Bedrock hydrogeochemistry Forsmark

Site descriptive modelling
SDM-Site Forsmark

Marcus Laaksoharju, Geopoint

John Smellie, Conterra

Eva-Lena Tullborg, Terralogica

Maria Gimeno, University of Zaragoza

Lotta Hallbeck, Microbial Analytics

Jorge Molinero, Amphos

Nick Waber, University of Bern

December 2008

SKB

Bedrock hydrogeochemistry Forsmark

Site descriptive modelling SDM-Site Forsmark

Marcus Laaksoharju, Geopoint

John Smellie, Conterra

Eva-Lena Tullborg, Terralogica

Maria Gimeno, University of Zaragoza

Lotta Hallbeck, Microbial Analytics

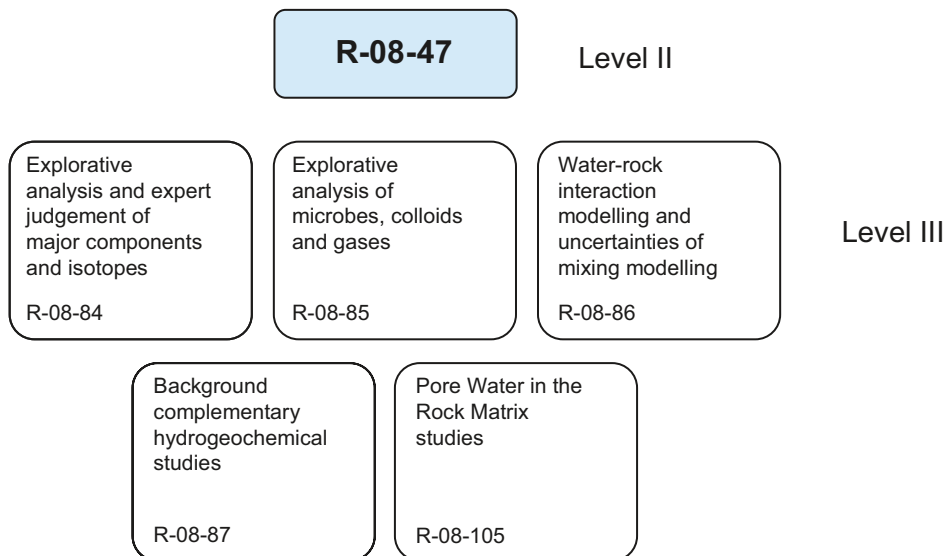Jorge Molinero, Amphos

Nick Waber, University of Bern

December 2008

Preface

This document forms the final part of the site investigation stage of the hydrogeochemical evaluation carried out at the Forsmark site leading to a Hydrogeochemical Site Descriptive Model version based on available data. It is the main hydrogeochemical report supporting the Forsmark Site Description (SDM-Site). SKB's ChemNet group, consisting of independent consultants and university personnel, carried out the data interpretation and modelling during the period September 2006 to December 2007. Several groups within ChemNet were involved and the evaluation was conducted independently using different approaches ranging from expert knowledge to geochemical and transport modelling. During regular ChemNet meetings the results were presented and discussed. The original work by the ChemNet participants is presented in /Smellie et al. 2008, Hallbeck and Pedersen 2008a, Gimeno et al. 2008/ and /Waber et al. 2008a/ in four level III reports containing complementary information for the bedrock hydrogeochemistry Forsmark Site Descriptive Model (SDM-Site Forsmark, R-08-47) level II report, as exemplified in the figure below. The work by Gascoyne and Gurban, Gurban, Molinero et al. and Nilsson is presented in /Kalinowski 2008/.

R-08-47		Level II

| Explorative analysis and expert judgement of major components and isotopes

R-08-84 | Explorative analysis of microbes, colloids and gases

R-08-85 | Water-rock interaction modelling and uncertainties of mixing modelling

R-08-86 | Level III |

Background complementary hydrogeochemical studies R-08-87	Pore Water in the Rock Matrix studies R-08-105

There is also another level III report: Fracture mineralogy of the Forsmark area by /Sandström et al. R-08-102/.

The views presented therein reflect those of the individual authors and are not neccessarily the views contained in this integrated Background Report. The ChemNet members contributing to this report are (in alphabetical order):

Patricia Acero, University of Zaragoza, Spain

David Arcos, Amphos, Barcelona, Spain

Luis Auqué, University of Zaragoza, Spain

Lara Duro, Amphos, Barcelona, Spain

Mel Gascoyne, GGP Inc. Pinawa, Canada

María Gimeno, University of Zaragoza, Spain

Thomas Gimmi, University of Bern, Switzerland

Javier Gómez, University of Zaragoza, Spain

Ioana Gurban, 3D-Terra, Montreal, Canada

Lotta Hallbeck, Micro Analytics, Gothenburg, Sweden

Jorge Molinero, Amphos, Barcelona, Spain.

Ann-Chatrin Nilsson, Geosigma AB, Uppsala, Sweden.

Karsten Pedersen, Microbial Analytics, Gothenburg, Sweden.

Björn Sandström, University of Gothenburg, Sweden

John Smellie, Conterra AB, Stockholm, Sweden

Eva-Lena Tullborg, Terralogica AB, Gråbo, Sweden

Nick Waber, University of Bern, Switzerland

Marcus Laaksoharju, ChemNet project leader

Summary

The overall objectives of the hydrogeochemical site description for Forsmark are to establish a detailed understanding of the hydrogeochemical conditions at the site, and to use this understanding to develop models that address the needs identified by the safety assessment groups during the site investigation phase. Issues of concern to safety assessement are radionuclide transport and technical barrier behaviour, both of which are dependent on the chemistry of groundwater and porewater and their evolution with time. The specific aims of the hydrogeochemical work were:

- To document the hydrogeochemistry at the Forsmark site with focus on the development of conceptual models to describe and visualise the site.

- To provide relevant parameter values to be used for safety assessment calculations.

- To provide the hydrogeochemical basis for the modelling work by other teams, in particular hydrogeology.

- To take account of the feedback from the SR-Can safety assessment work /SKB 2006ab/ that bears relevance to the hydrogeochemical modelling work.

The work has involved the development of descriptive and mathematical models for groundwaters in relation to rock domains, fracture domains and deformation zones. In this report, the groundwaters have been interpreted in relation to their *origin*, *evolution* and *composition*, which require close integration with geological, climatological and hydrogeological information. Past climate changes are one of the major driving forces for long-term hydrogeochemical changes (hundreds to thousands of years) and are, therefore, of fundamental importance for understanding the palaeohydrogeological, palaeohydrogeochemical and present evolution of groundwater in the Fennoscandian crystalline bedrock. In contrast, redox buffer capacity of the bedrock will minimise the effects on changes in alkalinity and redox at repository depths, therefore limiting the variations in pH and Eh significantly, regardless of major changes in groundwater composition.

The Forsmark 2.2 and 2.3 data have resulted in significant modifications in site understanding as compared to the situation based on data freeze 2.1. The many consistent temporal and spatial data support the description concerning the groundwater origin, most of the major end members and major hydrochemical processes. Integration with hydrogeology supports the palaeohydrogeological description of the site. Reaction modelling, different isotope ratios (Sr, S, C, B, Cl, O, H and the U-decay series), buffer capacity modelling and measurements of Eh, pH and microbe data, all support the process understanding. Matrix porewater compositions have now been well established and have contributed greatly to the present conceptualisation of the Forsmark area. Input from the fracture mineralogical studies have provided important support to the palaeohydrogeological and process understanding of the site. The confidence concerning the three-dimensional variability of processes and properties was improved due to the addition of both new data in previously drilled boreholes and from new boreholes in specific key areas.

Several groundwater types which are now present in the bedrock can be associated with past climatic events in the late Pleistocene, including interglaciations, glaciations, deglaciations, and associated shore level displacements in connection with with marine/non-marine transgressions and regressions. Among these, the last glaciation and post glacial period is the most important for the groundwater development in the Fennoscandian Shield, especially in terms of land uplift and shore level displacement and the development of the Baltic Basin. The description is not restricted to post glacial time since there is groundwater and porewater evidence that indicates a pre-Pleistocene warm-climate derived meteoric water component. The hydrochemistry of the Forsmark area cannot be explained without recognising this older (minimum 1.5 Ma) component. The present groundwaters therefore are a result of mixing and reactions over a long period of geological time. The interfaces between different water types are not sharp but reflect the variability in the structural-hydraulic properties.

Groundwaters in the uppermost 20–200 m of the bedrock display a wide chemical variability with chloride concentrations in the range 200–2,000 mg/L suggesting influence of both fresh meteoric water and brackish marine water (i.e Baltic Sea water and Littorina Sea relicts). Furthermore, a sharp decrease in tritium content at about 150 m depth, as well as ^{14}C data, indicate that these shallow groundwaters have short residence times that are mostly in the order of a few hundred years to only a few decades.

At depths greater than approximately 200 m, the water composition is indicative of a brackish marine water with chloride concentrations in the range 2,000 to 6,000 mg/L and with a clear Littorina component, as indicated by concentrations of magnesium and the bromide to chloride ratio concentrations. This water type is recognised down to 600 to 700 m depth in the transmissive gently dipping deformation fracture zones in the south-eastern part of the candidate area (hanging wall bedrock), whereas the penetration depth in the footwall bedrock (i.e. fracture domain FFM01, the target volume), where the frequency of water-conducting fractures is low, is restricted to around 300 m. Below these depths, the water composition indicates brackish to saline non-marine groundwaters (i.e. absence of Littorina influence), reflecting processes which have occurred prior to the intrusion of the Littorina Sea waters. These deep waters further show an increase in calcium with depth which, compared with sodium, represents a well recognised trend and is indicative for water/rock interactions that occur under low flow to stagnant groundwater conditions which increase with depth.

Analyses of the composition of rock matrix porewater also support the occurrence of low groundwater turnover in the footwall bedrock (i.e. fracture domain FFM01). Porewater from this location generally has lower chloride contents and is enriched in $\delta^{18}O$ compared with the fracture groundwaters, indicating a transient state between the porewater and groundwater down to at least 650 m depth. A signature with low chloride, low magnesium and enriched in $\delta^{18}O$ and δ^2H has been preserved far away from water-conducting fractures, suggesting that these porewaters have evolved from an earlier, very long lasting circulation of old dilute groundwaters in a few fractures. This is also consistent with the still prevailing transient state between this porewater and fracture groundwater from equivalent depths that, based on ^{36}Cl and ^4He dating, have residence times of more than 1.5 Ma. South-east of the target volume in the hanging wall bedrock, a situation close to steady-state is suggested between porewater and fracture groundwater down to about 200 m depth, reflecting the high frequency of water conducting, gently dipping deformation zones, and the rapid circulation of significant volumes of water in this area. At greater depth, the porewater has lower chloride contents than the fracture groundwater indicating a transient state down to about 650 m depth.

Transport of water volumes and mixing (both advection-dispersion and molecular diffusion) are major processes giving rise to present-day groundwater compositions. However, mixing also induces reactions and therefore the separation of these two processes is not only very challenging, but is also important for site understanding in order to indicate effects from past/present solute transport and reactions. Reactions involve interaction with the bedrock and fracture minerals, and in particular the alkalinity and redox buffering capacity of the bedrock is of key importance for groundwater composition and predicting future changes due to, for example, potential infiltration of dilute and oxidising waters.

Weathering and potential calcite dissolution under acidic conditions in the near-surface bedrock environment is promoted by the extensive presence of limestones in the overburden and controlled by biogenic input of carbon dioxide. This gives rise to pH values usually above 7, calcium concentrations mostly between 50 and 200 mg/L, and bicarbonate concentrations in the range 200 to 900 mg/L in the near-surface waters (down to about 20 m depth). Concentrations then decrease to very low values at greater depths. However, bicarbonate is relatively high in most of the brackish marine groundwaters hosted in the upper 600 m of the gently dipping deformation fracture zones in the hanging wall bedrock south-east of the target volume, whereas brackish non-marine groundwaters below 300 m depth in the footwall bedrock (i.e. fracture domain FFM01) have low bicarbonate contents.

The pH buffering capacity in the Forsmark groundwaters at depths greater than 100 m appears to be controlled by the calcite system, and modelling indicates that this water is in equilibrium with calcite. Investigations of fracture minerals show that calcite in fractures is abundant and that no extensive leaching has occurred in response to past glaciation/deglaciation events. These findings suggest that the buffering capacity against infiltrating dilute groundwater is sufficient, although no quantifications have been made yet. However, a study aiming at quantification of fracture minerals is currently on-going and will be reported separately as a complement to the site descriptive modelling reports.

According to data analyses and modelling of the redox system, reducing conditions currently prevail at depths greater than about 20 m. Most of the Eh values determined in brackish ground-waters (at depths between 110 and 646 m) seem to be controlled by the occurrence of an amorphous iron oxyhydroxide with higher solubility than a truly crystalline phase. This indicates that the iron system is disturbed, which also is supported by mineralogical investigations that have identified the presence of fine-grained amorphous to poorly crystalline phases now evolving towards more crystalline phases. At still greater depths the iron system seems to be limited by only crystalline iron hydroxides, mainly hematite. Despite the uncertainty of the measured data (e.g. due to sampling perturbations), the dissolved sulphide concentrations at shallow to intermediate depths are systematically low, possibly due to the precipitation of amorphous $Fe(II)$-monosulphides, linked to the activity of sulphate-reducing bacteria (SRB). At depths greater than 600 m, the dissolved sulphide concentrations increase, which is consistent with the occurrence of SRB and with the active precipitation of $Fe(II)$-monosulphides.

The behaviour of uranium is a special case at Forsmark. Elevated concentrations have been detected in groundwaters associated with a Littorina component and the highest concentrations are found in waters in the gently dipping deformation zones in the hanging wall bedrock south-east of the target volume. There are indications that these elevated concentrations are related to easy dissolvable uranium fractions in fracture coatings in contact with these waters. Speciation-solubility calculations support this conclusion and indicate that the high uranium contents are the result of the control exerted by an amorphous (and very soluble) uranium phase present in the system, and weakly reducing Eh values which may allow uranium complexation and re-equilibrium depending on Eh and dissolved carbonate.

The presence of goethite ($FeOOH$) in some hydraulically active fractures and fracture zones (mainly within the major gently dipping deformation zones ZFMA2 and ZFMF1) in the upper part of the bedrock indicates circulation of oxidising fluids during some period in the past (potentially Quaternary). However, the presence of pyrite in the same zones suggests that the circulation of oxidising fluids has been concentrated along channels in which different redox micro environments may have been formed. Furthermore, mobilisation as well as deposition of uranium in the upper 150 m of the bedrock is indicated by uranium-series decay analyses (USD) of fracture coatings.

The analyses of the current redox system at Forsmark have consistently indicated that sampling (or drilling induced) perturbation may have altered the original redox conditions of the hydrochemical system. Examples include oxygen intrusion and precipitation of amorphous iron oxyhydroxides, as indicated by the colloidal composition (see below) and mineralogical determinations. Additionally, there could have been modification of the original Eh and/or alkalinity by drilling waters, and the increase in dissolved uranium contents or changes in sulphide contents could have been caused partly by one or more of these disturbances. Despite these potential disturbances, the buffer capacity of the system maintains a marked alkalinity and a noticeable reducing character. Concerning the potential redox buffering capacity of the fracture system, it is concluded that previous oxidising episodes have not been intense enough to exhaust the reducing capacity of fracture filling minerals, which are still present in the shallow system (for example chlorite and pyrite).

Analyses of gases dissolved in groundwater at Forsmark have shown that the gas content increases with depth, but the waters are far from being oversaturated by gas. The major gas components are nitrogen and helium. Methane has also been detected, but generally in small amounts (less than 0.2 mL/L). Currently, it is not known whether the methane is of biogenic or non-biogenic origin, or a mixture of both.

Colloid amounts in Forsmark groundwater are comparable to that found in other granitic environments. The colloids are composed mostly of aluminum, silica, iron and sulphur. Uranium associated to the colloids was found in boreholes KFM02A and KFM06A, in line with the high groundwater uranium concentrations found in these boreholes. The uranium content on the colloids is about 10% of the uranium concentration in the groundwater and colloidal transport is, therefore, the result but not the origin to the high uranium content in the groundwater.

There is generally a high confidence in the description and understanding of the current spatial distribution of groundwater composition, mainly due to the consistency between different analyses and modelling of the chemical data, but also due to the agreement with the hydrogeological understanding of the area. The existence of a near-surface redox reaction zone appears to be plausible, but this is still unclear from uncertainties in data interpretation. Nevertheless, the abundance of calcite suggests there is active buffering capacity on dilute groundwaters low in calcite. Furthermore, even though quantification of the bedrock buffering capacity is not yet achieved, general indications from the Forsmark area as a whole point to a bedrock which has a sufficiently large buffering capacity to maintain pH values in the range 7 to 8.5 and Eh values lower than –140 mV. One important remaining uncertainty concerns the increase in sulphide concentrations measured in the on-going monitoring programme. Initial drilling and pumping may have disturbed the system or may have facilitated sulphate reduction, but this issue remains to be resolved. The monitoring programme will also support the overall understanding of the long term behaviour of other groundwater parameters such as uranium, DOC (dissolved organic carbon) and tritium.

Contents

1 Introduction

1.1 Scope and objectives

The Swedish Nuclear Fuel and Waste Management Company (SKB) has undertaken site characterisation at two different locations, the Forsmark and Laxemar-Simpevarp areas, with the objective of siting a geological repository for spent nuclear fuel. The investigations are conducted in campaigns with periodic 'data freezes', i.e. dates when no further data are incorporated in the database to allow for interpretation and modelling of that specific dataset. After each data freeze, the site data are analysed and site descriptive modelling is carried out with the purpose of developing a site descriptive model (SDM) of the site. This SDM is a synthesis of hydrogeochemistry, geology, rock mechanics, thermal properties, hydrogeology and surface system processes.

The overall objectives of ChemNet within the SDM for Forsmark are to first establish a detailed understanding of the hydrogeochemical conditions at the site, and to use this understanding to develop models that address the needs identified by the safety assessment groups during the site investigation phase. Issues of concern to safety assessement are radionuclide transport and technical barrier behaviour, both of which are dependent on the chemistry of groundwater and porewater and their evolution with time. The specific aims of the stage 2.2 and 2.3 hydrogeo-chemical work were:

- To document the hydrogeochemistry of groundwaters and porewaters at the Forsmark site with focus on the development of conceptual models to describe and visualise the site.

- To provide relevant parameter values to be used for safety assessment calculations.

- To provide the hydrogeochemical basis for the modelling work by other teams, in particular hydrogeology.

- To take account of the feedback from the SR-Can safety assessment work /SKB 2006ab/ that bears relevance to the hydrogeochemical modelling work.

The work has involved the development of descriptive and mathematical models for ground-waters in relation to rock domains, fracture domains and deformation zones. In this report, the groundwaters have been interpreted in relation to their *origin*, *evolution* and *composition*, which require close integration with geological, climatological and hydrogeological information. Past climate changes are one of the major driving forces for long-term hydrogeochemical changes (hundreds to thousands of years) and are, therefore, of fundamental importance for understanding the palaeohydrogeological, palaeohydrogeochemical and present evolution of groundwater (and porewater) in the Fennoscandian crystalline bedrock. In contrast, the buffer capacity of the bedrock will minimise the effects on changes in alkalinity and redox at repository depths, therefore limiting the variations in pH and Eh significantly, regardless of major changes in groundwater composition.

This background report provides an integrated link between the SDM main report (Level I), which provides a brief overview of the hydrogeochemical investigations, and the Level III reports which provide full documentation and in some cases a thorough interpretation of the hydrogeochemical data.

1.2 Methodology

The main task of the hydrochemistry evaluation work is to describe the hydrochemical conditions in and around the rock volume surrounding the repository. The investigations will fulfil various requirements, where one is related to information on features (parameters) used to calculate the long-term stability and safety of the disposal. A further requirement includes the understanding of the chemical conditions and their changes and development with time (palaeohydrogeochemistry).

Understanding the current undisturbed hydrochemical conditions at the proposed repository site is important when predicting future changes in groundwater chemistry that may be of importance to the long-term integrity of the currently planned SKB repository system, in particular copper corrosion and/or bentonite degradation. Therefore, the following variables are of particular interest for the hydrogeochemical site descriptive modelling: pH, Eh, sulphur system, iron, manganese, carbonate, phosphate, acetate, nitrogen species, total dissolved solids (TDS), isotopes, colloids, fulvic and humic acids, and microorganisms. In addition, dissolved gases (e.g. carbon dioxide, methane and hydrogen) are of interest because of their likely participation in microbial reactions.

In order to achieve site understanding the sequence of investigations, evaluations and modelling exercises outlined in Figure 1-1 were initially established as guidelines to the hydrogeochemical programme. Some of the investigation methods are based on expert knowledge, whereas others are based on mathematical modelling. The applied methodology is described in detail elsewhere /e.g. Smellie et al. 2002/ and the specific hydrogeochemical methodology used within the SKB site investigation programme is published in a special issue of Applied Geochemistry /Gascoyne and Laaksoharju (ed.) 2008/.
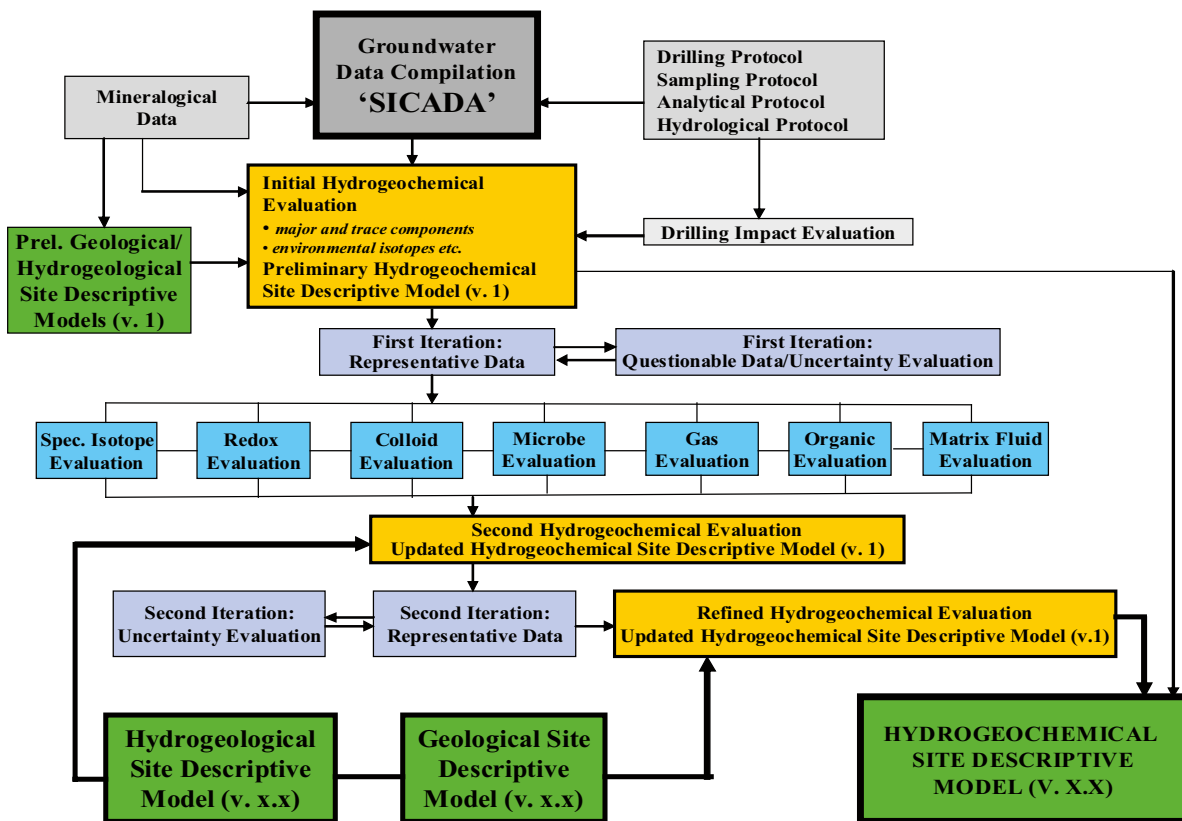

Figure 1-1. Schematic work flow and modelling steps for the implementation of the hydrochemical modelling /Smellie et al. 2002/.

In brief, the raw chemical data are initially screened to remove any obvious analytical or sampling artefacts based on specified laboratory and field procedures. These screened data are then entered into the SKB Sicada database and in this form delivered for hydrochemical evaluation. The quality of the data is then rigorously assessed with respect to their representativity based on an integrated hydrochemical, geological and hydrogeological approach. Specific data judged to be prerequisite for the understanding, interpretation and modelling of the groundwater conditions are then selected, and from these the most suitable samples are identified for different modelling purposes. Examples include field redox potential measurements and analysed Fe(tot) and Fe(II) values for redox modelling of the groundwater system, and major ion and environmental isotope data input to hydrogeological model calibrations.

The next step is a general examination of the data using traditional geochemical approaches to describe the data and provide an initial insight and understanding of the site, i.e. the construction of a preliminary conceptual model for the area. Based on this hydrochemical framework, selected data are further evaluated using different modelling approaches, for example, geochemical equilibrium modelling, mixing modelling and finally using coupled modelling codes. The results from these modelling exercises are presented as 2D/3D visualisations of the model volume based on the measured constituents from the modelled area. These descriptions are compared and integrated with independent modelled results for the area, for example, the geological and hydrogeological models.

The evaluation stages were repeated after each data freeze when new and modified data became available. Each data freeze represents data collected up to a predetermined date set by SKB, after which no new data are accepted; this allows all participant groups to share the same dataset. For internal consistency, at each new data freeze and modelling stage, the updated datasets are checked against the previous versions to identify anomalous or erroneous data which may require additional sampling and/or analysis to reduce uncertainties and increase reliability. Thus, the final site descriptive model as presented and described in this report is the result of an iterative, step by step development during the period of the site investigations, i.e. through modelling stages 1.2, 2.1, 2.2 and 2.3.

In general, the pre-investigation scheme outlined in Figure 1-1 was achieved in the respect that all components were addressed and accomplished to varying degrees, but the sequence of events leading to the final site description varied. This was partly due to the natural evolution of the site investigations, which must retain a degree of flexibility to decide quickly on additional boreholes or additional measurements and analysis, to accommodate time losses due to faulty equipment etc and also to impose time constraints on personnel activity to meet schedule demands etc.

The work within modelling stages 2.2 and 2.3 further developed the conceptual models and the understanding of the site as presented in earlier model stages. Integration with HydroNet, SurfaceNet and RetNet (SKB's hydrogeological, surface system and bedrock transport modelling groups, respectively) was more effective than was previously the case due to the large amount of new interpreted data which brought the hydrogeochemical programme into consistency with the progress of the other groups.

Further to the groundwater hydrochemical studies, detailed studies of porewaters have been carried out with success for the first time in any crystalline rock environment. In addition, the importance of mineralogy has been underlined in site understanding, for example, as input to the geochemical equilibrium modelling. From a palaeohydrogeological viewpoint, geochemical and mineralogical information from fracture minerals, altered rock and the reference rock matrix has been compiled in /Sandström et al. 2008/, where analysis of these data are restricted to the pH and redox buffering capacity of the host rock. The major findings from the fracture mineral and porewater investigations have been integrated into the site description.

Important feedback from SR-Can /SKB 2006ab/ and Insite (the review group established by the authorities) and Sierg (SKB's independent review group) was integrated into the modelling. The CRI issue list (e.g. CRI-list dated October 2006, established by the authorities, represents important input to the investigations, aiming to improve various aspects of the site descriptive model and site understanding. Of the issues proposed, some were addressed already in /SKB 2007/, but additional data during model stage 2.3 facilitated further modification. The issues addressed at different levels of detail were:

- Eh and pH buffering capacity.

- Interaction between deep and shallow groundwater systems.

- Elevated uranium content in some groundwater at intermediate depths.

- Alternative models, uncertainties and data bias.

- Confirming models of the site scale in relation to the groundwater flow system.

- Geochemical and isotopic data for palaeohydrogeology and groundwater evolution.

- Mineralogical and petrographical characterisation of fracture and matrix minerals.

- Groundwater compositions at repository depth.

- Spatial variability of hydrochemical data.

- Characterisation of colloidal, organic, microbial and gaseous species in groundwaters.

- Data from pre-existing boreholes in and near the sites.

- Geochemical analogues of safety-related radionuclides.

Details of the hydrogeochemistry work and the results of issue handling have been addressed in /Smellie et al. 2008, Hallbeck and Pedersen 2008a, Gimeno et al. 2008/ and /Kalinowski (ed.) 2008/.

1.3 Nomenclature and processes

The nomenclature and processes described in this report are important to understanding the various conceptual model approaches developed, both past and present.

The nomenclature of the groundwater types used in this report depends on the purpose of the modelling and a distinction can be made between the following:

1) *Current groundwater types*, i.e. these are the types that are now used to distinguish different waters as measured today. The nomenclature of these present water types are related to the perceived main origin of these waters (i.e. meteoric, Littorina, glacial meltwaters etc), but their compositions have subsequently been altered by mixing and reactions.

2) *Origins of current groundwater types*. This relates to the chemical composition of the real groundwater end members, i.e. the 'actual' precipitation, the 'actual' glacial meltwater, the 'actual' estimated Littorina sea water, etc. The end-member compositions used for the site modelling are listed in Table 1-1.

Description of the current groundwater types in Forsmark is based on the salinity content of the water (e.g. Fresh, Brackish, Saline). Brackish waters may be subdivided into Brackish Marine and Brackish Non-marine, mainly based on magnesium content and other marine indicators (e.g. chloride to bromide ratios). As a consequence, the same water type can be described as, for example, Brackish Marine or a mixture of Littorina and Glacial water. The compositions of the end members are described in detail by /Gurban 2008/.

Table 1-1. End-member compositions used for the Forsmark site groundwater modelling.

	Deep Saline Laxemar values	Values used for Forsmark modelling	Littorina	Glacial	Old Meteoric + Glacial	Altered Meteoric Forsmark #4919
pH	8	8	7.6			7.91
HCO_3^- (mg/L)	14.1	14.1	92.5	0.12	0.12	466.0
Cl (mg/L)	47,200	47,200	6,500	0.5	0.5	181
SO_4^{2-} (mg/L)	906.0	10	890	0.5	0.5	85.1
Br (mg/L)	323.7	323.7	22.2			0.57
Ca (mg/L)	19,300	19,300	151	0.18	0.18	1.6
Mg (mg/L)	2.12	2.12	448	0.1	0.1	41.1
Na (mg/L)	8,500	8,500	3,674	0.17	0.17	7.5
K (mg/L)	45.5	45.5	134	0.4	0.4	274.0
Si (mg/L)	2.9	2.9	3.94	–	–	5.60
δ^2H (‰ V-SMOW)*	–44.9	–44.9	–37.8	–158.0	–118	–80.6
$\delta^{18}O$ (‰) V-SMOW)*	–8.9	–8.9	–4.7	–21.0	–16.0	–11.1

* Vienna Standard Mean Ocean Water

The names of the water types used in the different evaluations and modelling activities based on /Smellie et al. 2008, Gimeno et al. 2008, Gurban 2008/, are:

1) *Palaeohydrogeochemical description:* Highly Saline, Old Meteoric ± Old Glacial, Last Deglaciation, Littorina and Present Meteoric.
   (Note: '± Old Glacial' means that the Old Meteoric water may or may not contain an Old Glacial component).

2) *Mixing end member (M3) modelling:* Deep Saline, Saline, Old Meteoric + Glacial, Glacial, Littorina and Altered Meteoric.

3) S*ite descriptive model:* Saline, Brackish Non-marine, Brackish Marine, Mixed Brackish and Fresh.

To understand, interpret and conceptualise the groundwater evolution, the following issues need to be considered:

1) *The 'original' composition of the groundwater present the bedrock:* This is essentially unknown, but evidence from fracture groundwaters and matrix porewaters indicates that resident groundwaters prior to the last deglaciation were a mixture of old meteoric ± old glacial and saline in type as a function of depth. Note that the uncertainty in recognising groundwater components older than the last deglaciation increases considerably with age see /Laaksoharju et al. 2008, Smellie et al. 2008/.

2) *Last deglaciation effects:* Includes incursion of glacial meltwater and subsequent Littorina Sea water.

3) *Introduction of more recent groundwater types:* Because the studied site is situated close to the Baltic Sea coast, it is evident that both fresh meteoric water and brackish-marine sea waters of different salinities may have played important roles, especially since the last deglaciation. Fresh meteoric waters from very different climates (e.g. ranging from temperate to cool) may also have been recharged repeatedly.

4) *Factors controlling groundwater flow that largely determine the resulting groundwater chemistry:* These include topography, bedrock transmissivitites, interconnection of different fractures and fracture networks, density differences and potential glacial loading and unloading.

5) *The reactions taking place in the soil cover and bedrock which modify the original signature of the recharge water:* Examples are redox reactions mostly mediated by microbial activity involving oxygen consumption, and reactions with manganese, iron, sulphide and carbon. In addition, water/rock reactions such as ion exchange, calcite dissolution/precipitation, and silicate weathering will occur, together with mixing and also diffusion (e.g. exchange with matrix porewater).

1.4   Abbreviations

Symbols, subscripts, and abbreviations used in this report are listed and explained in Table 1-2 below. These are provided to simplify reference in the text to special names, chemical and physical parameters, elements, compounds, isotopes and biochemical compounds.

Stable isotope ratios ($^2H/^1H$, $^{11}B/^{10}B$, $^{13}C/^{12}C$, $^{18}O/^{16}O$, $^{37}Cl/^{35}Cl$ and $^{34}S/^{32}S$) are referenced to a standard (e.g. V-SMOW, PDB or CDT) and expressed in per mil (‰) deviations (δ values) from the appropriate standard where δ is defined as:

$$\delta = [\ (R_{sample}/R_{standard})-1\ ] \times 1{,}000 \qquad \text{and R is e.g. } {}^{18}O/{}^{16}O.$$

Table 1-2. Explanation of symbols, subscripts and abbreviations used in this report.

Symbol/abbreviation	Description
^{40}Ar	Radiogen isotope formed from ^{40}K.
^{39}Ar	Isotope formed as a result of induced neutron activation of ^{39}K
ATP	Adenosine-Tri-Phosphate
AA	Autotrophic Acetogenic bacteria
HA	Heterotrophic Acetogenic bacteria
AM	Autotrophic Methanogenic bacteria
HM	Heterotrophic Methanogenic bacteria
AOM	Anaerobic Methane oxidation
$^{11}B/^{10}B$	Ratio for boron isotopes
pCO_2	Partial pressure of carbon dioxide
CCC	Complete Chemical Characterisation
CDT	Cañon Diablo Troilite (Standard used for $\delta^{34}S$)
CHAB	Cultivable Heterotrophic Aerobic Bacteria
Cond.	Electric conductivity (field)
^{12}C	Light stable carbon isotope
^{13}C	Heavy stable carbon isotope
^{14}C	Radioactive carbon isotope (half-life 5730 ± 40 years)
$^{14}C_{(TIC)}$	Carbon-14 concentration in total inorganic carbon
pmC	Percent modern carbon
^{35}Cl	Light stable isotope of chlorine
^{37}Cl	Stable isotope of chlorine
^{36}Cl	Radioactive isotope of chlorine (half-life = 301,000 years)
Deuterium	(^2H) The heavy stable isotope for hydrogen
DIC	Dissolved inorganic carbon
DOC	Dissolved organic carbon
Eh	Redox potential
Fe(II)	Ferrous iron
Fe(III)	Ferric iron
GMWL	Global Meteoric Water Line

Symbol/abbreviation	Description
^{4}He	Helium-4 (Heavy isotope of helium)
^{1}H	Hydrogen (stable isotope)
^{2}H	Deuterium (Heavy stable isotope of hydrogen)
^{3}H	Tritium (Radioactive hydrogen isotope. half-life = 12.43 years)
HCO_3	Bicarbonate
HRL	(Äspö) Hard Rock Laboratory
IRB	Iron-Reducing Bacteria
MPN	Most Probable Number
MRB	Manganese-Reducing Bacteria
M3	Program for calculation of groundwater mixing proportions
NRB	Nitrate-Reducing Bacteria
^{16}O	Light stable isotope of oxygen
^{18}O	Heavy stable isotope of oxygen
PHREEQC	A Computer Program for Speciation, Batch-Reaction, One-Dimensional Transport, and Inverse Geochemical Calculations
PDB	Standard according to Pee Dee Belemnitella Formation (used for ^{13}C as well as for ^{18}O, especially for carbonates)
PVB	Pressure Vacuum Beaker
REEs	Rare Earth Elements (La, Ce, Pr, Nd, Sm, Eu, Gd, Tb, Dy, Ho, Er, Tm, Yb and Lu)
Radioactive isotopes	Radioactive isotopes decay and produces isotopes (daughters) that can be either stable (radiogenic isotopes; see below) or radioactive (e.g. decay chains like the U- series). The decay rate for a specific isotope is constant and usually expressed as half-life
Radiogen isotopes	Radiogen isotopes are stable but formed by radioactive decay
^{87}Sr	Radiogen strontium isotope, produced by decay of ^{87}Rb
^{86}Sr	Stable isotope of strontium
SRB	Sulphate Reducing Bacteria
SDM	Site Descriptive Model
^{32}S	Light stable isotope of sulphur
^{34}S	Stable isotope of sulphur
$\delta^{34}S_{(SO4)}$	Stable sulphur isotope ratio in dissolved sulphate
TIC	Total Inorganic Carbon
TNC	Total Number of Cells
Tritium	Radioactive hydrogen isotope (^{3}H) half-life = 12.43 years
TU	Tritium Units
TDS	Total Dissolved Soilids
USD	Uranium-Series Decay analyses
V-SMOW	Vienna Standard Mean Ocean Water (Standard used for ^{18}O/ ^{16}O and ^{2}H/ ^{1}H ratios)

1.5   Conceptual mixing and reactions

As a result of the extensive site bedrock investigations in Sweden and Finland it is perceived that the hydrogeochemical evolution of fracture groundwater strongly results from advective mixing and water-rock interactions driven by past and present changes in the climate (e.g. /Laaksoharju and Wallin (eds.) 1997, Laaksoharju et al. 1999, Pitkänen et al. 1999/). Many of the evaluation and modelling steps used within ChemNet are focused on discriminating these effects by using different modelling approaches. Mixing modelling focuses on tracing the origin of the groundwater, whereas reaction modelling focuses on understanding the interaction between oxic/anoxic groundwaters and the bedrock and, for example, the mediating role microbial activity may play.

For modelling purposes, different approaches can be used leading to quite different descriptions of the system. When applying end-member mixing models, for example, the choices of end members are crucial for the description of both mixing and reactions. This does not necessarily mean that some models are right and some models are wrong. It is more a question of choosing the most suitable model available for describing the part of the system that is to be addressed, and also to focus on the time period of interest. All epochs and all parts of the system can never be described with high resolution using the same model; usually several models are required as well as different sets of end members and starting prerequisites.

Figure 1-2a to d illustrates the different approaches to model groundwater mixing and reactions, using sodium versus chloride as an example. The sodium content in groundwater can be altered by, for example, feldspar weathering or ion exchange, but chloride is regarded as a water conservative tracer not affected by reactions. The task is to model the reactions that have caused the measured sodium content. In Model 1 (Figure 1-2 b), the water composition is the result of reactions, for example, the sample with about 0.85 mol/kg Cl, indicated with the arrow, has gained about 0.28 mol/kg sodium due to reactions. There is no flux or mixing in the system since the system is closed. In Model 2 (Figure 1-2 c), the water composition is the result of mixing of two end members (indicated with the dashed black line); here the sample has gained about 0.07 mol/kg sodium. The water composition is described mainly as a result of two-component mixing with some gain of sodium by reactions. In Model 3 (Figure 1-2 d), the water composition is described almost exclusively as the result of mixing of several end members. Here the sample has not gained any sodium, since it plots on, or close to, the mixing line (black
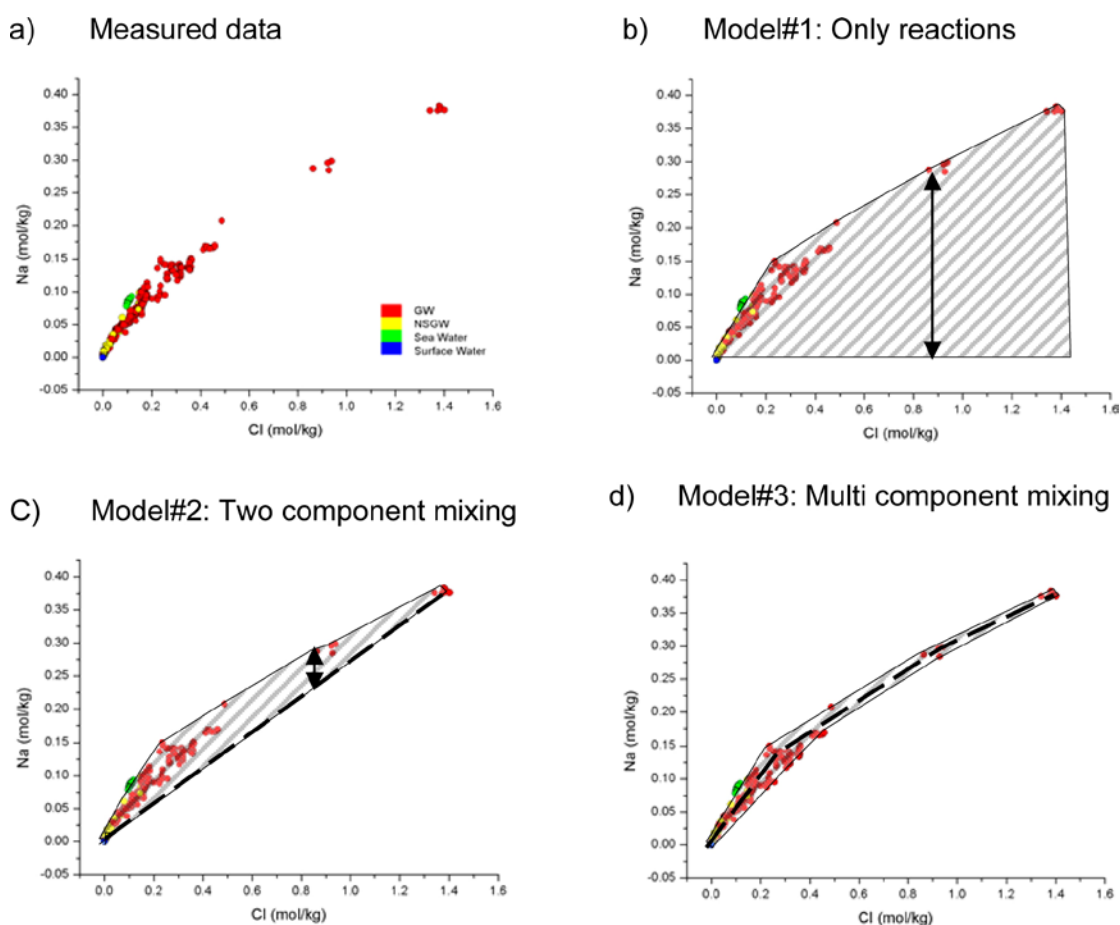
Figure 1-2. *Schematic presentation of how different models are used to describe the processes behind the measured Na content. The arrows indicate the amount of reactions taking place for a particular sample, the grey dashed area indicates samples affected by reactions and the black dashed line indicates the mixing line: a) Measured Na versus Cl, b) Model based on reactions, c) Model based on a mixture of two end members and, d) model based on several end members.*

dashed line). The water composition is described as the result of multi-component mixing and the sodium content is the result of pure mixing/transport. Plots above the mixing line indicate a gain of sodium, whereas plots below the mixing line indicate a loss of sodium.

The example given above clearly shows that the description of the groundwater system depends on the model selected. Model 1 describes the total amount of reactions taking place to obtain the sodium content measured in the sample. However, it does not describe where and when the reactions took place. Models 2 and 3 describe the water composition in relation to the endmember composition. Hence, these models can be used to calculate the mixing proportions of the endmembers. This, in turn, can be used not only to indicate the origin, but also to indicate the range of possible residence time in the bedrock. This is useful information when, for example, integrating the results with the hydrogeological modelling. Models 2 and 3 do not describe the evolution of the end-member composition, but assume that the processes responsible for this composition are implicitly considered (including all the reactions that ever took place).

It is generally a relatively easy task to construct Model 2, but with the risk that the system is oversimplified such that the effects from reactions are overestimated and the effects from transport underestimated. Model 3 can provide realistic descriptions of conservative and non-conservative compounds, but model uncertainties (such as uncertain end-member compositions and mathematical uncertainties in the model applied) can still lead to an erroneous conclusion concerning the gain/losses of element concentrations. The accuracy of Models 2 and 3 can be tested by, for example, plotting the model-predicted chloride and $\delta^{18}O$ contents versus the measured ones. The deviation from a perfect correlation will then indicate the model uncertainties /Laaksoharju 1999/. The uncertainties in the modelling are discussed in /Gimeno et al. 2008/.

The importance of mixing becomes apparent under the following circumstances:

- The palaeo- and present climate has a huge impact on the hydrogeology and, hence, on hydrochemistry in Fennoscandia /Laaksoharju et al. 2008/. This facilitates different water types, i.e. glacial, sea water and meteoric water, to enter or to be flushed out from the bedrock.

- The temperature in the rock is relatively low (at –200 m = 11C°; the gradient is 1.6C° per 100 m) and therefore most water/rock interaction processes generally are slow.

- The groundwater flow is faster and more dominating than the reaction times, i.e. for highly transmissive conditions.

The significance of reactions becomes apparent, particularly with respect to: a) redox conditions where microbiologically mediated reactions are rapid, and b) pH and alkalinity values buffered by kinetically fast calcite precipitation/dissolution reactions /Gimeno et al. 2008/.

As an example of the complexities involved, the chemical evolution of Littorina Sea water entering the bedrock at Forsmark was modelled /Gimeno et al. 2008/. The modelled results indicated that the major components Cl, SO_4, Na, Mg and Ca, and stable isotope values of $\delta^{18}O$ measured in the brackish marine groundwater with chloride contents around 5,500 mg/L, can be predicted without considering major influences from reactions, assuming that 20 to 60% Littorina sea water was infiltrating into a groundwater mixture consisting of 10% deep saline and 90% glacial water. This assumption is in agreement with the conceptual postglacial model of the site. However, detailed investigations /Smellie et al. 2008, Molinero et al. 2008/ indicate modifications of the water caused by the following reactions:

- Br/Cl typically show marine values in groundwater samples where the Na/Ca ratio and Mg contents are significantly reduced compared with marine values.

- The carbon system indicates HCO_3 production following the last deglaciation related to the intrusion of the Littorina water.

- The sulphur system indicates sulphate reduction (i.e. lowering of sulphate contents and increase in sulphur isotope values in the remaining sulphate).

- The strontium isotope ratios show no mixing line towards marine values which should be expected if only mixing had occurred; instead the strontium isotopes show clear signs of water/rock interactions which probably include ion exchange.

As to intrusion of the Littorina sea water, it can thus be concluded that mixing, together with reactions, have formed the composition of the present brackish marine groundwater. Furthermore, reactions modified, but did not mask the origin of the water. The exact quantification of the contribution from reactions versus mixing is complex, and at best semi-quantitative at the site scale, and requires different modelling approaches ranging from explorative analyses, mass-balance calculations, mixing calculations and coupled reactive transport modelling (see for example /Gimeno et al. 2008, Molinero et al. 2008/).

2 Previous model versions and input from other disciplines

2.1 Previous conceptual model

Two versions of the SDM (versions 1.1 and 1.2) have been developed for the Forsmark area. Version 1.1 /SKB 2004/ was completed during 2004 and version 1.2 in June 2005 /SKB 2005/. The aim of the work based on the 2.1 data freeze was to provide feedback to the site investigations /SKB 2006b/ and to address issues brought up by various review groups such as , Sierg and the ChemNet group itself /SKB 2007/. In total, three complete modelling steps have been carried out during the complete site investigation stage. The scope of the first two modelling steps, versions 1.1 and 1.2, was limited, whereas this final stage (the SDM-Site Forsmark modelling based on 2.2 and 2.3 data), has resulted in a modified and complete site description.

The earlier hydrogeochemical model version 1.2 and model stage 2.1 /SKB 2005, SKB 2006b/ concluded that the complex groundwater evolution and patterns at Forsmark were a result of many factors such as: a) the present-day topography and proximity to the Baltic Sea, b) past changes in hydrogeology related to glaciation/deglaciation, land uplift and repeated marine/ lake water regression/transgression, and c) organic or inorganic alteration of the groundwater composition caused by water/rock interactions and microbial processes. The chemistry of the sampled groundwaters reflected to various degrees processes relating to modern and ancient water/rock interactions and mixing.

The conceptual understanding of the Forsmark site based on the 2.1 data was that the groundwater composition showed an increase in salinity down to a depth of about 200 m, and tritium (^{3}H) data show no input of modern water at depths greater than 200 m. This indicates that groundwater types in the uppermost parts of the rock are of meteoric origin. At depths between approximately 200–600 m, the salinity remains fairly constant at a level between 5,000 and 6,000 mg/L which, together with high magnesium concentrations linked to a significant marine component, indicates input of Littorina Sea waters to these depths. At depths between 600–1,000 m, the salinity increases to higher values with a glacial and deep water signature. There are also indications that the salinity is higher at greater depths in the bedrock in the north-western part of the candidate area (i.e. in the target volume) when compared with the south-eastern part.

The Forsmark 2.1 groundwater data indicated relatively small modifications to the version 1.2 hydrogeochemical site description, but the overall geochemical understanding of the site has improved due to addressing certain review issues /SKB 2007/. These included confirmation of previous findings from version 1.2 and also support for the predictions made in version 1.2 based on the limited knowledge at that time. Confidence has improved in the three-dimensional variability of processes and properties due to the addition of new data from previously drilled boreholes and from new boreholes in specific key areas. This increased confidence in the overall understanding of three-dimensional variability of processes and properties at the site.

2.2 Geology model input

The geology of the Forsmark area has been described in /Olofsson et al. 2007, Stephens et al. 2007/ and the bedrock evolution from the Palaeoproterozoic through to the Quaternary in /Söderbäck 2008/. Furthermore, the interplay between, for example, structural geological and hydrogeological features at Forsmark have been addressed in /Follin et al. 2007ab, 2008ab/. The summary text below is based on the data evaluation and modelling work reported in these publications.

The Forsmark site is located north-east of Forsmark village along the Baltic Sea coast in an area that contains three regionally significant deformation zones (Singö, Eckarfjärden and Forsmark). These zones dip steeply and strike WNW-ENE and NW-SE (Figure 2-1). In several parts of the area, outcrops are limited, especially away from the coast. The bedrock is dominated by different types of metamorphosed granitoid with subordinate felsic to intermediate metavolcanic rocks, metamorphosed diorite or gabbro, pegmatite or pegmatitic granite and amphibolite (Figure 2-1). These rocks formed between 1.89 and 1.85 billion years ago (1.89–1.85 Ga).
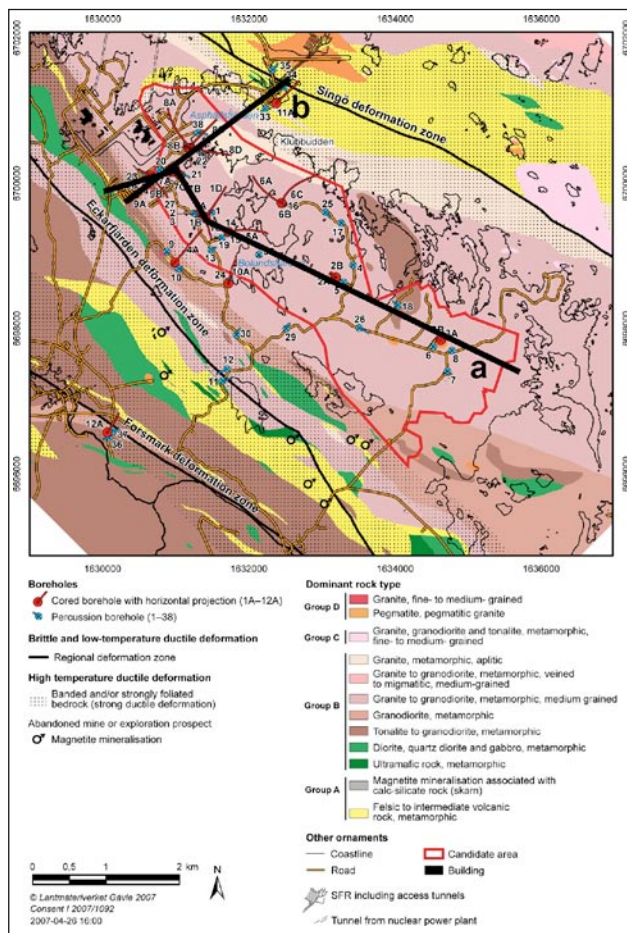
Figure 2-1. *Cored and percussion borehole locations in relation to the bedrock geology of the Forsmark area. The approximate positions of the WNW-ESE (a) and WSW-ENE (b) cross-sections described in chapter 7 are indicated. /Stephens et al. 2007/.*

A penetrative, ductile tectonic fabric developed between 1.87–1.85 Ga during the Svecokarelian orogeny, when temperatures exceeded 600°C and the rocks were situated at mid-crustal depths. After 1.85 Ga, the rocks started to cool below 500°C. Areas where the bedrock is banded and/ or affected by a strong, ductile tectonic foliation (dotted raster in Figure 2-1) can be separated from areas where the bedrock is folded and more lineated in character (dotted raster absent in Figure 2-1). The former are inferred to have been affected by higher ductile strain. They anastomose around the more folded and lineated bedrock with lower ductile strain that are restricted to several tectonic lenses. The candidate area is situated in the north-western part of one of these tectonic lenses and includes the target area in its north-westernmost part, between Lake Bolundsfjärden and the nuclear power plant. The bedrock inside this tectonic lens is relatively homogeneous and is dominated by medium-grained metagranite with subordinate pegmatite or pegmatitic granite, amphibolite and finer grained metagranitoid. The lithology and deformational characteristics are more complex outside the lens. The rocks in these marginal domains dip steeply towards the south-west.

Following these early developments, ductile-brittle and brittle deformation occurred several times during the Proterozoic, related to major tectonic activity probably during the later part of the Svecokarelian (1.80–1.70 Ga), Gothian (1.70–1.60 Ga) and Sveconorwegian (1.10–0.90 Ga) orogenies. This has resulted in the activation and subsequent reactivation of the different fracture systems. A second geological process has also affected the bedrock at several times during the Proterozoic and Phanerozoic. This process involved loading by sedimentary rocks or by ice during cold, glacial periods and, subsequently, unloading related to denudation of this younger material. This process has occurred at several times during the long geological history of the bedrock and each unloading phase resulted in exhumation of the Proterozoic crystalline bedrock.

The geological modelling work at Forsmark /Stephens et al. 2007/ has addressed rock domains, deformation zones and fracture domains in the bedrock. These three entities are summarised below. Rock domains occupy the whole rock volume. The bedrock in each rock domain consists of two components, the bedrock along deformation zones and the bedrock between deformation zones which comprises one or more fracture domains.

2.2.1 Rock domains

Rock domains refer to rock volumes where the bedrock shows similar composition, grain size, degree of bedrock homogeneity, and degree and style of ductile deformation. Rock domains RFM029 and RFM045 (Figure 2-2) comprise the target volume and are of most significance in the context of the site description and modelling work. Rock domain RFM029 dominates the central part of the target volume and is the volumetrically most significant domain from a repository construction viewpoint; the subordinate rock domain RFM045 occurs in the northern part of the target volume (Figure 2-2). The bedrock in these domains predominantly consists of medium-grained metagranite and, in order of decreasing importance, subordinate pegmatite or pegmatitic granite, amphibolite and fine- to medium-grained metagranitoid. The rocks are affected by regional amphibolite-facies metamorphism and, in rock domain RFM045, by the high-temperature alteration referred to as albitisation.
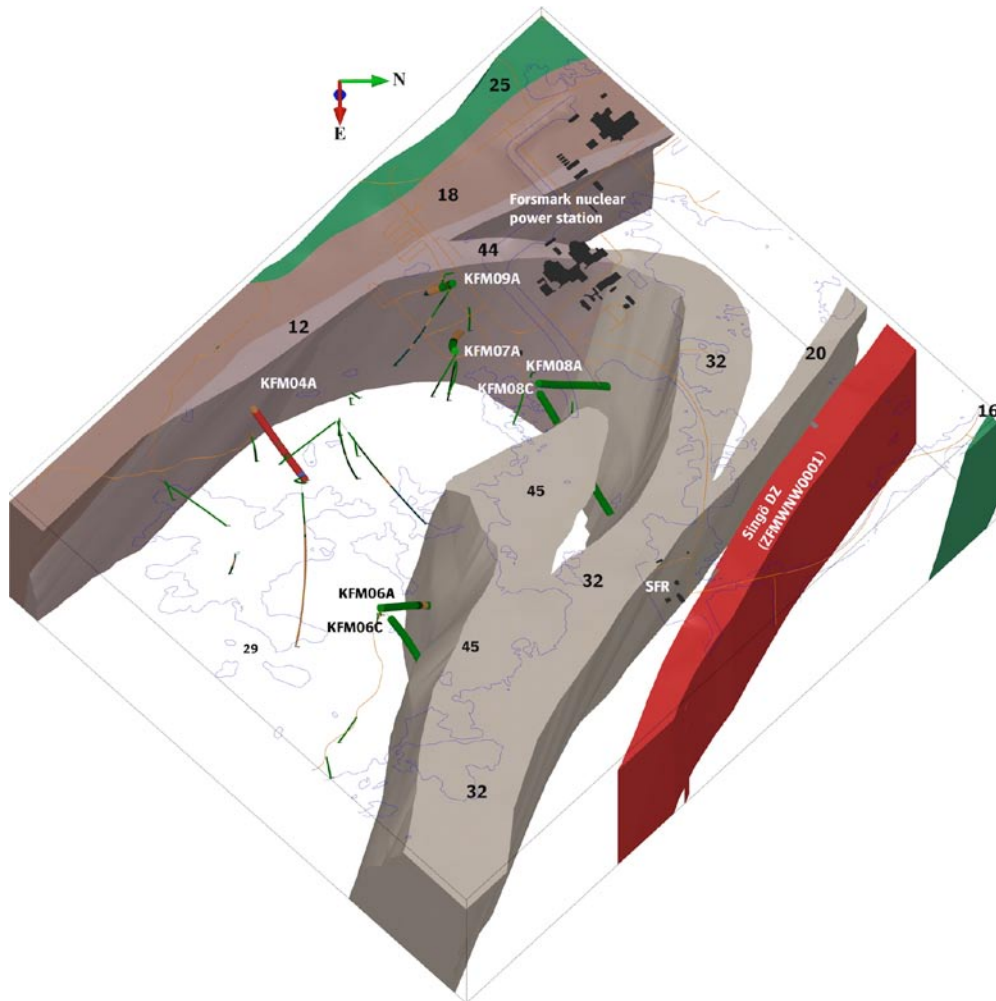
Figure 2-2. *Three dimensional model of the moderately- to steeply-plunging synform structure which characterises the target volume. The model is viewed to the west from approximately the position of SFR. The regionally significant Singö deformation zone is shown in the foreground. The rock domains inside the target volume are numbered; several domains, including RFM029, are unshaded in order to display the structural style at the Forsmark site. Note especially the moderately- to steeply-plunging synform that is defined by the boundary between domain RFM029 and domains RFM032 and RFM044. The dominant rock type in each domain is depicted by different colours (*see *Figure 2-1). Boreholes marked with the help of larger cylinders (KFM04A, KFM06A, KFM06C, KFM07A, KFM08A, KFM08C and KFM09A) constrain the boundaries between different domains. /Stephens et al. 2007, Figure 4-5/.*

Rock domains RFM029 and RFM045 are situated in the core of a major synform that plunges 55–60° to the SE (Figure 2-2). Folding of the ductile tectonic foliation inside these two domains and the development of a linear ductile fabric is a characteristic structural feature. Virtually all the other rock domains occur along the limbs of the major fold structure, both to the north-east and to the south-west (Figure 2-2). The marginal rock domains outside the target volume share the property that they are affected by intense ductile strain with strongly foliated and lineated rocks, and locally an intense tectonic banding.

2.2.2 Deformation zones

Deformation zones refer to parts of the bedrock along which there is a concentration of strain. Most deformation zones at Forsmark are brittle structures, i.e. they are fracture zones. Three important sets of deformation zones have been recognised (Figure 2-3 and Figure 2-4):

- Vertical and steeply dipping (to the south-west) deformation zones that strike WNW-ENE or NW-SE and are prominent outside the target volume. These zones generally show complex, ductile and brittle deformation and are represented by the Singö, Eckarfjärden and Forsmark zones. These three zones show a trace length at the ground surface which is longer than 10 km, i.e. they are regionally significant zones.

- Vertical and steeply dipping fracture zones that strike ENE-WSW to NNE-SSW and are prominent inside the target volume. The zones that belong to this set inside the target volume show a trace length at the ground surface which is about 3,000 m or less.

- Gently dipping fracture zones that dip to the SE and are conspicuous outside the target volume in the south-eastern part of the candidate volume. This set includes the gently dipping fracture zone ZFMA2 which effectively forms the southern boundary to the target volume. Relative to the other two sets of deformation zones, the gently dipping zones contain a higher frequency of open fractures (i.e. crush rock). Many of these zones extend to at least 1,000 m depth, and they play an important role both hydrogeologically and hydrogeochemically.
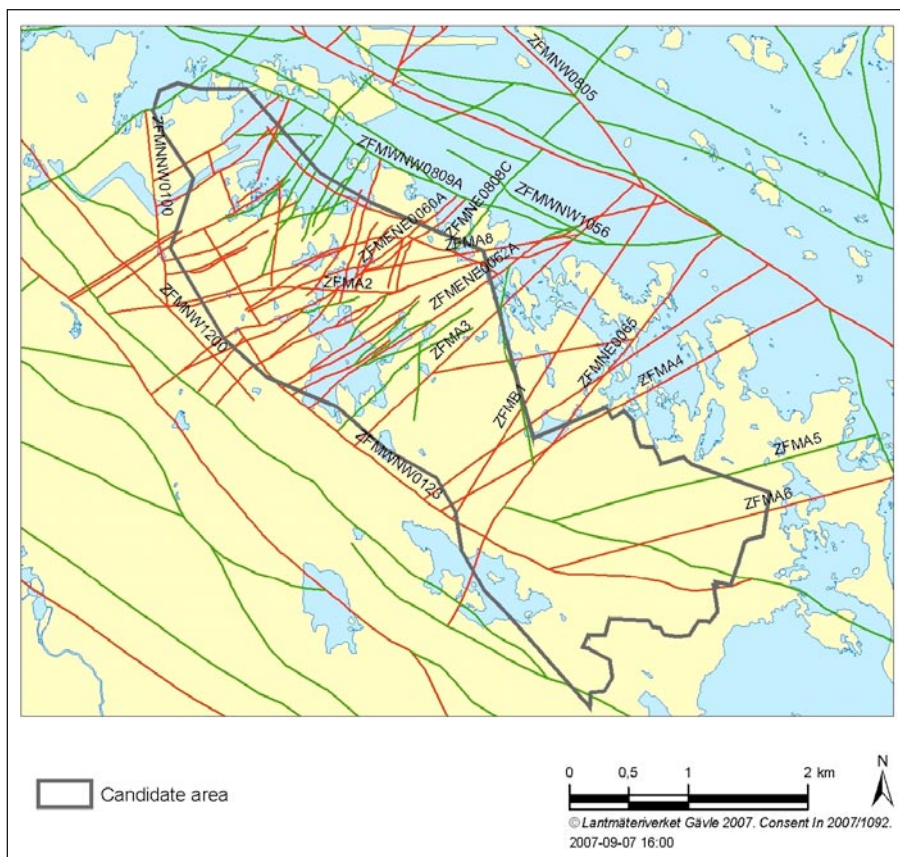
Figure 2-3. *Major deformation zones in the Forsmark area. Only the most relevant zones are labelled to correspond to the cross-sections later used to conceptualise and visualise the hydrogeochemical data /Stephens et al. 2007/. Red lines represent high confidence deformation zones and green lines low confidence deformation zones.*
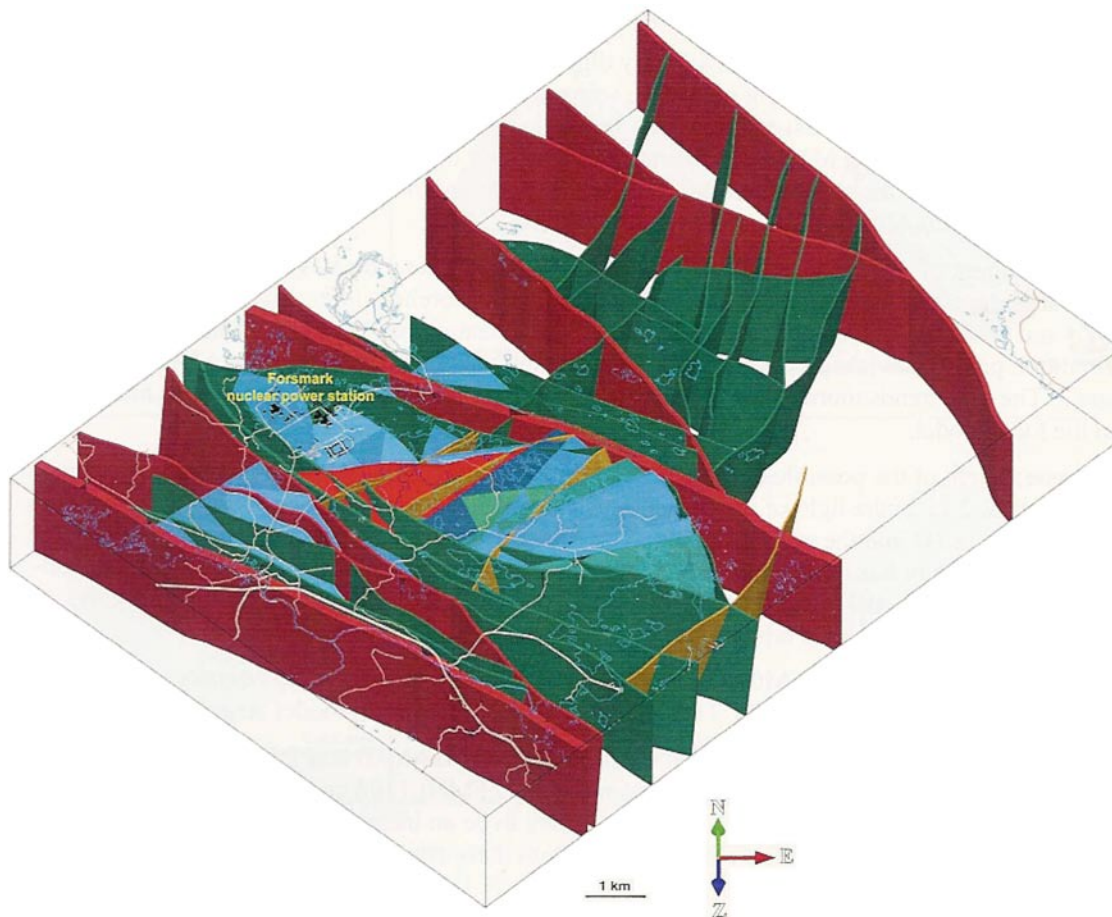
Figure 2-4. *Three dimensional model of all deformation zones at the regional scale (compare with Figure 2-3). Zones marked in red have a trace length at the surface longer than 10,000 m (regional deformation zones). Zones marked in green and beige are steeply dipping zones between 3,000 and 10,000 m in length. The beige colour indicates the few zones of this size that transect the tectonic lens. The zones marked in blue and red are gently dipping; the sharp red colour marks the major gently dipping deformation zone ZFMA2. The model is viewed from the south. /Stephens et al. 2007, Figure 5-20/.*

Extracts of the 3D deterministic models for deformation zones (stage 2.2; see /Stephens et al. 2007/), both on a regional and on a local scale, are shown in Figure 2-4 and Figure 2-5, respectively. The regional model (Figure 2-4) includes all the vertical and steeply dipping zones that are longer than 3,000 m at the ground surface and all the gently dipping zones inside this model volume. By contrast, the local model includes all the vertical and steeply dipping zones longer than 1,000 m and all gently dipping zones that are present inside this more restricted model volume. An extract of the local model, which only includes the dominant vertical and steeply dipping zones, is shown in Figure 2-5. The target volume is situated in the central part of the local model volume.
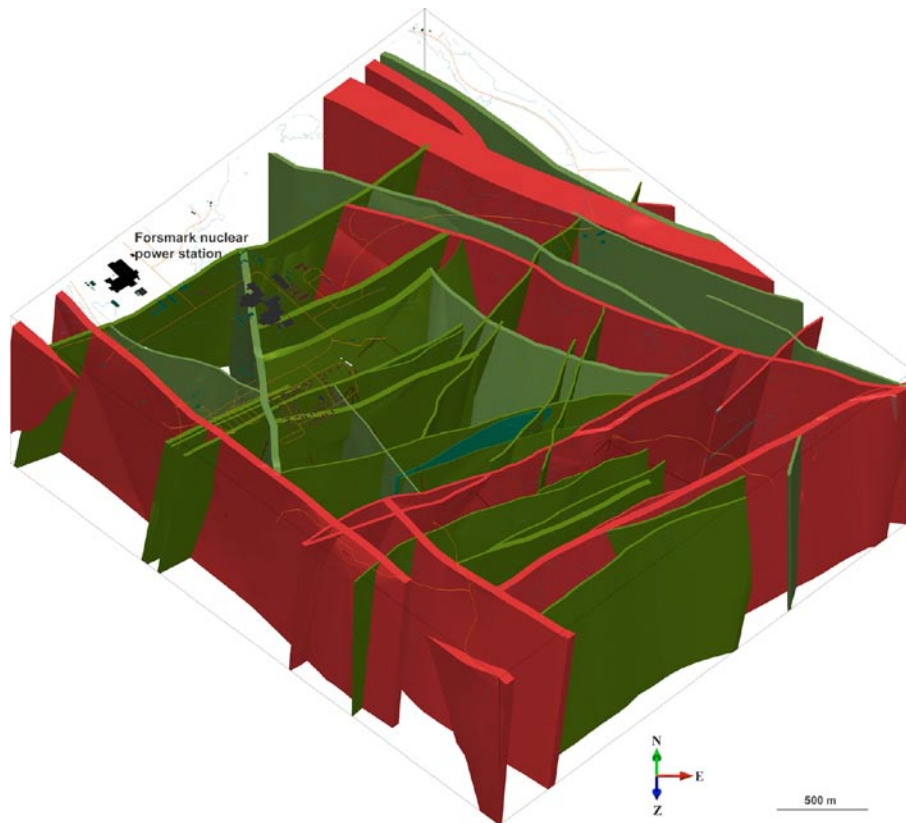
Figure 2-5. *Three dimensional model of the vertical- to steeply dipping deformation zones at the local scale. Note the concentration of vertical and steeply dipping deformation zones that trend ENE and NNE in the central part, i.e. the target volume. The model is viewed from the south. Zones marked in red have a trace length at the surface longer than 3,000 m; zones marked in green are less than 3,000 m in length. /Stephens et al. 2007, Figure 5-12/.*

2.2.3   Fracture domains

To further facilitate site description and modelling work, the bedrock in between deformation zones has been divided into several fracture domains, based on geological criteria, mainly frequency of open fractures and, in the case of one fracture domain (FFM06), character of rock type /Olofsson et al. 2007/. The extent of four of these domains within the target volume (FFM01, FFM02, FFM03 and FFM06) is shown in Figure 2-6, together with the associated rock domains and some deformation zones. Fracture domain FFM02, in the uppermost part of the target volume, is of particular interest, since it is characterised by a complex network of gently dipping and sub-horizontal, open and partly open fractures, which locally merge into fracture zones. Relative to FFM02, fracture domains FFM01 and FFM06 in the lower part of the target volume, which includes the potential repository depth, show a lower frequency of open fractures. The division into fracture domains is consistent with respect to hydrogeological criteria /Follin et al. 2007b/.

Profile 1 (drill site 6)

Profile 2 (drill sites 8 and 2)
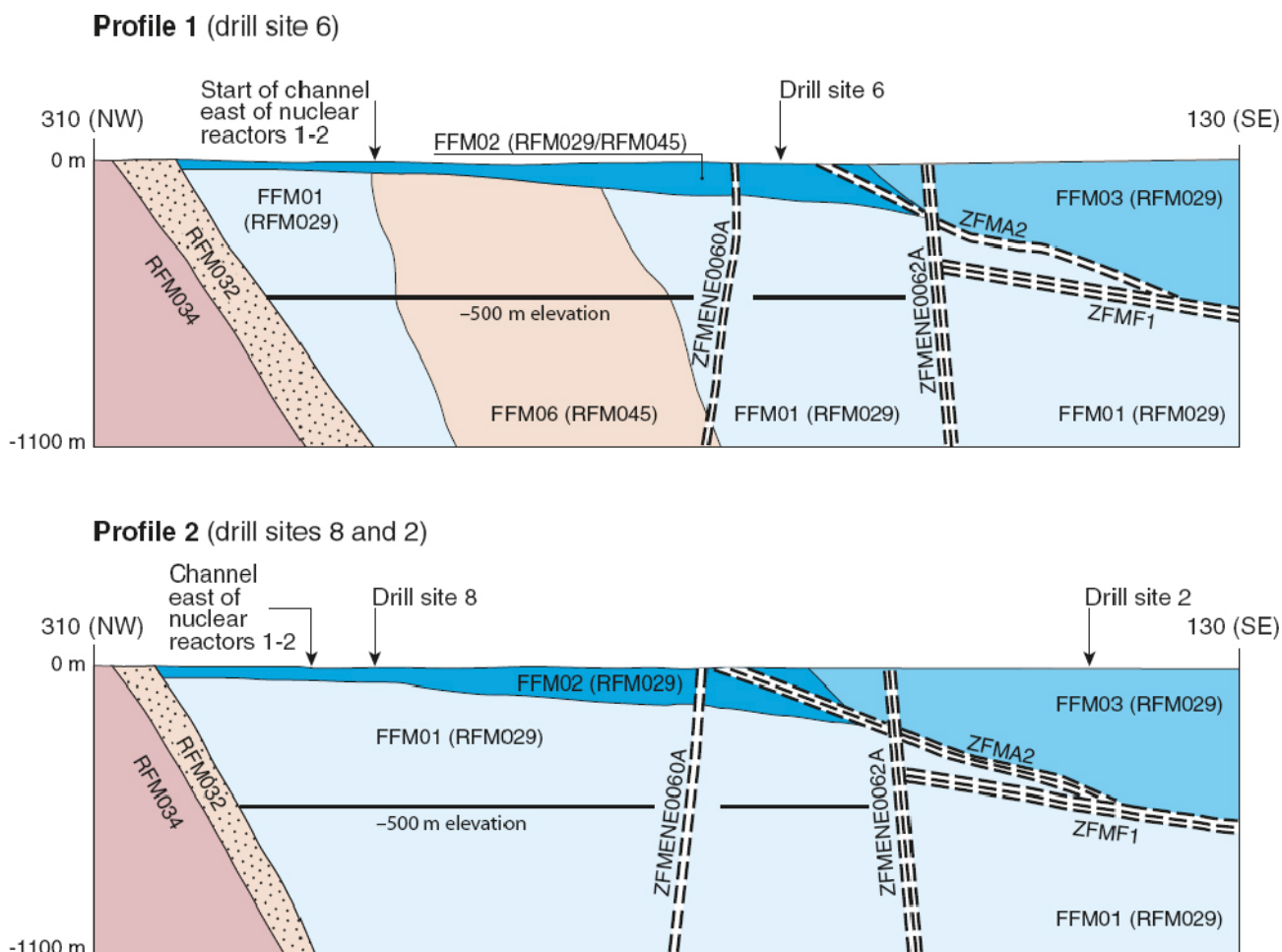
Figure 2-6. *Simplified NW-SE profiles across the target volume that intersect drill sites 2 and 8 (Profile 1) and drill site 6 (Profile 2) (cf. Figure 2-1 for location). The labelled fracture domains (FFM01, FFM02, FFM03 and FFM06) occur inside rock domains RFM029 and RFM045. Note the major gently dipping deformation zones ZFMA2 and ZFMF1, which essentially divide the candidate area into FFM03 (hanging wall) and fracture domains FFM01, 02 and 06 (footwall). The target volume is situated inside the footwall bedrock segment. Reference to average repository depth is shown by the black line at 500 m depth and 'channel' refers to an excavated link between the Baltic Sea and the nuclear power plant (not shown), /Olofsson et al. 2007, Figure 5-4/.*

Connected, open fractures have been modelled in 3D with a stochastic representation of the individual fractures using the discrete fracture network (DFN) concept /Follin et al. 2007b/. Figure 2-7 shows a NW-SE cross-section of a stochastic simulation of such features in fracture domains FFM01, FFM02 and FFM03 along the candidate volume (compare with Figure 2-6). The orientation of this cross-section is similar to that shown in Figure 2-8. The simulation indicates that these three fracture domains have significantly different intensities of connected open fractures. The intensity of such fractures is important when interpreting and discussing groundwater flow and the advective transport of different groundwater types (solutes) (cf. section 2.3 below). In particular, below 400 m depth in fracture domain FFM01, the connected open fractures are compartmentalised and the intensity of these fractures is close to the percolation threshold. As a result of the high horizontal stresses and the structural anisotropy in the bedrock, the connected open fractures in the bedrock segment structurally beneath the gently dipping zones ZFMA2 and ZFMF1, i.e. inside the target volume, are predominantly sub-horizontal or gently dipping, with second order steeply dipping sets around NE and NS. Moreover, the majority of the flowing fractures observed in the cored boreholes are sub-horizontal or dip gently (up to 80%).
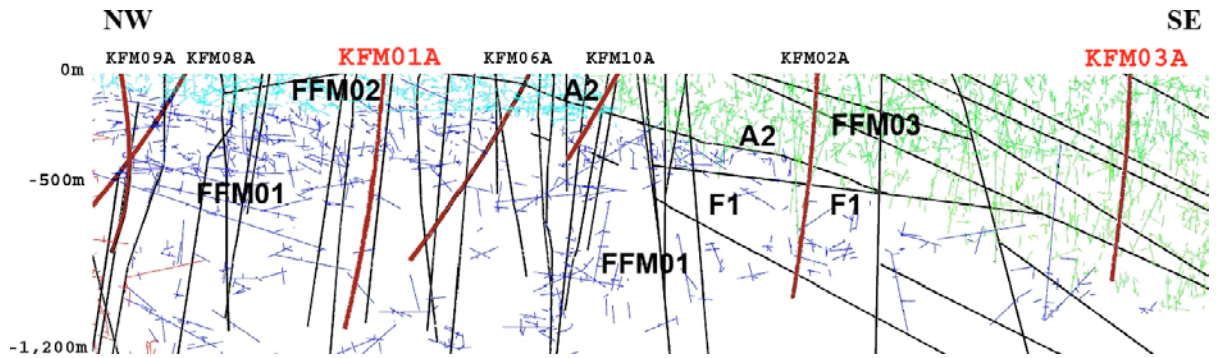
Figure 2-7. WNW-ESE cross-section through the central part of the candidate area showing an example of the DFN model realisation with connected open fractures in fracture domain FFM01 (dark blue), FFM02 (turquoise) and FFM03 (green). Note the absence of connected open fractures in KFM01A below approximately 300 m depth /Follin et al. 2008a/.
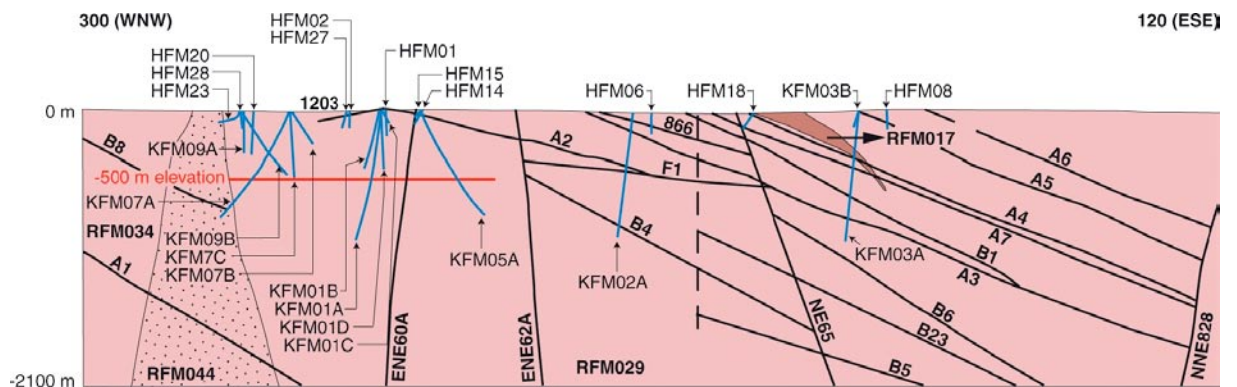
Figure 2-8. WNW-ESE 2D cross-section through the central part of the candidate area /Stephens et al. 2007, Figure 5-21a)/. The important, gently dipping deformation zones identified with reflection seismic data are highlighted in this schematic figure, in particular ZFMA2 and ZFMF1. Together with the steeply dipping zone ZFMNE0065, these zones essentially divide the candidate volume into hanging wall (to the SE) and footwall (to the NW) bedrock segments. Since this cross-section has been extracted from the regional model, rock domain 29 is referred to as RFM029R. The potential repository inside the target volume is located inside rock domain 29 in the footwall bedrock segment. See text for further description.

2.2.4 Two-dimensional cross-sections

The major geological features of the candidate volume are further detailed in two strategically selected cross-sections that integrate rock domains and deformation zones. These sections have been extracted from the regional geological models (stage 2.2) of the site /Stephens et al. 2007/. The location of the profile lines are shown in Figure 2-1:

- A WNW-ESE section (Figure 2-8) connecting boreholes KFM09A and B, KFM07A, B and C, KFM01A, B, C and D, KFM05A, KFM02A and B, KFM03A and B as well as the associated percussion boreholes.

- A WSW-ENE section (Figure 2-9) connecting boreholes KFM09A and B, KFM07A, B and C, KFM08A, B, C and D and KFM11A, as well as the associated percussion boreholes.

The geology of the WNW-ESE section through the central part of the candidate volume is dominated by medium-grained metagranite (rock domain RFM029) with minor metatonalite (rock domain RFM017). The bedrock in rock domain RFM044 consists of the same granitic rocks as in RFM029 but is affected by stronger ductile deformation, while the bedrock in rock domain RFM034 resembles that in RFM029.

29

There is a significant structural difference in the deformation zone pattern on both sides of the gently dipping deformation zones ZFMA2 and ZFMF1. These zones essentially divide the candidate volume into a hanging wall bedrock segment to the south-east and a footwall bedrock segment to the north-west (see also Figure 2-6). The hanging wall bedrock contains an increased number of gently dipping deformation zones, many of which extend down to at least 1,000 m depth (Figure 2-8). By contrast, there are very few gently dipping zones in the footwall bedrock (Figure 2-8). This difference is also steered by the older anisotropy at the site, with gently dipping ductile structures and rock contacts in the south-eastern part of the candidate volume. It is also evident in the hanging wall and more steeply dipping structures and contacts in the north-western part, in different parts of the major fold structure shown in Figure 2-2 and Figure 2-9 /Stephens et al. 2007/. In addition, it needs to be kept in mind that the bedrock in the north-western part of the candidate volume, in the footwall and hanging wall on both sides of zones ZFMA2 and ZFMF1, is intersected by a number of steeply dipping fracture zones, which strike ENE-WSW to NNE-SSW (see Figure 2-3).

The WSW-ENE 2D cross-section (Figure 2-1 and Figure 2-9) has largely been described above in the context of Figure 2-2. The cross-section represents a slice through the major SE-plunging synform. It shows how rock domain RFM029 forms the core of the major synform inside the tectonic lens and how other rock domains are situated along the limbs of this major structure. The potential repository inside the target volume is located within rock domain RFM029 in the core of the synform.

2.2.5 Concluding remarks

Most of the hydrochemical data evaluated originates from deformation zones and only a limited amount of data comes from the bedrock in the contiguous fracture domains. Moreover, some of the data in the fracture domains may have been influenced, to varying extent, by groundwater from nearby deformation zones, since sampling is possible only in fractures with groundwater flow. Such fractures need to be both transmissive and connected to these zones. Examples
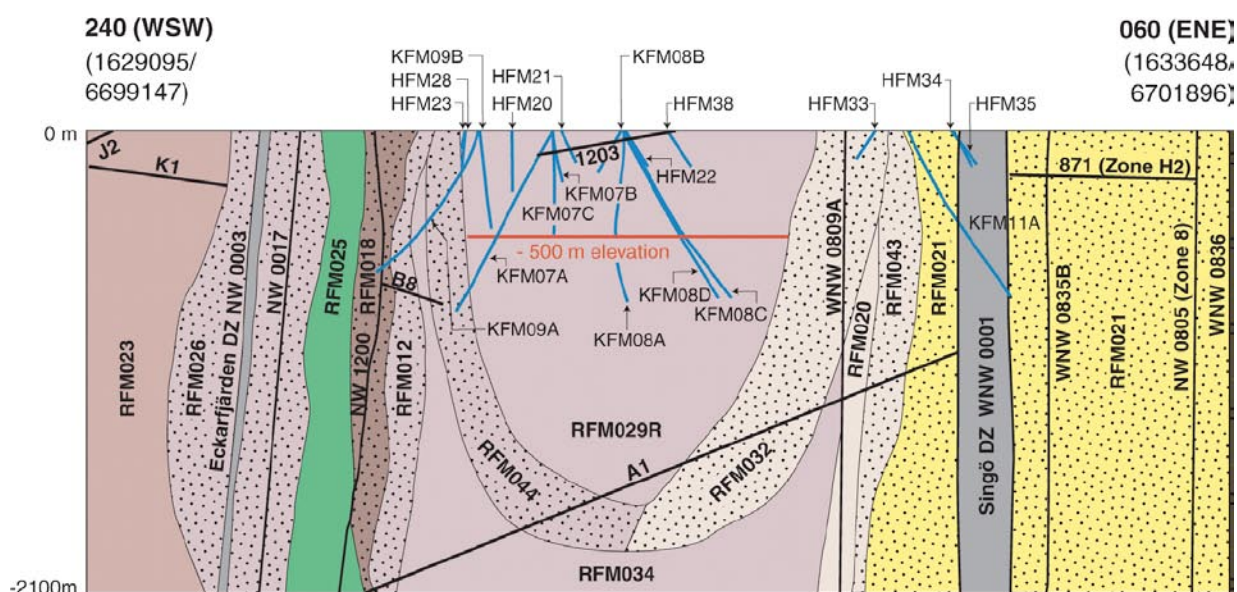
Figure 2-9. *The WSW-ENE 2D cross-section showing the main deformation zones, the borehole positions (marked in blue; some extrapolated), and the main rock domains constituting the tectonic lens and its surroundings. The estimated repository depth at 500 m is marked in red. Note that boreholes KFM08A/B/C, KFM07A/B/C and KFM09B are located within the tectonic lens, and that KFM09A, and the lower part of KFM07A and KFM11A, penetrate the periphery of the lens towards the Eckarfjärden deformation zone and Singö deformation zone, respectively. Since this cross-section has been extracted from the regional model, rock domain 29 is referred to as RFM029R /SKB 2008/.*

include the deepest groundwaters sampled from borehole KFM03A and some upper and intermediate groundwaters from borehole KFM01D. Furthermore, there is a spatial homogeneity in the fracture groundwater and matrix porewater chemistry which begins to become evident throughout the Forsmark candidate volume beneath about 600–700 m depth. As a consequence of these considerations, it has generally proven difficult to relate the hydrogeochemical data to the fracture domain concept. The only clear distinction is the hydrochemical difference between fracture domain FFM02 and the underlying FFM01 in the footwall bedrock segment (cf. section 4.1.1).

It is the hydrogeology of the water-conducting fractures within the fracture domains and the deformation zones embedded in the fracture domains which is of key importance to hydrogeochemistry. Together with the hydrogeochemistry, these water-conducting structures, in turn, will influence the distribution of the porewater chemistry in the rock matrix.

Bearing in mind the considerations above, it has proven more useful to address the hydrogeochemical data in relation to their spatial location with respect to the footwall and hanging wall bedrock segments as discussed above. The key features of the structural-mechanical properties of importance for the hydrogeochemical and hydrogeological modelling at Forsmark are as follows /Stephens et al. 2007, Follin et al. 2008a/:

• A pronounced bedrock anisotropy, established at an early stage in the geological history in the ductile regime, steered the overall occurrence and character of younger brittle structures at the site.

• The major gently dipping deformation zones ZFMA2 and ZFMF1 divide the candidate area bedrock into a footwall bedrock segment (i.e. target volume to the north-west) and a hanging wall bedrock segment to the south-east.

• The footwall bedrock is inferred to have higher rock stresses than the hanging wall and is primarily composed of fracture domain FFM01. Fracture domain FFM02 is situated closer to the surface, predominantly in the footwall bedrock, and contains a conspicuously higher frequency of open fractures relative to that observed in domain FFM01. Release of stress along sub-horizontal and gently dipping fractures characterise this domain. The fractures consist of both reactivated older fractures and newly formed sheet joints.

• The hanging wall bedrock is intersected by several gently dipping deformation zones, many of which extend to at least 1,000 m depth, or more. It is primarily composed of a single fracture domain, FFM03.

• The intensities of connected open fractures are significantly different for these three fracture domains. For instance, below 400 m in the footwall bedrock (i.e. fracture domain FFM01), the connected network of open fractures is considerably compartmentalised and close to the percolation threshold, which implies a restricted groundwater circulation at repository depth. The observed open fractures are predominantly sub-horizontal or gently dipping.

2.2.6 Fracture mineralogy input

Detailed investigations of the fracture mineralogy and altered wall rock have been carried out as part of the Forsmark site characterisation programme /Sandström et al. 2008/. This work summarises and evaluates the data obtained from the detailed fracture mineralogical studies, and also includes information derived from the extensive core mapping that has been carried out within the programme. This includes descriptions of the identified fracture minerals, their chemical composition and petrogeneses, and the sequence of fracture mineralisations in the area. Special focus has been put on the chemical and stable isotopic composition of calcite to obtain palaeohydrogeological information. Chemical analyses of bulk fracture filling material have been used to identify possible sinks for certain elements and also to identify minor mineral phases which can be overlooked by X-ray diffraction (XRD).

General characteristics

The relative abundance of the different fracture minerals have been evaluated based on core mapping (Boremap) data combined with supporting analyses to identify minerals difficult to determine macroscopically. The most common fracture minerals are chlorite/corrensite and calcite. Other minerals frequently found are laumontite, quartz, adularia, albite, prehnite, epidote, hematite and pyrite. Minerals found as minor occurrences include asphaltite, analcime and goethite.

Clay minerals have been identified using XRD analyses and the most common varieties are corrensite > illite > mixed layer clays > smectite > kaolinite, vermiculite and other swelling clays. No other carbonates than calcite have been identified and the only sulphate mineral identified is barite which is very rare (e.g. inclusions in galena); gypsum has not been identified in any of the fractures studies. Pyrite makes up more than 99% of the identified sulphides, together with small amounts of galena, chalcopyrite and sphalerite.

Potential differences in fracture mineralogy between the different fracture domains have been studied and it can be concluded that:

- With the exception of asphaltite and goethite, which almost exclusively are found in open fractures within the footwall (i.e. fracture domain FFM02) and probably in the upper part of the hanging wall (in fracture domain FFM03), the same fracture mineralogy is found in fracture domains FFM01, FFM02, FFM03 and FFM06, although the proportion of the different minerals may vary.

- Clay minerals also occur most abundantly in open fractures in the upper part of the footwall (fracture domain FFM02) but are found in all other fracture domains within the target volume as well.

As mentioned above, asphaltite and goethite are found in the upper part of the bedrock whereas other minerals (e.g. chlorite) show little or no variation with depth. Clay minerals (Figure 2-10) are found more abundantly in fractures in the upper part of the bedrock but are also found at greater depths. The calcite ± quartz ± pyrite assemblage (i.e. generation 3; see below) is most common in the upper 350 m of the bedrock, but in the near-surface environment there is no evidence that calcite and pyrite have decreased in frequency due to surface related oxidation or dissolution of calcite. The presence of goethite in hydraulically conductive zones, however, suggests an input of oxidising waters associated mainly with subhorizontal zones during some occasions in the past.
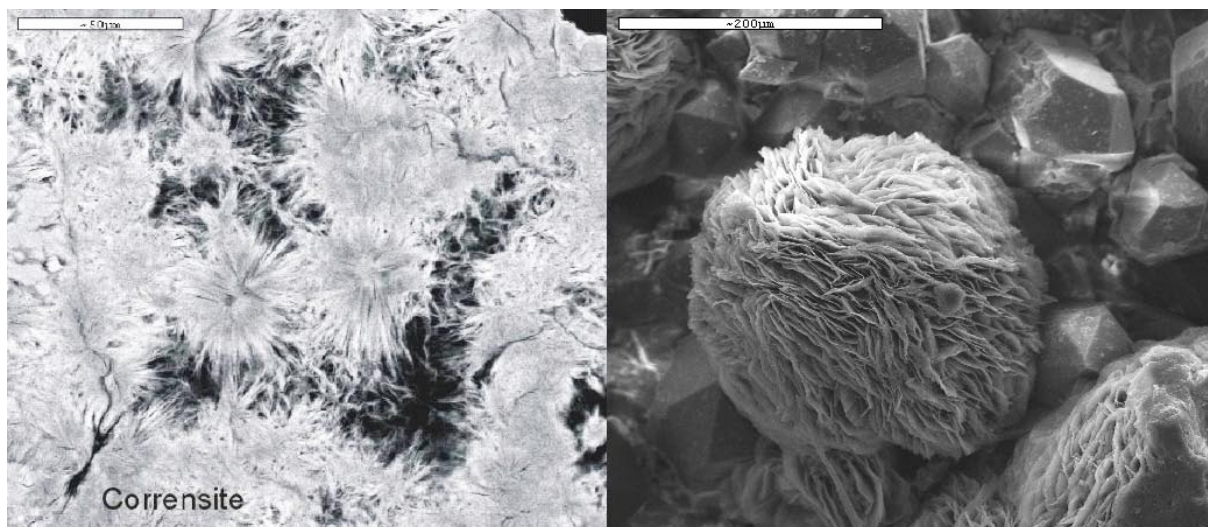
Figure 2-10. Backscattered electron images of corrensite. The left image is from a thin section from KFM05A 428.00–428.13 m, scale bar is 50 μm. The right image is from KFM05A 938.00–938.18 m, scale bar is 200 μm /Sandström et al. 2008/.

The dominating fracture assemblages in the hydraulically conductive fractures are chlorite + calcite ± others and calcite ± quartz ± pyrite (i.e. typical assemblage of the Palaeozoic Generation 3 fractures) /Sandström et al. 2008/.

Sequence of fracture mineralisation events

Four different generations of fracture mineralisation have been distinguished with high confidence /Sandström et al. 2006a, 2008/.

Generation 1 (Pre-Sveconorwegian)

Generation 1 is dominated by epidote, quartz and Fe-rich chlorite precipitated under hydrothermal conditions at temperatures higher than 150–250°C. These minerals are also found as sealing phases in brittle-ductile cataclasites. Generation 1 minerals are most conspicuous in subhorizontal and gently dipping fractures or in steeply dipping WNW-ESE to NW-SE fractures.

Generation 2 (Sveconorwegian)

Generation 2 consists of a sequence of fracture minerals precipitated during hydrothermal conditions at temperatures approximately 150–280°C, and comprising mainly adularia, albite, prehnite, laumontite, calcite, chlorite and hematite. Generation 2 minerals are particularly common along steep ENE-WSW to NNE-SSW and NNW-SSE fractures. $^{40}Ar/^{39}Ar$ ages from adularia indicate a major influence of early Sveconorwegian tectonothermal activity at 1.1 to 1.0 Ga which either affected or resulted in the development of fractures coated or filled by generation 2 minerals. Both reactivation of older fractures and formation of new fractures are inferred during this event. Dissolution of fracture minerals occurred prior to the formation of generation 3 minerals.

Generation 3 (Palaeozoic)

Generation 3 consists of minerals precipitated under low temperature conditions during the Palaeozoic. The most abundant minerals are calcite, quartz, pyrite, corrensite and asphaltite. The brine-type formation fluid was influenced by organic material that may have emanated from an overlying organic-rich sedimentary cover. The formation temperature was around 60–100°C, although higher temperatures (160–190°C) may have been reached locally in the fracture system. Generation 3 minerals are found in many types of fractures characterised by generation 1 and 2 minerals indicating extensive reactivation, but also formation of new fractures is inferred. Precipitation of generation 3 minerals has been demonstrated during the Late Palaeozoic (Permian), but fracture mineral formation probably occurred at several periods during the Palaeozoic

Generation 4 (Late Palaeozoic-Present)

Generation 4 is dominated by chlorite/clay minerals and thin precipitates of calcite, but also minor amounts of goethite and pyrite mainly associated with hydraulically conductive fractures and fracture zones. Precipitation of these minerals may have occurred over a long period of time (since the Late Palaeozoic?), and during different events and at different times. Most generation 4 minerals occur in sub-horizontal to gently dipping fractures but also in steeply dipping WNW-ESE to NW-SE, ENE-WSW to NNE-SSW and NNW-SSE fractures, i.e. in all the different sets of fractures. Most of the fractures with generation 4 minerals are ancient structures (Proterozoic-Palaeozoic in age). Fractures without any visible mineral filling are also interpreted to belong to generation 4 and are possibly young in origin. The majority of these structures are sub-horizontal or gently dipping, and most are present in the uppermost part of the bedrock and at greater depth along the gently dipping deformation zones /Stephens et al. 2007, Sandström et al. 2008/.

Wall rock alteration

Fractures sealed with generation 1 and 2 minerals are associated with red staining of the wall rock due to hematite dissemination (Figure 2-11). This alteration shows strong spatial association with deformation zones /Stephens et al. 2007/, but is also common adjacent to single fractures within the fracture domains. The character and properties of this altered (red-stained/partly oxidised) rock that occurs adjacent to generation 1 and 2 have been described by /Sandström and Tullborg 2006/. A summary of the main features associated with the altered red-stained rock is given in /Sandström et al. 2008/.

The major mineralogical changes in the altered rock are an almost complete saussuritisation of plagioclase chloritisation of biotite and to some extent hematisation of magnetite. The plagioclase of oligoclase composition has been replaced by a mineral assemblage consisting of albite, adularia, sericite, epidote, hematite and calcite. The red staining of the rock is due to the dissemination of sub-microscopic hematite grains within and along the grain boundaries of the saussuritised plagioclase.

This hydrothermal staining normally extends a few centimetres perpendicularly out from the fractures, although more extensive zones also exist, often associated with penetrative, interconnected networks of thin fractures. The alteration (especially the chloritisation), however, extends farther into the rock than the red staining suggests, and the amount of rock mapped as "oxidised" should therefore be seen as a minimum value.

The changes in geochemical composition between fresh and altered rock are relatively small. The major changes include an increase in Na and LOI (Lost On Ignition i.e. loss of lattice bounded water, and to lesser extent carbonate and sulphate/sulphide) whereas Ca, Fe and Si decrease in the altered rock.

An increase in the connected porosity in the altered rock can be seen, most likely due to the chloritisation of biotite and an increase in the number of microfractures.

A small increase in the degree of oxidation can be seen in the altered rock but this change is not as evident as may be suggested by the red staining of the rock. The measured mean total oxidation factor (Fe^{3+}/Fe_{total}) increases from 0.20 in fresh rock to 0.28 in altered rock, indicating that most Fe is still in the Fe^{2+} oxidation state even in the altered rock.
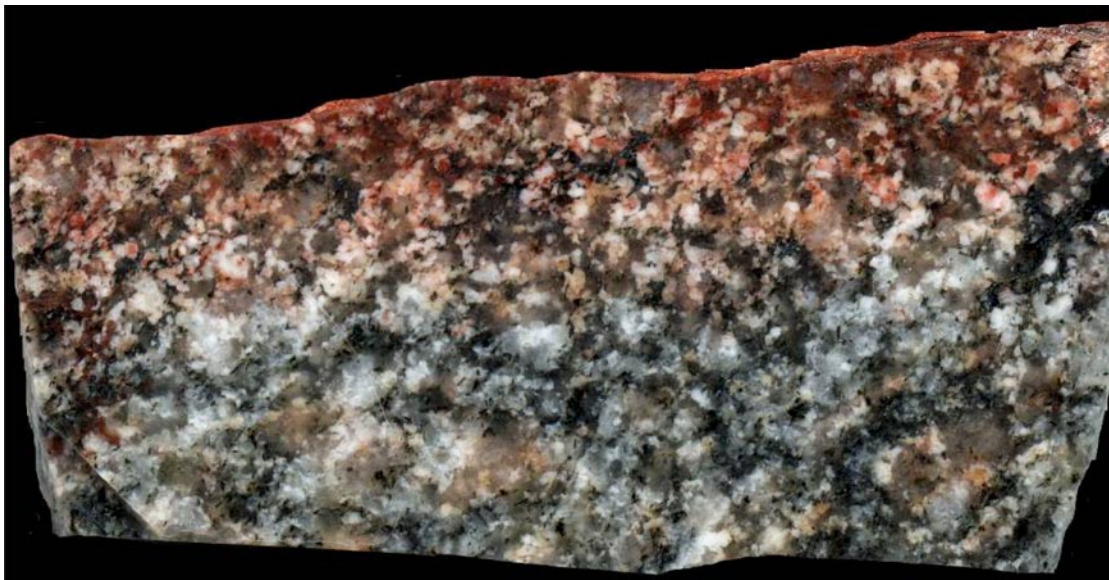
Figure 2-11. *Red stained hydrothermally altered rock adjacent to a laumontite sealed fracture. The red staining can be seen to gradually disappear about 1.5 cm out from the fracture. Sample KFM09A 145.84 m. The base of the picture is about 4.5 cm /Sandström and Tullborg 2006/.*

2.3 Hydrogeology model input

The input from hydrogeological modelling is important not only for understanding the interplay between surface water, near-surface groundwater and deep groundwater, but also provides greater understanding of the palaeohydrogeochemical evolution of the site. For example, input from the hydrogeology model can be in the form of conceptual model support and testing, and descriptions of flow directions and flow properties. Furthermore, it is important to bear in mind that the anisotropy in the structural geological model /Stephens et al. 2007/ effectively governs the pathways for flow at all depths.

2.3.1 Surface to near-surface features

The Forsmark candidate area is characterised by low relief with small-scale topography and is almost entirely located below 20 m.a.s.l. (for example /Bosson et al. 2008/). The Quaternary till deposits that characterise the surface are less than 20 m thick and cover around 90% of the ground surface; rock outcrops are common. All known regolith in the Forsmark area, as with the rest of north-eastern Uppland, has been deposited during, or after, the Weichselian glaciation (i.e. during the last 115,000 years /Söderbäck (ed.) 2008/). The oldest deposits are of glacial origin and are deposited directly from the Weichselian ice sheet or by water from the melting ice. The deposits typically are poorly developed comprising young and unweathered soils with a high content of calcium carbonate in the gravel and fine fractions, and the occurrence of till with a high clay content. Hydraulic conductivities vary within these deposits with the upper soil profile (to around 0.6 m) characterised by high values ($1.5 \cdot 10^{-5}$ m/s), the deeper coarse tills at lower values ($1.5 \cdot 10^{-6}$ m/s), and the underlying fine-grained till at even lower values ($1.5 \cdot 10^{-7}$ m/s).

The annual precipitation and runoff are 560 mm and 150 mm, respectively. Groundwater levels in these Quaternary deposits are very shallow and, on average, less than 0.7 m below ground surface during 50% of the year. With abundant recharge, the groundwater levels quickly rise resulting in lateral flow and surface water discharge; thus the region consists of small catchment areas characterised by localised shallow groundwater flow systems. Wetlands are frequent and cover between 25 and 35% of some of the delineated sub-catchments. The main lakes, i.e. Fiskarfjärden, Bolundsfjärden, Eckarfjärden and Gällsboträsket, are shallow with mean and maximum depths ranging from approximately 0.1 to 1 m and 0.4 to 2 m, respectively. Sea water flows into the most low-lying lakes during events of very high sea water levels.

2.3.2 Near-surface to bedrock interface

From a hydrochemical viewpoint the recharging waters entering the bedrock from the Quaternary deposits defines the important (altered) meteoric end member for the bedrock groundwater evaluation. For most of the target area there is a close correlation between the topography and the groundwater levels in the Quaternary deposits, which is not the case for the upper bedrock environment. For example, high transmissivity is indicated in the upper bedrock structures by low groundwater level gradients which contrast with groundwater levels in the till, which are in general considerably higher than in the bedrock. Hence, local, small-scale recharge (downward flow) and discharge (upward flow) areas, involving groundwater flow systems restricted to the Quaternary deposits, will overlie the more large-scale flow systems associated with groundwater flow in the bedrock. Also, in the middle of Lake Bolundsfjärden, located in the central part of the candidate area, the lake level and the groundwater level in the till are considerably higher than the groundwater levels in bedrock down to 200 m depth, indicating a downward flow gradient from the lake and Quaternary deposits to the bedrock /Follin et al. 2007a, Söderbäck (ed.) 2008/.

The flow systems around and below the lakes are quite complex. The lake water/groundwater level relationship, under natural as well as disturbed conditions, indicates that the lake sediments and the underlying till have low vertical hydraulic conductivities. This means that groundwaters below the lakes have relict marine chemical signatures, whereas groundwaters in the surface riparian zones are fresh.

The transition from near-surface to upper bedrock, referred to as the shallow bedrock aquifer, is illustrated in /Follin et al. 2007a/ and reproduced in Figure 2-12. This shallow bedrock aquifer comprises the horizontal/subhorizontal sheet joints shown in the figure. This part of the upper bedrock (0–150 m) is considered to be hydraulically anisotropic due to a lattice of intersecting near-surface joints and gently dipping single fractures. The groundwater flow field is considered horizontally anisotropic and flow rates are high. When the meteoric recharge waters enter the subhorizontal fractures they mix with existing groundwaters in the fractures and are rapidly transported laterally to be discharged towards the Baltic Sea to the north-east of the candidate area. Figure 2-13 shows the lateral extent of the shallow bedrock aquifer which underlines its importance to the target volume.

This shallow bedrock aquifer therefore limits direct meteoric recharge to deeper bedrock levels. Nevertheless, some deeper recharge of meteoric water is likely to occur where outcropping, steeply dipping deformation zones coincide with higher surface elevations south-west of the candidate area /Follin et al. 2007a/.

2.3.3 Bedrock features and fracture domains

The geological subdivision of the bedrock at Forsmark into fracture domains is also consistent with the hydrogeology /Follin et al. 2007b/. Early on in the site investigations, hydrogeological studies had indicated the possible subdivision of the bedrock present between the deformation zones (i.e. excluding the deformation zones) into four sub volumes based on the fracture intensity of flowing fractures, and this concept was tested subsequently by applying the geological criteria already mentioned in section 2.2. This showed that the six fracture domain subdivisions (FFM01-06) are largely in agreement with the earlier four hydrogeological sub-volumes in that the hydrogeological properties of fracture domain FFM01 are similar to domain FFM06 and those of fracture domain FFM03 are similar to domains FFM04 and FFM05, and therefore consistent with the definition of fracture domains based on geological data.
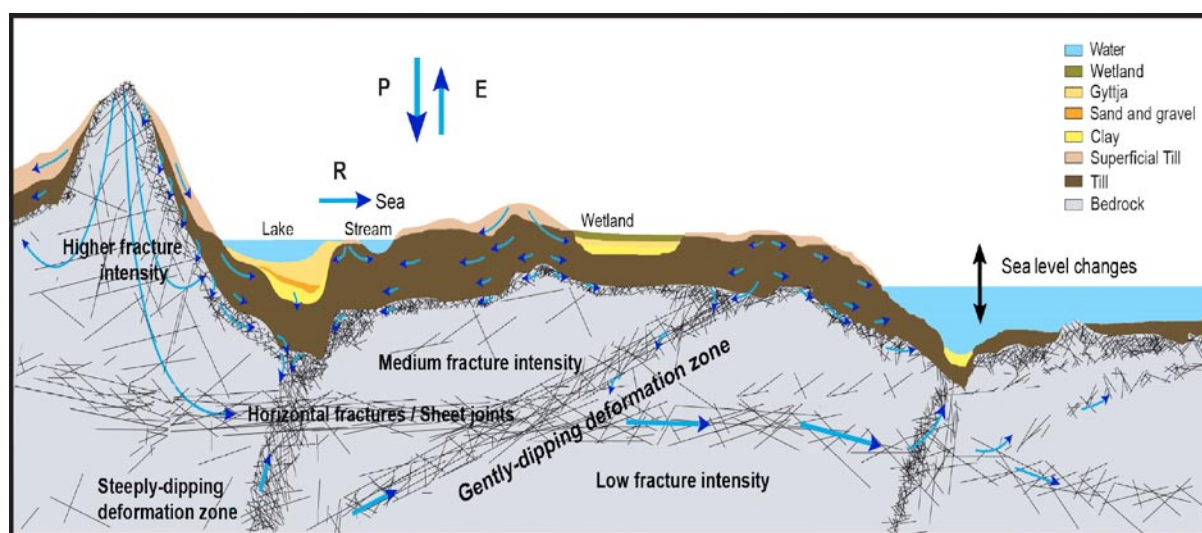
Figure 2-12. *East to west cross-section of the Forsmark target area illustrating the sequence and groundwater flow properties from surface Quaternary regolith sediments to the approximately upper 150 m of the bedrock which represents the shallow bedrock aquifer. P = precipitation, E = evapotranspiration, R = runoff. The lattice of horizontal fractures/sheet joints, outcropping deformation zones and single fractures in between the deformation zones is probably heterogeneous but in many places it is highly transmissive. The lattice is found to short circuit the recharge from above as well as the discharge from below. That is, the groundwater levels in the Quaternary deposits and at depth are both higher than in the near-surface bedrock. /Follin et al. 2007a/.*
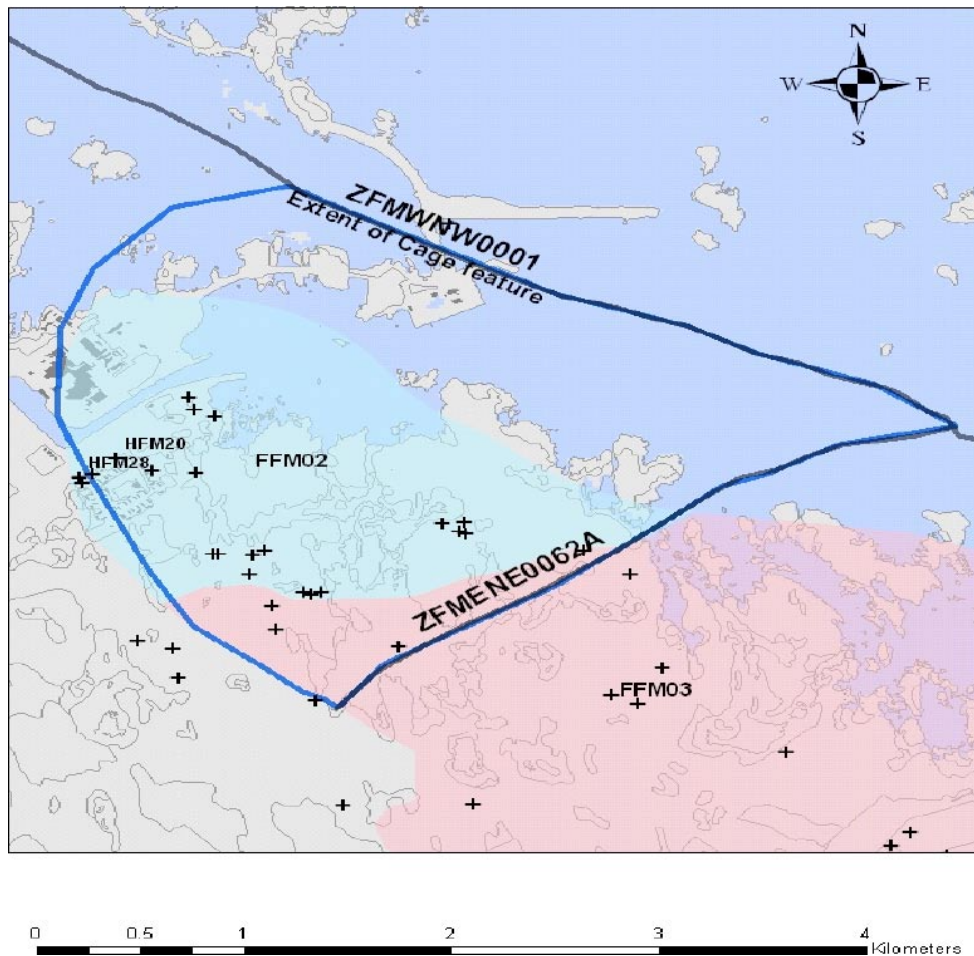
Figure 2-13. *The estimated lateral extent of the shallow bedrock aquifer (referred to in the figure as the now obsolete 'cage feature') covering the target area /Follin et al. 2007a/.*

Fracture domain FFM01, which comprises the major volume of the footwall, thus dominates the target volume (Figure 2-8 and Figure 2-9). It differs from fracture domain FFM02 in that at increased depths there is an overall lower intensity of open, flowing fractures and lower fracture transmissivity. These flowing fractures mostly consist of discrete, subhorizontal to gently dipping single fractures of fairly large extent /Follin et al. 2007a/.

Fracture domain FFM03 (Figure 2-8), effectively comprising the hanging wall, shows approximately the same low fracture frequency as fracture domain FFM01 but contains a significant number of highly transmissive, gently dipping deformation zones. The transmissivity of these zones is high in the upper 400 m and significantly lower below approximately 500 m, i.e. there is a significant depth trend in the transmissivity data gathered. Flow directions within the candidate area are primarily subhorizontal along the fracture planes towards the north-east with a weak upward component /Follin et al. 2007a, 2008b/.

The local, major steeply dipping deformation zones such as ZFMENE0060A in Figure 2-8 are also subjected to a significant depth trend in transmissivity. However, these zones are also found to be considerably more heterogeneous with both open and sealed flow channels, the former with measurable flow. The vast majority of these steeply dipping zones are parallel with the topographic gradient and transect the candidate area. However, it is difficult to generalise the flow pattern due to the shallow bedrock aquifer and the considerable heterogeneity of the zones that comprise it. Particle tracking simulations suggest that the flow gradient is predominantly upwards until the shallow bedrock aquifer is reached in the uppermost part of the bedrock /Follin et al. 2007a, 2008b/.

37

Fracture domain FFM06 is located in rock domain RFM045 within the target volume (Figure 2-8). It lies beneath fracture domain FFM02 and is closely similar to fracture domain FFM01 hydrogeologically. Geologically, it differs from fracture domain FFM01 by the wide-spread occurrence of fine-grained and altered (albitised) granitic rock with a higher quartz content /Stephens et al. 2007/.

2.3.4   Present conditions

Regional scale conceptualisation

Figure 2-14 shows the main regional hydrogeological features of the candidate area and sur-roundings. The major regional steeply dipping Forsmark (FDZ), Eckarfjärden (EDZ) and Singö (SDZ) deformation zones, which border the candidate area, run perpendicular to the regional groundwater flow direction which is to the northeast. The steeply dipping deformation zone ENE0060 (referred to as ZFMENE0060A in the previous section) therefore runs parallel to the regional groundwater flow direction. In the local scale ZFMA2 zone, which is gently dipping to the south-east, the groundwater flow is also dominantly to the northeast /Follin et al. 2008, R-08-95/.

Although not as well investigated as those structures within the candidate area, the major regional Forsmark, Eckarfjärden and Singö steeply dipping deformation zones are considered to be less important hydraulically than ZFMA2. They probably function as important recharge/discharge features both past and present; past evidence of probable discharge from the last deglaciation can be observed in borehole KFM12A (cf. section 2.4) where brackish glacial type groundwaters have been collected from quite shallow depths (around 300 m) within the Forsmark deformation zone.
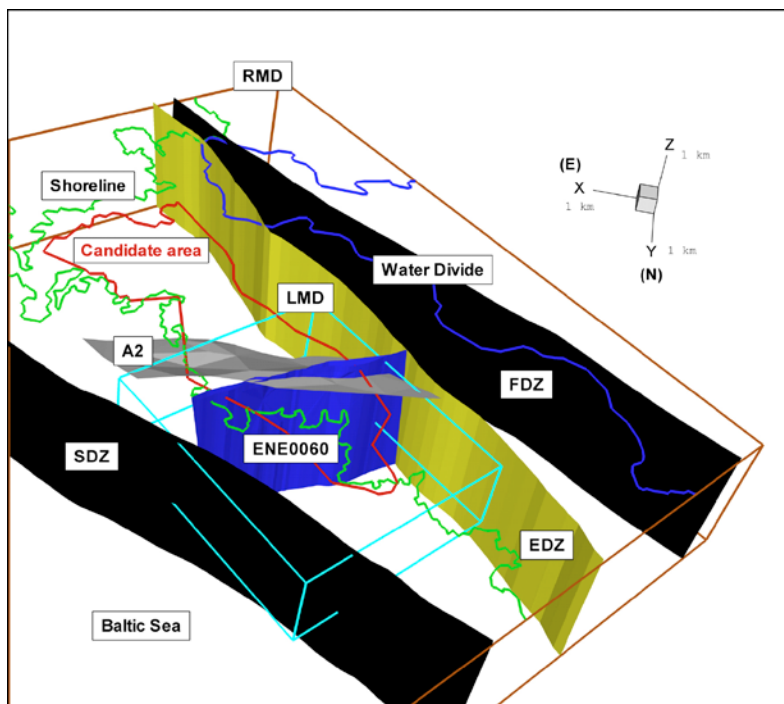
Figure 2-14. *The figure illustrates the primary hydrogeological characteristics of the Forsmark area. Shown are the candidate area, the regionally significant deformation zones of Forsmark (FDZ), Eckarfjärden (EDZ) and Singö (SDZ) which border the candidate area, and the local major deformation zones A2 and ENE0060. The solid blue line indicates the nearest regional topographical water divide. (LMD = the local model domain; RMD = the south-western part of the regional model domain). /Follin 2008, R-08-95 et al. 2007b/.*

Site scale conceptualisation

The integrated conceptual model of present-day hydraulic conditions and preliminary hydro-chemical data (stage 2.2) along a similar NW-SE profile as used in Figure 2-8 (Profile 2) is presented in Figure 2-15 /Follin et al. 2007a/. This figure conveniently summarises the interrelationship between the major gently dipping deformation zone ZFMA2 and the series of similarly gently dipping deformation zones of high transmissivity which are embedded in fracture domain FFM03 (i.e. the hanging wall). This contrasts with fracture domains FFM01 and FFM02 (i.e. the footwall) where such large-scale zones are absent, instead characterised by intensively fractured superficial bedrock (i.e. fracture domain FFM02) and very sparsely fractured bedrock below (i.e. fracture domain FFM01); see also Figure 2-9. The former hosts the horizontal sheet joints of high transmissivity (i.e. the shallow bedrock aquifer described in section 2.3.2) and the latter reflects a sharp decrease in transmissivity, which continues with increasing depth. As a consequence, the present-day groundwater composition varies within the bedrock depending on the geological structures and their hydraulic properties.

Figure 2-15 also shows the major groundwater types of the area, each reflecting different palaeohydrogeochemical events since the last deglaciation. Their depth relationships can be compared in the hanging wall (FFM03) and in the footwall (FFM01 and FFM02). The most striking difference is the major presence and depth of penetration of Littorina Sea water (maximum salinity lasted between 4500 and 3000 BC) in the hanging wall (to around 600 m) compared to the footwall (to around 300 m), which reflects mainly the difference in scale and transmissivity of the respective water-conducting fracture systems. In addition, the shallow bedrock aquifer in the upper part of the footwall wall has acted both as a hinder to the penetration of the Littorina Sea water and also has facilitated its flushing out following land uplift. Below respectively around 300 m and around 600 m depth, fracture transmissivities are low in both the hanging wall and footwall bedrock and the groundwater types and their mixtures are generally similar.
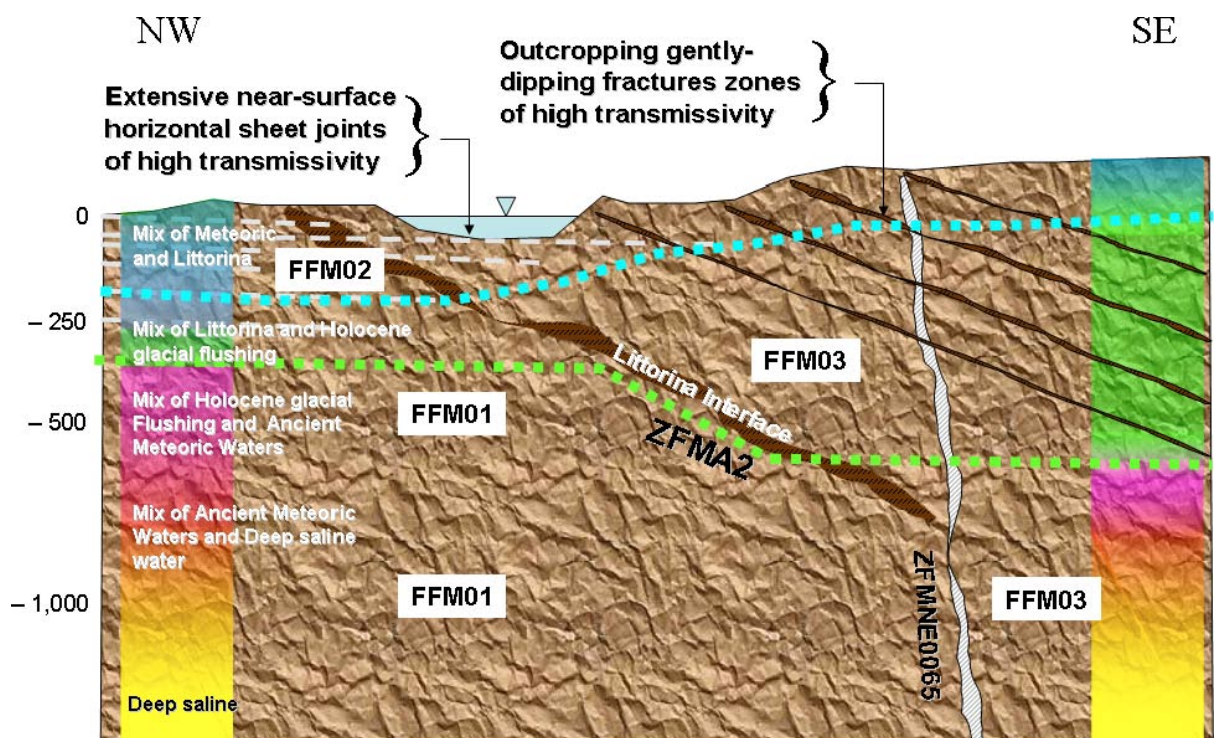
Figure 2-15. Conceptual model for Forsmark illustrating present hydraulic conditions and distribution of the different groundwater types (based on Figure 2-8 cross-section). Fracture domain FFM03 = hanging wall, and fracture domains FFM01 and 02 = footwall. /from Follin et al. 2007a/.

Based on /Follin et al. 2007a/ the local scale conceptual model was summarised as follows:

1. Glacial meltwater penetrated into the bedrock due to high water pressures below the retreating ice cap; the salinity of the glacial meltwater was assumed to be close to that of fresh water. At great depths in the bedrock the hydrogeochemical conditions are assumed to be unaffected. For modelling purposes, the salinity of the deep groundwater was set to approximately 10% TDS by weight at 2,100 m depth ('brine type' groundwater conditions). Data to support this assumption are based on groundwater samples from the approximately 1,660 m deep borehole KLX02 in Laxemar /SKB 2006cd/.

2. A density intrusion occurred during the Littorina Sea period (ca. 7000 to 3000 BC) due to a greater salinity at the surface than in the near-surface bedrock groundwater. Probably, the penetration of Littorina Sea water varied depending on the occurrence of geological structures and their hydraulic properties. The greatest penetration occurs in the hanging wall bedrock. A maximum salinity of about 1.2% TDS by weight was assumed for the Littorina water.

3. The flushing of the relatively flat and moderately undulating topography within the Forsmark candidate area by meteoric water probably became established ca. 900 years ago (for the regional model area the process started 2,500 years ago) as a result of the ongoing shore level displacement (present-day rate is 6–7 mm/year). The shore level displacement is a function of two processes; glacial rebound and global sea level changes. The salinity of the meteoric water was assumed to be close to that of fresh water. The flushing was assumed to be short-circuited by high-transmissive horizontal fractures/sheet joints in the uppermost part of the bedrock in the footwall (i.e. the shallow bedrock aquifer), thus leaving some fractions of deep saline, glacial water and Littorina Sea water behind.

2.4 Surface and near-surface model input

Possible hydrochemical indications of deep/old groundwater in near-surface locations at Forsmark have been investigated by both ChemNet /Smellie et al. 2008, Gimeno et al. 2008, Molinero et al. 2008/ and SurfaceNet modelling teams, providing an example of interdisciplinary interaction.

The SurfaceNet modelling work is reported in /Tröjbom et al. 2007/. The main purpose was to explore whether superficial observations of water chemistry in soil pipes, streams and lakes relate to the chemical composition of the deeper bedrock groundwaters, in particular, if there was any evidence of deep groundwater discharge. This was approached using multivariate Principal Component Analysis of all available groundwater data which resulted in a series of groups (beginning with Group A) which categorised the samples in terms of decreasing likelihood of having a deep groundwater chemical signature. Based on the hydrogeological model (cf. section 2.3), active discharge would not be expected in the target volume because of the shallow bedrock aquifer. In the areas peripheral to the target volume and to the south-east of the candidate area, and close to the major deformation zones, perhaps some localised occurrences might be expected.

According to /Tröjbom et al. 2007/, the main areas of interest (see Figure 2-1 for locations) included: a) a volume in the northwestern part of the candidate area where relatively shallow levels had been influenced close to the location of boreholes KFM06 and KFM07, b) a deeper volume located in the southeastern part centred around borehole KFM03, and c) an area outside the candidate area close to the Eckarfjärden deformation zone indicated in percussion boreholes HFM11and HFM12. All three cases confirmed observations already known from the exploratory analyses work and early 3D spatial analysis documented in/Smellie et al. 2008, Gimeno et al. 2008, Molinero et al. 2008/. Points (a) and (b) were interpreted as old/deep Littorina signatures in the ChemNet analysis, which is in agreement with SurfaceNet, and in point (c) the depleted $\delta^{18}O$ signatures from boreholes HFM11 and HFM12 indicated the presence of significant glacial water (probably from the last deglaciation) close to the surface (cf. Figure 4-13). /Tröjbom et al. 2007/ maintain that the observed signatures are most probably explained by relict remnants of

older groundwaters, not yet flushed out from the Quaternary deposits, according to the conceptual model and the present hydrological flow patterns. There is no clear indication of deep groundwater discharge into the freshwater surface system according to hydrochemical measurements from streams and lakes. This is largely consistent with the ChemNet interpretation.

2.5 Evolutionary effects

Palaeohydrogeochemistry has been an important and integral part of the SKB hydrogeochemical site investigations since the early 1980s. Considerable advances have been made since then, based on a greater geological understanding of Quaternary field evidence and on improved laboratory techniques. Such techniques have led to more quantitative isotopic and major and trace element geochemical evidence of palaeo-indicators from different sources, including groundwaters, matrix porewaters and mineral coatings from water-conducting fracture zones. In addition, isotopic systematics have helped determine the residence times of key groundwater and matrix porewater types, providing a time frame to more quantitatively conceptualise the hydrochemical evolution of the Forsmark site. Furthermore, there has been the recognition of an old, dilute meteoric water of warm-climate origin present before the last deglaciation. The age of this component is unknown, but possibilities include certainly pre-Holocene (> 10,000 years ago) and maybe pre-Pleistocene (> 1.8 Ma) or even further back in time, possibly to Tertiary times.

2.5.1 Quaternary evidence

After the last deglaciation

Quaternary studies have underlined the importance of major crustal movements that have affected and continue to affect northern Europe, following the melting of the latest continental ice, the Weichselian glaciation. These show the interplay between isostatic recovery on the one hand and eustatic sea level variations on the other. The net effect of these two processes in terms of elevation is called shore level displacement /Påsse 1997/. Detailed descriptions of the development at Forsmark after the last deglaciation, including shore level displacement and the development of the Baltic, is given in /Söderbäck (ed) 2008, Follin et al. 2007a, Smellie et al. 2008/ and is summarised below.

In northern Sweden, during the Weichselian glaciation, the heavy continental ice at its maximum depressed the Scandinavian Shield by as much as 800 m below its present altitude. Shortly after this glacial maximum, a marked climatic change occurred about 18,000 years ago, and the ice started to retreat, a process that was completed after some 10,000 years. This was followed by a major standstill and, in some areas, a re-advance of the ice front during a cold period ca. 13,000–11,500 years ago. The end of this cold period at approximately 10,000 years ago marked the onset of the present interglacial, the Holocene, whereupon the ice retreated more or less continuously during the early part.

 As soon as the vertical stress decreased after the ice recession, the basement and crustal rocks started to slowly rise (isostatic land uplift). This uplift started before the final deglaciation and, importantly, is still an active process in most of Sweden where the current rate of uplift is around 6–7 mm per year.

Figure 2-16 and Table 2-1 show the aquatic evolution in the Baltic basin since the last deglaciation characterised by a series of brackish and fresh water stages, which are related to changes in sea level. This evolution has been divided into four main stages: the Baltic Ice Lake, the Yoldia Sea, the Ancylus Lake, and the Littorina Sea /Björck 1995, Fredén 2002/. The most saline period during the Holocene occurred approximately 4500 to 3000 BC, when the surface water salinity in the Littorina Sea was 10–15‰ compared with approximately 5‰ today in the Baltic Sea /Westman et al. 1999/.
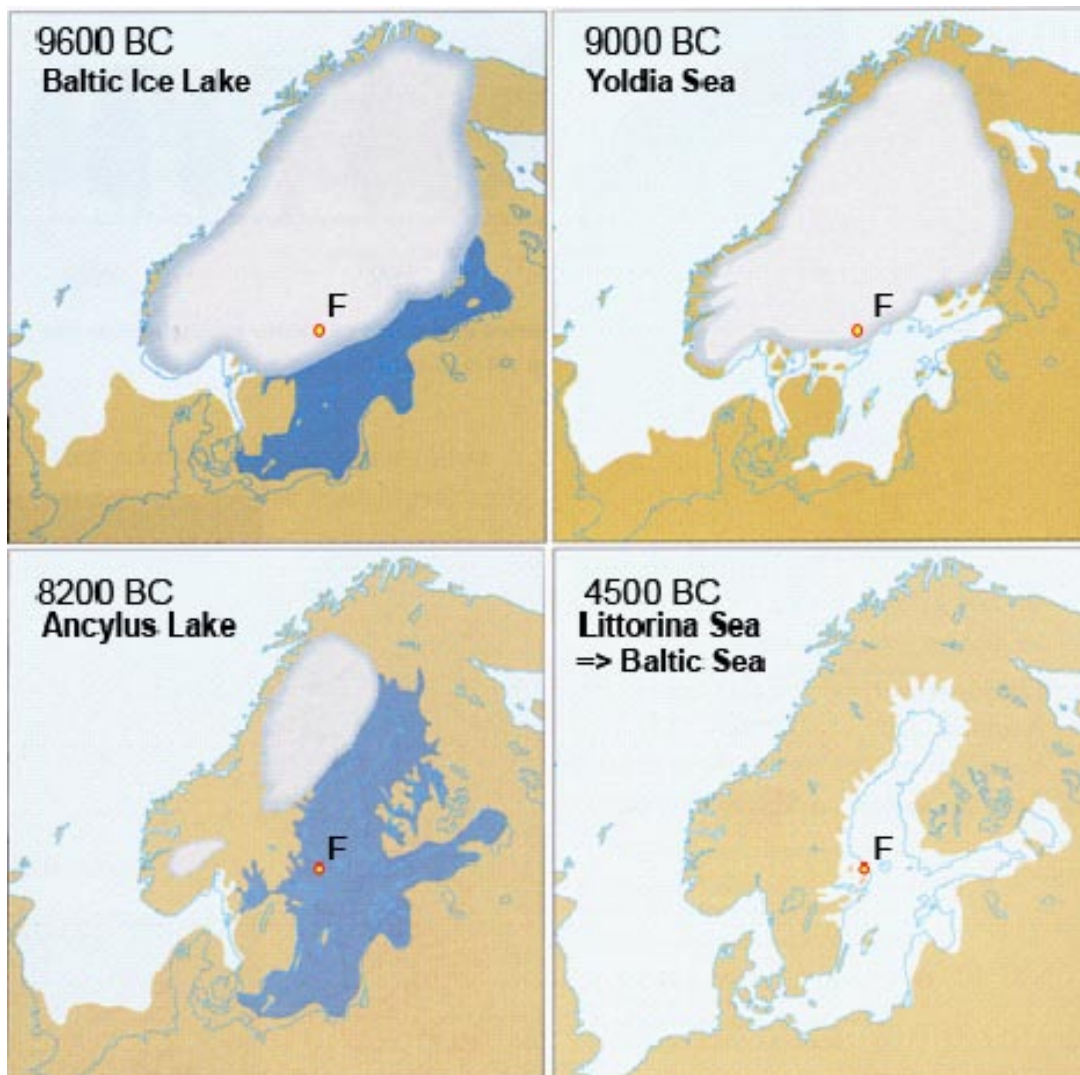
Figure 2-16. *Map of Fennoscandia with some important stages during the Holocene period. Four main stages characterise the development of the aquatic systems in the Baltic basin since the last deglaciation: the Baltic Ice Lake (13,000–9500 BC), the Yoldia Sea (9500–8800 BC), the Ancylus Lake (8800–7500 BC) and the Littorina Sea (7500 BC to present). Fresh water is symbolised with dark blue and marine/brackish water with light blue. The Forsmark area (notated 'F') was probably at or close to the rim of the retreating ice sheet during the Yoldia Sea stage (from /Follin et al. 2008a/).*

Table 2-1. Evolution of the Baltic Sea basin since the last deglaciation /Follin et al. 2008a/.

Baltic stage	Calender year BC	Salinity	Environment in Forsmark
Baltic Ice Lake (not applicable in Forsmark)	13,000– 9500	Glacio-lacustrine	Covered by inland ice.
Yoldia Sea (perhaps not applicable in Forsmark)	9500–8800	Lacustrine/Brackish /Lacustrine	At the rim of the retreating inland ice.
Ancylus Lake	8800–7500	Lacustrine	Regressive shoreline from about 140–75 m RHB 70.
Littorina Sea (→ Baltic Sea)	7500–present	Brackish	Regressive shoreline from about 75–0 m RHB 70. Most saline period 4500–3000 BC. Present-day Baltic Sea conditions have prevailed during the last ca. 2,000 years.

Permafrost

In general, but not always, glaciation is presumed to be preceded by tundra and then permafrost. Permafrost forms extensively when the mean annual temperature is colder than 2–3°C below zero, when there are dry conditions (i.e. insufficient moisture to create major glaciers), and when there is a time lapse before the ice covers the area. As indicated by present-day occurrences of permafrost in Greenland and Canada, depths of penetration can reach at least 500 m /Ruskeeniemi et al. 2004/ and take several thousand years to form. In north-east Siberia permafrost extends to 1,500 m depth and more, but this represents a very old accumulative effect incorporating input from several glaciations far back in time. No convincing evidence of remnant permafrost exists in northern Fennoscandia.

Prior to the Weichselian glacial maximum at approximately 18,000 years ago, the ice margin is thought to have been more permanently located across southern Fennoscandia some 30,000–50,000 years ago, and to have been subject to fluctuation. There is the possibility, therefore, that the Forsmark site has been subject to permafrost conditions for a long period of time until eventually overrun by the advancing continental ice sheet.

The impact of permafrost on groundwaters is largely unknown as most evidence has been removed/modified either during permafrost decay coeval with the advancement of the ice cover, and/or subsequently flushed out during deglaciation (see /Smellie et al. 2008/ for discussion). However, the possibility of preservation of such evidence in the matrix porewaters cannot be ruled out (see /Waber et al. 2008a/).
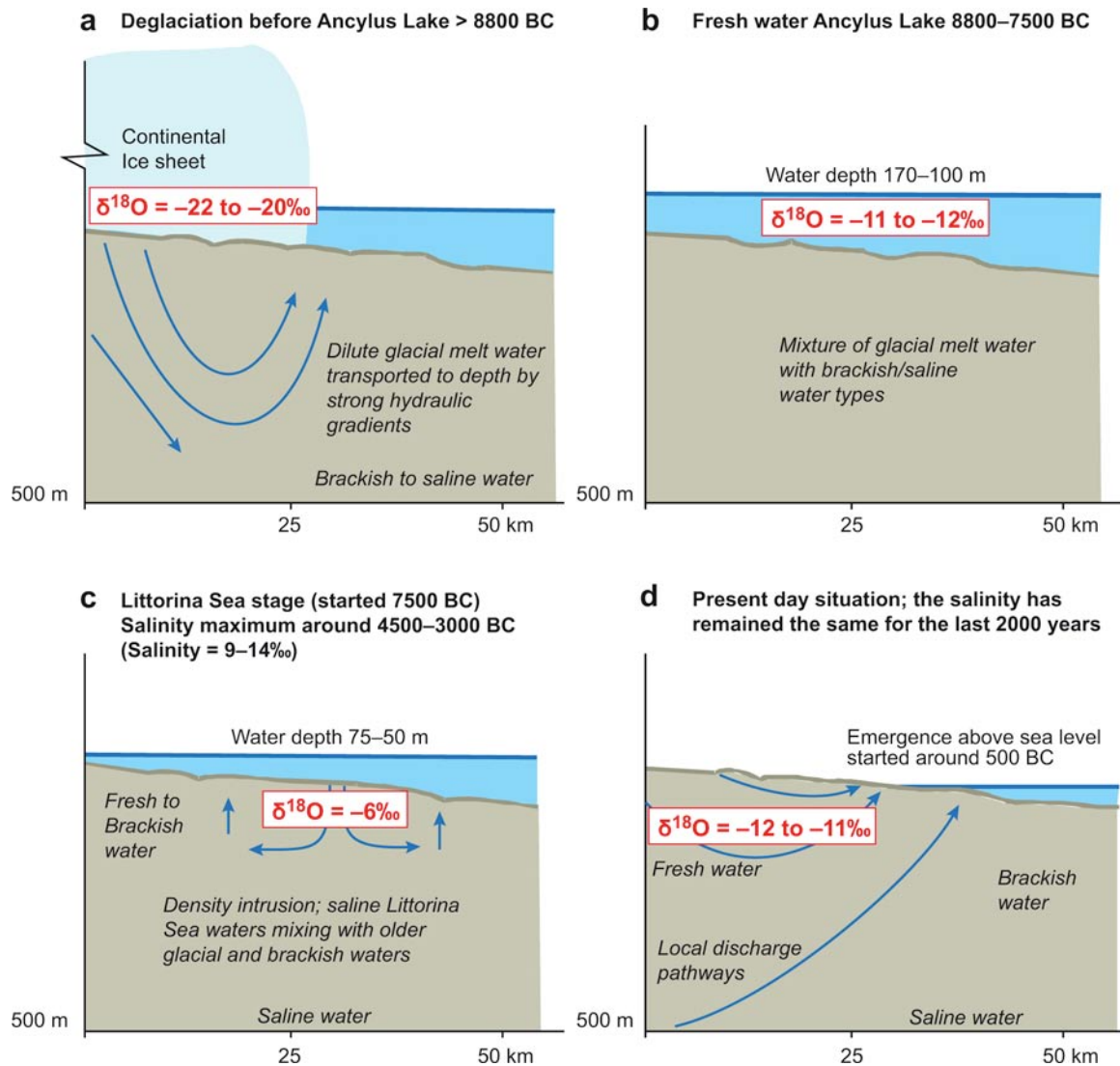
2.5.2 The scenario after the last deglaciation to the present day

During subsequent melting and retreat of the ice sheet the following sequence of events conceptualised in Figure 2-17 (compare with Figure 2-16) is thought to have influenced the Forsmark site.

When the continental ice melted and retreated (i.e. deglaciation stage approximately 18,000 BC to 8000 BC), glacial meltwater was hydraulically injected under considerable head pressure into the bedrock close to the ice margin. The exact penetration depth is still unknown, but depths exceeding several hundred metres are possible according to hydrodynamic modelling /e.g. Svensson 1996/. Any permafrost decay groundwater signatures may have been disturbed or destroyed during this stage, but also may have been preserved in some of the matrix porewaters.

Several different non-saline and brackish lake/sea stages then transgressed the Baltic Sea basin during the period ca. 9000 BC to 1500 AD. Of these, two periods with brackish water can be recognised; Yoldia Sea (9500 to 8800 BC) and Littorina Sea (from 7500 BC continuing to the present), with the Baltic Sea from 2,000 years ago to the present. The Yoldia period has probably resulted in only minor contributions to the subsurface groundwater since the water was very dilute to brackish in type from the large volumes of glacial meltwater it contained. Furthermore, this period lasted only for 700 years. The Littorina Sea period in contrast had a salinity maximum of about twice the present Baltic Sea and this maximum prevailed at least from 4,500 to 3000 BC; during the last 2,000 years the salinity has remained almost equal to the present Baltic Sea values (Westman et al. 1999 and references therein). Dense brackish sea water such as the Littorina Sea water was able to penetrate the bedrock resulting in a density intrusion which affected the groundwater in the more conductive parts of the bedrock. The density of the intruding sea water in relation to the density of the groundwater determined the final penetration depth (see section 6.2). As the Littorina Sea stage contained the most saline groundwater, it is assumed to have had the deepest penetration depth eventually mixing with preglacial groundwater mixtures already present in the bedrock.

These stages have influenced the Forsmark region apart from the Yoldia Sea transgression which was of less importance and may even be not applicable.

a Deglaciation before Ancylus Lake > 8800 BC

Continental Ice sheet

$\delta^{18}O = -22$ to $-20‰$

Dilute glacial melt water transported to depth by strong hydraulic gradients

Brackish to saline water

500 m

25   50 km

b Fresh water Ancylus Lake 8800–7500 BC

Water depth 170–100 m

$\delta^{18}O = -11$ to $-12‰$

Mixture of glacial melt water with brackish/saline water types

500 m

25   50 km

c Littorina Sea stage (started 7500 BC) Salinity maximum around 4500–3000 BC (Salinity = 9–14‰)

Water depth 75–50 m

Fresh to Brackish water

$\delta^{18}O = -6‰$

Density intrusion; saline Littorina Sea waters mixing with older glacial and brackish waters

500 m   Saline water

25   50 km

d Present day situation; the salinity has remained the same for the last 2000 years

Emergence above sea level started around 500 BC

$\delta^{18}O = -12$ to $-11‰$

Fresh water

Brackish water

Local discharge pathways

500 m   Saline water

25   50 km

Figure 2-17. The conceptual model for the Forsmark area following the last deglaciation. The different stages are: a) deglaciation before the Ancylus Lake (> 8800 BC), b) freshwater Ancylus Lake between 8800–7500 BC, c) density intrusion of Littorina sea water between 7500 BC to 0 AD, and d) the present day situation. Blue arrows indicate possible groundwater flow pattern.

When the Forsmark candidate area was sufficiently raised above sea level 1,000 to 500 years ago to initiate recharge of fresh meteoric water, this formed a lens on the surface of the saline water because of its low density. As the present topography of the Forsmark area is flat and the time elapsed since the area was raised above sea level is short, the flushing out of saline water has been limited and the freshwater lens remains at shallow depths (from the surface down to 25–100 m depending on hydraulic conditions).

Many of the natural events described above may be repeated during the lifespan of a repository (thousands to hundreds of thousands of years). As a result of the described sequence of events, brine, glacial, marine and meteoric waters are expected to be mixed in a complex manner at various levels in the bedrock, depending not only on the hydraulic character of the fracture zones and groundwater density variations, but also on anthropogenic activities including hydraulic testing and groundwater sampling.

2.5.3   The scenario from before the last deglaciation to the present day

Background

The climate changes discussed above in section 2.5 and in /Söderbäck 2008/ and /Follin et al. 2008a/ affect not only the precipitation and hence the amount of water, but also the type of water infiltrating the bedrock. The evolutionary aspects are discussed in detail in /Smellie et al. 2008/.

The infiltrating water can be glacial meltwater, precipitation, or sea water dependent of the prevailing climatic conditions. The hydraulic driving forces/or the density of these water types, together with hydrogeological properties of the bedrock, determine where and how deep the waters can penentrate. However, climatic change is a cyclic process and tends to flush out earlier water types, but the driving forces and conditions can vary and residuals of earlier climate input can be preserved. Extreme conditions, such as the maximum melting of the inland ice, the most saline sea water, or the longest wet period, provide the best possibility to leave an imprint on the bedrock groundwater. These palaeohydrogeochemical events therefore provide an important framework to understand the hydrogeochemical evolution of the bedrock groundwaters. However, to only consider scenarios occurring after the last deglaciation can be seriously misleading, especially considering hydrochemical input data to establish boundary conditions for hydrodynamic modelling of the Forsmark area. For example, analyses of porewaters and groundwaters from the relatively tight and isolated bedrock in the target volume of the candidate area show groundwater compositions not significantly influenced by either glacial meltwater (of unknown age) or brackish marine water (i.e. Littorina Sea and/or Baltic Sea origin). In other words, there is an important groundwater component from before the last deglaciation that has influenced to varying degrees the present-day hydrochemistry of the Forsmark site.

Working hypothesis

In the initial hypothesis /SKB 2005, 2006b/, the older component from before the last deglaciation was not considered and modelling was based on the post glacial scenario (see Figure 2-16 which illustrates the most important post glacial climatic phases (see also /Söderbäck (ed) 2008/). The post glacial hydrochemical conceptualisation was supported broadly by hydrogeological studies and subsequently integrated into the hydrodynamic models.

The conceptual model at that time considered four key water types that contributed to the Forsmark groundwater system and chronologically comprised: *Deep Saline Water* (oldest) > *Holocene Glacial Meltwater* > *Littorina Sea Water* (→ *Baltic Sea Water*) > *Present-day Meteoric Water* (most recent). Figure 2-16 illustrates the most important post glacial climatic phases /see also Söderbäck 2008/.

This early conceptual model was much improved during model stage 2.3, and now includes the recognition of older groundwater components from before the last deglaciation. The four key water types listed above, whilst simplified, essentially still reflect much of the present-day understanding although the following major groundwater types, in chronological order, are now recognised: *Saline Water* > *Brackish Non-marine Water* > *Last Deglaciation Meltwater* > *Brackish Marine (Littorina/Baltic) Water* > *Fresh Water* /Laaksoharju et al. 2008, Smellie et al. 2008/. (Note that Last Deglaciation refers to the period 18,000–8000 BC).

The present working hypothesis for the hydrogeochemical site conceptual model therefore recognises that Quaternary evolution has influenced the groundwater chemistry, especially in the most conductive parts of the bedrock. This is not restricted to post glacial time as there is groundwater and porewater evidence that indicates an old, warm-climate derived meteoric water component. The age of this component is basically unknown, but possibilities include certainly pre-Holocene and maybe pre-Pleistocene or even further back in time. Without recognising this older component the hydrochemistry of the Forsmark area cannot be adequately explained. The

present groundwaters, therefore, are a result of complex mixing and reactions over a long period of geological time. Mixing will be more important in those parts of the bedrock with dynamic hydrogeological properties. In other less dynamic parts, the groundwater chemistry will be more influenced by water/rock interaction processes.

Present conceptual model

Porewater analyses and groundwater samples from the relatively tight and isolated bedrock volumes in the target volume of the candidate area show groundwater compositions not significantly influenced by either glacial meltwater (of unknown age) or brackish marine water (i.e. Littorina Sea or Baltic Sea origin). These groundwaters are brackish to saline non-marine in type (4,000–10,000 mg/L Cl), are usually found from 300–700 m depth and deeper, and are significantly influenced by mixing, reactions and interaction with pore fluids in the rock matrix (diffusion processes). Furthermore, portions of these groundwaters have resided in the bedrock for very long periods of time (at least around 1,5 Ma as indicated by ^{36}Cl dating techniques and supported by helium systematics), for example, long enough to change the δ^{18}O and δ^{2}H ratios causing small positive deviations from the Global Meteoric Water Line. At greater depths (> 1,500 m), highly saline groundwater of brine character of unknown age and origin can be expected to show some similarities to that sampled at the Laxemar subarea and supported by surface geophysical measurements /Thunehed and Pitkänen 2007/. However, available chloride and bromide ratios, as well as lithium and strontium contents, show clear differences when compared with typical deep saline groundwaters samples at the Laxemar and Olkiluoto sites (cf. section 4.9 and /Smellie et al. 2008/). This may reflect variations in the bedrock geochemistry. At the moment considerable uncertainty exists around this particular issue because of the lack of groundwater data from depths greater than 1,000 m.

Figure 2-17 illustrates the conceptualisation of the Forsmark groundwater system from before the last deglaciation to the present day. In the context of geological time scales, fluid inclusions in calcite of Palaeozoic origin show the presence of very saline (around 20wt%) mainly Ca-Cl fluids /Sandström et al. 2008/. It can be assumed, therefore, that during the Late Palaeozoic when several kilometres of marine and terrestrial sediments covered the Precambrian Shield area of south-east Sweden, brine solutions were formed allowing these brine waters to slowly penetrate and saturate both the fractures and eventually the interconnected pore spaces in the underlying crystalline bedrock (Figure 2-18). Figure 2-19a, shows a tentative distribution of groundwater types and salinity gradients in the Forsmark area before the intrusion of the last deglaciation meltwater just prior to the Holocene. Based on an understanding of the climatic changes that have occurred since the last deglaciation, it is logical to presume that there must have been at this time old meteoric waters comprising components derived from both temperate and cold climate events. These waters would have intruded the bedrock and have had long times to interact with the minerals. Assuming there were favourable gradients, old meteoric waters could have been partially mixed with deeper, more saline groundwaters, but the high density contrast would have prevented further mixing. What can be said with confidence is that the residual old brackish waters in Forsmark do not have a marine signature. This situation seems to be still valid for the most isolated parts in the bedrock, for example, in the deeper footwall bedrock segment including fracture domain FFM01. However, along the more hydraulically conductive gently dipping deformation zones in the hanging wall bedrock segment, the last deglaciation meltwaters were intruded to several hundreds of metres (Figure 2-19b) and mixed with previously more or less fresh waters that resided in the upper 400–500 m in the most conductive zones.

During the subsequent Littorina Sea stage (Figure 2-19c), the Forsmark area was covered by brackish marine water assumed to be at around 6,500 mg/L Cl /Pitkänen et al. 1999, 2004/. This maximum salinity (twice the present salinity of the Baltic Sea) lasted at least between 4500 and 3000 BC. Due to the unstable density situation generated by the higher density Littorina Sea water located over previously infiltrated last deglaciation meltwater of lower density, the Littorina Sea water entered the deformation zones and fractures and mixed/displaced the previously resident fresh water of glacial and old meteoric character (Figure 2-19c).

250 Ma

Sedimentary cover

Present bedrock
surface

Brine

~10 000   Cl mg/L   >100 000
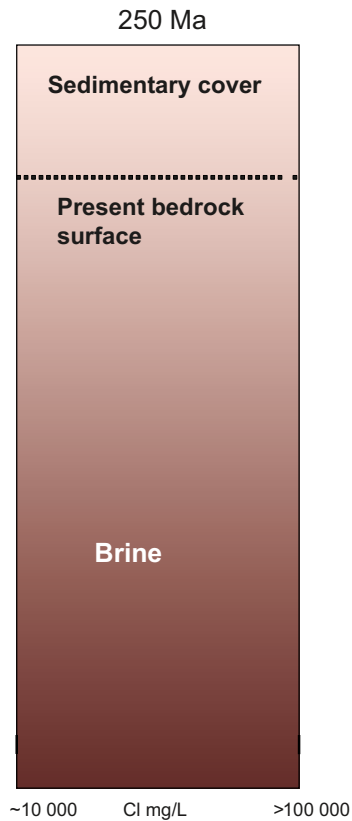
Figure 2-18. *A simplified sketch of the groundwater situation during the Late Palaeozoic when the Forsmark area was covered by large thicknesses of marine and terrestrial sediments /Cederbom et al. 2000, Söderlund 2008/.*
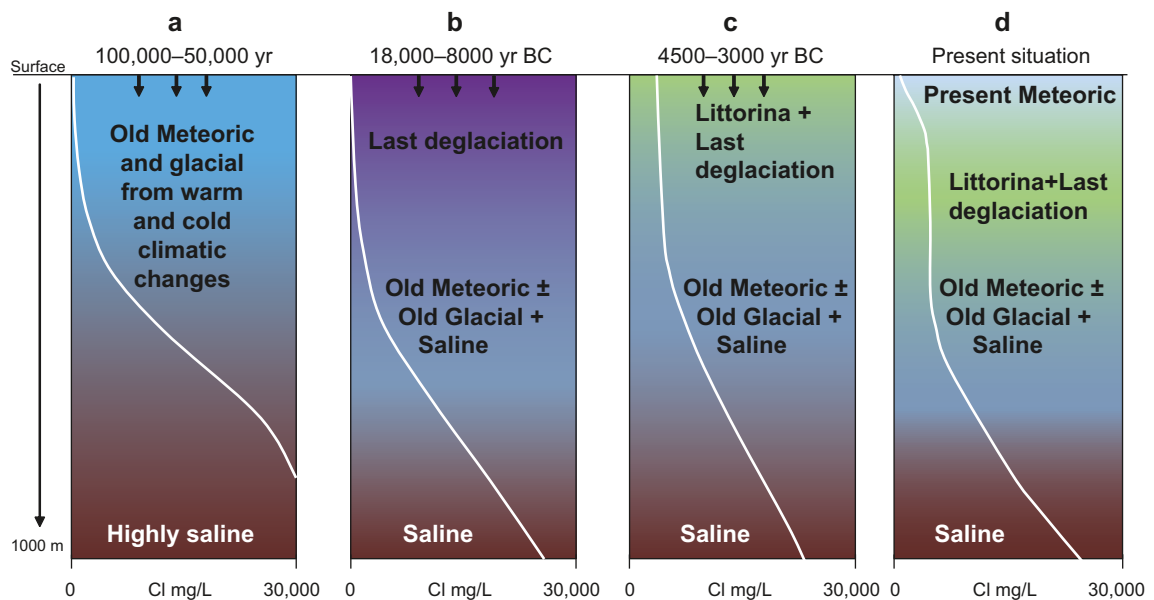
Figure 2-19. *Sketch showing tentative salinities and groundwater-type distributions versus depth for the transmissive zones at Forsmark. From left to right: a) situation prior to the last deglaciation, b) last deglaciation and intrusion of Late Weichselian meltwater, c) the Littorina Sea water penetration caused by density intrusion, and d) the present situation.*

The present situation is shown in Figure 2-19d, which illustrates the flushing out of the brackish marine groundwater (i.e. dominantly Littorina Sea water) in the upper part of the bedrock by recharged meteoric groundwaters during the last approximately 900 years. This flushing process commenced when land uplift of the Forsmark region above sea level was sufficiently advanced to establish hydraulic gradients and is continuing at the present day. Today, the most recent glacial water can no longer be identified as a major component in the bedrock, but rather could constitute a minor part in the Littorina-dominated groundwater and perhaps also in the older brackish non-marine groundwaters where depleted glacial water isotopic signatures have been measured.

The above description is valid generally for areas in the Forsmark bedrock where first the last deglaciation meltwater and then later the brackish marine (Littorina Sea) water have been introduced. Further conceptual development of the Forsmark area, for example, the land uplift processes, are described in /Söderbäck (ed) 2008, Tröjbom et al. 2007/.

An outstanding issue still to be resolved satisfactorily in the conceptual model is the porewater and fracture groundwater evidence of an older dilute meteoric water component (cf. sections 4.8 and 4.9), that may have existed as far back as the Tertiary based on fracture groundwater [36]Cl age dating. This possibility leaves an immense time span of several hundreds of thousands of years to explain prior to the last deglaciation at 18,000–8000 BC. At the moment there are too few data to be more specific than to point out that there is consistent evidence, but no proof (cf. /Waber et al. 2008a/).

3   Hydrogeochemical data

3.1   Databases

The Forsmark dataset which formed the basis for model stages 2.2 and 2.3 comprised quality assured field data that were available in the SKB Sicada databases at the time of the 2.3 data freeze. These data contain complete hydrogeochemical analyses including microbes, colloids, gas analysis and porewater analyses from bedrock samples. These data are compiled in /Kalinowski 2008/, stored in the SKB model data base Simon and described in detail in /Smellie et al. 2008, Gimeno et al. 2008/. The dataset also incorporates version 1.2 and stage 2.1 with modifications to some of the data based on delayed or additional chemical analyses. The groundwater data from other Nordic sites and SFR (Final Repository for Radioactive Operational Waste) have been used for comparison /Kalinowski (ed) 2008/.

The objective was to base the Forsmark hydrogeochemical modelling on data in the 2.2 data freeze and to use new data in the 2.3 data freeze and in the later extended 2.3 dataset for comparison and as a model check. The use of data and the data versions involved are described in detail in /Smellie et al. 2008, Hallbeck and Pedersen 2008a, Gimeno et al. 2008, Kalinowski (ed) 2008/. Data input for the hydrogeological modelling group (HydroNet) was based on the 2.2 data with the 2.3 data restricted to strengthening the choice of boundary conditions (i.e. end-member input for hydrodynamic modelling) and to support the development of the conceptual model common to both hydrogeochemistry and hydrogeology.

3.2   Available data

The locations of the percussion and cored borehole are shown in Figure 2-1 and in more detail in Figure 3-1 and Figure 3-2 were each drill site is featured. A total of 25 cored and 38 percussion boreholes have been drilled at 12 drill sites. Of these, cored boreholes KFM04B, KFM07A and KFM09A are located peripheral to the candidate area to the north-west, and boreholes KFM11A and KFM12A lie outside the candidate area and positioned to investigate the large-scale Singö and Forsmark deformation zones. Seventeen cored boreholes were sampled for hydrochemical evaluation representing locations within, peripheral and outside the candidate area. Of these seventeen cored boreholes, 10 were sampled also for microbes and gases, and five for colloids.

The dataset extracted from Sicada as data freezes 2.2 (October, 2006) and 2.3 (April, 2007), included old data from earlier data freezes and the new data stored up to April 2007. Additional data from the monitoring programme and three deep boreholes were included in the 'Extended 2.3 data freeze' (October, 2007). Table 3-1 summarises the number and type of the samples included in the 2.2–2.3 and extended 2.3 data freezes.
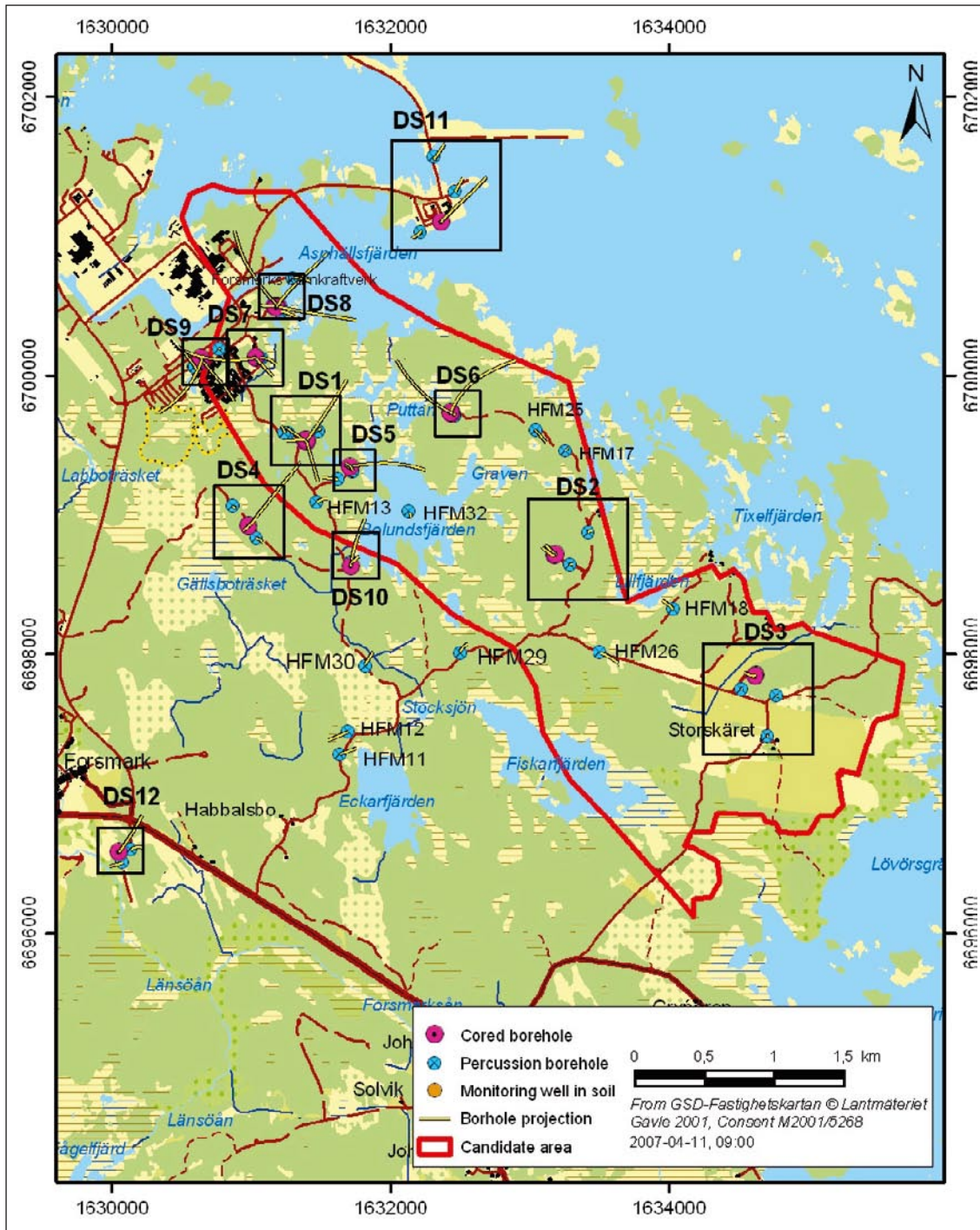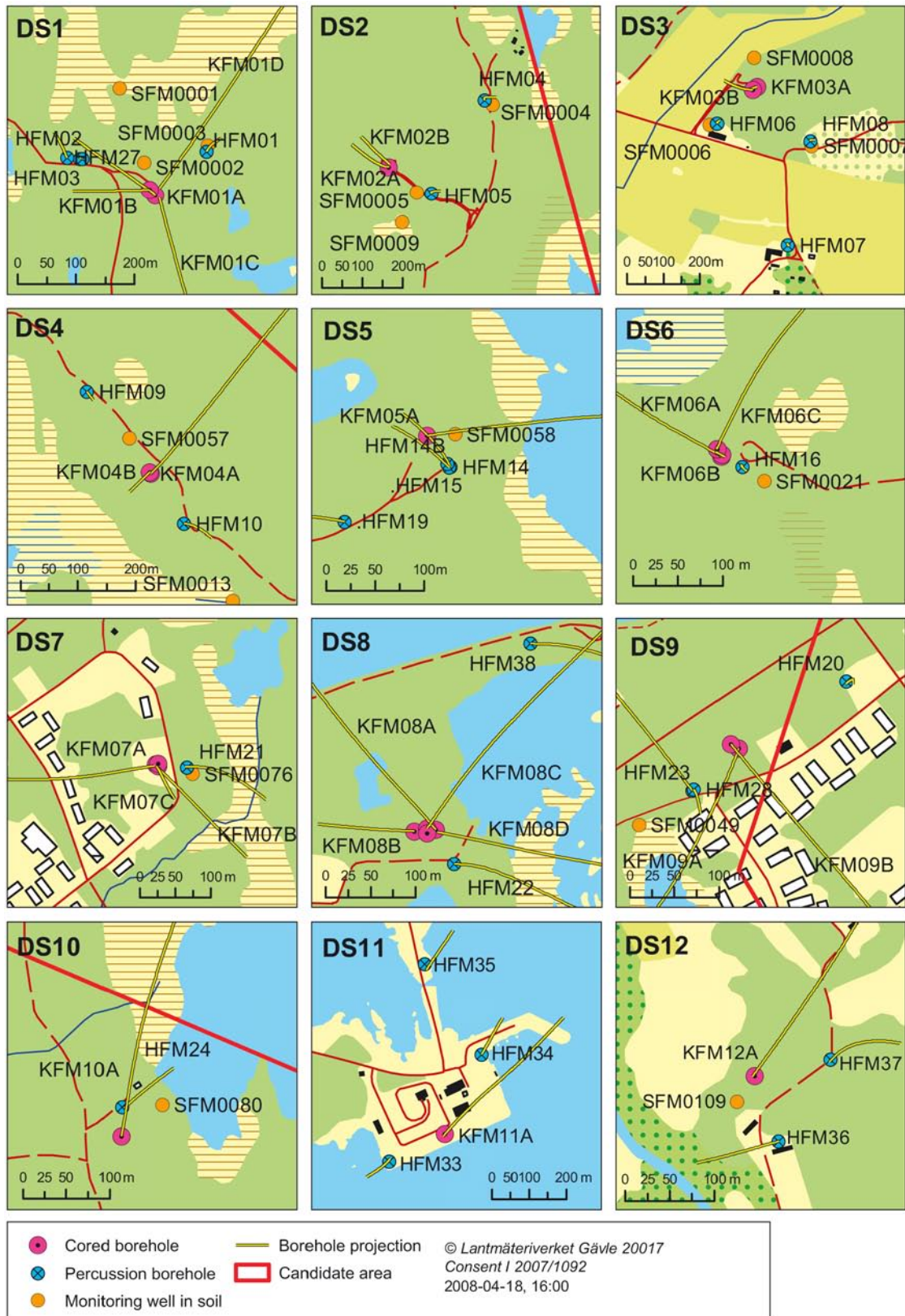
Figure 3-1. *Location of the 12 drill sites within, peripheral and outside the demarcated Forsmark candidate area.*

Figure 3-2. *Details of the 12 drill sites in the Forsmark area, showing the cored boreholes and the accompanying percussion boreholes at each site.*

Table 3-1. Number and type of samples included in data freezes 2.2 and 2.3 and the extended 2.3 data freeze. These include all categories (1–5); see section 3.3 for details.

Type of sample	Number of samples in data freezes F2.2–2.3	Extended data freeze F2.3
Percussion boreholes	154	13
Cored boreholes	178	27
Process control	13	
Drilling sample	7	
Tube sampling	65	
Shallow groundwater	317	
Sea water	277	
Lake water	404	
Stream water	398	
Precipitation	31	
Colloids	37	
Microbes	50	
Gas	42	
Rock matrix porewater	52	39

3.3 Quality assured data

3.3.1 Hydrochemical data

The complete groundwater dataset has been evaluated systematically with respect to quality, and an assignment of different categories was made with respect to their value for further hydrogeochemical interpretational work /Smellie et al. 2008/. This was based on an integrated geological, hydrogeological and hydrochemical approach. A separate small-scale feasibility study of some selected borehole sections was made to determine the possibility of further quantifying the effects from drilling and pumping /Gascoyne and Gurban 2008/, but this did not affect the categorisation of the dataset. Of the five categories chosen, Categories 1–3 primarily meet the requirements of hydrogeochemical (but also hydrogeological) modelling, category 4 primarily meets hydrogeological requirements (but may also be of use for more qualitative hydrogeochemical modelling with caution), while category 5 generally needs to be used with great caution in the context of both hydrogeochemistry and hydrogeology, in particular the tube sample data. A colour code was introduced to quickly distinguish between sample quality when, for example, data are presented in spread-sheet tables or as symbols in scatter plots. In the database, the classification category is indicated numerically in a separate column in addition to the colour coding. An outline of the classification into the various categories for the cored boreholes is presented in Table 3-2. The number of samples and the allocated category are listed in Table 3-3 and the complete tables are stored in the SKB model database Simon.

Table 3-2 lists the most important criteria used to categorise the groundwater samples. For example, a Category 1 sample has less than 1% drilling water, adequate time-series data to assess groundwater chemical stability when sampled, an adequate section length based on the hydraulic properties of the borehole, a charge balance within ± 5%, complete major ion and isotope data and, finally, no evidence of short circuiting either within the borehole around the packed-off section or between different fracture systems in the surrounding bedrock. In comparison, a Category 3 sample may have some of the Category 1 criteria but will differ in failing to satisfy all the criteria, for example, the sample may be characterised by inadequate time series data and/or more than 5% drilling water. At the other extreme, a Category 5 sample may still record less than 1% drilling water and have a complete set of analytical data, but fail

Table 3-2. Classification criteria for cored boreholes /Smellie et al. 2008/.

Cored Boreholes Aspects/Conditions	Category 1	2	3	4	5
Drilling water (≤ 1%)	x	x	x	x	x
Drilling water (≤ 5%)		x	x	x	x
Drilling water (≤ 10%)			x	x	x
Drilling water (> 10%)				x	x
Time series (adequate)	x	x	x	x	x
Time series (inadequate)			x	x	x
Time series (absent)				x	x
Suitable section length	x	x	x	x	x
Sampling during drilling				x	x
Sampling using PLU hydraulic testing equipment			x	x	x
Tube sampling					x
Charge balance ± 5% (± 10% for < 50 mg/L Cl)	x	x	x	x	x
Major ions (complete)	x	x	x	x	x
Major ions (incomplete)			x	x	x
Environmental isotopes (complete)	x	x	x	x	x
Environmental isotopes (incomplete)		x	x	x	x
Hydraulic effects (short circuiting)					x

to meet several or all of the other criteria, for example, long sampled section, inadequate time-series data and influenced by short-circuiting effects etc. Type samples in this category include those collected during drilling and using PLU (site investigation) hydraulic testing equipment. Samples of tube sample origin also fall within this category because of open-hole mixing effects.

It should be noted that the amount of uranine spiked water used for drilling is based on an average value of the uranine. This introduces a degree of uncertainty which may influence the calculated percentage of drilling water for any one borehole section sampled for groundwater. However, this is not considered to be at a level to negatively influence the categorisation procedure.

The main criteria used to categorise the groundwaters sampled from percussion and cored boreholes are:

Category 1 Samples: Characterised by good time-series data (i.e. stable chemistry recorded over an adequate time period of days to weeks) and accompanied by complete analytical data (i.e. particularly all major ions and environmental isotopes); a charge balance of ± 5% and less or close to 1% drilling water. In addition, reliable redox values; a good coverage of trace elements (including U, Th and REEs), and, if possible, microbe, organic and dissolved gas data, is also recommended. Note, however, that the quality of these parameters is not considered in the categorisation because they require a different set of criteria.

Category 2 Samples: Of similar quality to category 1 but marked by incomplete analytical data (usually restricted to an absence of ^{14}C and ^{13}C and less trace element, microbe, organic and gas data) and/or with elevated concentrations of drilling water (1–5%).

Category 3 Samples: This category differs from Categories 1 and 2 in terms of inadequate time-series data; time-series data that indicate instability during sampling; incomplete analytical data (such as absence of some isotopic and trace element data, microbe, organic and gas data, and redox values); elevated drilling water concentrations (5–10%).

Category 4 Samples: Samples are mostly restricted to Cl, Br, ^{18}O, Mg, HCO_3, Na, Ca, SO_4; elevated drilling water concentrations (> 10%); absence or very incomplete time-series data. Type samples are often of an exploratory nature, i.e. mostly taken to see if there is adequate water volume and to check strategic indicators such as drilling water content, salinity (electrical conductivity) ± pH ± major ions (Cl, Br, SO_4, HCO_3) ± ^{18}O. Some samples taken during drilling and those sampled using PLU hydraulic testing equipment also fall within this category.

Category 5 Samples: Samples with some major ions or ^{18}O missing; no charge balance values; elevated drilling water concentrations (> 10%); absence or very incomplete time-series data. Type samples in this category include those collected during drilling and those sampled using PLU hydraulic testing equipment. Samples of tube sample origin also fall within this category because of open hole mixing effects. Note, however, that in some cases the uppermost tube sample (usually near-surface groundwater from highly transmissive zones) and the deepest sample (usually the most saline accumulation due to density constraints) may be quite representative.

Table 3-3 gives a breakdown of the different categories represented by the Forsmark groundwaters.

The highest quality data are required, for example, for geochemical equilibrium calculations, modelling of redox conditions, and reliability for specialised studies involving microbes, organics and colloids. On the other hand overall site understanding (e.g. groundwater distribution, origin and evolution and its integration with hydrogeology) is adequately addressed by a combination of all categories with the obvious proviso that the lower the category used, the more caution is required in their interpretation. In such cases the inclusion of high quality data provides an important check or control on data quality and interpretation as shown in Figure 3-3 and Figure 3-4.

The behaviour of chloride (conservative ion) with depth is illustrated in Figure 3-3, where all five categories are plotted. The figure shows that the general trends and important outliers indicated by all data are strengthened and constrained by the higher category samples (1–3), and even some of the category 4 samples. As expected, the low quality category 5 samples show the greatest scatter, but even so many follow the major trends. The green rectangle demarcates the extent of the strongest Littorina Sea component, i.e. a narrow range of salinity from around 5,330–5,550 mg/L Cl and within an approximate 130–550 m depth range.

As an example of a less conservative ion, Figure 3-4 shows the distribution of magnesium. However some general trends, once again strengthened by the higher quality data, can be clearly seen: a) low magnesium groundwaters extending from shallow fresh groundwaters to deeper, saline groundwaters, b) Littorina-type brackish groundwaters with higher magnesium (> 140 mg/L) which extend to around 500 m depth (i.e. corresponding to the chloride distribution in Figure 3-1), and c) groundwaters with a weak Littorina Sea component (50–140 mg/L Mg), exemplified by the ringed groundwaters in the figure.

Table 3-3. Number of samples from percussion and cored boreholes allocated to each category.

	Cat. 1	Cat. 2	Cat. 3	Cat. 4	Cat. 5
Percussion boreholes	3	2	7	13	87
Cored boreholes	1	15	15	8	80

Elevation versus Chloride
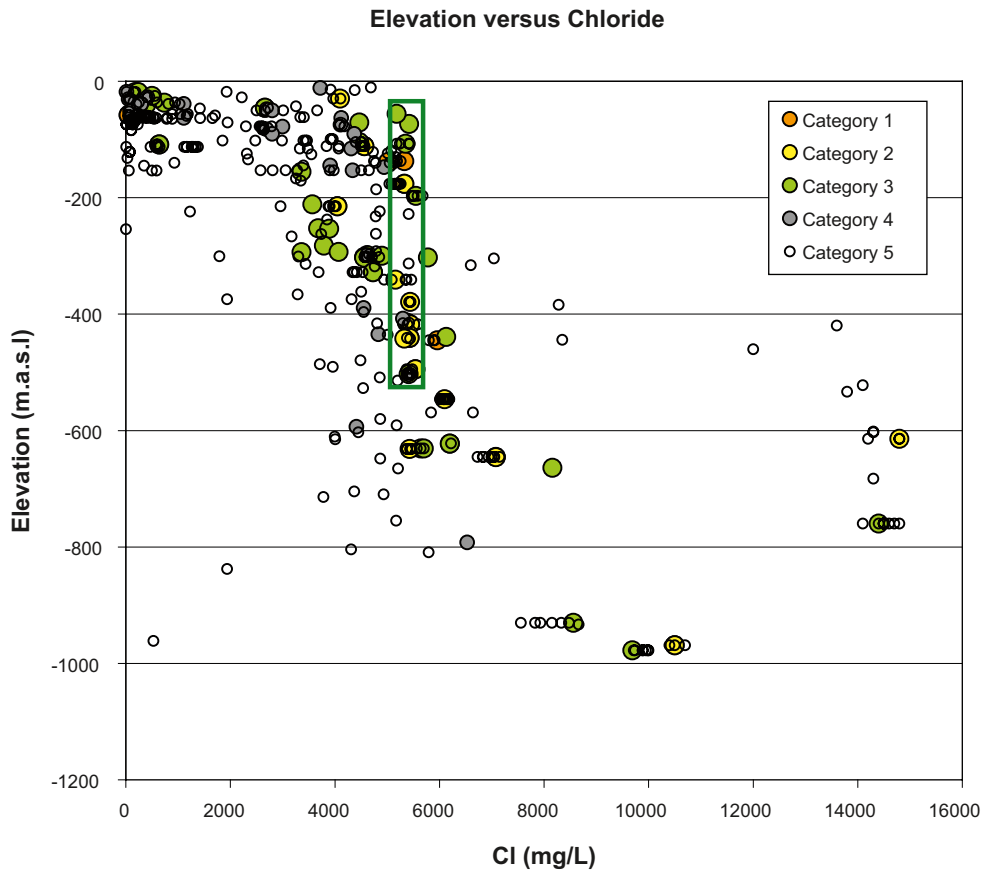
Figure 3-3. *Chloride data plotted versus elevation showing all categories. Green rectangle demarcates the extent of the strongest Littorina Sea component (around 5,330–5,550 mg/L Cl).*

All Magnesium Data versus Elevation
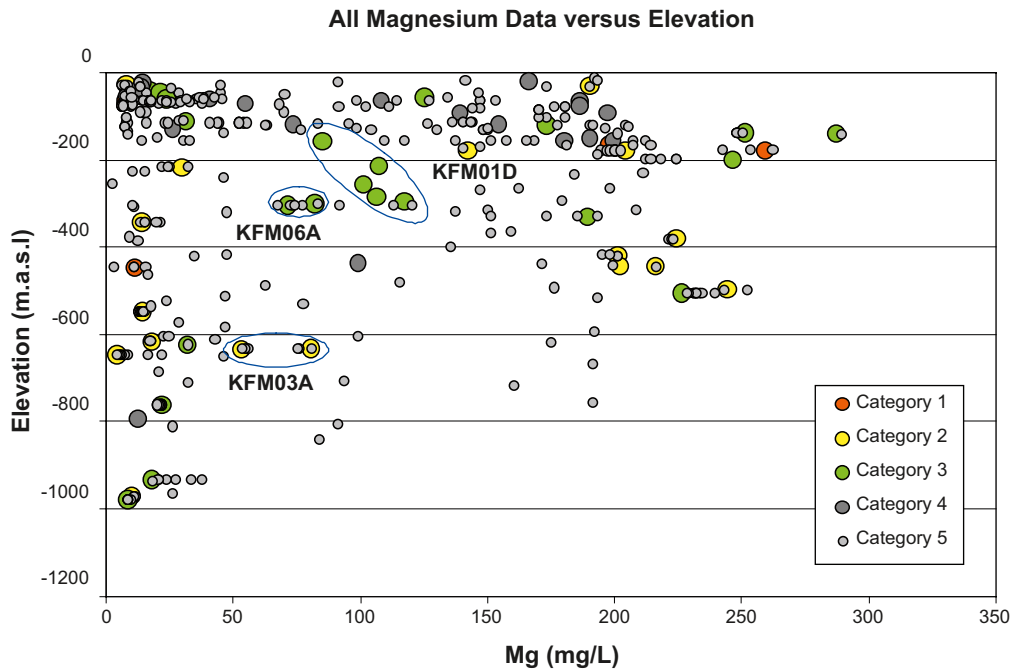
Figure 3-4. *Magnesium data plotted versus elevation showing all categories. Ringed and labelled borehole samples represent a weak Littorina Sea component in the groundwaters (50–150 mg/L Mg) compared to the higher magnesium-rich samples (> 150 mg/L). The remaining weakerLittorina Sea components are represented by groundwaters with > 25 mg/L Mg.*

Questionable data

Questionable data refer to those data that appear to be reasonably representative but still may reflect a wide range of possible influences such as limited hydraulic short-circuiting effects during sampling, small-scale contamination from different borehole activities, and induced mixing over large distances by long-term draw-down hydraulic pumping tests and dilution and tracer tests to determine groundwater flow conditions. Some issues of concern were identified, which included:

- The hydraulic tracer test programme involved at different stages the injection of uranine and additionally caesium in one test. In some of the sampled groundwaters, especially from monitoring sections, this has resulted in an increase of uranine which may be incorrectly interpreted as an artefact of the introduced uranine during initial drilling of the boreholes. Furthermore, in two of the monitoring samples there were anomalous increases in caesium. This was investigated and the tested borehole sections identified and documented.

- Low but detectable tritium contents (around one or a few TU) have been detected in brackish and saline groundwaters from intermediate depth at Forsmark. These types of groundwaters, brackish marine and brackish to saline non-marine, are usually tritium-free and therefore the risk of artificial contamination had to be addressed. Possibilities included: a) enhanced mixing of surface and especially modern Baltic Sea water through time partly caused by the extensive pumping related to dilution and tracer experiments, and long-term draw-down hydraulic pumping tests, b) enhanced mixing of waters from SFR, which are enriched in tritium these waters are mostly brackish marine waters of variable chloride contents, and c) contamination of tritium in the pumping equipment caused by high tritium in deionised water occasionally used during routine Complete Chemical Characterisation (CCC) sampling. In situ production of tritium in the bedrock and laboratory contamination were considered less probable.

- During sampling, fracture networks intersecting the boreholes may lead to short-circuiting of the groundwater flow in the surrounding bedrock and also to bypassing the packer systems used to isolate the borehole sections being sampled. This effectively means that the section sampled may have been supplied by mixed groundwaters from higher or lower levels in the bedrock, and/or mixed borehole waters above or below the packer systems. In both cases the sampled groundwaters when interpreted in isolation may be evaluated erroneously as being of suitable quality.

Each of these issues were addressed in detail during the quality evaluation of the data and appropriate action taken in the categorisation process /Smellie et al. 2008/.

3.3.2 Microbiological data

For microbiological field investigations, in common with colloids (section 3.3.3) and gases (section 3.3.4) below (and generally with most all trace components), the sampling of quality groundwaters has been overshadowed to a degree by their sensitivity to drilling and sampling activities. In cases this has resulted in uncertainties due to suspected contamination caused by, for example, pumping rates and artefacts from drilling, insufficient sampling time, short-circuiting during sampling etc.

During the drilling of boreholes used for microbiological sampling a thorough cleaning and sterilisation programme was applied /Pedersen 2005/. The effectiveness of this programme was tested during each drilling operation from boreholes KFM01A to KFM06A. This was conducted by analysing the Total Number of Cells (TNC), Adenosine-Tri-Phosphate (ATP) and the number of Cultivable Aerobic Heterotrophic Bacteria (CHAB) in the drilling water. It has previously been demonstrated at the Äspö Hard Rock Laboratory (HRL) that contamination of groundwater by drilling water does not create a sustained contamination of the intersected aquifers /Pedersen et al. 1997/. In line with these results, a correlation could not be demonstrated between the amount of drilling water in the samples and any of the microbiology parameters measured in the Forsmark site investigation samples /Hallbeck and Pedersen 2008a/. The quality and reproduc-

ibility of the applied methods for microbiological analyses were tested and are discussed in detail by /Hallbeck and Pedersen 2008a/. The reproducibility of all analyses was found to be within the standard deviation of the methods used. The analysis of TNC and ATP has been demonstrated to agree and to give reliable results on numbers and biomass in Fennoscandian shield groundwaters /Eydal and Pedersen 2007/. The analysis of TNC, ATP, CHAB and MPN as conducted on the Forsmark groundwater samples was applied in parallel on 60 independent groundwater samples from between 3.9 and 450 m depth in Olkiluoto, Finland /Pedersen et al. 2008/. Significant correlations were found between groundwater chemistry and borehole conditions with cultivable numbers, diversity and biomass, suggesting a mutual dependency between microbiological processes and the groundwater geochemistry. In conclusion, the analysis of microbiology in Forsmark was based on a solid scientific basis with methods that are well established, quality assured and published in peer-reviewed scientific journals.

3.3.3   Colloid data

The silicon data were excluded for borehole KFM01A, 112 m in some of the analyses because of likely sampling artefacts. In addition, no total amounts of colloids were available for this borehole /Hallbeck and Pedersen 2008a/.

With respect to calcite and sulphur, the calcite values were subtracted from the total amount of colloids, while the sulphur values were not recalculated as pyrite because this phase could not be confirmed. Sulphur is therefore represented as that recorded in Sicada. Calcium and sulphur colloids are commonly regarded as pressure drop related and their actual concentrations in the sampled groundwater can not be safely inferred from the data.

3.3.4   Gases

The sampling of gas was performed using a Pressure Vacuum Beaker (PVB) which has occasionally been linked with some pressure gas leakage problems into the sample, which elevates the argon or nitrogen concentration of the sample being collected /Hallbeck and Pedersen 2008a/. There are two possibilities to track such effects. One is to take two samples with nitrogen and argon respectively; however, this indicated in both cases a reverse relationship between argon and nitrogen. This contamination effect becomes almost impossible to compensate for in the calculations of gas concentrations unless samples are duplicated every time they are collected (not done in the present study), because the degree of contamination for one of the two gases will remain unknown. The best possible way, presently, is to judge a sample result in relation to several other results for samples from similar depths. A large discrepancy between a particular sample result and the average result for samples from the same depth region indicates a sampling artefact. Several possible such cases were found related to KFM07A, 08A, 10A (215 m) and 11A. These samples contain more nitrogen, and also more total gas, than do all other samples in relation to depth, which may suggest leaking PVB vessels. Consequently, all other gases in these potentially contaminated samples were diluted resulting in an underestimate of the actual values.

4 Explorative analysis and modelling

Explorative analysis involves an initial general examination of the groundwater data using traditional geochemical approaches to describe the data and provide an early insight and understanding of the site, i.e. the construction of a preliminary conceptual model for the area (section 2.6.3). Based on this hydrochemical framework, selected data are further evaluated using different modelling approaches such as data evaluation and visualisation, mixing modelling, equilibrium modelling, redox modelling and evaluation of microbes, colloids and gases.

The computer codes that were used in the hydrogeochemical evaluation are listed below.

- PHREEQC: Code for calculations of chemical equilibrium, reaction, advective transport and inverse modelling /Parkhurst and Appelo 1999/. Thermodynamic data base: WATEQ4F /Ball and Nordstrom 2001/, distributed with the PHREEQC code, with some modifications, see details in /Auqué et al. 2007/.

- M3: Mixing and mass balance calculation program /Laaksoharju et al. 1999, Gómez et al. 2008/.

- CORE^{2D}: Coupled hydrochemical/hydrogeological modelling code /Samper et al. 2000/.

- OpenDX: 3D visualisation (IBM Open Visual environment, OpenDX).

Studies of fracture fillings, composition of the porewater in the bedrock and groundwater residence times are important information for the site description. The background data, the explorative analysis and the modelling are detailed in /Smellie et al. 2008, Gimeno et al. 2008, Kalinowski (ed) 2008/. The most important results are described in the sections below.

During the explorative analyses of the groundwaters it became apparent that a subdivision of the sampled groundwaters into four major groundwater types would facilitate the description and interpretation of the figures and diagrams. The major water types distinguished are; Fresh, Brackish Marine, Brackish Non-marine and Saline Non-marine. Because of the lack of deep groundwater hydrochemical data, the brackish and saline non-marine groundwaters have been combined. In addition, two groundwater types were included to accommodate important mixing processes resulting from anthropogenic and natural processes: a) a near-surface 'Mixed Brackish' type mainly comprising fresh and brackish marine groundwaters, and b) a deeper 'Transition Zone' type comprising degrees of mixing between brackish marine and brackish to saline non-marine groundwaters. The main chemical and isotopic character of each groundwater type, and their respective colour codes used in the plots, can be summarised as follows.

Fresh (Light Grey colour code)

Water type: Fresh (< 200 mg/L Cl; < 1.0 g/L TDS); Mainly meteoric in origin, i.e. Na(Ca)-HCO$_3$(SO$_4$)-(Cl) in type, $\delta^{18}O$ = –12 to –11‰ V-SMOW.

Mixed Brackish (Light Green colour code) (Not a specific groundwater type)

Waters of mixed Fresh and Brackish Marine origin (200–2,000 mg/L Cl; 1.0–3.5 g/L TDS); is usually sampled at 50–150 m depth in relatively long boreholes sections mainly from percussion boreholes. They may be the result of natural and/or anthropogenic mixing during drilling activities and sampling.

Brackish Marine (Green colour code)

Water type: Brackish Marine (2,000–6,000 mg/L Cl; 3.5–10 g/L TDS; Mg > 100 mg/L); variable Littorina Sea component (± modern Baltic Sea) + Last Deglaciation meltwater ± Saline component; Na-Ca-Mg-Cl-SO$_4$; δ^{18}O = –11.5 to –8.0‰ V-SMOW.

Transition zone samples (Not a specific water type) (Turquoise colour code)

Waters sampled in the transition zone between Brackish Marine and Brackish Non-marine groundwaters. These waters range from 4,000–6,500 mg/L Cl and from 25–100 mg/L Mg. They may be the result of natural and/or anthropogenic mixing during drilling activities and sampling.

Brackish to Saline Non-marine (Blue colour code)

Water type: Brackish to Saline Non-marine (4,000–15,000 mg/L Cl; 8.5–16 g/L TDS; Mg < 25 mg/L); Old Meteoric ± Old Glacial ± Last Deglaciation meltwater ± Saline component, i.e. Ca-Na-Cl in type, δ^{18}O = –16.0 to –10.5‰ V-SMOW.

This subdivision into different groundwater types corresponds to the division used in the conceptual visualisation (section 6) with the exception that Brackish Non-marine groundwaters (4,000–10,000 mg/L Cl) and Saline Non-marine groundwaters (10,000–20,000 mg/L Cl) are treated separately and are given turquoise and dark blue colour codes respectively.

4.1 Initial data evaluation and visualisation

This section is based primarily on the work of /Smellie et al. 2008, Gimeno et al. 2008, Molinero et al. 2008/, with limited input from /Hallbeck and Pedersen 2008a/. Addressed are the primary major ions and isotopes for site understanding; some strategic minor ions (uranium, phosphate, nitrate and ammonia) and the trace elements (including REEs) are briefly presented and discussed.

For the visualisation and interpretation of primary data, use has been made of: a) x-y plots to demonstrate depth variations of the major ions and also their association with fracture domains and deformation zones, and b) a 3D presentation of the same data in order to quickly locate and orient the boreholes to achieve a better physical understanding of the site. Because of a lack of deep groundwater data, the brackish non-marine and saline groundwater types in the x-y plots have been combined for convenience under the general heading of 'brackish to saline non-marine groundwater type' identified with a blue colour code. Otherwise in the site description sections of this report the 'brackish' and 'saline' non-marine groundwater types are dealt with separately and discriminated using a turquoise and blue colour code respectively.

Strictly the x-y plots should be presented always showing the analytical error bars on each sample point and, in the case of elevation, an error bar relating to the uncertainty of the depth measurement. This has not been routinely done (except for the porewaters which require micro-analytical techniques) because in many cases the error bars interfere with the main illustrative objectives of the plots. To compensate for this, examples of plots are illustrated in section 4.10.1 selected to cover the variation in uncertainties of some commonly used major ions and isotopes. For specific, more exotic constituents plotted (e.g. ^{37}Cl), the analytical uncertainties are given in the text.

Three of the most important hydrochemical signatures have been selected to describe the groundwaters (i.e. Cl, Mg and δ^{18}O) based on the conceptual understanding of the Forsmark area.

As part of this initial evaluation stage, the fracture domain concept (cf. section 2.2.4) was addressed by applying the approach outlined by /Olofsson et al. 2007/ to see if there was any hydrogeochemical consistency with the geology and hydrogeology. The results from this exercise essentially confirm the findings reported in /Olofsson et al. 2007/ in that many

of the differences observed between the fracture domains are mostly restricted to the type and transmissivity of the water-conducting fractures within the fracture domains and the deformation zones embedded in the fracture domains. For example, the hanging wall bedrock segment is characterised by a series of highly transmissive gently dipping deformation zones. Here, different water types (e.g. Littorina Sea) penetrated to around 600 m. This compares with fracture domains FFM02 and FFM01 (i.e. the upper part of the footwall), where the Littorina Sea influence has been restricted to maximum depths of around 300 m.

4.1.1 Depth trends of selected major ions

Figure 4-1a, c and e, plotting Cl, Mg and $\delta^{18}O$ against elevation, shows the association of the different groundwater types (colour coded) with the defined fracture domains and the embedded water-conducting deformation zones; Figure 4-1b, d and f shows the distribution of the different groundwater types with increasing depth. Figure 4-2 represents a three-dimensional visualisation of the boreholes showing the variation of chloride with depth along the boreholes. Combining these three methods of presenting the hydrochemical data provides a rapid and very informative insight to the vertical and lateral spatial distribution of the measured parameters, and the geological association of the various groundwater types.

Chloride is one of the main components in these groundwaters and it is directly correlated with their salinity. The uppermost 100–150 m in the Forsmark area (Figure 4-1a and b) display a wide variability in chloride and generally fall under the heading of mixed brackish groundwaters, due partly to the mixing of discharging brackish marine (Littorina) groundwaters (and/or residual near-surface saline waters of Baltic Sea origin) with recharging meteoric waters. In the footwall bedrock segment (including fracture domains FFM01 and FFM02), this shallow system is controlled by flow along highly transmissive, well-connected system of sub-horizontal fractures (i.e. the shallow bedrock aquifer), which is still in the process of flushing out residual brackish marine (Littorina) groundwaters. This also produces a mixing effect between recharging meteoric waters and residual brackish (possibly including Baltic Sea) groundwaters.

Below this shallow bedrock aquifer, the chloride content varies significantly with depth. Groundwaters from the footwall bedrock (including fracture domains FFM01 and FFM02) show a progressive increase of chloride from 100 m down to 600 m. This represents the passage from brackish marine groundwaters of Littorina type (present to a maximum depth of around 300 m) followed by the transition to brackish non-marine groundwaters to around 600 m, and saline non-marine types at greater depths. Although only a few samples of the more saline non-marine groundwater exist, examples include groundwaters from fracture domain FFM04 (and FFM05 not shown), outside the target volume (boreholes KFM07A and 09A), which show an important shift to the highest chloride concentration values measured at Forsmark (14,000–15,000 mg/L Cl; Figure 4-1a, b). This higher salinity appears to be associated with a larger proportion of a deeper, more highly saline component /Smellie et al. 2008/.

The presence of greater salinity at such intermediate depths is considered to reflect natural and/ or anthropogenic effects either due to glacial rebound (after the maximum glacial loading) or upconing resulting from different borehole activities including groundwater sampling. The first possibility is indicated by the presence of equally high chloride concentrations in porewater from borehole KFM09B collected at a distance of one metre from a water-conducting fracture, but considerably lower chloride further into the intact rock matrix (see section 4.8). This suggests a recent, but long interaction time between a high chloride fracture groundwater and the matrix porewater. The second possibility is supported by heavy pumping carried out to flush, for example, borehole KFM07A prior to sampling, and the only source of such saline groundwater below 250 m is believed to originate from a highly conductive fracture at around 800 m depth /Berg et al. 2006, Olofsson et al. 2007/. A similar explanation may be valid also for borehole KFM09A and in both cases upconing may have been facilitated by steeply dipping deformation zones with a high transmissivity. With the available data, however, a definitive interpretation cannot be presented that supports either a natural or anthropogenic origin to these anomalous groundwater compositions.
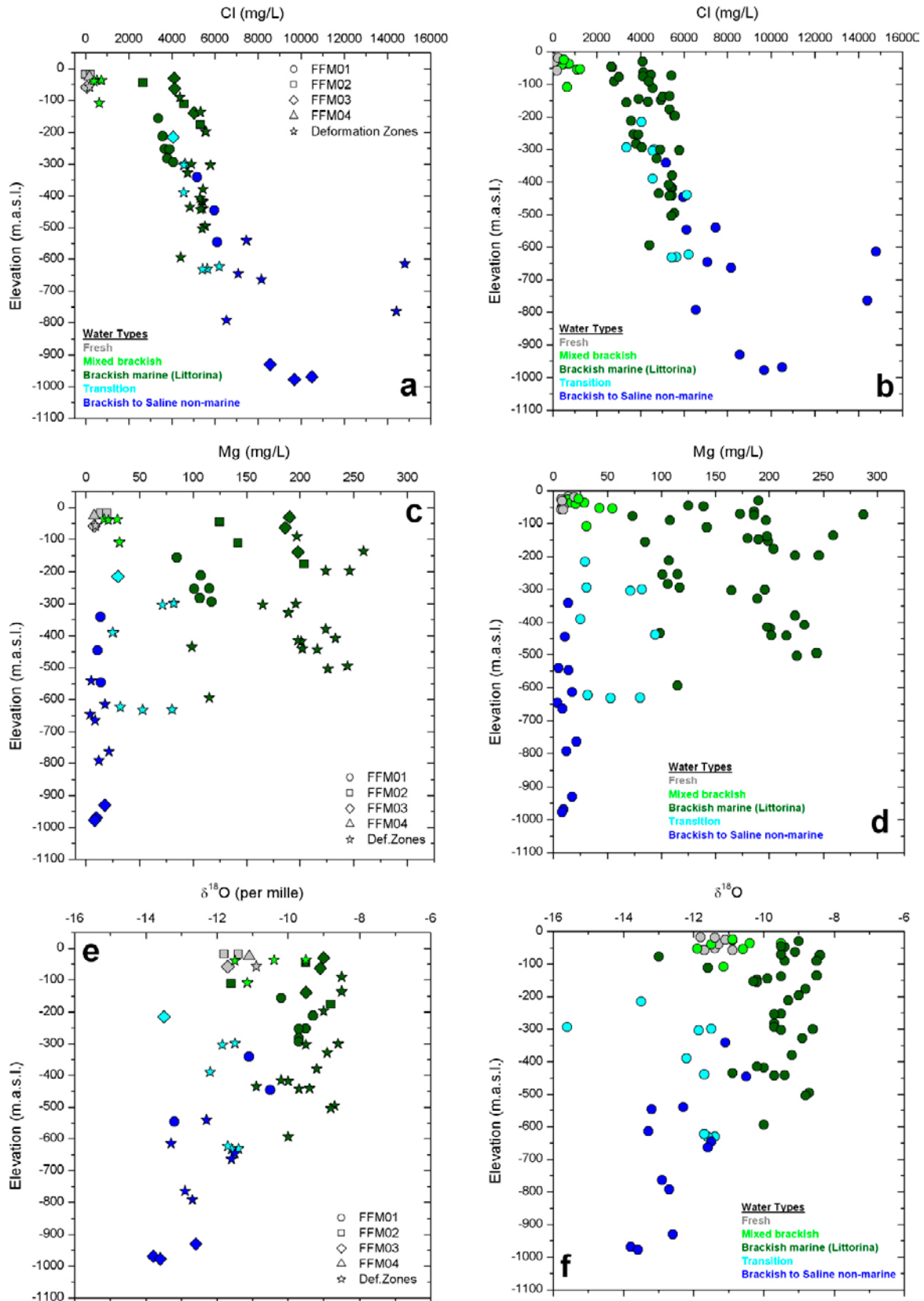
Figure 4-1. *Distributions of chloride (a, b), magnesium (c, d) and δ¹⁸O (e, f) in the two main systems in the Forsmark candidate area (i.e. hanging wall and footwall). Left-hand plots represent groundwaters sampled from the hanging wall (fracture domain FFM03) and the footwall (fracture domains FFM01 and FFM02). Also included is fracture domain FFM06 within the candidate area (same colour code as samples from the footwall) and those groundwaters from marginal areas to the target volume (fracture domains FFM04 and FFM05; in grey). Right-hand plots represent the same sampled groundwaters subdivided into the different major groundwater types used in the site description.*

Brackish marine groundwaters sampled from the hanging wall bedrock (i.e. fracture domain FFM03) mostly originate from the series of highly transmissive, gently dipping deformation zones. These deformation zone groundwaters have a wide range of chloride contents down to around 200 m depth, some achieving values as high as 5,000 mg/L (i.e. strong Littorina Sea signature). From 200–600 m, the chloride remains fairly constant around this value before increasing progressively up to 10,000 mg/L Cl at around 1,000 m depth, i.e. to a brackish and then saline non-marine groundwater type.

This increased salinity gradient with depth in the Forsmark area from around 600 m is believed to reflect processes that have occurred prior to the incursion of the Littorina Sea waters (and also the meltwaters from the last deglaciation) (cf. section 2.5.3). At that time, mixing and dilution of a deeper, more highly saline (or possibly brine type) with lower saline groundwaters at shallower depths (i.e. footwall bedrock including domain FFM01), can be attributed to advection, whereas at greater depths where groundwater flow decreases towards stagnant conditions, mixing is driven by upward molecular diffusion. Nevertheless, under both conditions it is the same deep saline or brine component that is being modified.

The three-dimensional chloride distribution with depth is illustrated also in Figure 4-2. Here it is possible to obtain a feel for the spatial distribution of the chloride laterally across the candidate area, for example, the anomalously high salinity in borehole KFM07A discussed above, and also to relate the borehole groundwater chemistry to potentially important surface and near-surface features such as discharge and recharge areas or complex shallow aquifer conditions reflected by variations in the salinity. Comparing near-surface groundwaters from the vicinity of Bolundsfjärden and Fiskarfjärden illustrates the general contrast of higher salinity in the former and less salinity in the latter. As discussed in section 2.3.1, below Lake Bolundsfjärden, in contrast to Lake Fiskarfjärden, there exist relict marine chemical signatures in the groundwaters. Noticeable, however, is the higher salinity under the centre of the Lake Bolundsfjärden indicating a localised point of discharge.
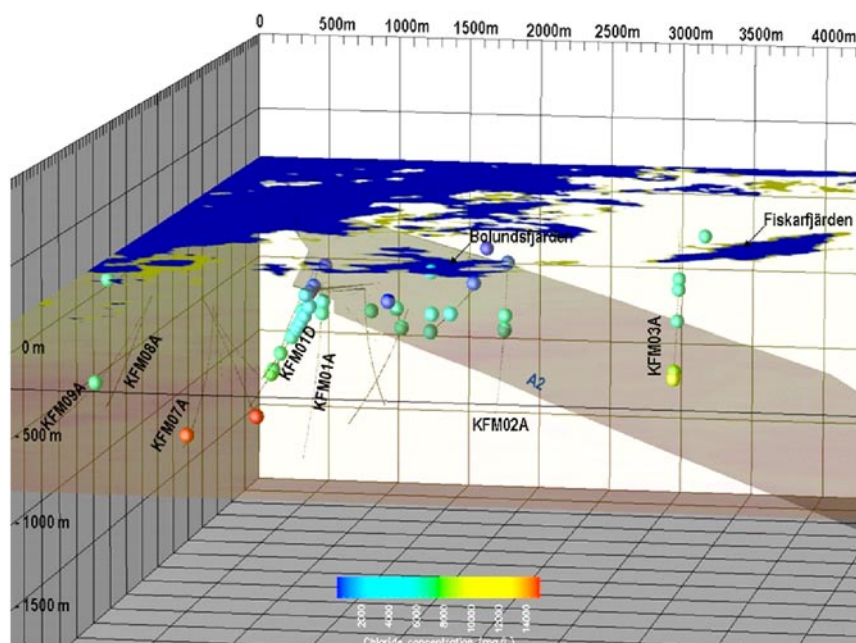
Figure 4-2. *3D visualisation of chloride concentrations and their lateral and vertical distribution related to the major gently dipping deformation zone ZFMA2 which, together with ZFMF1 (not shown), effectively divide the candidate area into the hanging wall (above ZFMA2) and footwall (below ZFMA2 – denoted by A2). (SE-NW view of the Forsmark area showing the main surface features such as lakes and coastline and the borehole names; the length and depth scales shown are common for all similar style 3D figures in sections 4.1.1 and 4.2 of this report).*

The magnesium concentration (Figure 4-1c, d and Figure 4-3), further emphasises the strong marine (i.e. Littorina Sea) influence in the candidate volume as a whole but again much more marked in the hanging wall bedrock in association with the gently dipping deformation zones, including ZFMA2. The brackish marine groundwater transition to brackish non-marine groundwater is quite sharp and clearly observed from around 500–650 m depth in the hanging wall bedrock, but is generally more diffuse from around 200–650 m in the footwall bedrock. In the part of the footwall bedrock where the frequency of water-conductive fractures is low (i.e. fracture domain FFM01), represented by borehole KFM01D, the maximum Littorina penetration is to around 300–350 m depth.

In the brackish to saline non-marine groundwaters, magnesium quickly drops to less than 25 mg/L below around 650 m in the hanging wall bedrock and (at around 300 m in borehole KFM01D). This is an important observation, suggesting that below these respective levels any significant hydrochemical distinction ceases between the footwall bedrock (i.e. fracture domain FFM01) and hanging wall bedrock (i.e. fracture domain FFM03). Furthermore, below this levels the fracture transmissivity is also very low.

With respect to oxygen-18 (Figure 4-1e, f and Figure 4-4), four main distinguishing observations can be made: a) typical near-surface meteoric recharge values around –12 to –10.5‰ V-SMOW), b) enriched values ranging from $\delta^{18}O = -10$ to –8.5‰ V-SMOW representing the brackish marine (Littorina) groundwaters, c) depleted values of $\delta^{18}O = -14$ to –12‰ V-SMOW for brackish to saline non-marine groundwaters, and d) the most depleted sample at $\delta^{18}O = -15.6$‰ V-SMOW from a mixed brackish groundwater with a significant glacial component (KFM12A) from the regional scale Forsmark deformation zone located outside the candidate area. Groundwaters from fracture domains FFM04 and FFM05, located outside the target volume, show weak but noticeable depleted glacial signatures (i.e. KFM07A at –12.9‰ V-SMOW and KFM9A at –13.3‰ V-SMOW). The most depleted sample from within the candidate area is $\delta^{18}O = -13.8$‰ V-SMOW from borehole KFM03A (960 m) in the hanging wall bedrock. Furthermore, porewater studies show that a glacial water component is present in the footwall bedrock (i.e. KFM08C at –13 ‰ V-SMOW; around 400 m depth) and hanging wall bedrock (i.e. KFM02B at –15 ‰ V-SMOW; around 170 m depth) bedrock.

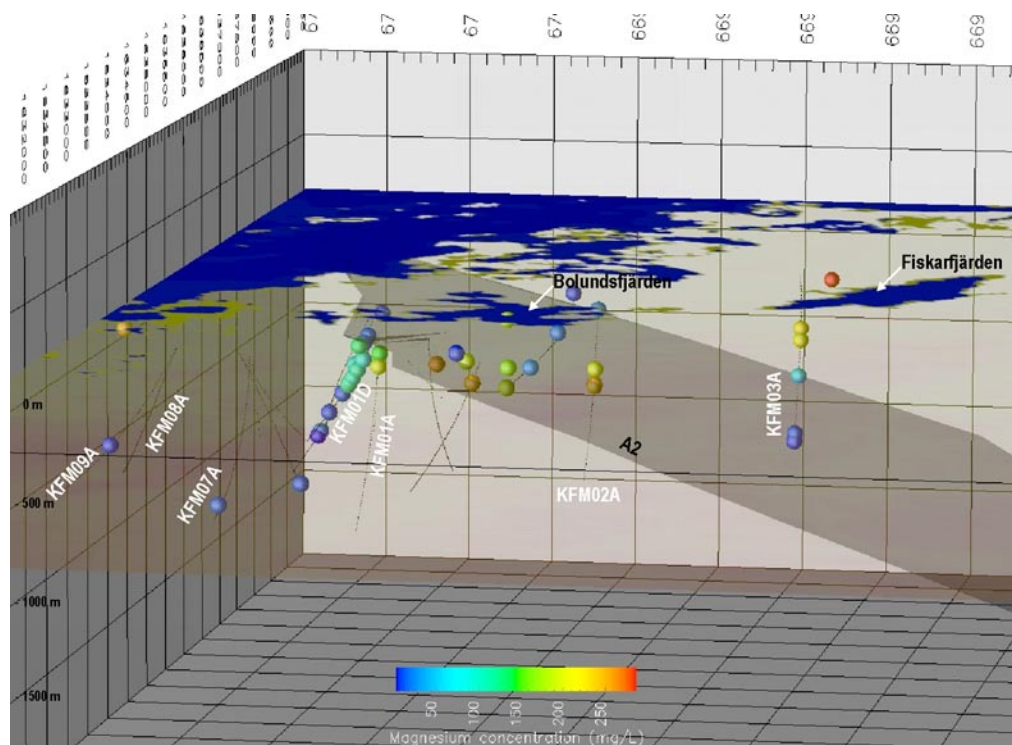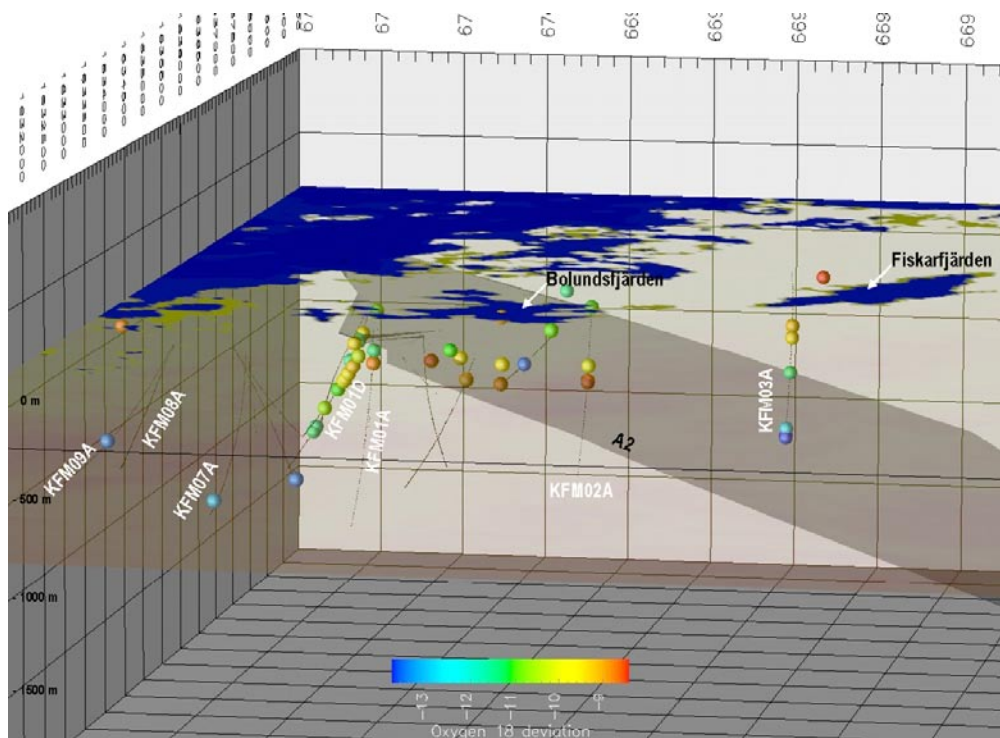***Figure 4-3.*** *3-D visualisation of magnesium concentrations and their lateral and vertical distribution.*

Figure 4-4. *3-D visualisation of δ¹⁸O contents and their lateral and vertical distribution.*

Also apparent is the depleted signature under the centre of Lake Bolundsfjärden indicating, together with chloride and magnesium, the local discharge of a groundwater of deeper origin mixed with some residual glacial meltwater from the last deglaciation (Figure 4-4).

These oxygen-18 data collectively show that a cold climate water component persists within the brackish to saline non-marine groundwaters, and probably also within the brackish marine (Littorina Sea) type groundwaters. However, any meltwater from the last deglaciation in the brackish marine (Littorina) groundwaters will be partly masked by the enriched $\delta^{18}O$ signature of these groundwaters. This $\delta^{18}O$ distinction with depth also reflects the change to lower transmissivity at 500–600 m depth associated with the gently dipping deformation zones within the hanging wall bedrock.

Figure 4-5 (a–d) shows the variation of sodium, calcium, potassium and sulphate with depth (see also /Smellie et al. 2008/). In all cases, in common with chloride, magnesium and $\delta^{18}O$, the subdivision of the groundwater types is reflected clearly in the chemistry. By comparing the brackish marine (Littorina) and brackish to saline non-marine groundwater types, the brackish marine groundwaters show generally, to varying degrees, higher sodium, potassium and sulphate with correspondingly lower calcium. With increasing depth, the brackish to saline non-marine groundwaters increase steadily with respect to calcium, and maybe to some small extent for sodium, but no clear trends can be observed for potassium and sulphate which are low in content. The increase in calcium is a well recognised trend, for example, in many deep groundwaters from the Fennoscandian and Canadian Precambrian Shield areas with calcium enrichment from water/rock interaction occurs as groundwater flow decreases towards stagnant conditions with increasing depth /Frape and Fritz 1987, Smellie et al. 2008/.
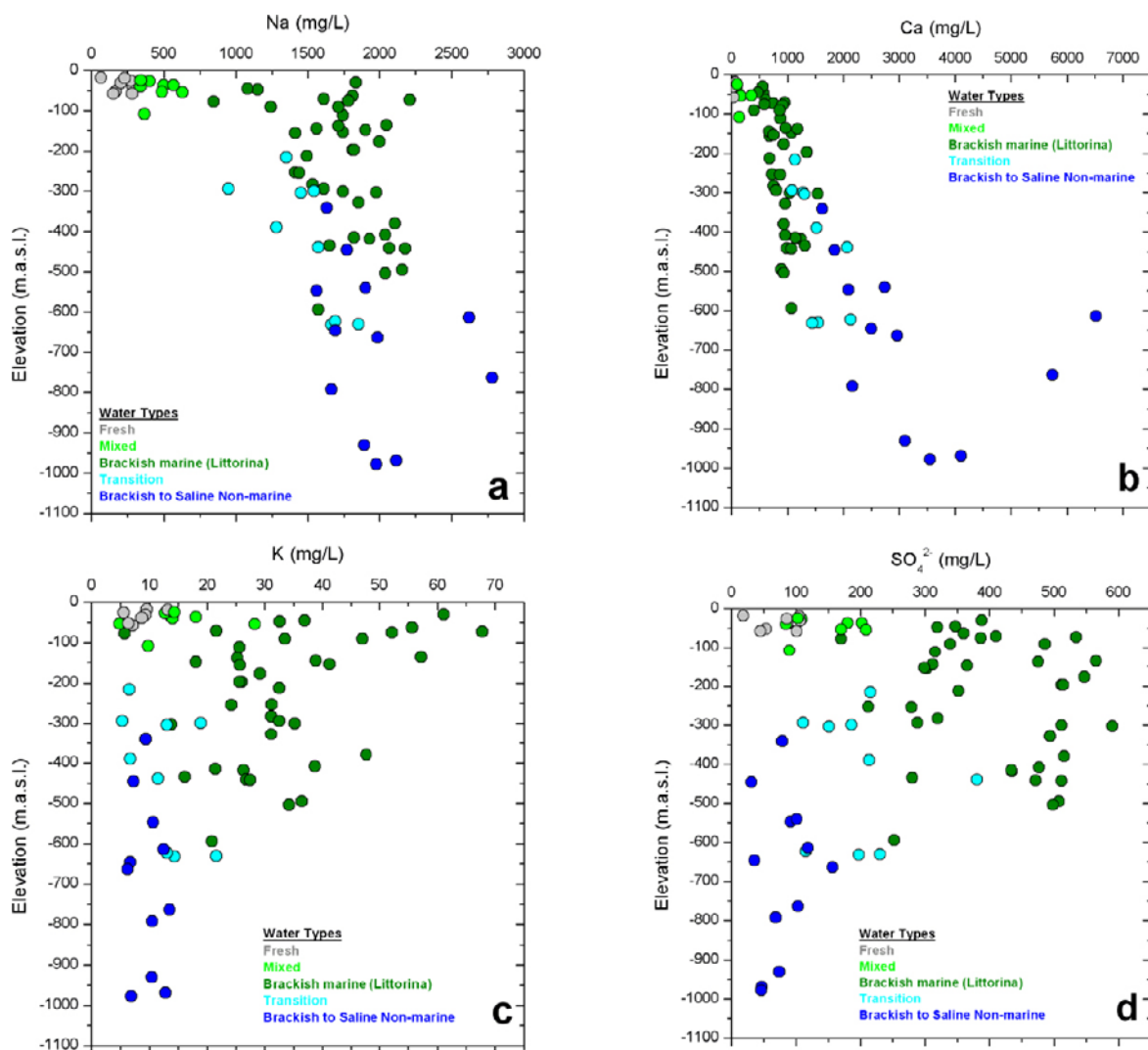
Figure 4-5. *Distributions of sodium (a), calcium (b), potassium (c) and sulphate (d) with depth related to the different groundwater types that typify the Forsmark area.*

Bicarbonate contents are highly variable in the first 150 m of the footwall bedrock segment (i.e. including fracture domain FFM02; Figure 4-6b) where the carbonate system and the microbial production of CO_2 are very active /Gimeno et al. 2008/. Concentrations then decrease to very low values at greater depths in both the footwall bedrock (including fracture domain FFM01) and hanging wall bedrock at those levels already demarcated by the other parameters. However, bicarbonate is relatively high in most of the brackish marine groundwaters characterising the upper 600 m of the hanging wall bedrock distinguished by the gently dipping deformation zones The brackish non-marine groundwaters below 300 m depth in the footwall bedrock (i.e. fracture domain FFM01), in contrast, have low bicarbonate contents for the same depths. At these depths this could be consistent with a higher carbon dioxide consumption by silicate weathering and increasing residence time of the groundwater mixtures. In any case, it can be concluded that the bicarbonate contents are generally low in the brackish to saline non-marine groundwaters, with the lowest values recorded from the deepest and most evolved groundwaters (at 600–800 m depth) from steeply dipping fracture zones to the north-west and south-west in the adjacent bedrock outside the target volume (i.e. fracture domains FFM04 and FFM05 (not plotted)). The dissolved organic carbon (DOC) show similar behaviour to bicarbonate, i.e. the content is generally decreasing with depth Figure 4-6c).
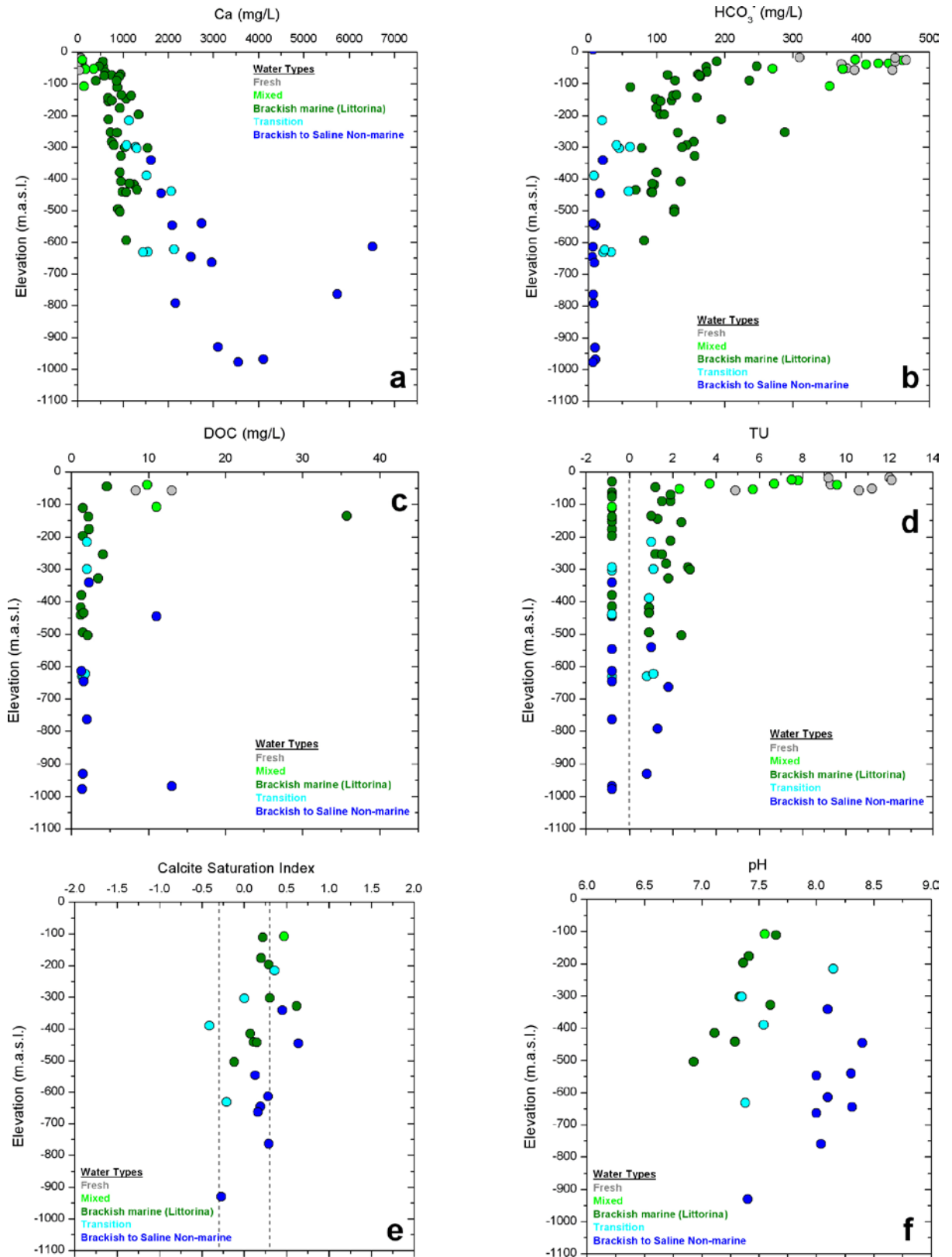
Figure 4-6. *Influence on the carbonate system with increasing depth: a) calcium, b) bicarbonate, c) dissolved organic carbon (DOC), d) tritium (values under detection limit is negative), e) calcite saturation index (uncertainty area of $\pm$ –0.3 is demarcated by the dotted vertical lines), and f) pH.*

The DOC values at depth are expected to be close to the detection limit but generally the values at depths greater than 100 m are between 1 and 5 mg/L with a few exceptions where the values are higher. The reason for these slightly increased values (also found in Laxemar) is not known. Contamination during drilling/sampling, new routines for cleaning the equipment, natural sources such as asphaltite /cf. Sandström et al. 2006b/, Littorina Sea etc have been discussed. It is hoped that additional data from the monitoring programme will help clarify the long-term behaviour for DOC.

In Figure 4-6d, showing tritium against depth, there is a clear trend with <less than 3 TU at depths greater than 100 m, indicating in most cases little or no influence of modern water (cf. discussions on uncertainties in some of the tritium data in section 3.3.1, and also in section 4.9.3).

With respect to pH (Figure 4-6f), apart from one sample taken in borehole KFM06A, the rest of the groundwater samples from the footwall bedrock comprising the target volume (i.e. fracture domain FFM01), and fracture domains FFM04 and FFM05 (not plotted) outside the target volume, have pH values between 8 and 8.5. As expected, pCO_2 in equilibrium with these waters decreases with depth as CO_2 is consumed by: a) microbially-mediated reactions, b) water/rock interaction, and/or c) decreased by mixing with saline waters with very low carbon contents. Most groundwaters are in equilibrium with calcite (Figure 4-6e) /Gimeno et al. 2008/. Groundwaters mostly of brackish marine water type and mainly from the gently dipping deformation zones in the hanging wall, have lower pH values (around 7.5) and higher pCO_2 /Gimeno et al. 2008/ although most of the waters are also in equilibrium with calcite (within the uncertainty range of 0.3 SI units). Studies of fracture filling calcites /Sandström et al. 2008/ indicate only minor recent changes (either precipitation or dissolution), in accordance with the recorded close to equilibrium conditions.

4.1.2 Major ion-ion/isotope plots

Figure 4-7 and Figure 4-8 show a collection of ion-ion/isotope cross plots which can provide additional insight to the origin and evolution of the groundwaters, such as revealing whether the groundwater composition is affected by processes other than mixing.

Sodium shows an overall positive correlation with chloride (Figure 4-7a) which reflects generally that mixing is the main process controlling its composition. In detail, however, two different sodium/chloride trends can be seen, one represented by the brackish to saline non-marine groundwaters (clearly affected by a deeper more saline component), and the other by the brackish marine (Littorina) groundwaters with a maximum up to 5,500 mg/L of chloride. These two mixing trends are also recognisable in the bromide versus chloride plot (Figure 4-8c). In addition, magnesium (Figure 4-7b) and sulphate (Figure 4-8b), both susceptible to reactions (e.g. ion-exchange and/or microbial processes), show a clear contrast between the pre-Littorina brackish to saline non-marine groundwaters (low values from older mixtures between deep saline and more dilute groundwaters) and the more recent Littorina Sea component (comparatively higher values). Furthermore, bicarbonate contents, related to the microbial breakdown of organic material (Figure 4-7c) are as expected, i.e. highest in the dilute near surface waters, but are also significant in the brackish marine waters. This is in contrast with the brackish to saline non-marine waters, which show extremely low values (thus excluding ^{14}C dating of these waters).
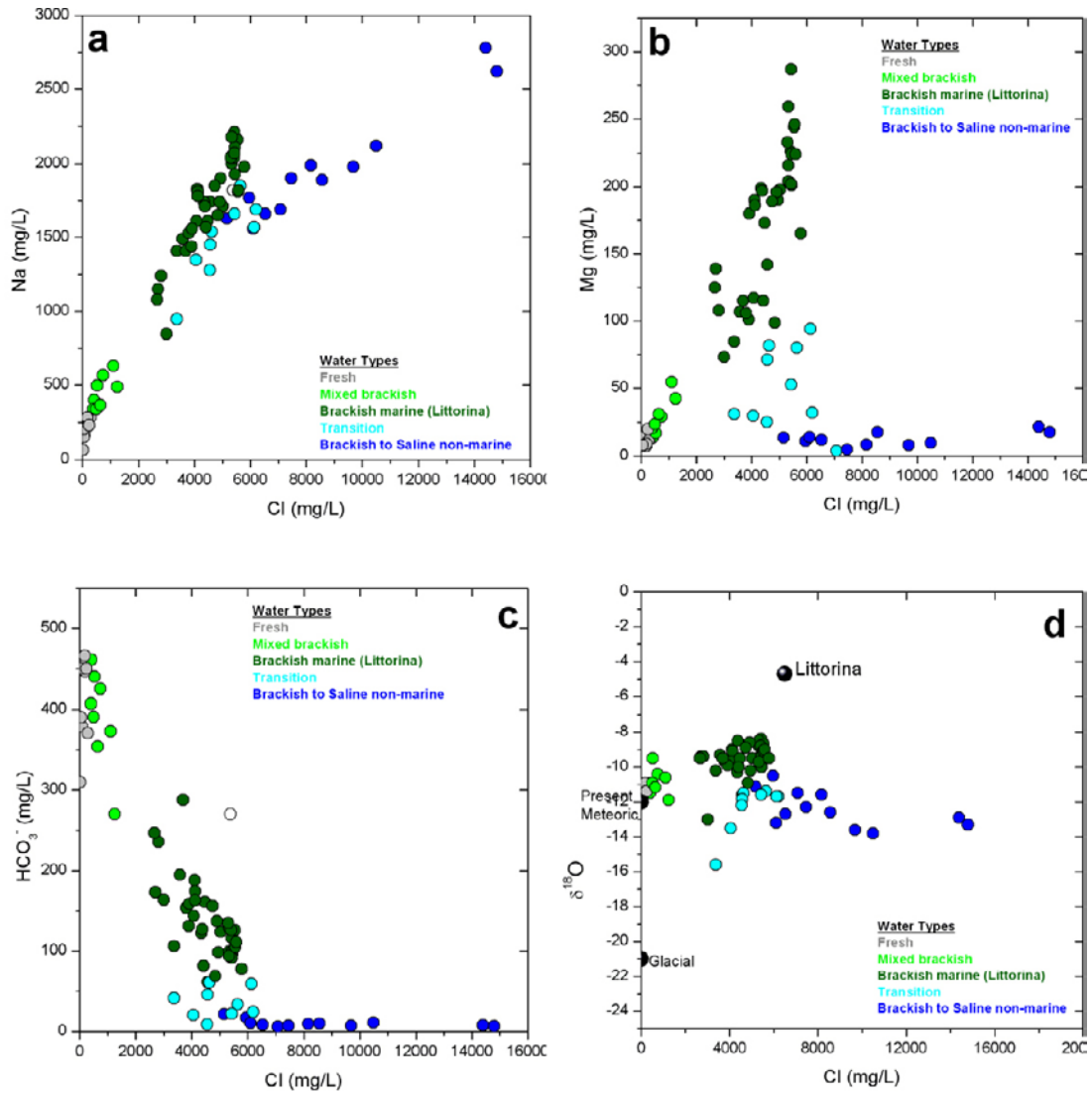
Figure 4-7. *Plots of sodium (a), magnesium (b), bicarbonate (c) and δ¹⁸O (d) versus chloride related to the two main groundwater systems in the Forsmark candidate site.*

The sulphate and sulphide and their variability in groundwaters and bedrock are presented in more detail in /Smellie et al. 2008/. From Figure 4-8b it is clear that the major source of sulphate is marine and mainly associated with the brackish marine water of Littorina type, and to lesser extent in the upper part of the bedrock were recharge type groundwaters have been influenced sometimes by present Baltic Sea waters. Stable sulphur isotope ratios, expressed as $\delta^{34}S$ CDT (Cañon Diablo Troilite), have been determined in sulphate from surface waters and groundwaters. Considering the shallow waters, /Tröjbom et al. 2007/ have made a thorough evaluation of the possible origins of sulphur in the surface water system. It was concluded that atmospheric deposition and oxidation of sulphides in the soil cover constitutes the most important sources, together with marine sulphate.
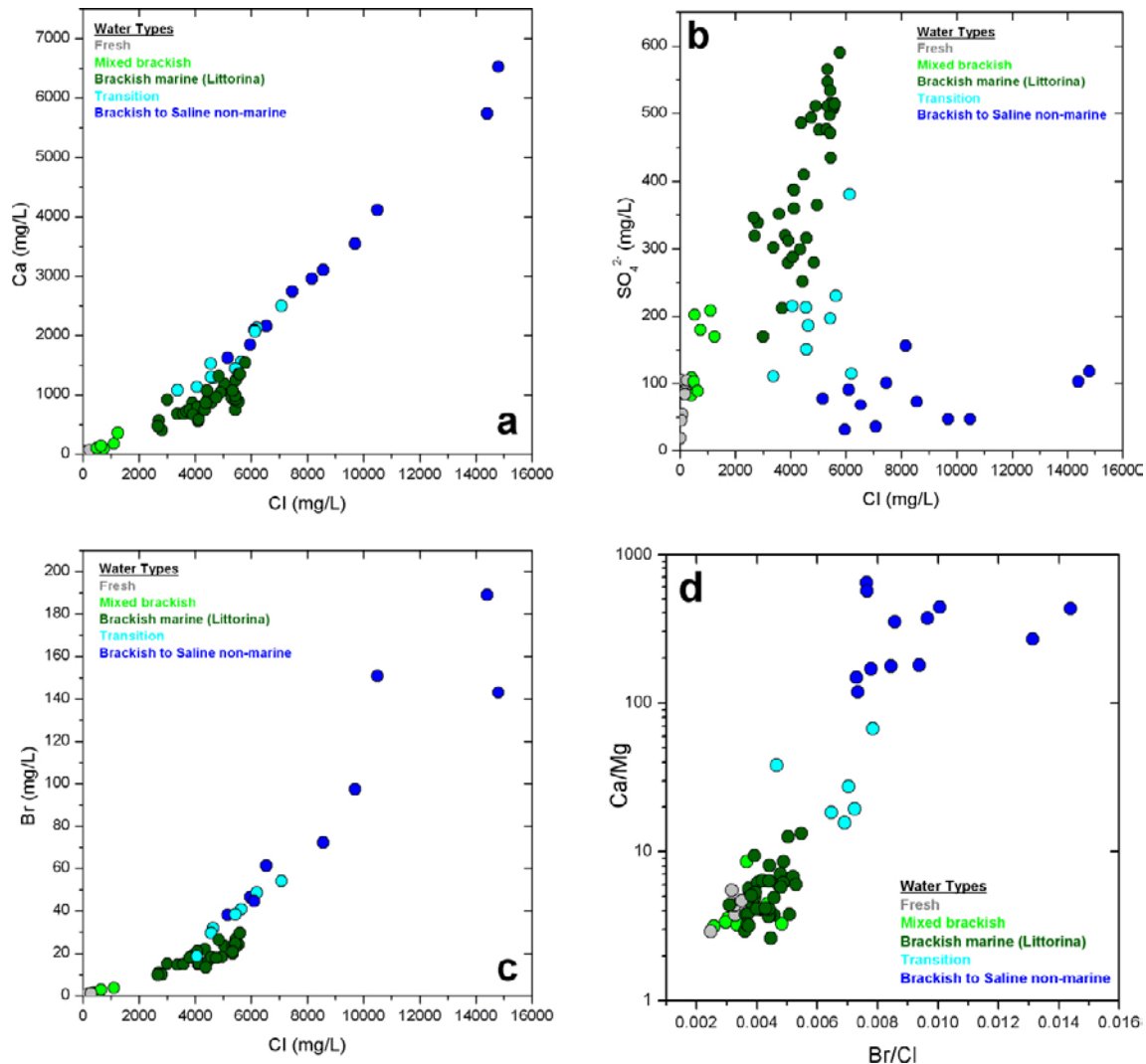
Figure 4-8. *Plots of calcium (a), sulphate (b) and bromide (c) versus chloride, together with an ion ratio plot of Ca/Mg versus Br/Cl. All are related to the main groundwater types that characterise the Forsmark candidate site.*

To better describe possible mixing trends, the sulphur isotope ratios $\delta^{34}S_{(SO4)}$ plotted against chloride content are shown in Figure 4-9. The fresh waters show low sulphate contents and a large variation in $\delta^{34}S_{(SO4)}$ compatible with input from several different sources of which, as mentioned above, oxidised sulphur from sulphides in the soil cover may be one /Tröjbom et al. 2007/. Unfortunately, there are no isotopic analyses of sulphides in the overburden, but $\delta^{34}S$ values of pyrites in fracture coatings have been analysed and show a very large spread in values (5.4–31.5‰ CDT with the majority of samples showing values of less than 17‰ CDT /Sandström et al. 2008/).

With further respect to sulphide, measurements have been carried out in groundwaters from the cored boreholes during the complete chemical characterisation (CCC) programme. These values are generally low (< 0.1 mg/L for the majority of samples) but show a slight increase with depth and a correspondence between sulphide and the number of sulphate-reducing bacteria has been indicated /Smellie et al. 2008/. However, during the subsequent groundwater monitoring programme a number of isolated borehole sections have been resampled at different time intervals. This has shown that some sections have much higher (but usually variable) sulphide contents during the monitoring phase than was recorded during the CCC sampling programme. This variation casts a degree of uncertainty over the sulphide data in general and consequently interpretation should be approached with caution.

70
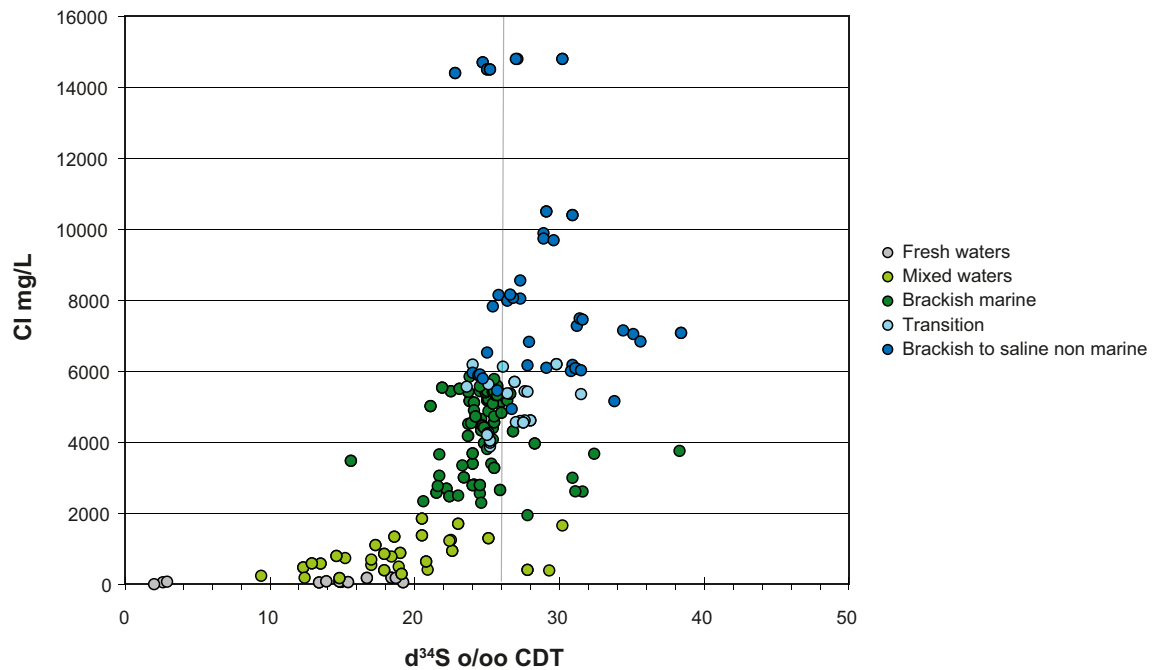
Figure 4-9. *Cloride versus δ³⁴S (CDT) for different groundwaters types at Forsmark based on all data (categories 1–5) but excluding tube samples and samples with more than 15% drilling fluid. The marine value (around 21‰ CDT) is indicated by the lighter grey vertical line.*

The main conclusions from the sulphate and sulphide studies are:

- The major sulphur source in the Forsmark groundwaters is marine in origin, in particular due to the intrusion of Littorina Sea water. However, most of the resulting brackish marine waters show relatively homogeneous $\delta^{34}S_{(SO4)}$ values between 24–26‰ CDT, which is higher than expected for marine sulphate, irrespective of sulphate content.

- The addition of sulphate caused by dissolution and oxidation of sulphides is very limited and seems only to occur at or close to the surface.

- Sulphate reduction mediated by SRB has decreased the sulphate content in the original marine waters and modified their $\delta^{34}S_{(SO4)}$ values. This has occurred during partly open conditions, for example, modification of the Littorina Sea water relatively close to the surface, or in large pools of sea sediments which have not been entirely isolated. At greater depth, sulphate reduction during closed condition have resulted in very low sulphate contents and correspondingly high $\delta^{34}S_{(SO4)}$ values (> 30‰ CDT). SRB also are indicated as active at depth in the Forsmark groundwaters /Hallbeck and Pedersen 2008a/.

- Measurements of sulphide at different sampling occasions have yielded very different results and continued sampling in association with the monitoring programme is needed before more detailed interpretations should be attempted. However, because Fe^{2+} is produced in the system, it is probable that S^{2-} will be controlled by Fe-monosulphide solubility during undisturbed conditions.

- Fracture pyrite of Palaeozoic origin is relatively common, but recent deposition of sulphides has been difficult to identify, therefore suggesting only minor occurrences.

Concluding remarks

There is strong evidence that the Forsmark groundwaters are characterised by two distinct generations of groundwater mixing. All the described plots suggest that the deep brackish to saline non-marine groundwaters represent an origin much older than the last deglaciation. These older trends are preserved in groundwaters from the less water conductive bedrock volumes and also

in the rock matrix porewaters (cf. section 4-8 and /Waber et al. 2008a/. In contrast, at shallower depths and representing the period following the last deglaciation, mixing with recent Littorina Sea waters is widespread in the more conductive parts of the bedrock, disturbing or removing the older groundwater mixing trends.

These two major mixing trends can be clearly illustrated by plotting Ca/Mg against Br/Cl (Figure 4-9d). This figure shows a cluster of young to recent fresh, mixed and brackish marine groundwaters with low ratios, and a change to much older and deeper, brackish to saline non-marine groundwaters at higher ratios. Between these two 'end members' there are several transition groundwaters indicating variable degrees of mixing. Many of the Forsmark samples, therefore, represent groundwaters which contain a component of an old, highly saline non-marine or non-marine/old marine mixing end member that increases in amount with depth.

4.1.3 Depth trends of selected minor ions

Uranium

Elevated uranium concentrations (< 20 µg/L) have been detected in some of the sampled ground-waters at Forsmark (Figure 4-10). These elevated concentrations correspond to a narrow range of chloride concentrations which mostly, but not totally, coincide with the brackish marine (Littorina Sea) groundwaters. As an integral part of the hydrogeochemical studies, but also from a safety assessment viewpoint, the importance of explaining these elevated uranium concentrations was given high priority.

The uranium and its variability in groundwaters and in the bedrock are also discussed in detail in /Smellie et al. 2008, Sandström et al. 2008/, summarised in this report in the redox section 4.3, and commented on in the fracture filling section 4.7.3.
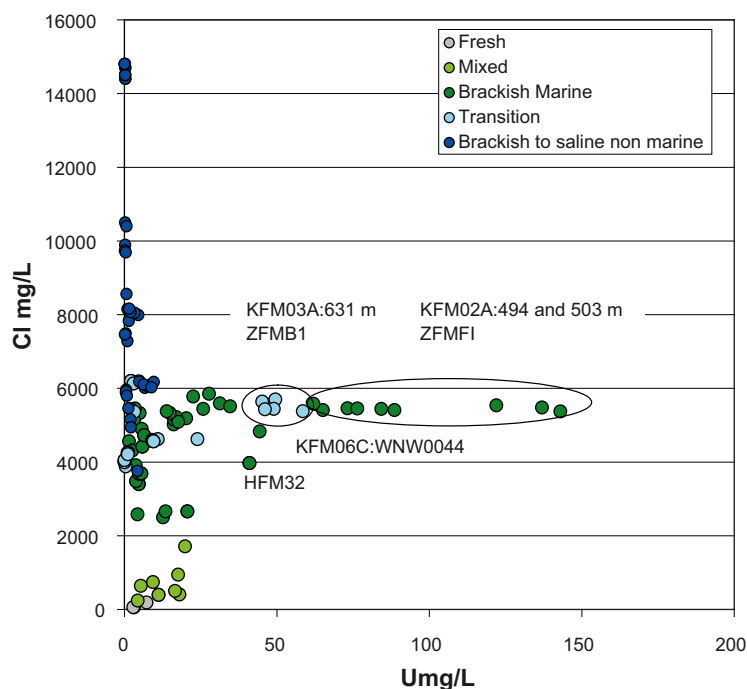

Figure 4-10. *Cloride plotted versus U for groundwaters from Forsmark. A large number of data are plotted for KFM02A around 500 m depth representing groundwaters from the gently dipping deformation zone ZFMF1.*

Phosphate, nitrate and ammonia

Phosphate, nitrate and ammonia can cause stress corrosion of the copper canisters and are therefore of special interest within the site investigation programme.

The phosphate concentrations (PO_4^{3-}) in the Forsmark groundwaters are low due to precipitation (apatite?) and removal by the relatively high Ca^{2+} concentrations. Maximum concentrations (near 0.1 mg/L) are even lower than those detected in other crystalline environments like Simpevarp, Olkiluoto /Pitkänen et al. 2004/ or the Lac du Bonet Batholith in Canada /Gascoyne 2004/. As these environments show, the highest variability and contents of dissolved PO_4^{3-} in the Forsmark area are associated with the near surface groundwaters (with maximum values near 0.1 mg/L), although some very shallow fresh and mixed groundwaters also show relatively high concentrations (from 0.015 to 0.065 mg/L;). The PO_4^{3-} concentrations in deeper groundwaters are always below 0.05 mg/L or even below the detection limit at 0.7 µg/L (Figure 4-11a).
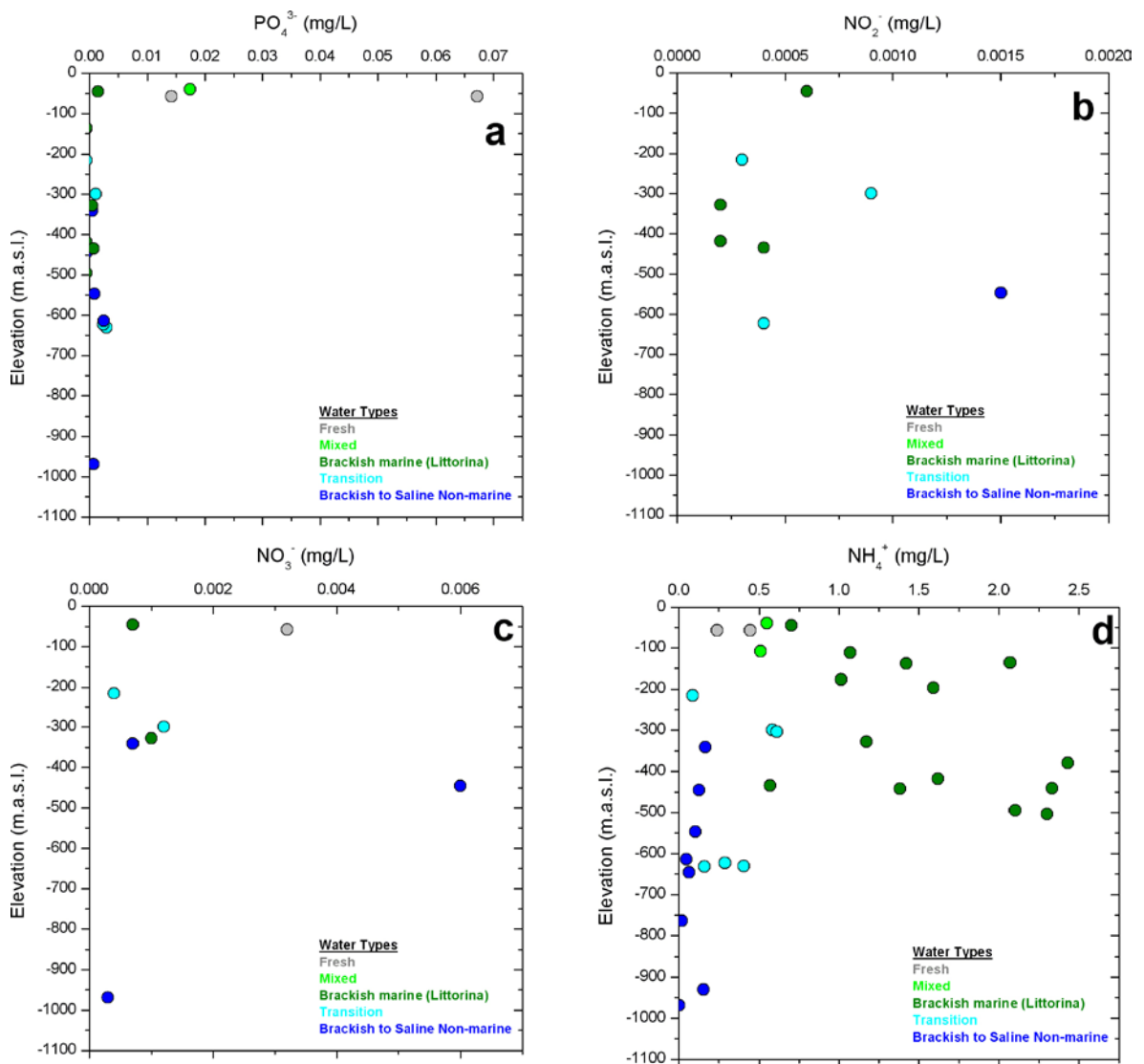
Figure 4-11. *Distribution of: a) phosphate, b) nitrate, c) nitrite and, d) ammonia with depth related to the different groundwater types that typify the Forsmark area.*

Nitrate, nitrite and ammonium nitrogen concentrations show the largest variability and highest concentrations in the near surface groundwaters, achieving values up to 0.48 mg/L for nitrate, 0.02 mg/L for nitrite and 8.7 mg/L for ammonium. Nitrate and nitrite contents are commonly at trace levels which is normal for most natural (non-contaminated) systems /Appelo and Postma 2005/. Maximum concentrations are around 0.0015 mg/L for nitrite and 0.006 mg/L for nitrate (Figure 4-11b and c). The major part of the total nitrogen usually occurs as ammonium or dissolved organic nitrogen /Tröjbom and Söderbäck 2006/ showing a temporal variability due to seasonal variations in biological activity /Berg et al. 2006/.

Compared to other crystalline environments (e.g. in the granitic batholith from Lac du Bonnet, Canada /Gascoyne 2004/) dissolved nitrite and nitrate concentrations in the Forsmark groundwaters are very low. Nitrate levels may be low due to the presence of nitrate reducers, and the lack of nitrite can simply be an indication that it is also being rapidly consumed /Hallbeck and Pedersen 2008a/.

The dissolved NH_4^+ shows a very different pattern from that of NO_2^- and NO_3^-. Although the highest concentrations are also found in the near surface groundwaters (with values up to 9 mg/L), high values are also found in the groundwaters of brackish marine (Littorina) type (almost 2.5 mg/L) even at 500 m depth (Figure 4-11d). The highest NH_4^+ concentrations (between 1 and 2.5 mg/L) are systematically associated with brackish marine (Littorina) groundwaters (Figure 4-11d) where chloride concentrations are between 5,000–5,500 mg/L. The same association is observed also in the Olkiluoto groundwaters /Pitkänen et al. 2004/. These observations indicate that the high NH_4^+ concentrations found in the groundwaters from Forsmark represent an inherited character from their old marine signature. Seawater shows generally low NH_4^+ concentrations (usually well below 0.05 mg/L in the available samples from the Baltic Sea) but marine sediments with organic matter can contain significantly higher contents produced by bacterial activity /Pitkänen et al. 2004 and references therein/. Increased ammonium concentrations with depth in the interstitial waters from sediments of the Baltic Sea have been observed with concentrations frequently ranging from 4 to 16 mg/L /Carman and Rahm 1997/. Therefore, infiltration of the recharging Littorina waters through marine sediments can justify increments in dissolved NH_4^+, although this has to be balanced by decreases with depth due to microbial consumption and ion exchange on clays.

Trace and rare-earth elements

Trace elements and rare-earth (REE) components generally occur in groundwaters at concentrations of less than 1 mg/L /Drever 1997/. The following elements have been analysed within the Forsmark site characterisation programme: Al, B, Ba, U, Th, Fe, Mn, Li, Sr, Sc, Rb, Y, Zr, In, Sb, Cs, Ba, La, Ce, Pr, Nd, Sm, Eu, Gd, Tb, Dy, Ho, Er, Tm, Yb and Lu. Also included are commonly occurring heavy trace elements such as Cu, Ni, Cr, Zn, Pb and Mo even though these may be influenced by contamination related to borehole activities discussed below. The risk of contamination is large also for aluminium, but this is still reported due to its importance for the modelling work; analytical results are, however, very uncertain and their usefulness can be questioned.

From the total trace element inventory, specific groups have been addressed separately depending on their use in understanding particular aspects of groundwater origin and behaviour /Smellie et al. 2008/. For example, to establish accurately the groundwater distribution of certain trace elements of interest to repository performance assessment (e.g. Mo, Ni, Zn, Ba, Sr and REEs) and the mineralogy of the water-conducting fractures sampled, provides the opportunity to calculate their solubility limits and test models of speciation and transport.

In summary, the behaviour of certain trace metals (e.g. Mo, As, Cr, Co, Cu, Pb and Ni) is difficult to evaluate in the Forsmark groundwaters because of:

• Incursion and mixing of different groundwater types at different stages in the past, particularly since the last deglaciation.

• Contamination resulting from borehole activities which may have affected mainly low transmissive fractures characteristic of fracture domain FFM01. Subsequent pumping when sampling may have served to mobilise many of these residual elements resulting in elevated values. This further underlines the importance of adequate pumping prior to sampling to help remove excess trace metals.

• Periodic monitoring of borehole sections where high pumping rates are used to prepare the section for sampling, i.e. by removing three section volumes of water followed by immediate sampling. This activity may also have served to mobilise many of these elements, both residual types from drilling activities and those natural-occurring elements from mixed sources loosely bound along the fracture systems.

• In some cases a groundwater sample characterised as being of good quality, based on major ions and isotopes etc (i.e. categories 1–3), was sampled when the trace element contents had stabilised. There are other cases, however, when the chosen groundwater sample had not achieved stability, therefore suggesting contamination.

The relationship of some metals with uranium was tested to shed some light on the possible origin of the elevated uranium in some of the Forsmark groundwaters (cf. section 4.3 in Smellie et al. 2008). Uranium is naturally often found in association with As, Mo, V (or PO_4); however no obvious correlation was found.

The REE contents in the Forsmark groundwaters are generally low and below detection levels in the deeper groundwaters characterised by saline non-marine waters. From ten cored borehole sections, however, representing depths from 100–500 m, it was possible to analyse the REEs; for the chondrite normalised curves (see Figure 4.2-1 in /Smellie et al. 2008/. Eight of the analysed samples consisted of brackish marine waters, one has a close to fresh water composition (Cl = 640 mg/L, KFM02A: 108 m) and one was classified as brackish non-marine (KFM10A: 215 m). Interestingly, the latter showed the lowest REE contents and only La and Ce were above detection limit. The other samples showed largely similar uniform REE patterns with a slight increase in HREEs (heavy rare earth elements). This is normally interpreted as typical for dominantly carbonate complexation. Sample KFM01D: 253 m elevation deviates from the rest of the samples in having a positive Eu-anomaly. The representativity of the REE analyses seems to be good (apart for Eu for which there was only one collected sample to date) judged from repeated analyses of time series samples.

4.2   Mixing calculations

Multivariate Mixing and Mass-balance Modelling (M3) /Laaksoharju et al. 1999, SKB 2006bd, 2007/ uses the Principal Component Analysis (PCA) method to analyse variations in groundwater compositions so that the mixing components, their proportions, and chemical reactions can be indentified. The PCA method is statistical and identifies the principal components, in terms of linear combinations of the concentrations of those species analysed, that best explains the spread in data. The method quantifies the contribution to hydrochemical variations by mixing of groundwater masses in a flow system by comparing groundwater compositions with identified end-member waters. However, groundwater mixing proportions computed with M3 should be

considered semi-qualitative (i.e. due to the complex influence of mixing and reactions) as evaluations of the groundwater signatures have shown that over- or under-estimations of the actual groundwater signatures can result /Laaksoharju et al. 1999, Molinero et al. 2008/. The choice of end members is crucial for modelling the mixing proportions. Calculated mixing proportions showing a deep saline water component at very shallow depths is an example of model errors introduced when assuming that all end members contribute to the groundwater formation. The uncertainties of the method are described by /Gómez et al. 2008/ and the end member test performed is described in section 4.10. The M3 modelling is discussed in /Gimeno et al. 2008, Gurban 2008, Molinero et al. 2008/. Below, the M3 mixing proportions are shown together with scatter plots indicating the end-member contribution in relation to the resulting water and the end-member mixing proportions in 3D visualisations with a SE-NW view. For the M3 calculations the following end-member compositions were used: Deep Saline-Old Meteoric + Glacial-Littorina-Altered Meteoric and their chemical compositions are given in /Gimeno et al. 2008, Gurban 2008, Molinero et al. 2008/.

Figure 4-12 shows the mixing proportions of Deep Saline water. The water type classification of the Deep Saline water is mainly based on the salinity contents together with the absence of marine indicators such as Mg, K and, in the Forsmark area, also SO_4. The resulting water, Brackish to Saline Non-marine water, contains the largest proportion of Deep Saline (i.e. water up to 35%). The most saline waters with the highest Deep Saline signatures are associated with the deepest samples taken from boreholes KFM07A and KFM09A. These two samples have been collected in deformation zones outside the target volume (i.e. fracture domains FFM04 and FFM05; cf. Figure 2-6). Upconing of the saline water is indicated by the hydogeological modelling and also the chemistry, with the result that the true depth profile is not known in this part of the site. On the other hand, the deepest sample at KFM03, also characterised by a high Deep Saline signature (around 25%), corresponds to a depth of around 960 m (bottom right in Figure 4-12) within the Forsmark candidate area but outside the target volume. This correspond to the series of gently dipping deformation zones including the major ZFMA2 and ZFMF1 gently dipping deformation zones of the hanging wall bedrock segment. From this information it can be concluded that there is a salinity increase with depth and there exists the possibility of higher salinity at even greater depths below KFM03A, coupled to the lower hydraulic conductivity in the part of the footwall bedrock segment (i.e. fracture domain FFM01) under the deformation zones ZFMA2 and ZFMF1 (Figure 4-12).

In Figure 4-13 the Old Meteoric-Glacial end member corresponds to the depleted $\delta^{18}O$ signatures indicative of influx of cold climate water such as glacial meltwater or old meteoric water prior to the last deglaciation. The resulting transition to Brackish to Saline Non-marine water contains the largest proportions of the Old Meteoric-Glacial end member. It can be seen that a high Old Meteoric-Glacial end-member signature (75%) is found in the deepest available sample, collected from borehole KFM03A (960 m) outside the target volume. However, the percussion borehole HFM12 shows a clear indication of Old meteoric-Glacial water close to the ground surface, probably associated with the Eckarfjärden deformation zone, one of the WNW regional zones outside the southern border of the Forsmark tectonic lens. It can be seen in Figure 4-4 the depleted values of $\delta^{18}O$ near Lake Eckarfjärden and the correspondence with the relatively high (31%) glacial water signature computed by M3 (Figure 4-13). This signature is consistent with an independent hydrochemical study by SurfaceNet /Tröjbom and Söderbäck 2006, Tröjbom et al. 2007/, which identified the Eckarfjärden area as a potential discharge zone with deep groundwater signatures (right-hand figure in Figure 4-13). Additional information on the consistency between ChemNet and SurfaceNet hydrochemical interpretation is described in /Molinero et al. 2008/. Deep groundwaters in boreholes KFM07A and KFM09A also show noticeable Old Meteoric-Glacial end-member signatures (> 30%).
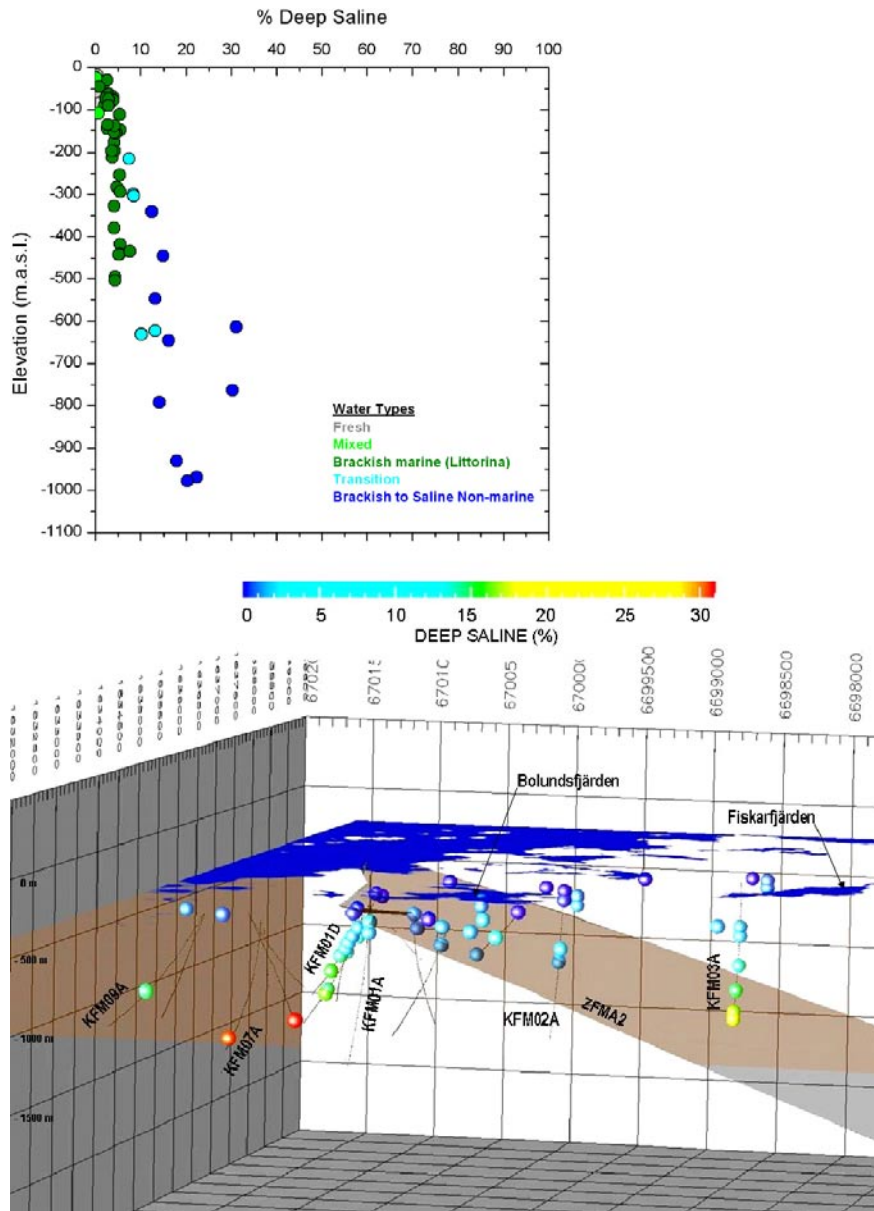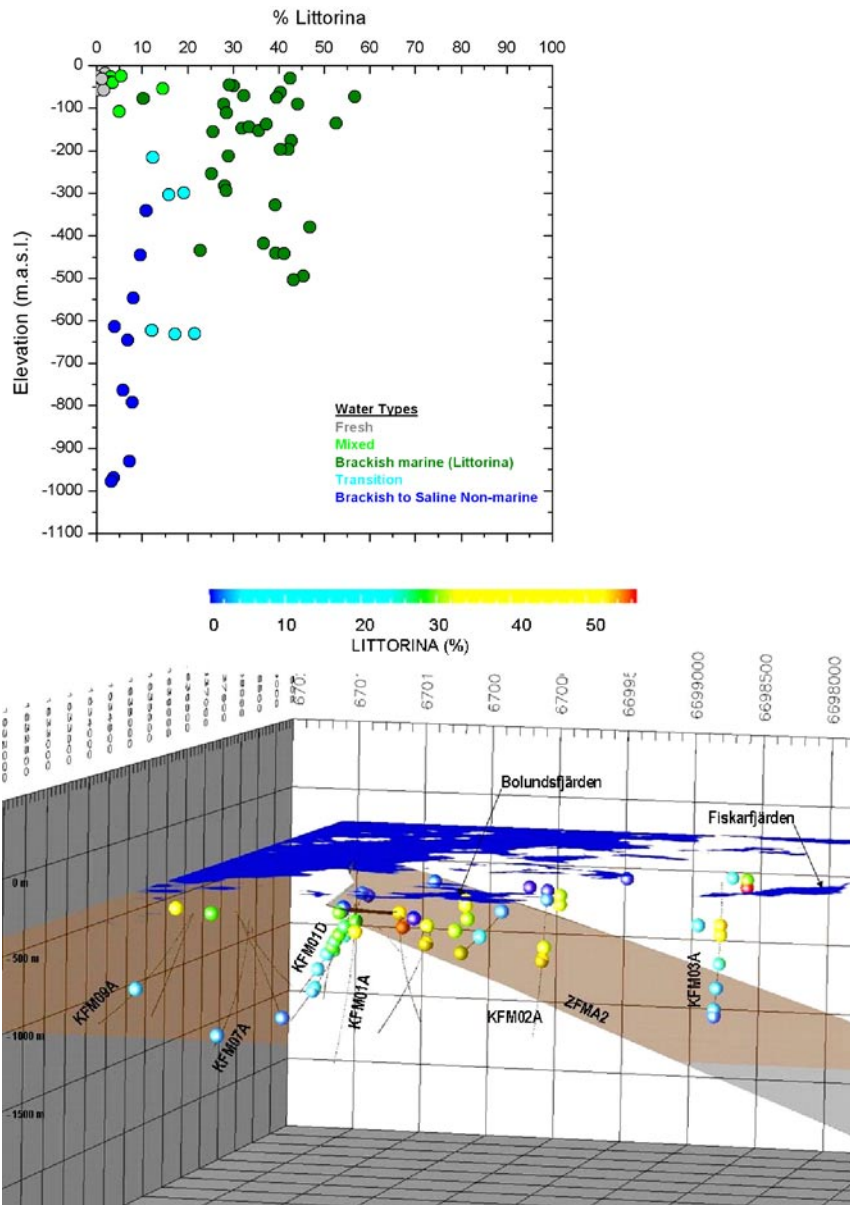
Figure 4-12. *Computed M3 mixing proportions of the Deep Saline end member compared with the resulting water types (top figure) and shown in 3D in relation to the major gently dipping deformation zone ZFMA2 (bottom figure).*
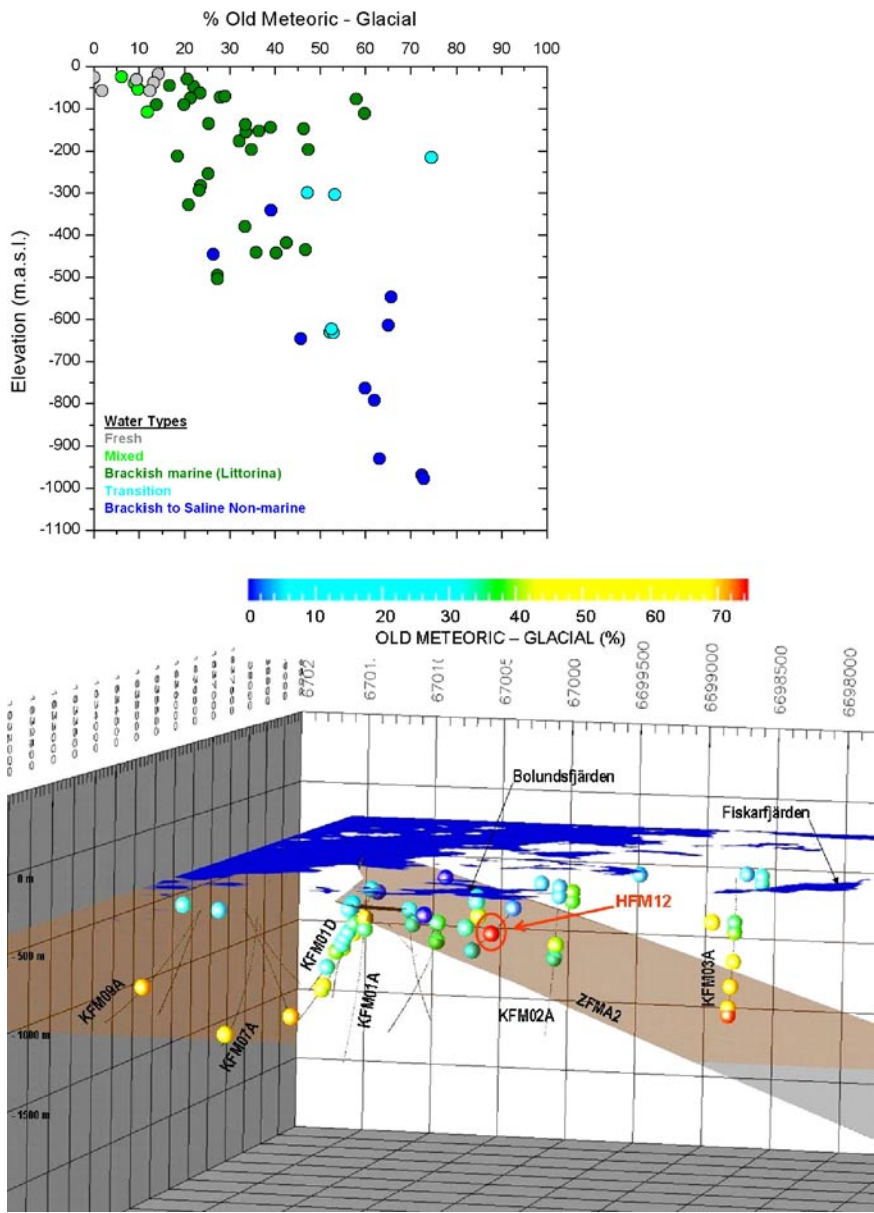
Figure 4-13. *Computed M3 mixing proportions of the Old Meteoric-Glacial end member compared with the resulting water types (top figure) and shown in 3D in relation to the major gently dipping deformation zone ZFMA2 (bottom figure).*

Groundwaters with a Littorina Sea water end-member signature (Figure 4-14) have been detected at depths between 100–600 m, mainly in the hanging wall bedrock, and to a lesser degree (down to 300 m) in the footwall bedrock (i.e. fracture domains FFM02 and FFM01). At depths greater than 600 m in the hanging wall, the gently dipping deformation zones contain groundwater devoid of marine signatures. The Littorina end member corresponds to the high measured magnesium (cf. Figure 4-3) and sulphate values, and the resulting Brackish Marine water from mixing of the Altered Meteoric and Littorina Sea end members should contain the largest proportions of the Littorina Sea end member. Computed Littorina mixing proportions indicates that the M3 model underestimates the actual marine component. This is supported by independent evaluations of Littorina signatures based on chloride and bromide mass ratios, which indicate that the M3 model could underestimate the actual marine signature in the groundwaters /Molinero et al. 2008/. This is explained by the modification of the original Littorina Sea signature (used as an end member) by different reactions, such as microbial sulphate reduction and production of bicarbonate etc.

Figure 4-14. *Computed M3 mixing proportions of the Littorina end member compared with the result-ing water types (top figure) and shown in 3D in relation to the major gently dipping deformation zone ZFMA2 (bottom figure).*
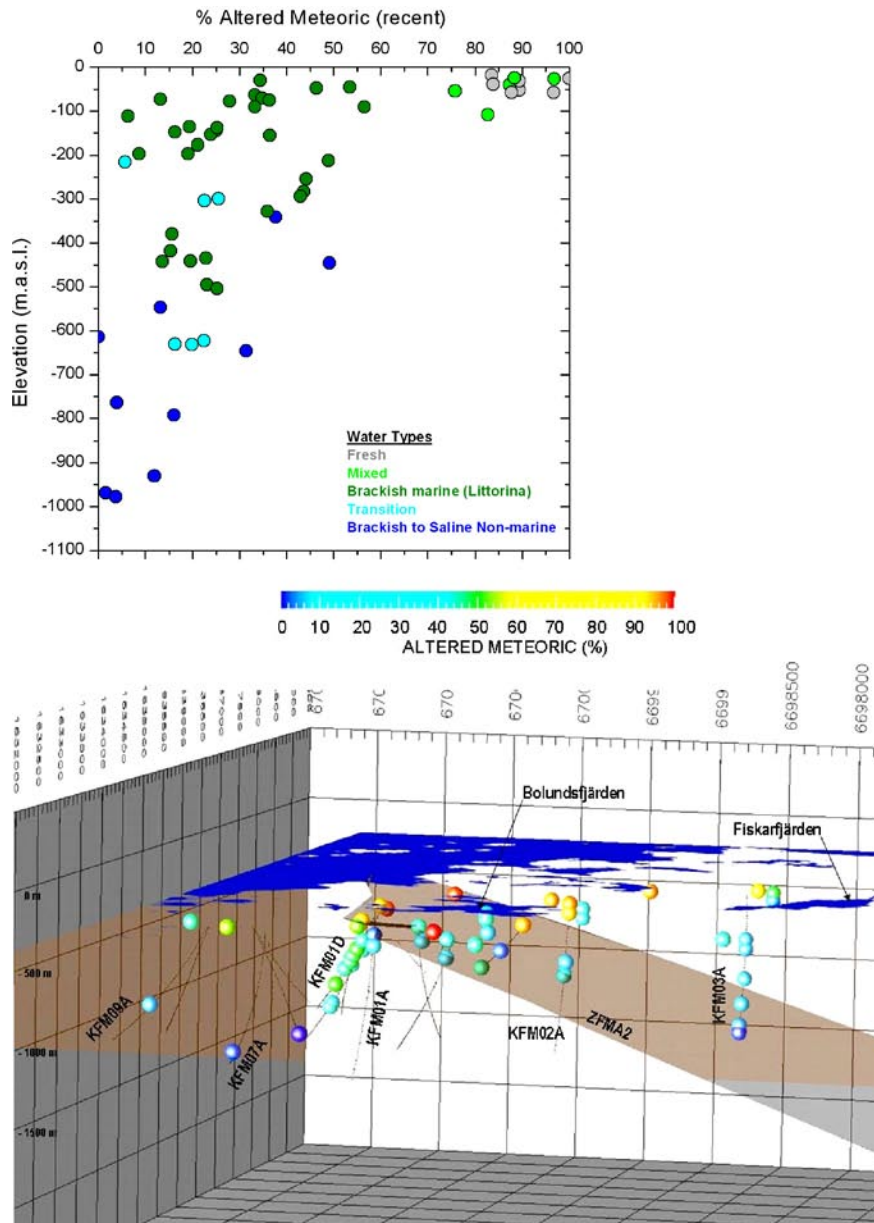
Figure 4-15 shows the mixing proportions of the recent Altered Meteoric end member. The water samples with an Altered Meteoric end member portion more than 80% correspond generally to waters with measurable tritium contents (restricted to the first 100–200 m, mainly in the upper footwall bedrock; i.e. fracture domain FFM02). This means that the dilute water constitutes a very active hydrogeological system, developed through the subhorizontal open and highly conductive fractures existing in the upper part of the footwall bedrock, which is respon-sible for the shallow bedrock aquifer in the Forsmark area. As expected, the resulting 'Fresh' and 'Mixed' waters show large proportions of the Altered Meteoric end member.

Figure 4-15. Computed M3 mixing proportions of the recent Altered Meteoric end member compared with the resulting water types (top figure) and shown in 3D in relation to the major gently dipping deformation zone ZFMA2 (bottom figure).

The above information shows that despite some reservations of underestimating the groundwater marine component, the M3 calculations support interpretations of measured ions and isotopes and can be used to indicate major features such as the groundwater origin in terms of relative mixing proportions and the penetration depth or location of different groundwaters. This allows focus on specific areas of significance to the site characterisation and eventual performance assessment analysis. These results can be checked and supported by various types of independent mixing models /Molinero et al. 2008/ and can be used as an important tool for establishing the site boundary conditions as supporting integration with hydrogeological modelling.

80

4.3 Redox modelling

To evaluate the redox system is one of the most important requirements for repository safety assessment, but also one of the most complicated tasks in hydrogeochemistry /Auqué et al. 2008/. For the analyses of the site investigation data, an integrated modelling approach was applied where hydrogeochemical information was combined with mineralogical and microbiological information /Gimeno et al. 2008/. However, as a first step, the results from the actual measurements of Eh and redox-sensitive elements (i.e. Mn, Fe, S and U) are discussed. Subsequently, these results have been integrated with the results obtained from redox pair calculations, speciation-solubility calculations and microbiological analysis to identify the main controls of the redox state in groundwaters.

4.3.1 General trends of measured Eh and redox sensitive elements

Potentiometric Eh measurements have been performed in most of the sections sampled for Complete Chemical Characterisation (CCC). Such measurements can be subject to both technical and interpretative problems. However, over the last 25 years, SKB has developed methodologies for the measurement of this parameter /Auqué et al. 2008/ and the results obtained provide, at the very least, useful information for the study of the complex redox system /Gimeno et al. 2008/.

Eh values measured at Forsmark range from −143 to −281 mV, and their distribution with depth is shown in Figure 4-16 where the scarcity and heterogeneous distribution of the data are obvious. This heterogeneity with depth does not seem to reflect trends observed in other crystalline systems (e.g. in Palmottu, where a similar methodology for Eh measurement was used) and in most other aquifers where a regular and marked decrease of redox potential is observed as the residence time and depth of the waters increase /e.g. Drever 1997, Blomqvist et al. 2000/.

However, when the different groundwater types are distinguished (right-hand Figure 4-16) it is clear that the brackish to saline non-marine waters (4 samples) show generally low Eh (< –240 mV) in the less water conductive part of the system, from 300 m depth down to 1,000 m. In contrast, four out of five brackish marine (Littorina-type water) samples show values between –140 to –200 mV, extending down to 600 m in the more conductive part of the system. The exception is KFM10A showing a value of –256 mV. The relation between Eh and groundwater types may therefore be more relevant than any depth trend Figure 4-16.
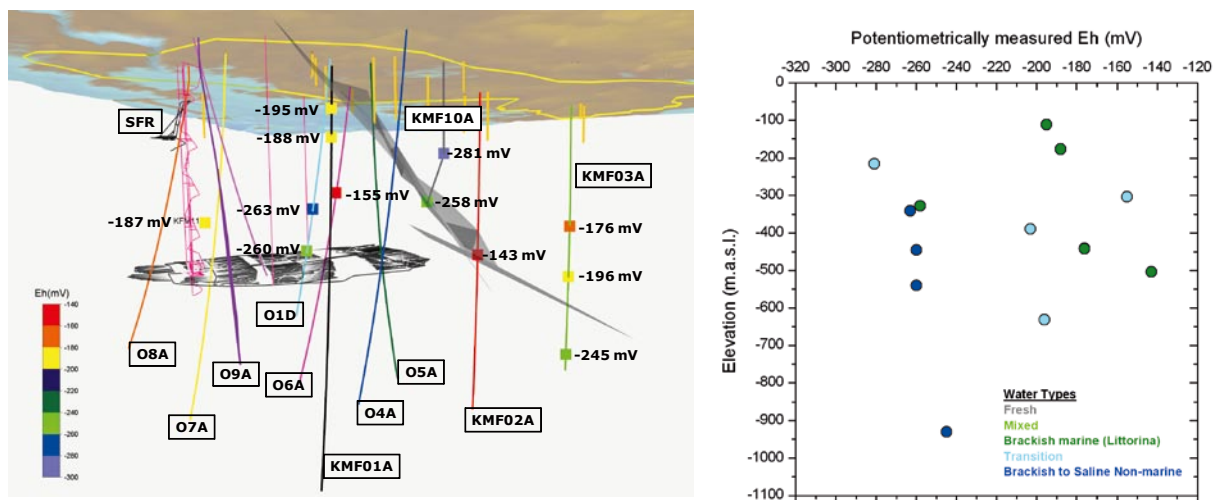
***Figure 4-16.*** *Left diagram: 3D plot of the site with the available Eh values superimposed on a simplified sketch of the system showing the position of the boreholes, the major gently dipping deformation zone ZFMA2 and the schematic layout of the repository (horizontal grey structure). Right diagram: Distribution of potentiometric Eh measurements with depth subdivided into the main groundwater types.*

81

Iron, manganese, sulphide and uranium concentrations do not show a clear trend variation when plotted with the chloride concentrations. This is mainly due to the wide range of concentrations of these elements in the brackish marine (Littorina-rich) groundwaters with up to 5,500 mg/L Cl, and where also the maximum concentrations of these elements are found. Therefore, instead of plotting these elements against chloride, their distribution against depth and groundwater types is more useful Figure 4-17. The first interesting observation is the lack of any clear depth dependence, and the second is that the highest values (over one order of magnitude in most cases) are associated with the brackish marine groundwater types mainly from water-conducting fractures in the upper part of the footwall bedrock (i.e. including fracture domain FFM02) and also from the series of gently dipping deformation zones in the hanging wall bedrock.

Ferrous iron values below 200 m depth are always less than 3 mg/L except for the high values in KFM10A at 328.08 m depth (section 478–487.5 m) with a range of concentrations from 7.4–15.4 mg/L (Figure 4-17a).

Manganese contents are low (< 0.5 mg/L, Figure 4-17b) in the brackish to saline non-marine groundwaters at depths typical for fracture domain FFM01 in the footwall bedrock and the groundwaters from fracture domains FFM04 and FFM05 outside the target volume. The brackish marine groundwaters, in contrast, have very high manganese contents, not only in the
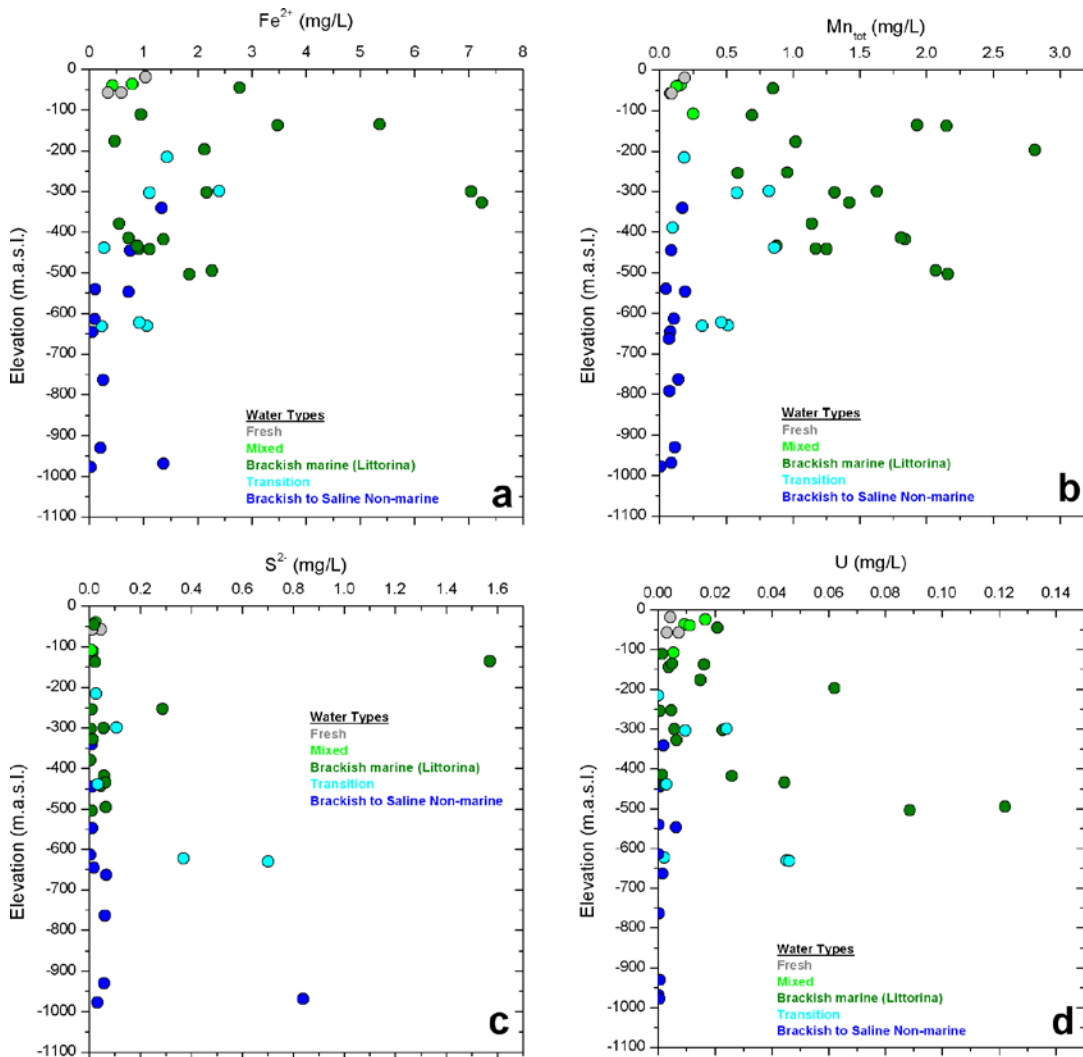
Figure 4-17. Distribution of Fe^{2+} (a), Mn_{tot} (b), S^{2-} (c) and U (d) with depth in the Forsmark area groundwaters (groundwater categories 1–4 have been plotted).

shallow part of the system, but also down to 500 m depth which is atypical for most investigated granitic systems. There is no clear correlation between Mn^{2+} and Fe^{2+} but the brackish to saline non-marine groundwaters show generally low contents of both elements, while the levels are, as mentioned above, significantly higher in the brackish-marine groundwaters.

The sulphide measurements have been difficult to evaluate due to uncertainties in measured contents. Except for two samples in HFM19 at 150 m depth (with S^{2-} about 1.5 mg/L), S^{2-} contents in groundwaters from the surface down to 600 m depth are very low (even below detection limit) (Figure 4-17c). During the ongoing groundwater monitoring programme much higher sulphide contents (> 1 mg/L) have been measured in some sections, whereas others show little difference or only a moderate increase in sulphide. The explanation for this is not clear; there are indications that the CCC sampling may produce low values due to large disturbances related to drilling and flushing /Hallbeck and Pedersen 2008a/. Equally, the very high values measured during monitoring may also be a result of disturbances and mixing of different waters. More measurements and especially time-series data are essential for understanding this very complex system.

Uranium shows variable concentrations, but these are usually higher in the brackish marine and transition water types /Smellie et al. 2008/. The variation is large; from a few µg/L up to 143 µg/L U. The most elevated uranium concentrations correspond to a narrow range of chlorinity coinciding with the brackish marine (Littorina Sea) groundwaters or transition samples from the boundary between the brackish marine and brackish non-marine groundwaters (Figure 4-17d). At depths below 650 m the uranium concentrations decrease dramatically. Resampling of the groundwater sections (i.e. during the monitoring-programme) shows that high uranium values remain high or become even higher.

As an integral part of the hydrogeochemical studies, but also from a safety assessment viewpoint, the importance of explaining these elevated uranium concentrations became an important priority. Several different hypotheses have emerged which have been individually addressed in /Smellie et al. 2008/.

The large variability in the uranium concentrations in the groundwaters and the detection of elevated uranium concentrations in some fracture coatings (up to 2,300 ppm), led to the conclusion that in situ water/mineral interactions are important to explain the highest uranium values at depth in the groundwater /Smellie et al. 2008, Sandström et al. 2008/. However, it has also been concluded that the high uranium contents are only found in groundwaters with Eh higher than –200 mV and HCO_3 contents more than 30 mg/L (and in most cases above > 50 mg/L), and solubility calculations show that a stable U(VI)-carbonato complex is probably responsible for the higher concentrations observed in these waters.

4.3.2   Redox pair modelling

In this section, the measured electrode Eh values are compared with independently calculated values, and/or are tested and confirmed using other data. This was carried out to: a) confirm or support the redox field measurements, and b) confirm the redox pair(s) believed to control the redox conditions in the groundwater. The redox pairs that have been analysed are the dissolved SO_4^{2-}/S^{2-} and CO_2/CH_4 redox pairs, and the heterogeneous couples $Fe^{2+}/Fe(OH)_3$, $HS^-/S_{(c)}$, SO_4^{2-}/FeS_{am} and $SO_4^{2-}/$ pyrite /Gimeno et al. 2008/.

PHREEQC, and the thermodynamic data included in the WATEQ4F database, have been used for the calculations, except in the case of the heterogeneous pair $Fe^{2+}/Fe(OH)_3$ for which three different sets of log K values have been used for the solid phase, /see SKB 2007/. These are: a) the set of values proposed by /Nordstrom et al. 1990/ corresponding to amorphous to microcrystalline hydrous ferric oxides, HFOs, or ferrihydrites (log K = 3 to 5,); b) the value derived from the calibration proposed by /Grenthe et al. 1992/ for a wide spectrum of Swedish groundwaters (log K = −1.1 for a crystalline phase such as hematite or goethite); and c) the value of log K =

1.2 defined by /Banwart 1999/ using the same methodology as /Grenthe et al. 1992/ but working with groundwaters from the Äspö Large-scale Redox Experiment (REX) /SKB 2007, Banwart 1999/. The redox potential corresponding to the $Fe^{2+}/Fe(OH)_3$ heterogeneous redox pair has been obtained in all these calculations using the already-mentioned equilibrium constants and the Fe^{2+} activity calculated with PHREEQC. Alternatively, this redox potential has also been calculated from the calibration model defined by /Grenthe et al. 1992, Banwart 1999/ as a function of pH and the total concentration of Fe^{2+}. The results are summarised in Figure 4-18.

As already reported in /SKB 2007/, the Eh values obtained with the $Fe^{2+}/Fe(OH)_3$ redox pair considering a microcrystalline $Fe(OH)_3$ are more oxidising than the electrode potentials, and therefore they are not included in the plots.

The Eh values calculated with the $Fe^{2+}/Fe(OH)_3$ redox pair using the calibration of /Grenthe et al. 1992/ (or the corresponding equilibrium constant) are in good agreement with the Eh values measured in two deep samples from KFM03 (930.5 m and 631.9 m; Figure 4-18a). For the rest of the samples, this calibration gives more reducing values than those measured. This lack of agreement is clearly seen in Figure 4-18a.
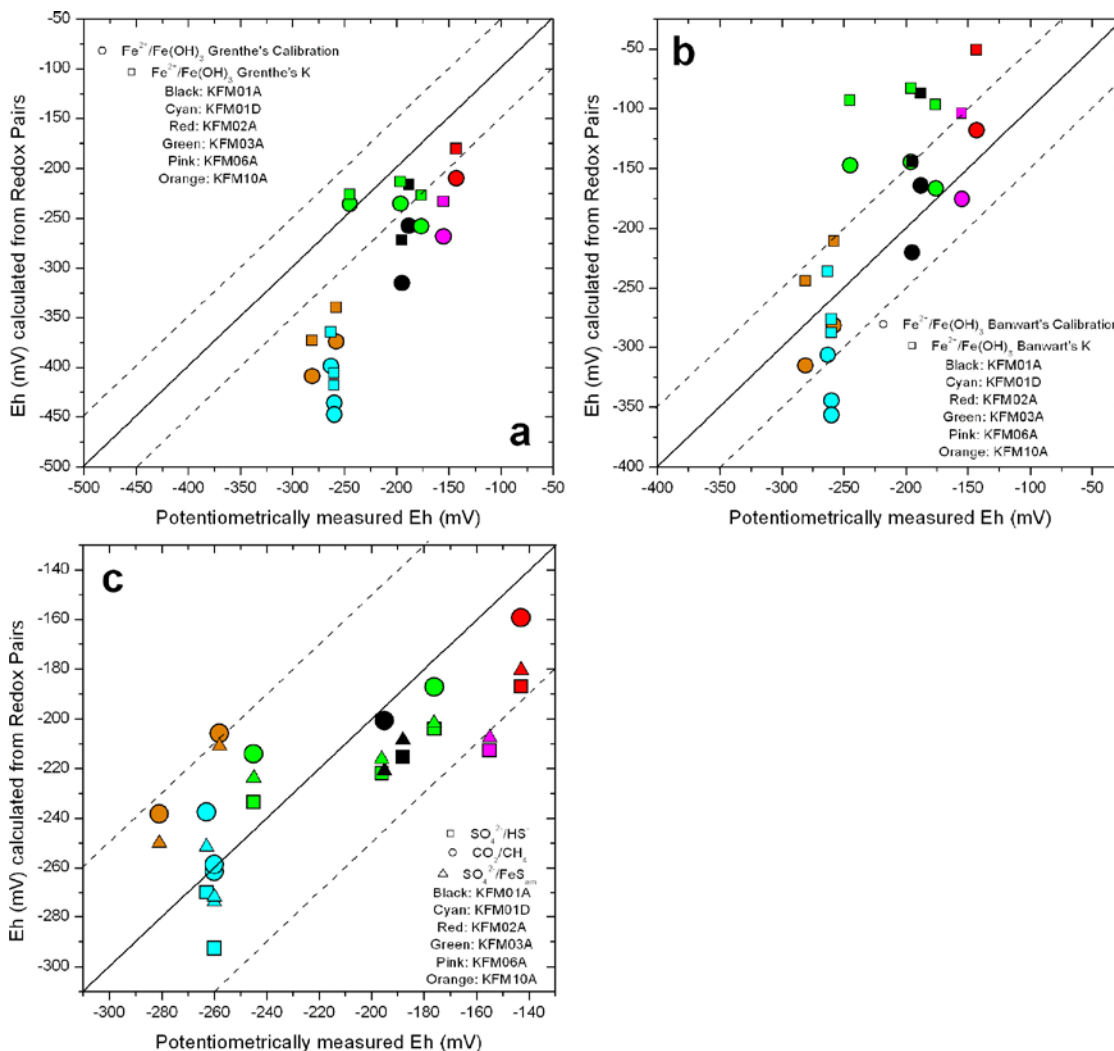
Figure 4-18. *Comparison of the Eh values potentiometrically measured with Chemmac and the Eh values calculated using the different redox pairs. (a) and (b) panels: $Fe^{2+}/Fe(OH)_3$, and (c) panel, SO_4^{2-}/HS^-, SO_4^{2-}/FeS_{am} and CO_2/CH_4. The dashed lines indicate the accepted range of Eh variability of ± 50 mV /e.g. Garrels and Christ 1965, Kölling 2000/.*

On the contrary, the Eh calculated with the same redox pair and using the calibration proposed by /Banwart 1999/ (or the corresponding equilibrium constant) is in good agreement (Figure 4-18b) with all measured values in the brackish groundwaters except for the two deepest samples from borehole KFM03A (mainly the deepest saline groundwater). This suggests that the redox state of the brackish to saline groundwaters could be controlled by different iron oxyhydroxides (or by iron oxyhydroxides with a different degree of crystallinity).

The sulphur redox pairs show, in general, good agreement with the potentiometrically measured Eh values (Figure 4-18c). The results obtained with the homogeneous SO_4^{2-}/HS^- pair and the heterogeneous SO_4^{2-}/FeS_{am} redox buffers agree very well with the measured ones (as also found in Laxemar) /SKB 2004, Gimeno et al. 2008/, usually better than with the redox buffer $SO_4^{2-}/pyrite$.

Speciation-solubility calculations (ferrous iron monosulphide equilibrium /Gimeno et al. 2008/) and microbiological data /Hallbeck and Pedersen 2008a/ support the influence of the sulphur system in the redox control of the groundwaters in Forsmark.

Finally, Eh values obtained with the non-electroactive pair, CO_2/CH_4, are also in fairly good agreement with measured values (within a range of ± 50 mV). In fact, the homogeneous sulphur and the methane redox pairs define a range of Eh, and the middle of this range is always represented by the heterogeneous SO_4/FeS_{am} pair (Figure 4-18c).

The sulphur and the CO_2/CH_4 redox pairs used here provide similar potentials (within the usually accepted uncertainty range of ± 50 mV), which is to be expected as the redox 'windows' for these redox pairs are very close.

4.3.3 Summary of the redox systems

The number of samples with representative and complete data for the analysis of the redox system (Eh values, Fe^{2+}, S^{2-}, Mn, U, microbial and mineralogical data) have increased during the hydrogeochemical programme, especially in the number of Eh determinations, but the amount of data are still very low. Integrated evaluation shows that the rock/water system (including microbial activity) maintains a buffer capacity that ensures a reducing character at depths greater than 100 m /Laaksoharju et al.2008/. This conclusion holds true even considering some problems with the data. The analyses performed have confirmed that sampling (or drilling-induced) perturbation may have influenced the original redox conditions of the hydrochemical system /Gimeno et al. 2008/. Examples include oxygen intrusion and precipitation of amorphous iron oxyhydroxides, modification of Eh or alkalinity by drilling waters, and the increase in dissolved uranium contents, or changes in sulphide contents, caused by one or more of these disturbances.

The available information on the redox system is summarised below.

The iron system is most clearly affected by drilling and sampling disturbances. For example, recent and detailed mineralogical determinations in borehole KFM02A indicate the presence of fine-grained amorphous to poorly crystalline phases (including some other, more ordered, structures, e.g. goethite) induced by drilling /Dideriksen et al. 2007/. However, most of the Eh values determined in brackish groundwaters (at depths between 110–646 m) seem to be controlled by the occurrence of an oxidised iron phase with an intermediate crystallinity, such as that considered by /Banwart 1999/ in the Äspö REX Experiment. This intermediate phase would represent a recent microcrystalline iron oxyhydroxide recrystallised from an amorphous one.

The presence of an intermediate iron oxyhydroxide with higher solubility than a truly crystalline phase is considered possible in these brackish groundwaters if a brief oxidising disturbance has taken place. This supports the result obtained from the redox pair calculations /Gimeno et al. 2008/.

In the deeper saline groundwaters this situation has not been detected. The redox potential measured in the deepest groundwaters in Forsmark is one of the most reducing in the system, and is in agreement with the modelled value derived according to /Grenthe et al. 1992/. This indicates that the Eh value of these groundwaters is undisturbed and appears to be controlled by a clearly crystalline iron oxide such as hematite.

With respect to the *manganese system*, low total manganese contents and undersaturation with respect to rhodochrosite are typical for saline Forsmark groundwaters, as also observed in many other granitic groundwater systems. However, brackish marine groundwaters with an important Littorina component usually have high manganese concentrations and reach equilibrium with respect to rhodochrosite. This is very uncommon in other granitic systems in the Fennoscandian Shield unless the Littorina component happens to be in the same range as that at Forsmark /Pitkänen et al. 2004/. This suggests that the high manganese contents and the equilibrium with rhodochrosite in brackish marine groundwaters are a characteristic that may have been imposed by the superficial marine environment prevailing during the Littorina stage, involving microbial activity in the sea floor sediments. In addition, measureable manganese contents provide independent support for reducing conditions. Furthermore, manganese reducing bacteria have been idenitified in most of the groundwater samples analysed for microorganisms (cf. section 4.4).

The sulphur system is important for the general understanding of the redox processes in Forsmark groundwaters. Studies of the sulphate contents in the groundwaters show decreasing values with depth and the highest sulphate values are associated with the presence of brackish marine groundwaters of Littorina-type whereas the brackish to saline non marine groundwater are low in sulphate (cf. section 4.1). However, the SO_4/Cl ratio is less than expected for marine waters. This, in combination with the sulphur isotope data ($\delta^{34}S$), which shows values higher than marine signatures (+21‰ CDT), suggests some modification caused by SRB. These bacteria have also been identified in most of the boreholes at Forsmark, although the numbers of SRB were very low in some of the samples /Hallbeck and Pedersen 2008b, Smellie et al. 2008, section 4.4/. In conclusion, this means that sulphide is, or has been, produced at various depths in the groundwater system, although the available data do not allow quantitative estimates of its production over time.

Actual measurements of sulphide indicate a complex pattern with evidence of perturbations (mainly anthropogenic) in the original sulphide contents deduced from the increases observed with time in most of the resampled and monitored sections (additional data are not included in the modelling). Based on the modelling of stage 2.3 data, precipitation of "amorphous" monosulphides occurs only locally (mainly associated with deformation zones). In the brackish marine groundwaters between 220 m and 600 m depth, dissolved sulphide contents are low, possibly due to localised precipitation of monosulphides in ferrous iron-rich environments /Gimeno et al. 2008/. Another possibility is that the measured sulphide may be too low due to flushing in connection with drilling and sampling /Hallbeck and Pedersen 2008a/, making interpretations based on present data uncertain.

With respect to *the uranium system*, the simplest explanation to the available data is that the elevated dissolved uranium contents detected in the Forsmark brackish marine groundwaters associated with the deformation zones, are related to local uranium anomalies or mineralisations in contact with these groundwaters. Limited mineralogical data seem to confirm this point /cf. section 4.7, Sandström et al. 2008/.

Speciation-solubility calculations support this conclusion and indicate that the elevated uranium contents are the result of two factors: (a) the solubility control exerted by an amorphous (and very soluble) uranium phase present in the system, and (b) the redox system which supports uranium complexation and reequilibrium depending on Eh (–200 to –180 mV) and dissolved carbonate.

High uranium groundwaters in Forsmark have a range of uranium concentrations that span one order of magnitude. This variation could be justified easily by equilibrium situations under slightly different conditions. Within the Eh and alkalinity ranges that characterise the Forsmark

groundwaters, uranium speciation is very sensitive to minor modifications in these parameters because they affect the extent of uranium carbonate complexation and, therefore, the solubility of the solids. This is important when considering the possible modification of the natural conditions undergone by these groundwaters. The alteration of an originally more reducing environment, and/or the increase of dissolved carbonate (e.g. by mixing with drilling waters), could have caused the increase in uranium-carbonate complexation enhancing the dissolution of uranium phases and increasing the contents of dissolved uranium with respect to that originally present in the system.

4.4 Microorganisms

4.4.1 Introduction

Microbiology included determination of the total number of cells (TNC) and concentration of adenosine-tri-phosphate (ATP). Cultivation methods consisted of aerobic plate counts and most probable number (MPN) determinations of anaerobic microorganisms including nitrate-reducing bacteria (NRB), iron-reducing bacteria (IRB), manganese-reducing bacteria (MRB), sulphate-reducing bacteria (SRB), acetogenic bacteria (AA, HA) and methanogens (AM, HM), /Hallbeck and Pedersen 2008ab/. A degree of uncertainty in the data may have resulted from the effects of drilling and sampling that have not been possible to quantify; sampling techniques and uncertainties are presented in section 3.3.2, in this report.

4.4.2 Characterisation of microorganisms

Size and activity of microbial populations

Investigations of the two different biomass parameters TNC and ATP in groundwaters from the Fennoscandian Shield have previously shown good agreement between these two parameters /Eydal and Pedersen 2007/. Similar data from the site investigation in Forsmark also showed very good agreement with a correlation at p = 0.002 /Hallbeck and Pedersen 2008a/. When plotted, these data show one group of data that has high TNC and ATP values and another group with lower TNC and ATP values (Figure 4-19). The highest ATP and TNC values were found in borehole KFM10A at 328 m depth, followed by the 445 m section in KFM01D (Figure 4-20). In fact, these two sections had stacked MPN values that were the highest found during the site investigations carried out in Forsmark (Figure 4-20) and in Olkiluoto, Finland /Pedersen et al. 2008/. Comparing TNC and ATP in the Forsmark groundwaters shows no clear relation with the groundwater types which is expected, since the microbial population is regulated by the available energy, which is not directly related to the groundwater types found at depth.

Diversity and dominating microbial groups

The microbial populations in the two sections with the highest stacked MPN values, KFM10A at 328 m depth and the 445 m section in KFM01D, consisted of auto- and heterotrophic acetogens, and iron-, manganese- and sulphate-reducing bacteria. This diversity distribution is found in most of the samples but with different values. There are some exceptions from this pattern; the shallow samples in KFM01A at 112 and 176 m depth and the samples from KFM06A at 302 m and 645 m depth, have high numbers of IRB and MRB, but close to zero numbers of SRB. The opposite is found in the deepest sections in borehole KFM03A at 930 m and 978 m depth with close to zero numbers of IRB and MRB, but with the presence of SRB. The dominating group in all sections is the acetogens. This group of organisms produces acetate, either from organic compounds in combination with production of hydrogen gas, or in an autotrophic way from carbon dioxide and hydrogen gas.

Acetate is an excellent carbon and energy source for most microorganisms. Autotrophic production of acetate has been suggested as a base for subsurface ecosystems that are independent of organic material supply from photosynthesis /Pedersen 2001/.
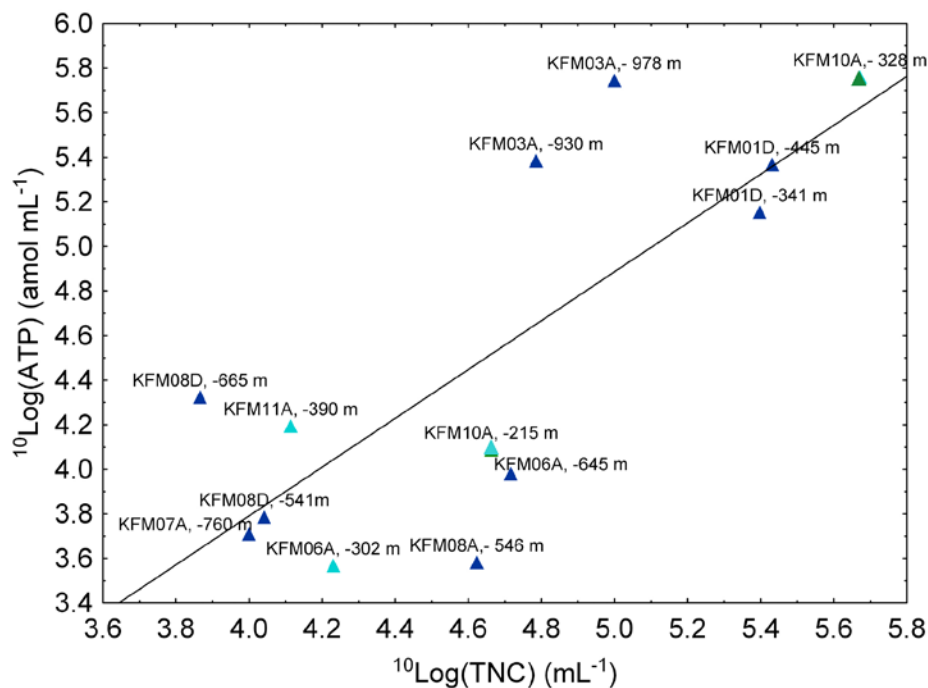
Figure 4-19. *The relation between ^{10}log total number of cells (TNC) and ^{10}log (ATP) in relation to the groundwater types. Statistics: ^{10}Log(ATP) = –06 + 1.09 ^{10}Log(TNC), r = 0.77, significant at p = 0.002, n = 13. Colour code: Brackish Marine (Littorina) = green, Transition = turquoise, Brackish to Saline Non-marine = blue.*
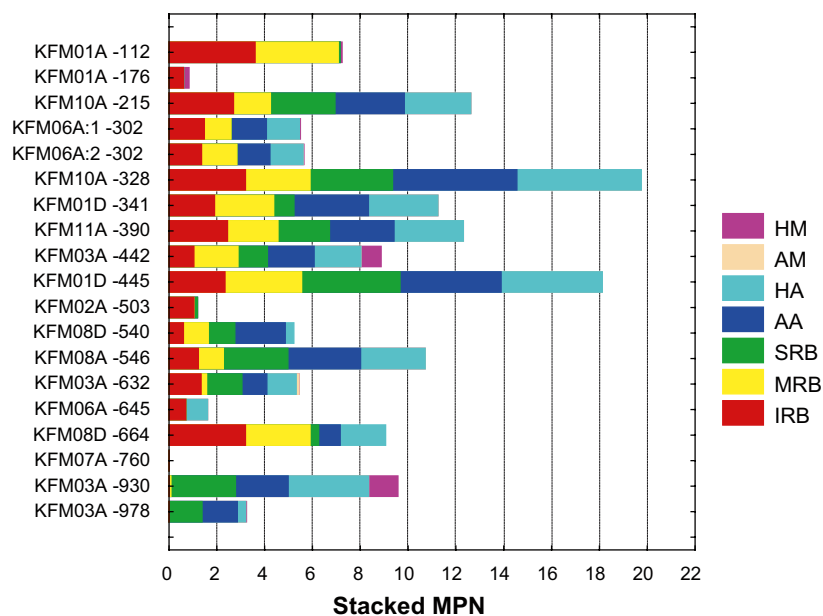
Figure 4-20. *Stacked ^{10}log MPN values for samples from Forsmark sorted by depth. IRB = iron-reducing bacteria, MRB = manganese-reducing bacteria, SRB = sulphate-reducing bacteria, AA = autotrophic acetogens, HA = heterotrophic acetogens, AM = autotrophic methanogens, and HM = heterotrophic methanogens. KFM06A was sampled twice during a control test /Hallbeck and Pedersen 2008a/.*
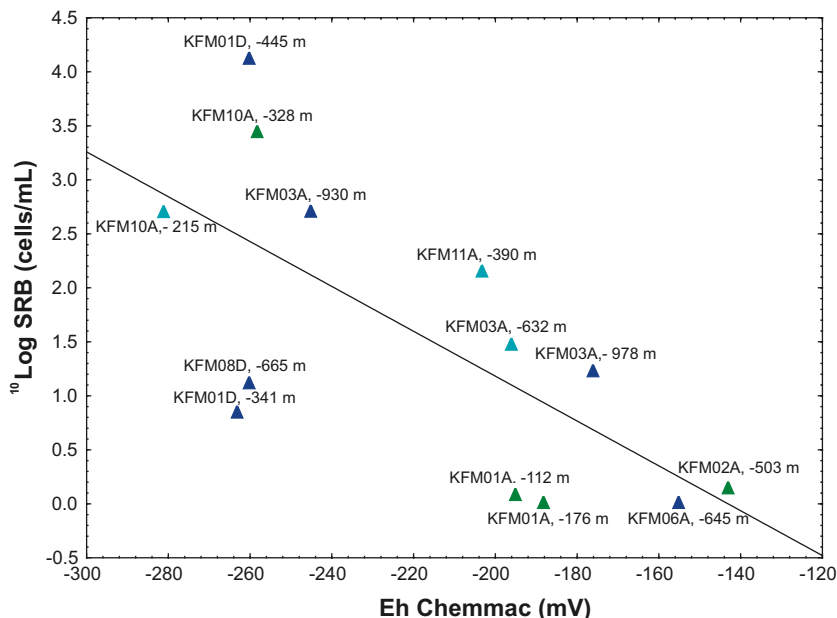
4.4.3 Sulphate-reducing bacteria, sulphide, sulphate and Eh

One of the main negative effects of microorganisms in the context of the final repository concept is the production of sulphide by SRB. The sulphide data, from groundwaters sampled at the same time for microbes, where generally very low (from below detection up to about 0.1 mg/L). The possible influence of pumping during sampling on sulphate reduction and the concentration of sulphide was discussed by /Hallbeck and Pedersen 2008a/. The increased flow rates that pumping generates, may reduce the sulphate reducing activity of SRB and increase the ferrous iron production by IRB as observed in the Äspö HRL /Pedersen 2005/. A correlation matrix with the microbial parameters and chemical parameters possibly influenced by microbial activity is shown in /Hallbeck and Pedersen 2008a/. One of the most important and significant correlations found (at $p = 0.009$) was the relation between Eh measured with the Chemmac and the MPN of SRB (Figure 4-21). This correlation suggests that the sulphide-producing activity of SRB may play an important part in controlling Eh as measured by the Chemmac probe. However, no correlation was found between the microbial or chemical parameters and the modelled values of E_h for the SO_4^{2-}/FeS redox pair.

4.4.4 Conclusions

The most important findings from the microbiological investigations at Forsmark are:

*   Sulphate-reducing bacteria are present at all depths, but showed wide variations in population levels.

*   Iron- and manganese-reducing bacteria are present at all depths, except for near-zero numbers in samples from the deepest groundwaters in KFM03A at 930 m and 978 m.

*   Acetogens are the dominating physiological group of microorganisms.

*   Measured Eh values correlated with the number of sulphate-reducing bacteria suggesting that the SO_4^{2-}/S^{2-} system, catalysed by sulphate-reducing bacteria, probably plays an important role in the redox state of the system.

Figure 4-21. *The relation between the number of sulphate-reducing bacteria and E_h analysed with the Chemmac system in relation to the groundwater types. Statistics: $^{10}Log\ (SRB) = 3.44\text{–}0.023 \times Eh$, $r = \text{–}0.69$, significant at $p = 0.009$, $n = 13$.* r = slope, p = significance coefficient and n = number of observations. *Colour code: Brackish Marine (Littorina) = green, Transition = turquoise, Brackish to Saline Non-marine = blue*

4.5   Colloids

4.5.1   Introduction

Suspended groundwater particles in the size range from 1×10^{-3} to 1 µm are regarded as colloids /Stumm and Morgan 1996/. Radionuclides can sorb (or adhere) or be incorporated in colloids and be transported or retarded with them. It is therefore important to estimate to what extent such colloids can occur or be formed in the groundwater, and for what time periods these colloids can be stable. The aim of the study of colloids was to quantify and determine the composition of natural colloids in bedrock groundwater samples.

Both inorganic and organic colloids exist and these types were measured at Forsmark. Micro-organisms must also be considered as colloids, as there are many groundwater examples ≤ 1 µm in size. The results of the organic colloid analyses are presented in /Hallbeck and Pedersen 2008a/. In addition, a recent study of groundwater in the Äspö HRL tunnel has found a variety of viruses in the water; these are protein particles, approximately 200 nm in diameter that can infect microbial cells. Additional investigations are needed to assess the importance of these colloids considering that colloids have to be stable in order to facilitate transport (e.g. radionuclide) to the biosphere.

4.5.2   Concentration of colloids with depth

Plotting colloid concentration versus elevation (Figure 4-22) shows that the colloid concentration was greatest at the shallowest depth, i.e. 112 m, although the concentration was also high in KFM03A: 442 m, and KFM10A: 328 m, which represent brackish marine water. The
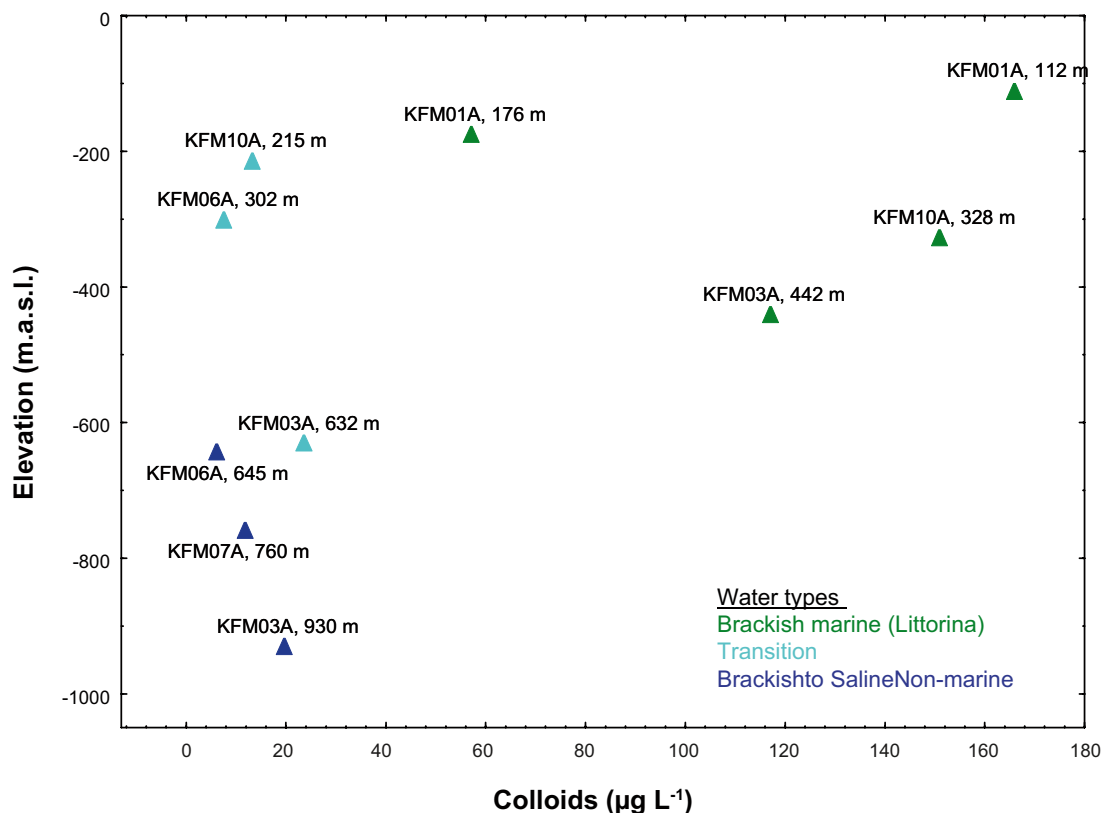
Figure 4-22. *Colloid concentration (µg/L) plotted against depth related to the different groundwater types. Data from /Hallbeck and Pedersen 2008a/ but omitting silica data for KFM01A: 112 m and KFM08D due to sampling artefacts .*

lowest concentration was found at a depth of 645 m in KFM06A which represents a brackish non-marine groundwater. The total range of measured colloid concentrations in the study is 5–170 µg/L and the average concentration is 58.4 µg/L, which compares with average concentrations from crystalline rock groundwaters in Switzerland (30 and 10 µg/L /Degueldre 1994/) and in Canada (300 µg/L /Vilks et al. 1991/), where the same sampling approach was used.

4.5.3   Conclusions

The major conclusions from the colloid characterisation study are listed below /Hallbeck and Pedersen 2008a/:

- The number of colloids found in Forsmark groundwaters is 2 to 6×10^5 /mL except in borehole KFM10A at a depth of 328 m, where the number is 2×10^6 /mL and in borehole KFM08D where the number of colloids is between 1×10^7 and 2×10^8 /mL. The measured colloid concentration is in agreement with measurements from other granitic environments.

- The filtration and fractionation method showed that the colloids were composed mostly of iron and sulphur compounds. LIBD (Laser-Induced Breakdown colloid Detection) with EDX (Energy-Dispersive X-ray analysis) show, on the other hand, that the colloids are composed mostly of aluminium, silica and iron compounds. Uranium associated with colloids is found in boreholes KFM02A and KFM06A, in line with the high groundwater uranium concentrations found in these boreholes. The uranium content associated with the colloids is about 10% of the uranium concentration in the groundwater and colloidal transport is therefore the result, but not the origin, of the elevated uranium content in the groundwater.

- The mass concentration of the colloids differs considerably depending on the detection method used. The highest values are obtained using the filtration method, whereas fractionation gives very low values. However, filtration values are in the same order of magnitude as the LIBD values, and most of the samples were found to contain colloid concentrations below 100 µg/L.

- Colloids can consist of microbial cells and potentially viruses (i.e. phages) and therefore should be taken into consideration when studying colloids in groundwater. The long-term stability and concentration of these colloids and their impact on radionuclides transports require additional study.

Note: Sampling and borehole activities can increase the formation of colloids, and therefore the results obtained can be regarded as maximum values.

4.6   Gases

4.6.1   Introduction

Dissolved gases in groundwater contribute to the mass of dissolved species. The gases can be defined as chemically reactive or conservative and some reactive dissolved types participate in biological processes. Chemically active species are oxygen and hydrogen sulphide with its anionic dissociation products HS^- and S^{2-} and carbon dioxide (with the dissolved species HCO_3^- and CO_3^{2-}), methane and hydrogen. Chemically inactive, inert gases, include the noble gases and to some extent nitrogen. Nitrogen fixation and denitrification by microorganisms may possibly influence the resevoir of nitrogen gas in groundwater, making nitrogen a gas difficult to define as purely (bio) chemically active or inactive. Finally, gases such as ethane and propane and their reduced forms can be found in deep groundwater.

At Forsmark, a total of 19 gas samples from ten boreholes have been analysed with an analytical precision of 20%. The sampling of gas was performed using the PVB pressure vessel; see section 3.3.4 and /Hallbeck and Pedersen 2008a/.

4.6.2 Total gas volumes

Plotting the total volumes of gas at atmospheric pressure in groundwater samples from Forsmark against elevation (Figure 4-23) shows an increasing trend with depth /Hallbeck and Pedersen 2008ab/.

4.6.3 Composition of dissolved gases

The major dissolved gases in groundwaters from the Fennoscandian Shield and in Forsmark are nitrogen, carbon dioxide, helium, methane and argon, and the gas composition varies with depth (Figure 4-23). The carbon dioxide concentration is greatest in shallow groundwaters, but the helium concentration increases with depth. The main component in all gas samples is nitrogen and the second most common gas is helium.

A saturation calculation for nitrogen is reported in /Hallbeck and Pedersen 2008a/ for the samples from KFM07A at 760 m depth, which had the highest gas volume of all samples at Forsmark. The calculation showed that 1,200 mL of nitrogen gas could be dissolved in one kg of water at 700 m depth and at a temperature of 10°C, indicating that the gas pressure in the Forsmark groundwater is far from saturation. This suggests that the amount of the gas, not possible to explain with exchange with the atmosphere, comes from deeper in the Earth, i.e. the majority of the nitrogen therefore appears to originate in the mantle.
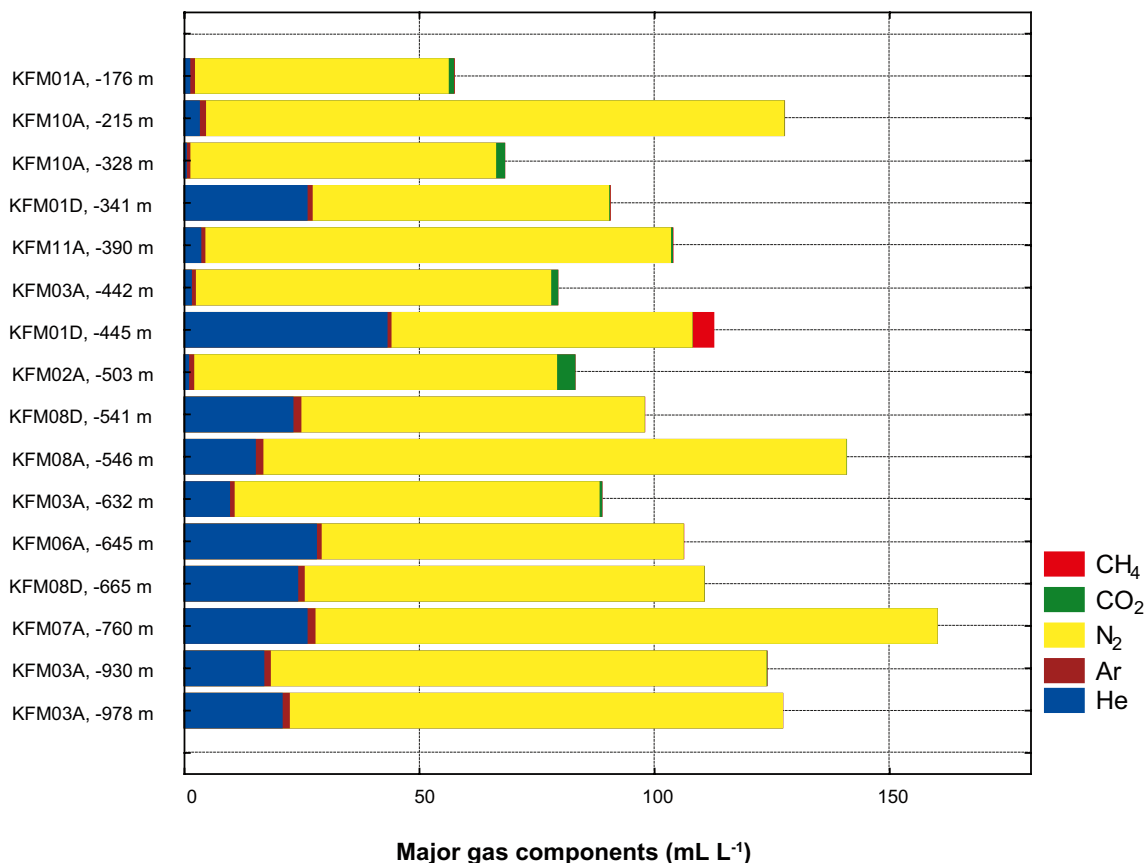
Figure 4-23. *Stacked values of the gas volume of major gas components in samples from Forsmark, sorted by depth.*

4.7 Groundwater mineral interaction

4.7.1 Background

Water/mineral reactions (that may or may not involve biogenic activity) are important for the hydrogechemical understanding and detailed description of the groundwater environment for two main reasons: a) recent water/mineral interaction with the groundwaters influences the present groundwater chemistry (e.g. dissolution/precipitation of calcite; oxidation/production of pyrite, ion exchange etc), and b) the distribution and chemical/isotopic composition of certain minerals (e.g. calcite, pyrite and Fe-oxyhydroxide) provide information on former physico-chemical conditions which are important for the description of the long-term stability of the site /Smellie et al. 2008/. Fracture minerals, and to some extent the adjacent bedrock, participate most actively in water/mineral interaction. Furthermore, the fracture minerals may also serve as a redox and pH buffer in the case of recharging oxidising groundwaters (e.g. during glaciation/deglaciation). The most common fracture minerals in the crystalline rocks at Forsmark are chlorite, calcite, Ca-Al silicates (laumontite, epidote, prehnite), sulphides and Fe-oxides.

To understand the fracture mineral system, it is important to have sound knowledge of the fracture mineral evolution in the area, and therefore a relative sequence of fracture mineralisations has been established for Forsmark based on general macroscopical observations and detailed microscopy /Sandström et al. 2008/. Four generations of fracture mineralisation can be distinguished (see section 2.2.5). and several generations of calcite occur in the fractures (see section 4.7.2).

It is well known that stable isotope and trace element composition of fracture filling calcites can be used as indicators of past and present hydrogeological conditions, for example, due to their relative fast response to changes in fluid chemistry and temperature /e.g. Wallin and Peterman 1999, Blyth et al. 2000, Tullborg et al. 2008/. The $\delta^{18}O$ of the calcite depends on the $\delta^{18}O$ value in the fluid responsible for precipitation and the formation temperature, whereas $\delta^{13}C$ gives mainly information on the carbon source and the process involved in the bicarbonate production.

$^{87}Sr/^{86}Sr$ isotopes do not fractionate during precipitation and calcite inherits therefore the $^{87}Sr/^{86}Sr$ ratios from the precipitating fluid. The $^{87}Sr/^{86}Sr$ ratios in the groundwaters and hydrothermal fluids are largely determined by water/mineral interaction and to lesser degree by the different origins of the fluids (e.g. marine/non marine). Since the fraction of radiogenic strontium is steadily growing in the rock and fracture minerals with time, higher $^{87}Sr/^{86}Sr$ ratios in the calcite may reflect younger ages of the calcite.

4.7.2 Calcites

The application of isotope systematics and detailed microscopy on the Forsmark calcites has resulted in identifying three general types of calcites based on stable isotope composition: a) hydrothermal calcite (generation 2), b) warm brine-type calcite originating from a fluid influenced by organic material (generation 3), and c) low temperature calcite precipitated from different groundwaters at temperatures close to present groundwater temperatures (generation 4). Calcites of the latter type occur only in small amounts but have been preferentially sampled for stable isotope analyses since they may provide information on the latest groundwater evolution in the area. Note that the fracture mineral assemblage characteristic for generation 1 does not contain calcite (cf section 2.2.5).

Generation 2 calcite (Pre-Sveconorwegian and/or Sveconorwegian)

Generation 2 calcites (Figure 4-24) show relatively small variations in $\delta^{13}C$ with values between −1.6 to −7.1‰ PDB (standard according to Pee Dee *Belemnitella* Formation). The majority of these calcites have low $\delta^{18}O$ values (< -14‰ PDB) although calcites showing a shift toward enriched $\delta^{18}O$ values are also found (Figure 4-25). Depleted $\delta^{18}O$ values and $\delta^{13}C$ values between −1 to −7‰ PDB are typical for calcite precipitating under hydrothermal conditions.
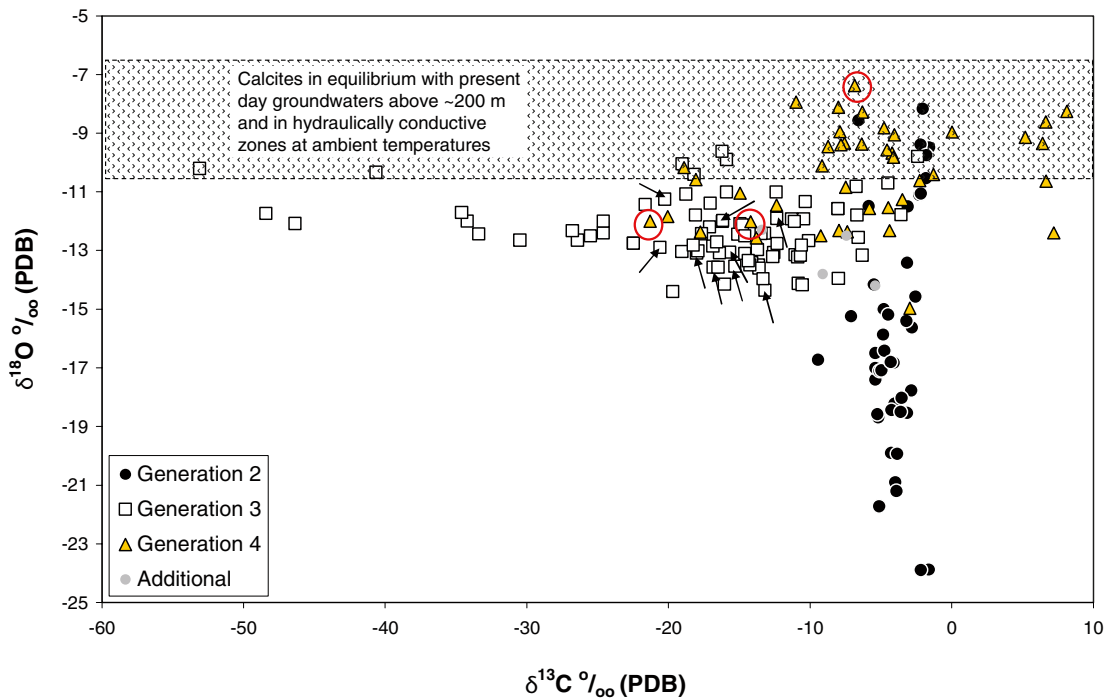
Figure 4-24. *δ¹³C versus δ¹⁸O in fracture filling calcite. The isotopic composition of groundwaters above ~ 200 m depth, and in hydraulically conductive zones, are dominated by brackish-marine waters (–10 to –8.5‰ SMOW) and, in the upper 100 m, by fresh meteoric water (–12 to –10.5‰ SMOW). For calculation of δ¹⁸O in calcite in equilibrium with these waters, the fractionation formula by /O'Neil et al. 1969/ has been applied at a temperature of ~ 7°C. Calcites marked as 'Additional' have not been possible to relate to the relative sequence of fracture mineralisations. Three generation 4 calcites with ⁸⁷Sr/⁸⁶Sr overlapping with the present groundwaters are marked with red circles. The samples marked with arrows represent calcite found coevally intergrown with quartz and represent an early event of generation 3 calcite precipitation. Analytical errors are less than 0.1‰, and fall within the size of the symbols.*
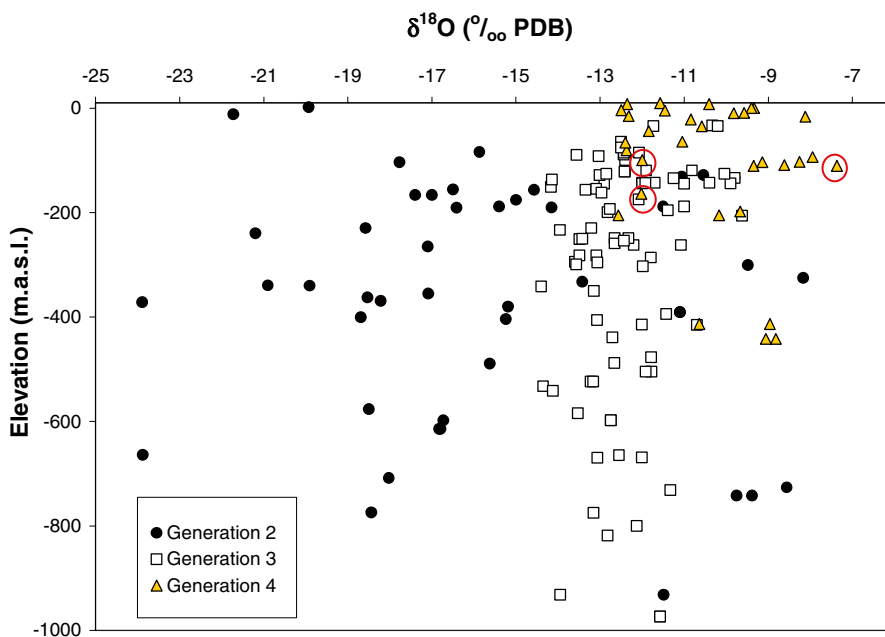
**Figure 4-25.** *δ¹⁸O in calcite versus elevation. Three generation 4 calcites with ⁸⁷Sr/⁸⁶Sr overlapping with present groundwaters are marked with red circles. Analytical errors are less than 0.1‰, and fall within the size of the symbols.*

94

The trend toward enriched $\delta^{18}O$ values in many of calcites is probably due to an 'oxygen shift' where interaction with the wall rock increases the $\delta^{18}O$ value of the fluid /e.g. Drever 1997/ which is subsequently inherited by the calcite during precipitation. Intensive water/rock interaction is supported by the observed wall rock alteration (cf. section 2.2.5) associated with precipitation of the hydrothermal calcite and is also in agreement with the variation in $^{87}Sr/^{86}Sr$ ratios (0.707 to 0.713 in all with one exception of 0.715).The overlapping $^{87}Sr/^{86}Sr$ ratios in calcite coeval with adularia, prehnite and laumontite of generation 2 indicate that these minerals did not precipitate during distinctly separated periods (Figure 4-26).

Generation 3 calcite (Palaeozoic)

Generation 3 calcite shows a narrower span in $\delta^{18}O$ values (–9.6 and –14.4‰ PDB) compared with the older calcite (Figure 4-26). In contrast, extreme variation in $\delta^{13}C$ values spanning –2.4 to –53.1‰ PDB (Figure 4-24) is shown. The $\delta^{13}C$ values in calcite between –7 and –30‰ PDB indicate an organic influence on the fluid which is in agreement with the proposed downward penetration of fluids from an organic rich sedimentary cover as suggested by the presence of asphaltite in the upper parts of the bedrock /Sandström et al. 2006b/. More extreme $\delta^{13}C$ values ($< –30$‰ PDB) are due to microbial oxidation of organic matter under in situ non-equilibrium conditions resulting in extreme depletion of ^{13}C in the produced HCO_3^-/CO_2 which subsequently is inherited into the precipitating calcite /Pedersen et al. 1997, Budai et al. 2002/. The variations seen in the $\delta^{18}O$ values could be due to temperature variation during precipitation and/or variation in the isotopic composition of the fluid. A moderate interaction with the wall rock is also possible.
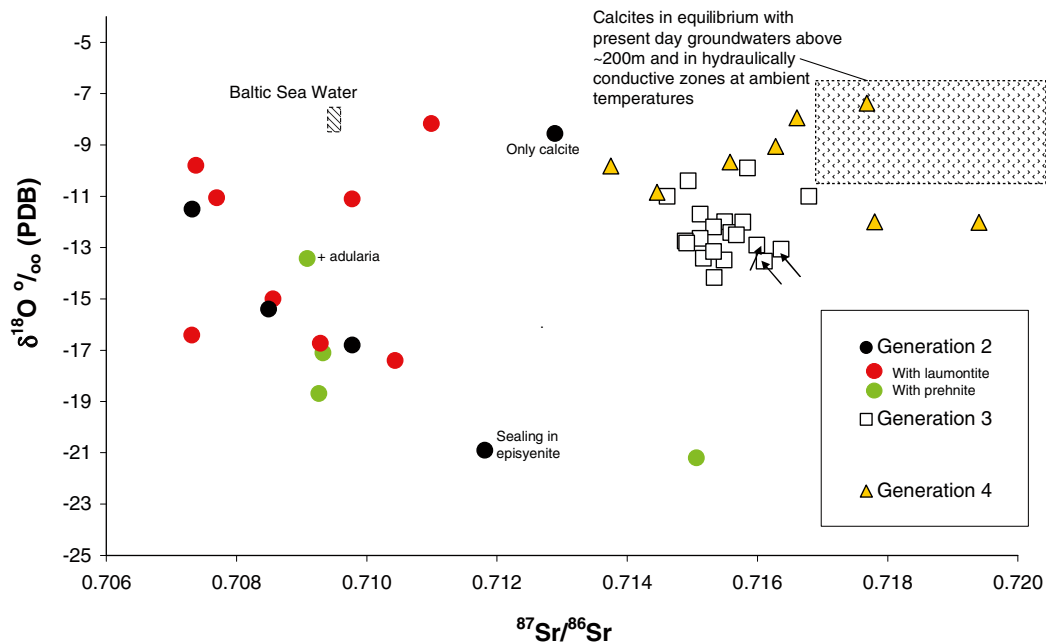
Figure 4-26. *$^{87}Sr/^{86}Sr$ ratio plotted versus $\delta^{18}O$ (PDB) in fracture filling calcite. Cogenetic minerals for generation 2 calcites are colour coded. Note: a) the overlap in $^{87}Sr/^{86}Sr$ ratios in calcite cogenetic with prehnite and laumontite, b) the isotopic composition of Baltic Sea Water and groundwaters down to around 200 m depth and in hydraulically conductive zones, c) the Brackish marine groundwaters (–10 to –8.5‰ SMOW) which dominates the conductive zones, and d) the Fresh meteoric water (–12 to –10.5‰ SMOW) in the upper 100 m of the bedrock. For calculation of $\delta^{18}O$ in calcite at equilibrium with these waters, the fractionation formula by /O'Neil et al.1969/ has been applied at a temperature of approximately 7°C.*

There is evidence for more than one event of calcite precipitation during the Palaeozoic, but it is not possible to distinguish between these calcites based on stable isotopic composition. In Figure 4-24, calcites representing an early event of generation 3 calcite precipitation are marked with arrows; both events are characterised by an organic $\delta^{13}C$ signature and show similar $\delta^{18}O$ values.

Most generation 3 calcites have $^{87}Sr/^{86}Sr$ ratios between 0.7149 and 0.7164 and can thus be distinguished from older calcites usually showing significantly lower $^{87}Sr/^{86}Sr$ values (Figure 4-26). The limited range in strontium isotopic composition of generation 3 indicates a relatively homogeneous strontium isotope ratio in the fluid, possibly due to the fact that the calcite precipitated from an old water/brine which had equilibrated with mineral phases in the rock.

Homogenisation temperatures (T_H) obtained from fluid inclusions in Generation 3 calcite separate into two groups; T_H 161–186°C and T_H 64–109°C /Sandström et al. 2008/. Fluid inclusions with lower T_H are found in calcites that have grown on quartz coatings and represent a shift towards more saline compositions (12–19wt% CaCl eq.). From a palaeohydrogeological perspective it is of interest to note the strong evidence of a highly saline organic rich fluid present in the crystalline rock aquifer during this time period (i.e. the Palaeozoic).

Generation 4 calcites (Late Palaeozoic-Present)

Generation 4 calcites overlap in both $\delta^{13}C$ and $\delta^{18}O$ values with the Palaeozoic (generation 3) calcite, although a shift towards higher values can be seen in both $\delta^{13}C$ and $\delta^{18}O$ values. Some of this overlap could be due to overgrowth of younger calcite on older Palaeozoic calcite, but a large part of the variation can be assumed to correspond to precipitations from very different groundwaters. Generation 4 calcite is expected to represent calcites formed mainly during the Caenozoic. During this period marine to brackish to meteoric waters have recharged during temperate and cool climate conditions and these may have taken part in the calcite dissolution/ precipitation processes. Calcites with $\delta^{18}O$ values between –11 and –7‰ PDB may have precipitated from waters similar to the present groundwater in the upper 200 m of the rock (Figure 4-25). Calcites with lower $\delta^{18}O$ could have been precipitated from a groundwater influenced by a larger glacial component. A few calcites display positive $\delta^{13}C$ values, possibly due to in situ microbial activity involving CH_4-CO_2 fractionation processes. Eight samples of the younger generation 4 calcites were analysed for $^{87}Sr/^{86}Sr$ and of these, five samples show values similar to the Palaeozoic calcites, although three show more radiogenic signatures. Only one calcite has been identified that is in equilibrium with both $\delta^{18}O$ and $^{87}Sr/^{86}Sr$ in the present groundwater at ambient temperatures. Two calcites have been identified which have $^{87}Sr/^{86}Sr$ ratios overlapping with the present groundwaters, but are not in equilibrium with the $\delta^{18}O$ values measured in groundwaters above 200 m depth. These calcites could have been recently precipitated during a colder climate, but could also have precipitated during different climatic periods when the groundwater had a similar composition. As shown in Figure 4-25, generation 4 calcites are generally found in the upper 200 m of the bedrock except for some samples selected from 400 m depth in deformation zones ZFMA2 and ZFMA7.

4.7.3   Fracture minerals as indicators of pH and redox conditions

Different mineralogical and geochemical indicators, such as the distribution of Fe(II)/Fe(III) minerals and behaviour of redox sensitive elements such as cerium and uranium, can be studied in order to reveal possible redox front development, for example, in the near-surface bedrock environment.

In addition, although calcite is not redox sensitive, there is a secondary dependency due to interactions between the biosphere and the bicarbonate. However, there are major problems locating bedrock evidence of a downward-propagating redox front at the Forsmark site. The most important of these are: a) most of the core drilling did not start at the bedrock surface,

which means that suitable data are restricted to only 8 boreholes where core mapping is absent for the upper 5–10 m, and b) the uppermost hundred metres of the bedrock are characterised by sub-horizontal to gently dipping, highly transmissive fractures (i.e. the shallow bedrock aquifer), which create strong horizontal, rather than vertical, flow conditions.

However, based on mineralogy and the analysis of redox-sensitive elements, the following observations of redox response to geological events can be made /Sandström et al. 2008/.

- The two earliest events of fracture mineralisation (generation 1 and 2 of Proterozoic age) are characterised by the presence of oxidised ferric iron (in hematite) and a number of cerium anomalies in fracture coatings. These observations are interpreted as indicative of oxidising conditions coeval with their formation. On the other hand, chlorite with a significant ferrous iron content is also part of the generation 1 and 2 parageneses, suggesting variable redox conditions both in time and space. Related to these two fracture generations are also hydro-thermal alteration/oxidation of the wall rock adjacent to the fractures (some centimetres), where the overall increase in $Fe^{3+}/Fe(tot)$ is small (about 10%). The major mineralogical changes in these altered rims (which normally extend a few centimetres into the wall rock) are almost complete saussuritisation of plagioclase, chloritisation of biotite and to some extent hematisation of magnetite.

- Generation 3 (Palaeozoic age) is characterised by reducing conditions as indicated by pyrite precipitation and also supported by the organic influence on the formation fluid during this period. Well-preserved pyrite crystals of Palaeozoic origin (generation 3) in many of the transmissive fractures suggest that reducing conditions have prevailed in large parts of the fracture system since this period.

- The presence of goethite (FeOOH) (generation 4) in some hydraulically-conductive fractures and fracture zones (mainly within the gently dipping deformation zone ZFMA2) in the uppermost part of the bedrock, indicates circulation of oxidising fluids during some period in the past (potentially Quaternary). This is also supported by a high oxidation factor ($Fe^{3+}/Fe(tot)$ determined from Mössbauer spectra), seen in a few fracture coatings from the upper 100–200 m. However, the presence of pyrite in the same zones suggests that the circulation of oxidising fluids has been concentrated along channels in which different redox micro-environments may have been formed.

- Uranium-rich phases are present in some of the fracture coatings although to date only one small grain of pitchblende has been identified /Sandström et al. 2008/. The origin of these phases is largely unknown but it can be concluded that uranium has been circulating through-out the geological history of the site. For example, some of the pegmatites show slightly elevated uranium values (a maximum value of 62 ppm is indicated by gamma spectrometric data /Stephens et al. 2007/). Even more importantly, there is evidence of redistribution and deposition of uranium irregularly along permeable structures during the Proterozoic /Welin 1964/. Moreover, during the Palaeozoic, potentially uranium rich Alum shales covered the area /Sandström et al. 2006a and references within/, and these may have contributed uranium to the system. Of special interest for understanding the present groundwater/mineral systems is the potentially late (Quaternary) redistribution of uranium. The use of uranium series decay isotope analyses (USD) on groundwaters and fracture coatings concluded that part of this uranium has been mobile during the last 1 Ma /Sandström et al. 2008/. Mobilisation, as well as redeposition of uranium in the upper part of the bedrock (150 m) is indicated. This is ascribed to the transition from near-surface oxidising conditions to more stable reducing con-ditions at depth. However, some of the deeper samples show similar behaviour which may be explained by the presence of an easily dissolvable and partly oxidised uranium phase, i.e. possibly altered pitchblende in type. Mobilisation and redeposition of this phase does not mean that oxidising water has penetrated to this depth. However, of greater importance is, irrespective of the aqueous phase which has mobilised the uranium, that the present mildly reducing groundwaters with sufficient bicarbonate (> 30 mg/L) are capable of keeping U(VI) mobile, resulting in variable accumulations occurring within the fracture zones to maximum depths of around 600 m (cf. section 4.3).

- Any potential build up of reducing capacity in the fracture minerals during recent periods of reducing groundwater conditions is difficult to estimate. Processes that may contribute to increase the redox capacity include the microbial production of Fe^{2+} and Mn^{2+} that may either precipitate (e.g. coprecipitation in calcite) or be sorbed on mineral surfaces due to ion exchange. In addition, iron sulphides may be formed due to bacterial activity of sulphate reducers. However, it can be concluded that the amounts of recent (Quaternary) minerals formed is very small.

No significant decrease in the frequency of calcite coated fractures in the uppermost part of the bedrock can be seen, indicating that no extensive calcite leaching has occurred in response to Quaternary glaciation/deglaciation events. However, no data are available from the upper 5–10 m and it is possible that calcite leaching and/or pyrite oxidation is visible close to the bedrock surface.

Ion exchange capacity is another parameter of importance and the few data available are reported in /Byegård et al. 2008/.

4.8   Porewater in the rock matrix

4.8.1   Background

The term 'porewater' as used here refers to the water in the connected pore space of the rock matrix that is accessible for diffusion-dominated interaction with groundwater circulating in nearby (micro-)fractures /Waber and Smellie 2008/.

The mass of porewater contained in the low-permeability matrix of the crystalline rock at Forsmark is significant compared to the mass of groundwater circulating in the fractures, and therefore its influence on the fracture groundwater and a future deep repository needs to be understood. The interaction between porewater in the low permeable bedrock and groundwater in transmissive fractures depends on the degree of connectivity of the pore system, where solute transport can take place in the porewater, and on the differences in the chemical composition between the two systems. Porewater and fracture groundwater always tend to reach chemical and isotopic equilibrium given a long enough period of stable conditions. Thus, the porewater acts either as a sink or a source for solutes depending on the concentration gradient established between porewater and fracture groundwater, and therefore becomes an archive of past fracture-groundwater compositions and the palaeohydrogelogical history of a site.

Once established, the chemical and isotopic signature might be preserved in the porewater over long periods of geological time. The degree of preservation of such signatures depends on: a) the distance of the porewater sample to the next conducting fracture in three dimensions (i.e. the fracture network), b) the solute transport properties of the rock (i.e. diffusion coefficient, porosity), and c) the period of constant boundary conditions (i.e. constant fracture-groundwater composition). Constant boundary conditions over the time period considered greatly facilitate the interpretation of an observed porewater signature. In reality, however, overlap of changes induced by variable boundary conditions seem more common, certainly in the first few metres of the rock matrix closest to a water-conducting fracture, and especially during the Holocene and Pleistocene periods when frequent climatic and hydrogeological changes occurred (see section 2.5). In addition, the significance of the signature (taking account of the measurement error) depends on the chemical gradient between porewater and fracture groundwater /Waber and Smellie 2008, Waber et al. 2008a/.

Porewater investigations at Forsmark were aimed at elaborating the hydrogeochemical evolution of the site based on the potential of porewater acting as an archive to events that have happened over recent geological time (i.e. several hundreds to a few millions of years). Porewater studies also can play an important role in defining the potential contribution of matrix diffusion to the retardation of radionuclide transport in the geosphere, and defining the interaction between porewater and repository barrier materials.

Within the SKB site investigation programmes at Forsmark and Oskarshamn, porewater investigations have been developed and tested for the first time in crystalline rocks /Waber and Smellie 2004, 2005, 2007/ and summaries in /Waber and Smellie 2008/ and /Waber et al. 2008ab/.

4.8.2 Sampling strategy, methods and data uncertainty

Porewater from the rock matrix cannot be sampled by conventional groundwater sampling techniques, but needs to be characterised by indirect methods based on drillcore material (see /Waber and Smellie 2008, Waber et al. 2008a/ for details). Furthermore, it is obvious that porewater data obtained for a single sample from a borehole can only be interpreted to a very limited degree. Consequently, profiles have been sampled systematically along borehole lengths and, if possible, along small-scale profiles extending several metres from a water-conducting fracture into the host rock matrix. These two sets of data are then compared to the present-day fracture-groundwater compositions characterising the closest water-conducting fracture to the selected porewater samples.

The success of porewater investigations relies on obtaining the originally saturated rock material. This requires freshly drilled cores from boreholes and the immediate on-site conditioning of such material within minutes after drillcore recovery (see /Waber et al. 2008a/ for details/. In addition, rather large-sized core samples are required to compensate for the low porewater content and to minimise possible artefacts induced from the time of drilling to the time of analysis. Furthermore, there is also great difficulty attached to predicting the location and orientation of a demarcated water-conducting fracture for profile sampling prior to drilling. Finally, a borehole provides only a one-dimensional section of a rock volume, i.e. along the borehole length. In the other dimensions a water-conducting fracture might indeed occur closer to a selected porewater sample than observed from the core material alone.

The chemical and isotopic compositions of porewater were derived using indirect methods such as out-diffusion and diffusive-exchange techniques on originally saturated and intact drillcore material. All applied techniques have been continuously improved upon during the site investigation programme to minimise induced artefacts and the experimental and analytical errors /Waber and Smellie 2005, 2007, 2008, Waber et al. 2008ab/.

The large drillcore size of approximately 200 x 50 mm (approximately 1 kg) was chosen to minimise artefacts induced by the drilling process, by stress release, and by desaturation during sample handling and transport. These possibilities have been thoroughly addressed and found to contribute a maximum contamination of about 8% of the chloride concentration derived from the out-diffusion experiment (Waber et al. 2008a). Such a small contamination lies within the experimental and analytical uncertainty of the experiment. The uncertainty attached to the derived porewater chloride concentration thus mainly depends on the accuracy of the water-loss measurements, and consequently on rapid measurements and on the heterogeneity of the rock sample. The uncertainty range of the obtained chloride concentrations in the porewater was thus estimated from the standard deviation of multiple water-loss measurements.

The concentrations obtained in the out-diffusion experiment solutions are converted to porewater concentrations using the geochemical porosity for chemically conservative components, while those for reactive components need to be corrected for water/rock interaction during the experiment by applying geochemical modelling. Geochemical model calculations using mineral dissolution kinetics are particularly important to show that the contribution of magnesium (marine indicator) from mineral dissolution during out-diffusion to the experiment solution, contributes only a small fraction of the magnesium concentration measured in the experiment solution /Waber et al. 2008a/. This allows, as a first assumption, the re-calculation of the magnesium concentration in the porewater in a similar way as for the conservative chloride. Whereas the uncertainty attached to such calculations might be somewhat larger compared to that of the porewater chloride concentration, it allows the distinction between Mg-rich porewater (e.g. >100 mg/kg$_{H2O}$) and Mg-poor porewater (e.g. < 20 mg/kg$_{H2O}$). Therefore, the so derived porewater concentration of magnesium can be used to identify a brackish marine (e.g. Littorina

or Baltic type) component in low to moderately brackish porewaters (i.e. Cl < 6,000 mg/kg$_{H2O}$). In general, such calculations show that the contribution from mineral dissolution during the experiment is limited and within 10 percent of the measured concentration in the experiment solutions. Chemical porewater concentrations are given in units of mg/kg$_{H2O}$ rather than mg/L because of the mass-based basis of their derivation by indirect methods.

The water isotope composition, $\delta^{18}O$ and δ^2H, of porewater was derived using the isotope diffusive-exchange techniques on originally saturated and intact drillcore material /Waber and Smellie 2008, Waber et al. 2008a/. Continuous improvement of this technique allowed a reduction in the cumulated error as calculated by Gauss' law of error propagation for the first investigated borehole (KFM06A) to the last (KFM02B), from about ± 2.5‰ and ± 25‰ to about ± 1.3‰ and ± 12‰ for $\delta^{18}O$ and δ^2H, respectively. In spite of the still substantial experimental error, the obtained results allow certain statements about possible origins of the porewater when combined with other parameters.

4.8.3 Sampled localities and integration with fracture groundwaters

Rock matrix porewaters have been analysed from five boreholes (Figure 2-1). Boreholes KFM01D, KFM08C, KFM09B, and KFM06A, are located in or close to the target volume (i.e. the footwall bedrock including fracture domains FFM01, FFM02, and FFM06), in the north-west sector of the candidate area (Figure 2-1 and Figure 6-2). Borehole KFM02B is located in the south-east sector of the candidate area (i.e. in the hanging wall bedrock; fracture domain FFM03) and intersects the major gently dipping deformation zones ZFMA2 and ZFMF1 (Figure 6-1). With the exception of KFM09B, samples for study were collected at regular intervals along the complete core lengths. In addition, the focus of boreholes KFM02B and KFM09B was on continuous sampling of profiles along the drillcore from a water-conducting fracture and from a higher transmissive episyenite zone, respectively, into the surrounding, undisturbed rock matrix. No drillcore samples exist from any of the upper 100 m percussion drilled lengths of the boreholes.

Where available, the chemical and isotope composition of the porewaters are compared to that of fracture groundwaters sampled from nearby water-conducting fractures, preferably in the same borehole, or in neighbouring boreholes at similar depth. During porewater/fracture groundwater interaction, the porewater composition is subjected to modification by the diffusional exchange (transient vs. steady-state, species-specific diffusion coefficients) and water-rock interactions (larger reactive mineral surface area, longer residence time) in addition to the evolutionary processes identified for the fracture groundwaters. Furthermore, several of the fracture groundwater end members have similar $\delta^{18}O$ and δ^2H values, but different chloride compositions and vice-versa. It is therefore not surprising that a different relationship between these natural tracers is established in the porewaters compared to the fracture groundwaters where these components have been used successfully in this report to trace the input of post-glacial meltwater, brackish marine (e.g. Littorina/Baltic sea) and recent meteoric end member types into the bedrock groundwater system. The varying distances of the porewater samples to the next water-conducting fractures, and the species-specific diffusion coefficients, means that the superposition of two sequential events will result in different signatures. The behaviour of porewater signatures therefore differs strongly from that of two mixing components mainly because it strongly depends on the time of interaction with a specific fracture groundwater composition.

4.8.4 Porewater composition

The porewater data show a distinction between bedrock characterised by low transmissivity and low frequency of water-conducting fractures (i.e. fracture domain FFM01 within the footwall; boreholes KFM01D, KFM08C, KFM09B and the lower part of KFM06A) and bedrock characterised by high transmissivity and a high frequency of water-conducting fractures (i.e. fracture domain FFM03 comprising the hanging wall, Borehole KFM02B, and fracture domain FFM02 in the footwall involving the upper part of borehole KFM06A). In general, chloride contents in the porewater increase towards greater depth, whereas the isotope composition displays a more complex distribution in both areas. However, there is a strong dependency between porewater composition and the distance along the borehole between the porewater sample and the next water-conducting fracture, and there are differences in the degree of compositional changes between the two areas (Figure 4-27 and Figure 4-28; cf. also Figure 6-3).
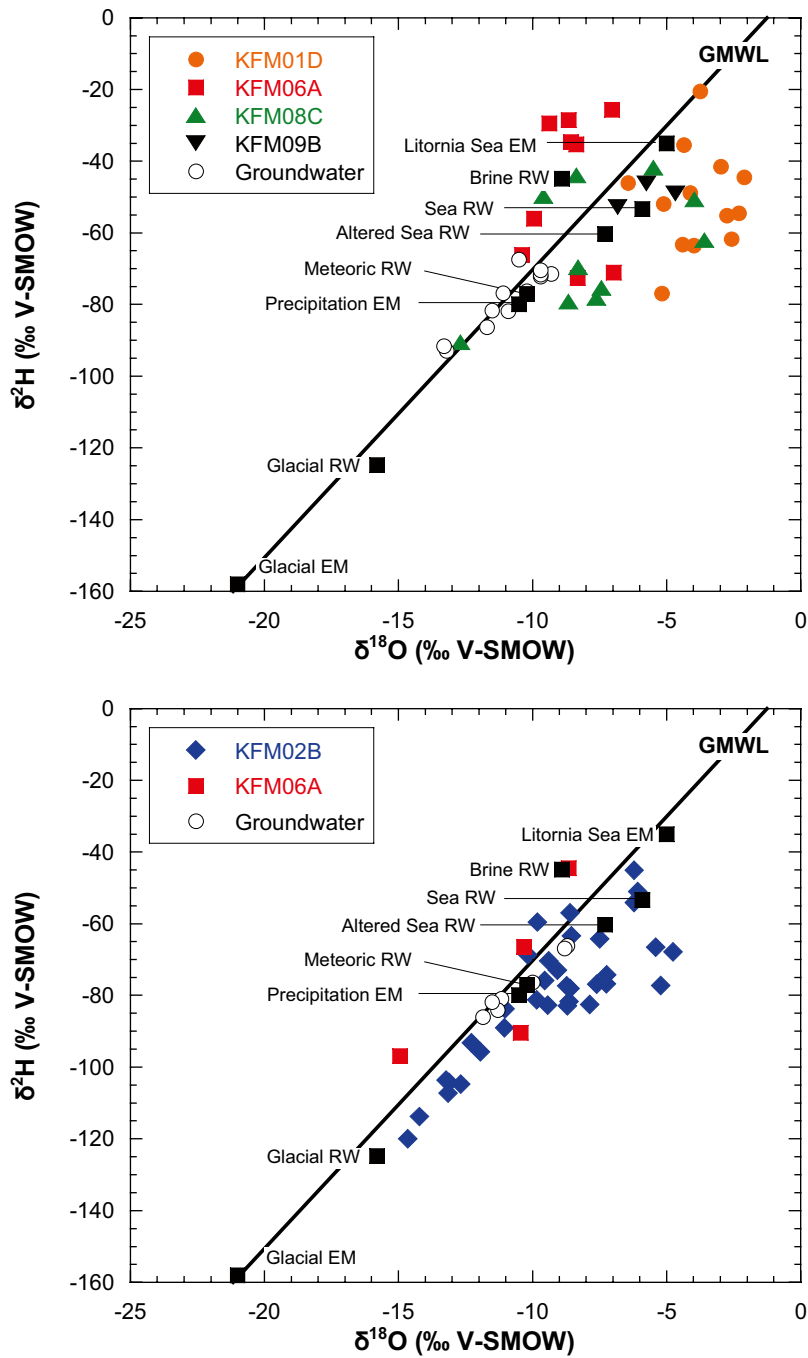
In the target volume (i.e. footwall bedrock comprising fracture domains FFM01 and FFM02), chloride contents in the porewater are between 2,000 and 3,500 mg/kg_{H2O} down to about 350 m depth (borehole KFM08C) and 500 m depth (boreholes KFM01D and KFM06A), respectively. Chloride contents at these depths are correlated to the frequency of water-conducting fractures /Waber et al. 2008a/ and the distance along the borehole between the porewater sample and the next water-conducting fracture (Figure 4-27). At greater depth, where the fracture frequency decreases and the distance between porewater samples and water-conducting fractures increases, the chloride contents increase continuously to about 10,000 mg/kg_{H2O} in all three boreholes, with the highest chloride content of 14,600 mg/kg_{H2O} occurring in porewater of a non-fractured section in borehole KFM08C at a depth of about 620 m (Figure 4-27). Deviations from this general pattern occur, for example, in borehole KFM09B where a chloride content of more than 10,000 mg/kg_{H2O} is already present at about 440 m depth in porewater adjacent to a water-conducting fracture in a zone of episyenite.

The general chemistry of the porewater in the target volume (i.e. the footwall bedrock; boreholes KFM01D, KFM08C, KFM09B, and lower part of KFM06A) changes from a Na-HCO$_3$ type at shallow depth to Na-Cl and Ca-Na-Cl types with increasing depth and chloride concentration. In the fracture groundwater magnesium was found to be a good indicator for the presence of a brackish marine component (e.g. Littorina and/or Baltic type seawater) /Smellie et al. 2008/. In the porewater of the footwall bedrock, high magnesium contents (>100 mg/kg_{H2O}) are only found at very shallow levels down to about 200 m depth in borehole KFM01D, i.e. corresponding to the maximum influence of the shallow bedrock aquifer.

South-east of the target volume (i.e. hanging wall bedrock; fracture domain FFM03, borehole KFM02B, and using values from the equally transmissive upper part of KFM06A in the footwall bedrock), the high frequency of highly transmissive fractures associated with the two major gently dipping deformation zones, ZFMA2 and ZFMF1, show porewater chloride concentrations mainly below 1,500 mg/kg_{H2O} down to a depth around 550 m (Figure 4-27). This pattern is interrupted with contents up to 3,000 mg/kg_{H2O} between about 360 m and 450 m depth, which coincides with an increased accumulation of water-conducting fractures and the intersection of deformation zones ZFMA2 and ZFMF1 in borehole KFM02B. This increase in porewater chloride content is associated with a distinct increase in magnesium contents (up to 200 mg/kg_{H2O}). In borehole KFM06A a similar increase in chloride occurs between 250–335 m associated with less elevated magnesium contents (up to 50 mg mg/kg_{H2O}). In these highly transmissive localities a weak Littorina signature is still evident in groundwaters from the nearby water-conducting fractures at depths down to at least 300 m in accordance with the elevated magnesium in the porewaters.
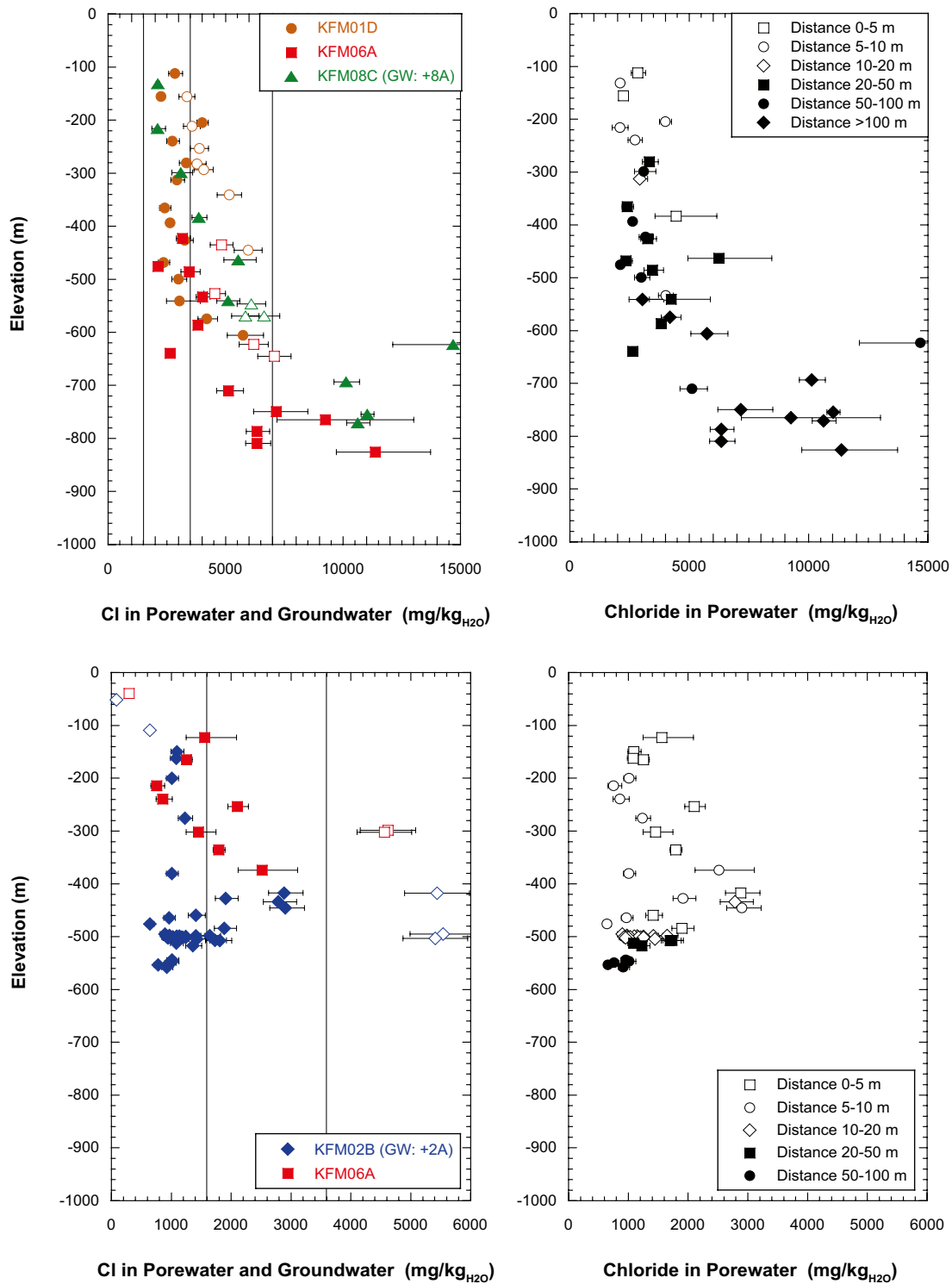
Figure 4-27. *Chloride concentration in porewater (closed symbols) and related fracture groundwater (open symbols) on the left, compared with the distance of the porewater samples to the next water-conducting fracture on the right. The top figures show the boreholes representing mainly low transmissive, low fracture frequency conditions (KFM01D, KFM08C and the deeper part of KFM06A) and the bottom figures show the boreholes representing high transmissive, high fracture frequency conditions (KFM02B and upper KFM06A). Indicated is the arbitrary subdivision of porewater Cl contents as used in the hydrogeochemical site descriptive model /Smellie et al. 2008; cf. Figure 6-3/; note the different scale on the x-axis. Fracture groundwater samples, GW, taken from other boreholes orientated in different directions from the same drilling sites are indicated in the legend. Error bars show cumulated error (see discussion in /Waber et al. 2008a/).*

Figure 4-28. δ*¹⁸*O-δ*²*H *diagram of porewater and related fracture groundwater in the target volume (footwall bedrock; boreholes KFM01D, KFM08C, KFM09B, and lower part of KFM06A, top) and the area southeast (hanging wall, borehole KFM02B and values from the upper part of KFM06A in the footwall, bottom). Porewater in the footwall is isotopically more enriched compared to the porewater in the hanging wall, which has isotope signatures similar to the fracture groundwater.*

4.8.5 Isotope composition of porewater

The oxygen and hydrogen isotope compositions of porewater from the target volume (i.e. footwall bedrock including fracture domain FFM01) differ clearly from that of porewater sampled in the area south-east of the target volume in the hanging wall bedrock (i.e. fracture domain FFM03). Porewater in the target volume is generally more enriched in the heavy isotopes compared to porewater of the hanging wall bedrock and also compared to fracture groundwater sampled from this area. Thus, porewater from boreholes KFM01D and KFM08C with low to moderate chloride contents (i.e. footwall; including fracture domain FFM01) plots further to the right of the Global Meteoric Water Line (GMWL) than sea water, suggesting the presence of a warm-climate component. However, high chloride porewaters from greater depths (around 820 m) in borehole KFM06A (i.e. also footwall; fracture domain FFM01) plot to the left of the GMWL near-by the Brine end member (Figure 4-29). In contrast, porewater from the hanging wall area plots over a large range of isotope compositions parallel to the GMWL, with the bulk of samples being located between the end-member compositions of sea water and present-day infiltration (Figure 4-29). Here, the porewater seems isotopically more similar to the fracture groundwaters sampled from this area. As shown below, based on the oxygen isotope composition, these differences result also in different distribution patterns with depth.

In the target volume two major depth trends are observed for the isotopic composition of porewater in boreholes KFM01D and KFM08C and the deeper levels in KFM06A. From shallow to intermediate depth at around 600 m the $\delta^{18}O$ values vary between about $-8.5‰$ and $-5.5‰$ V-SMOW in boreholes KFM08C and KFM06A, but are more enriched in ^{18}O in borehole KFM01D with $\delta^{18}O$ values of generally more than $-5.5‰$ V-SMOW (Figure 4-29). At increasing depth below about 550 m, the distance along the borehole to the next water-conducting fracture is generally more than 50 m. Here, the oxygen isotope composition becomes more depleted in ^{18}O and varies generally between $-10.5‰$ and $-8.5‰$ V-SMOW in porewaters from boreholes KFM08C and KFM06A, whereas it remains enriched in ^{18}O in borehole KFM01D. Deviations from these trends occur in borehole KFM08C at a depth of about 380 m with a $\delta^{18}O$ value of $-12.7‰$ V-SMOW in a porewater sample collected 5 m from the next water-conducting fracture and with $\delta^{18}O$ values of around $-4‰$ V-SMOW between depths of about 750–770 m (Figure 4-29). The depleted oxygen isotope signature at 380 m suggests the presence of a cold-climate or possible glacial component in the porewater. In turn, the enriched oxygen isotope compositions at 750–770 m depth are similar to those observed in porewaters from borehole KFM01D, but are associated with much higher chloride contents (> 10 g/kg_{H2O} vs. < 3 g/kg_{H2O}). This large difference in chloride content indicates that these porewaters have little or nothing at all in common in spite of the similar oxygen isotope composition.

South-east of the target volume in the hanging wall bedrock (i.e. fracture domain FFM03) the distance along the borehole between porewater samples and the next water-conducting fracture is generally 5–10 m in the highly transmissive zone down to a depth of about 520 m and seems to become only greater below about 550 m towards the bottom of the KFM02B borehole (Figure 4-29). These short distances are reflected in the porewater isotope compositions that are similar to the possible end members from brackish marine (e.g. Baltic/Littorina seawater types) signatures to cold-climate (glacial?) type signatures, which have circulated in the fractures over the last few thousand years. In contrast to the target volume area, however, older signatures seem not to be or only very weakly preserved in these porewaters.

There are no porewater data down to depths of around 160 m in the hanging wall bedrock segment but it can be assumed to show similarities with the upper, transmissive part of borehole KFM06A (fracture domain FFM02); this indicates porewater isotope signatures similar to present-day infiltration. Below 160 m in the hanging wall (borehole KFM02B) the isotopic signatures become typical of cold-climate (glacial?) infiltration, and then changes below around 200 m to values enriched in ^{18}O, similar to Baltic type signatures. Down to a depth of about 420 m the oxygen isotope signatures become increasingly depleted in ^{18}O towards cold-climate type signatures (Figure 4-29).
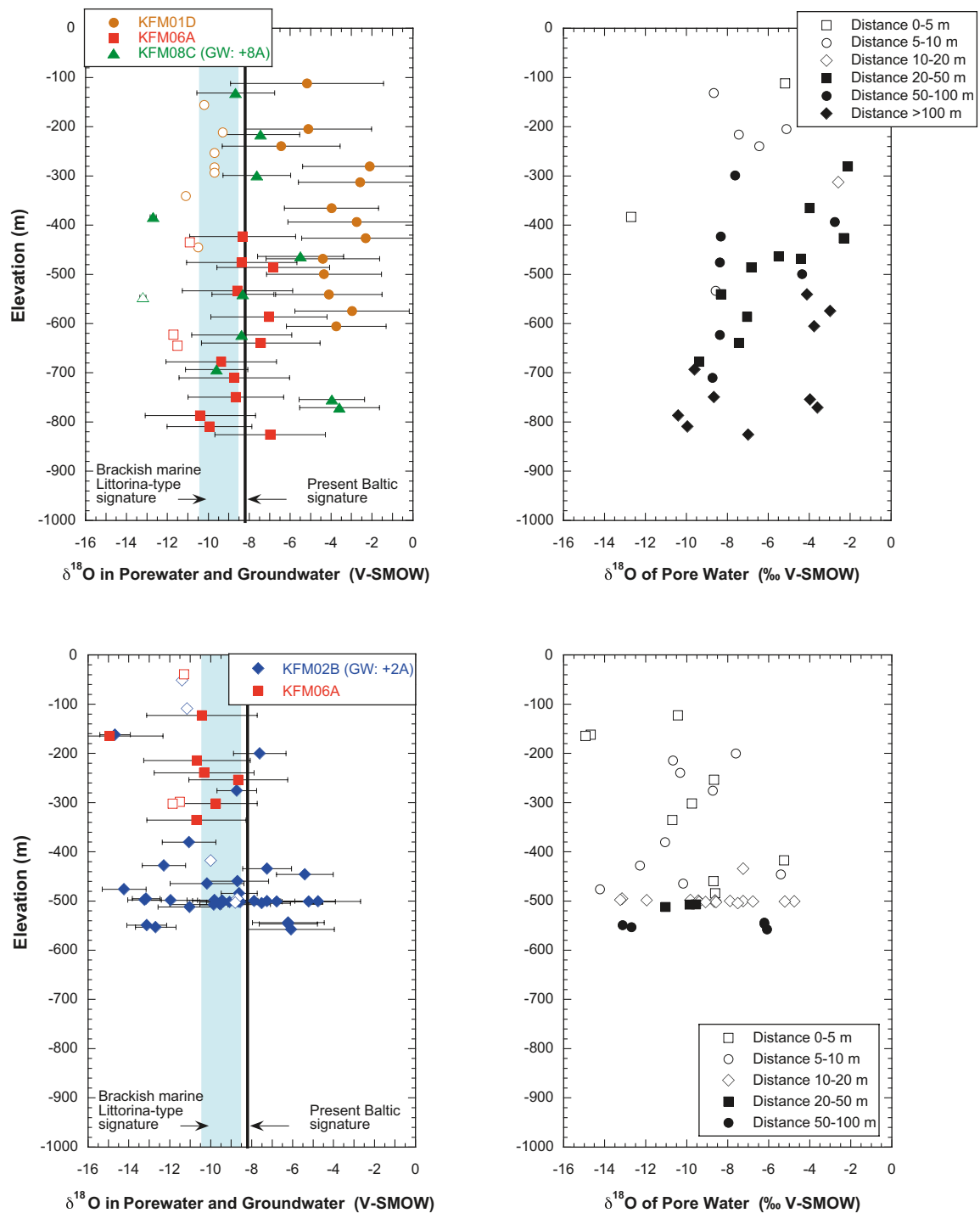
Figure 4-29. $\delta^{18}O$ *of porewaters and related fracture groundwaters (left) in comparison with the distance of the porewater samples along the borehole to the next water-conducting fracture (right). Top: low transmissive, low fracture frequency conditions; bottom: high transmissive, high fracture frequency conditions (error bars indicate propagated error according to Gauss). In left-hand figure, blue shaded column = 'Modified (present) Littorina signature', and the black column = 'Original Littorina signature'.*

The 420 m depth marks the intersection of borehole KFM02B with deformation zone ZFMA2 and around 495 m the intersection with deformation zone ZFMF1. The continuous sampled profile then extends from around 512–530 m depth in the rock matrix. This explains the variation of $\delta^{18}O$ values from about –4.7‰ (brackish marine-type) adjacent to the two major deformation zones, to about –14‰ (cold-climate to glacial type) further into the rock matrix. Close scrutiny can resolve a repetition (three times) where the distance along the borehole to the water-conducting fracture is within a few metres only, and the most negative values occur at depths of 480 m, 500 m, and 550 m (Figure 4-29; bottom). At each of these locations, the gradient described by the porewater isotope composition is steep and the change from a cold-climate type to a brackish-marine type isotope signature occurs within some decimetres to a few metres. Such steep gradients are typical for (geologically) short-term changes in the boundary conditions, i.e. in the fracture groundwater composition. All three inclinations to very negative isotope signatures are correlated with low chloride contents and clearly related to water-conducting fractures indicating that in these fractures cold-climate (glacial?) type groundwater must have circulated prior to the groundwater sampled today.

4.8.6   Solute transport in the rock matrix

To interpret the porewater data in a hydrogeological context, the solute transport, or more specifically the diffusion properties of the rock matrix, need to be known. Such information has been derived from measurements and modelling of chloride concentration time series obtained from the out-diffusion experiments using large-sized (about 1 kg) samples with their original saturation intact /Waber et al. 2008a/. The derived parameters account therefore to a greater degree for the heterogeneity of the rock than conventionally used small-size and resaturated samples, thus reducing the experimental/analytical error.

For all samples, the chloride time-series data obtained from the out-diffusion experiments can be described by radial diffusion from a rock cylinder indicating that equilibration between porewater and the surrounding solution was attained by diffusion only. Furthermore, and as mentioned in section 4.8.2, in situ experiments showed that perturbations of the rock samples and their transport properties due to stress release and contamination with drilling fluid were less than 8% of the obtained chemical and porosity data, thus being within the overall analytical uncertainty /Waber et al. 2008a/.

The obtained pore diffusion coefficients of chloride are largely independent of rock type and depth of the sample and vary for the modelled samples between 4.05×10^{-11} m^2/s and 2.46×10^{-10} m^2/s at a corresponding water-loss porosity of 0.38–0.89 Vol.% (Figure 4-30). Variations observed in the chloride pore-diffusion coefficient appear to be mainly related to the proximity along the borehole of a porewater sample to the next hydrothermally altered and tectonised zone of rock and the rock texture /Waber et al. 2008a/.

Differential flow logging of water conducting fractures in the bedrock at Forsmark show large differences in distance along the borehole between the fractures, for example, distances up to 100 m have been measured in the target volume. It is, however, important to keep in mind that these measurements cannot give a 3-D picture of the fracture network. For the samples analysed for porewaters, differences in concentration between porewater samples and fracture groundwaters are especially observed if the distance to the nearest fractures along the borehole exceeds 5 to10 m. The chemical and isotopic signatures preserved in such porewater samples have been established a long time ago by palaeowaters. These palaeowaters differed in their composition from the fracture groundwaters sampled today, which at repository depth in the target volume are characterised by having residence times in the bedrock of several tens to hundreds of thousands of years (cf. section 4.9).
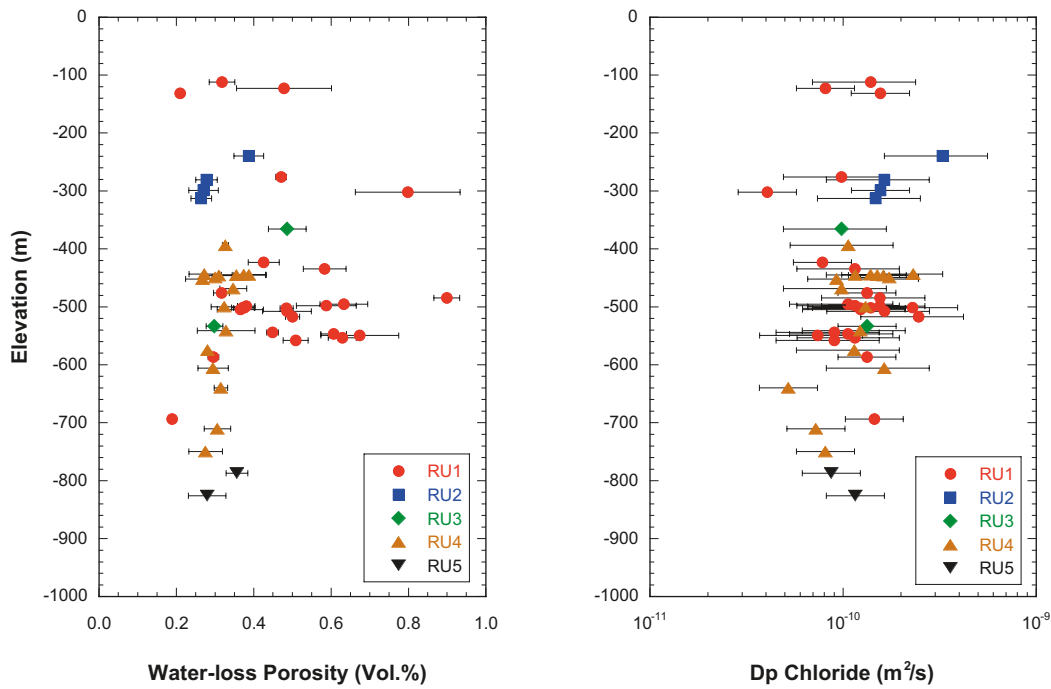
Figure 4-30. *Water-loss porosity (left) and pore diffusion coefficient of chloride (right) as a function of rock unit (for explanation see /Olofsson et al. 2007/) and sample depth.*

Even when taking into account the limitation of observations along the borehole, the porewater investigations show that given enough time, matrix diffusion of solutes is efficient over at least decametres in the intact rock matrix /Waber et al. 2008ab/. The implications of these data for radionuclide retardation in the repository host rock should be examined in detail in any future site-specific performance assessment.

With diffusion being identified as the dominant solute transport process in the rock matrix, the chemical and isotopic concentration of the porewater sample can be brought into an evolutionary context as a function of time (or space) using the fracture groundwater as boundary conditions for the diffusion domain. Figure 4-30 illustrates schematically the concentration change induced in a porewater sample as a function of distance to the next water-conducting fracture and for time periods of 6,000 years and 12,000 years, corresponding very approximately to the time of ingress into the system of Littorina water and the last deglaciation meltwater, respectively. A pore diffusion coefficient for chloride, Dp_{Cl}, at 25°C of 1.29E–10 m²/s, corresponding to the average of the measured values, was used for the calculations. Note that at in situ temperatures of 10°C the Dp_{Cl} would be reduced by about a factor of 1.5 and the distances shown in Figure 4-31 and given below would be reduced by about a factor of 1.2 ($\sqrt{1.5}$). From Figure 4-31 it can be seen that, for example, a signature of a once established chloride content of Littorina water (e.g. 6,500 mg/L) would be completely diluted in a porewater sample located 3.5 metres or less from a fracture above and below (i.e. distance between fractures = 7 m or less) or reduced by about 90% (i.e. to 650 mg/L) in a porewater sample located 5 metres from a fracture above and below, if fresh water would have circulated in both these fractures over the last 6,000 years (Figure 4-31, left). Similarly, a once established glacial isotope signature in a porewater sample (e.g. modern glacial with $\delta^{18}O$ of –17‰) between two fractures would be completely erased over a distance of 10 metres or less, changed to about 40% of the fracture water value (e.g. to about –14.6‰ with a fracture water of –11‰) at a distance of 20 metres, or still be preserved at a distance of more than about 50 metres between the two fractures, and assuming constant fracture water isotope composition over 12,000 years of interaction.
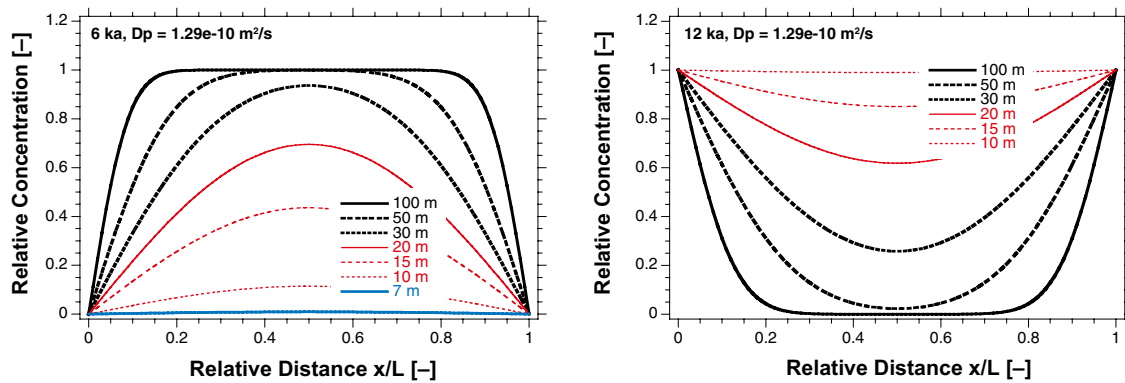
Figure 4-31. *Relative concentration changes induced on the porewater composition of a sample located at different distances between two water-conducting fractures for a time period of 6,000 years (left) and 12,000 years (right). The measured average pore diffusion coefficient for chloride, Dp_{Cl}, of 1.29E–10 m^2/s was assumed.*

4.8.7 Palaeohydrogeochemical evolution

Footwall bedrock observations

Based on the compositional differences of the porewater as function of depth and distance to the next water-conducting fracture, and the fact that solute transport in the rock matrix occurs predominantly by diffusion, the porewater data allow, in combination with the fracture groundwater data, a (partial) reconstruction of the palaeohydrogeological evolution of the site.

In the footwall bedrock of the target volume (boreholes KFM01D, KFM08C, and lower part of KFM06A), the porewaters and groundwater are in a transient state with the porewater having retained older signatures compared with the groundwater. The greater demarcation between porewater and fracture groundwater increases down to a depth of about 600 m, and supports the fact that the porewater has retained a very old, dilute and warm-climate water signature. In the upper footwall bedrock down to a depth of about 150 m, this old signature is modified by a younger brackish marine (i.e. Littorina-type) water while a glacial water signature is not resolved, except for possibly one sample collected close to a water-conducting fracture in borehole KFM08C (about 390 m depth). At greater depths down to about 640 m (600 m in borehole KFM08C), signatures with low chloride, low magnesium and enriched in ^{18}O and ^{2}H have been preserved far away from conducting fractures. Thus, these porewaters must have evolved from an earlier, very long term circulation of dilute groundwaters in the few water-conducting fractures. These signatures cannot be explained by interaction with recent fracture groundwater types and they undoubtedly date back to before the last deglaciation. The isotope composition of these porewaters indicates that they may have originated from a warm climate period, for example, possibly as far back as Tertiary times. Such very old and dilute porewater is consistent with the still prevailing transient state between this porewater and fracture groundwaters from equivalent depths, the latter being more mineralised and less enriched in the heavy isotopes and with estimated residence times of at least 1.5 Ma based on ^{36}Cl and ^{4}He /Smellie et al. 2008, Laaksoharju et al. 2008, also section 4.9/.

The porewaters in the footwall bedrock thus indicate that before the beginning of the Pleistocene-Holocene the entire rock volume was saturated with dilute meteoric water of warm-climate origin, possibly as far back as Tertiary times, down to at least 640 m below (present-day) sea level before intrusion of the last deglaciation meltwater and post-glacial brackish marine water types.

Below an elevation of about 640 m the porewater becomes increasingly saline and the associated isotope composition for some porewater samples is similar to that of the highly saline groundwater in the Laxemar KLX02 borehole ($\delta^{18}O = -8.9‰$ V-SMOW), i.e. more enriched in ^{18}O and ^{2}H than for other samples. Unfortunately, mainly due to the absence of fracture groundwater data from these depths at Forsmark, it can not be distinguished if the (unknown) brine end member in the porewater became mainly diluted (by diffusion) by the old, dilute meteoric water of warm-climate origin observed further up in the rock matrix, or if it became diluted only recently by last deglaciation meltwater or post-glacial fracture groundwaters. The large distances along the borehole between porewater samples and the closest water-conducting fractures, and the general hydraulic observations, however, argue against these latter possibilities.

In highly altered and/or tectonised zones, the porewater appears to record rather recent imprints of higher saline groundwater in the first few metres from a water-conducting zone, for example, as evidenced by the samples taken adjacent to vuggy episyenite in borehole KFM09B. This suggests that the saline groundwater similar to the present one was circulating in the fractures to depths of at least 440 m in the last few thousands of years. This observation is interesting as it suggests that the present-day level of groundwater of similar high salinity, and believed to have originated by upconing from depths greater than 1,000 m in boreholes KFM07A and KFM09C, may at one time have existed at much shallower levels in the bedrock. Although the timing and exact processes of such 'upconing' of deeper, more saline and evolved groundwaters cannot be further defined based on the present data, the indications are that residual highly saline groundwaters have circulated in the past, and are probably not only the result of anthropogenic 'upconing' as presently considered (cf. section 4.1.1).

Hanging wall bedrock observations

At shallow depths down to about 150 m in the hanging wall bedrock (borehole KFM02B) and from shallow depths in the footwall bedrock (borehole KFM06A), the distances along the boreholes to water-conducting fractures are within a similar range (Figure 4-27). The lack of porewater data within this interval precludes any quantitative interpretation, but the limited chloride data available are assumed to indicate a transient state between porewaters and fracture groundwaters, while a situation closer to steady-state is suggested for the isotope composition. The porewaters at this level are considered to reflect an interaction between brackish marine water (based on Cl and Mg). In contrast, just below at about 160 m, the porewater represents a meteoric water of uncertain age, similar in type to the present day or colder climate groundwater (based on $\delta^{18}O$ and $\delta^{2}H$).

At still greater depths in this area, an overall transient state between porewater and groundwater is established down to a depth of about 560 m with lower chloride contents in the porewater compared to the groundwater. In turn, the isotope composition of the few fracture groundwater samples is similar to that in porewater of rock matrix samples collected close to the fractures. Yet, the depleted $\delta^{18}O$ values of less than $-13‰$ V-SMOW preserved further away from the water-conducting fractures indicate that cold-climate glacial water was circulating for a considerable time period in the fractures at these depths. Since the last deglaciation, this cold-climate porewater signature has become overprinted with a brackish marine-type signature as indicated by chloride, magnesium and $\delta^{18}O$ in porewaters sampled closer to the conducting fracture. In the shallow zone, this brackish marine signature is now becoming overprinted by the circulation of present-day meteoric groundwaters.

4.8.8 Conclusions

- Porewater compositions (mainly chloride, $\delta^{18}O$ and magnesium) act as an archive of the past hyrogeologic history and its composition puts strong constraints on the interpretation of the palaeohydrogeological evolution of a site.

- Solute transport in the intact rock matrix appears to be dominated by diffusion and matrix diffusion was identified to occur at least over several decametres into the rock matrix.

- Differences in the preserved porewater compositions indicate a different hydrogeologic evolution for the footwall bedrock (i.e. target volume; fracture domains FFM01 and FFM02) to the north-west, and the hanging wall (fracture domain FFM03) to the southeast, in agreement with the hydrogeological site model.

- In the target volume the porewater composition is dominated by an old, dilute meteoric water of warm-climate origin (Tertiary?) indicating that the rock mass was once saturated with such water down to at least 560 m below surface.

- Adjacent to the gently dipping deformation zone ZFMA2, separating the footwall and hanging wall, the porewater reflects a more recent, mainly Holocene hydrogelogical evolution, with clear indications of cold climate and glacial water together with Littorina-type water intrusions down to about 550 m.

4.9 Groundwater residence time

4.9.1 Background

A key factor in understanding past and present groundwater evolution in the Forsmark area is to constrain the average residence time for each of the major groundwater types. This can be approached qualitatively in terms of the major and trace element compositions of the groundwaters, i.e. based on aspects of water/rock reaction kinetics. Considering different groundwaters that have evolved in a similar geologic environment such as the granitic rocks at Forsmark, a greater groundwater mineralisation can be indicative of a greater residence time (i.e. higher contents of dissolved species as a result of water/rock interaction). Stable isotopes, such as δ^2H, $\delta^{18}O$, $^{11}B/^{10}B$, ^{37}Cl, $\delta^{13}C$, $\delta^{34}S$ and $^{86}Sr/^{87}Sr$, may also give qualitative information on residence times, such as indications of climate change during recharge etc. On a more quantitative level, because of their known half-life decay character, the radioactive isotopes of tritium (^3H), carbon-14 (^{14}C), and chlorine-36 (^{36}Cl) and non-radioactive helium-4 (^4He) are used in the hydrochemical evaluation programme (for details see /Smellie et al. 2008/).

The complex issue of addressing residence times is fully acknowledged and the isotopic methods used can only suggest different times of isolation from the atmosphere. For further discussion see /Smellie et al. 2008/.

4.9.2 Qualitative information on residence time

Granite and granodiorite comprise the main rock types within the Forsmark target volume. The major rock-forming minerals susceptible to groundwater reaction and alteration are K-feldspar, plagioclase, quartz and micas (biotite/muscovite), giving rise respectively to the redistribution and potential concentration in the rock matrix porewaters and fracture groundwaters of, for example, commonly Na, K, Ca, Rb, Ba, Sr and Fe, based on aspects of water-rock reaction kinetics and sorption. With increasing low flow to stagnant groundwater conditions with depth, accompanied by greater water/rock interaction, these constituents should also increase in concentration accordingly. There are clear indications from chloride, calcium and sodium of a steady increase in mineralisation with depth supporting the concept that very old groundwaters are present at the maximum depths sampled /e.g. Smellie et al. 2008, Gimeno et al. 2008/. The amounts of trace elements such as Sr, Rb, Cs and Li in groundwaters are rock dependent but

they all show a tendency to increase in concentration with depth when away from the influence of the brackish marine Littorina type groundwaters. These groundwaters tend to complicate depth trends at shallower depths, often masking them /Smellie et al. 2008/.

Additional qualitative indications of increased water/rock interaction with depth are provided by the behaviour of the stable isotopes $\delta^{18}O$ and δ^2H. Deep basement groundwaters from Canada (in particular) and Fennoscandia (to a much weaker extent) show a deviation from the Global Meteoric Water Line (GMWL) coeval with increased salinity and enrichment in deuterium (^2H) /Smellie et al. 2008, Gimeno et al. 2008/. Forsmark groundwaters show only a weak deviation as highly saline groundwaters are not present at the depths investigated, but comparison with other Fennoscandian sites strengthens this possibility. Based on such observations, rock matrix porewaters would be expected also to have similar δ^2H enrichments, which indeed is the case /Waber and Smellie 2008, Waber et al. 2008a/.

4.9.3 Quantitative information on residence time

Quantitative information on groundwater residence time can be derived from short-lived and long-lived radioisotopes. Within the Forsmark hydrochemical programme the radioisotopes ^3H and ^{14}C are analysed routinely. In addition, ^{36}Cl analysis has been carried out on strategically-related groundwaters at a late stage in the programme. Helium (^4He) gas samples are routinely collected and analysed at selected locations, and this input has been used as support, when possible, to the other dating methods, in particular the ^{36}Cl method.

Short residence times

Understanding present-day flow conditions is crucial in determining, for example, the recharge input chemistry to the bedrock, the starting point for much of the bedrock hydrochemical modelling. Meteoric recharge waters of a young age (i.e. less than 55 years), can be traced by its contents of atmospheric thermonuclear tritium from the 1950's still present in the recharge precipitation and shallow groundwaters. Figure 4-32 show tritium versus depth and includes
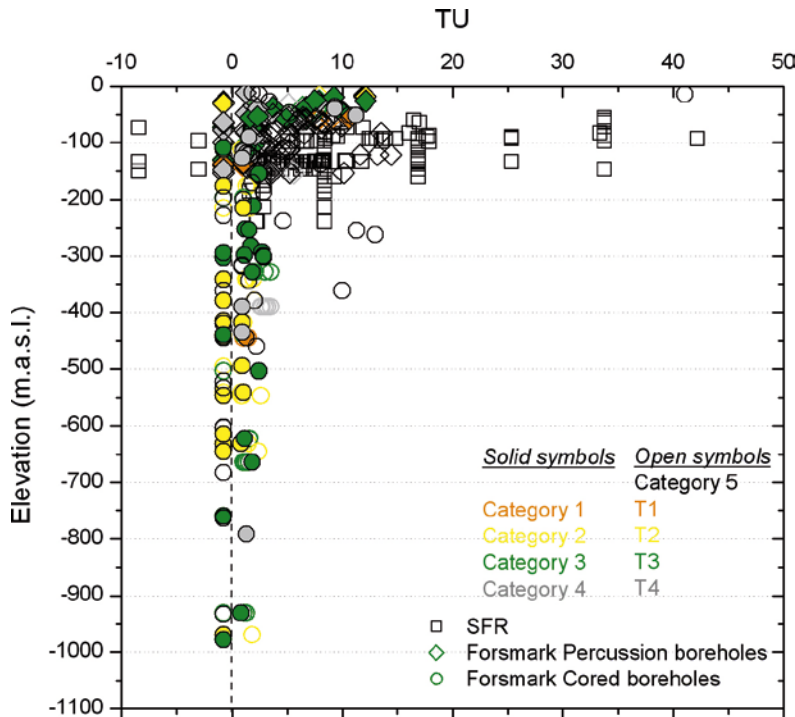

Figure 4-32. *Tritium versus elevation based on category 1–5 data from percussion and cored boreholes, and category 5 data from SFR. Different negative symbols represent different levels of detection.*

category 1–5 data from percussion and cored boreholes within and close to the candidate area, and category 5 data (i.e. all available data are of low or uncertain quality) from the SFR site. The plot shows a characteristic groundwater decrease in tritium at a depth of around 150–200 m, which represents the limit of fresh meteoric recharge waters of a young age. The persistent 1–3 TU with increasing depth is due to various sources of contamination /Smellie et al. 2008/.

Radiocarbon (^{14}C), with a half-life of 5,730 years, extends the range of detection up to 30,000 years for groundwater residence time. Theoretically, this range should cover comfortably the period since the last deglaciation, in particular confirmation of the Littorina Sea transgression. However, radiocarbon dating is complex and a major problem at Forsmark has been to constrain the ^{14}C input signature to the bedrock, and the reactions involving carbonate dissolution and breakdown of recent and old organic material that will affect the $^{14}C_{(TIC)}$ content in different groundwaters. This is discussed in more detail in /Smellie et al. 2008/. Figure 4-33 shows $^{14}C_{(TIC)}$ versus elevation for the Forsmark groundwater samples. The brackish marine waters show $^{14}C_{(TIC)}$ values in the range of 7–34 pmC, HCO$_3$ at 45–160 mg/L and δ^{13}C at –4 to –10‰. Attempts have been made to correct the ^{14}C contents for reactions, mainly based on δ^{13}C. Straight forward calculation from a source term and processes identified, however, has failed to determine the ^{14}C age; the uncertainty is simply too large (G. Buckau, pers. comm. 2007).

Three of the brackish marine waters have also been analysed for ^{14}C (organic) yielding values of 45–53 pmC in samples with $^{14}C_{(TIC)}$ at 13–17 pmC. Lower ^{14}C content in bicarbonate compared with TOC in the same groundwater is usual and normally attributed to reaction involving dissolution of ^{14}C-free carbonates. In conclusion, the radiocarbon analyses support a postglacial origin for the brackish marine (Littorina) groundwater, and 45–53 pmC in the organic phase is in accordance with ages of about 5,000–6,000 years covering the period of maximum salinity during the Littorina stage (4500–3000 BC).
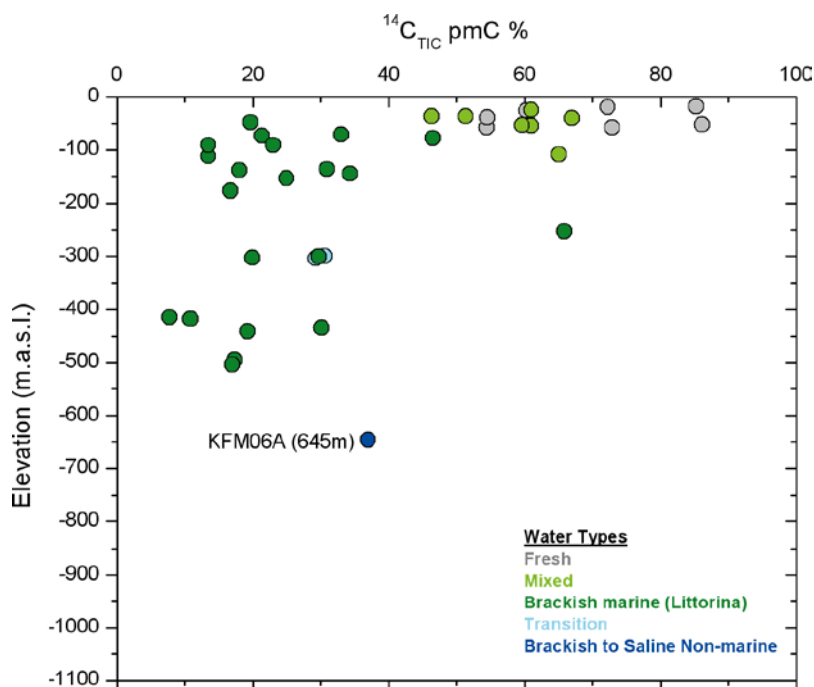

Figure 4-33. *$^{14}C_{(TIC)}$ versus elevation. Only one sample of brackish non-marine water-type was analysed and this indicated contamination during sampling.*

Long residence times

By comparing the measured ^{4}He-concentrations in groundwater with the calculated in situ ^{4}He-production rate (based on uranium and thorium concentrations in the host rock), information about groundwater residence time under closed system conditions, and/or indications of possible external input of helium into the system, can be obtained.

In Figure 4-34 the ^{4}He-concentrations measured in the Forsmark groundwaters are plotted versus the ^{4}He calculated to be produced over a certain period of time in the bedrock from which the groundwaters were sampled. As can be seen from this figure, the ^{4}He concentrations increase from brackish marine (Littorina) to those of transition variants, and eventually to those of the brackish to saline non-marine groundwaters. For the measured ^{4}He concentration in the brackish marine (Littorina) groundwaters it would have required more than 500 ka to produce the equivalent ^{4}He concentration in situ in the rocks by radioactive decay. Even if these Littorina-type groundwaters should contain a certain percentage of a very old component, these calculated time intervals are unrealistically long and, in turn, indicate that there is a contribution of helium flux from greater depth.

For the brackish to saline non-marine groundwaters it would require more than 1.5 Ma to produce the measured ^{4}He concentration in situ. This is in accordance with the ^{36}Cl data for the two saline groundwaters from greatest depths (KFM07A and KFM03A), where secular equilibrium has been achieved, thus giving an identical residence time. This is strong evidence that at these depths the average groundwater residence time is indeed in the order of 1.5 Ma. At shallower levels, where there may be an increased fracture frequency and transmissivity, similar groundwater types with similar ^{4}He concentrations may receive some helium flux from below, thus leading to an overestimation of their residence time. Furthermore, ^{4}He may have originated from only weakly fractured rock portions where localised in situ production may also be occurring, where groundwater flow is also limited, and where the calculated water residence time would therefore be overestimated.
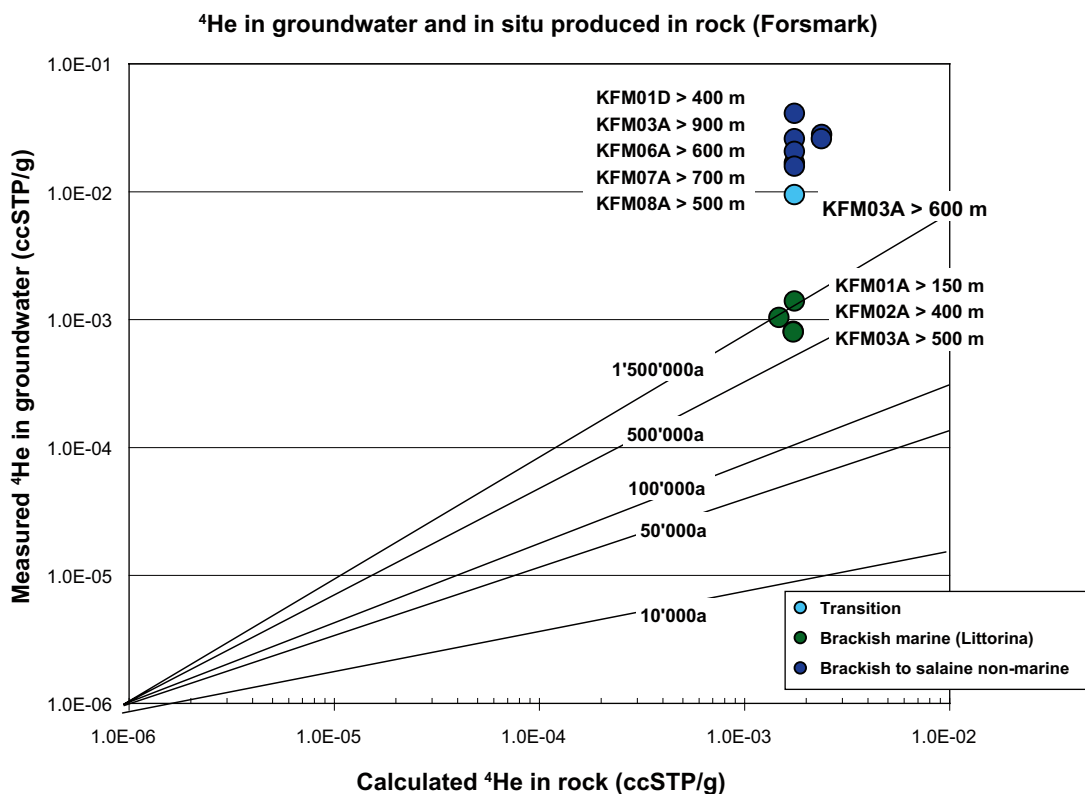
Figure 4-34. *Helium in groundwater and the calculated in situ production (age trendlines neglect He-flux from great depth).*

This latter hypothesis is supported by the trends developed between ^{4}He, δ^{18}O and δ^2H, for example for δ^{18}O in Figure 4-35. Here the ^{4}He concentrations increase from brackish marine (Littorina) to brackish to saline non-marine groundwaters coeval with a simultaneous depletion of δ^{18}O (and δ^2H), i.e. more depleted when compared to the Forsmark groundwaters plotted. This can be explained by an increasing amount of an old, cold-climate water with a longer residence time and thus higher ^{4}He concentration than the brackish marine (Littorina). A second increase in ^{4}He concentrations is then observed within the brackish to saline non-marine groundwaters, but here under simultaneous enrichment of δ^{18}O (and δ^2H). This indicates the increasingly long residence times of these groundwaters with an increasing proportion of either deep saline or warm-temperature climate infiltration, both consistent with the ^{36}Cl data.

4.9.4   Conclusions

In summary, there is a range of qualitative trace and major ion and stable isotope evidence and quantitative isotopic evidence, based on depth relationships, that generally support hydrogeo-logical observations, see also /Smellie et al. 2008/. This evidence shows:

- Recent to young fresh groundwaters, some showing signs of mixing with Littorina-type groundwaters especially in the hanging wall, characterise the upper approximately 100–150 m of the bedrock. At these depths, because the hydraulic system is more dynamic, climatic changes have resulted in the cyclic introduction and flushing out of different groundwater types over tens of thousands of years such that residence times for individual groundwater types seem relatively short, i.e. probably some hundreds to a few thousand years. This situation is common to both the hanging wall and footwall, and is borne out by tritium and ^{14}C which indicate that near-surface groundwaters have short residence times in the order of only a few decades to a few hundred years. This is in agreement with palaeohydrogeological evidence which indicates emergence from the Baltic Sea occurring at some 2,500 years ago with subsequent land uplift establishing meteoric water recharge some 900 years ago.
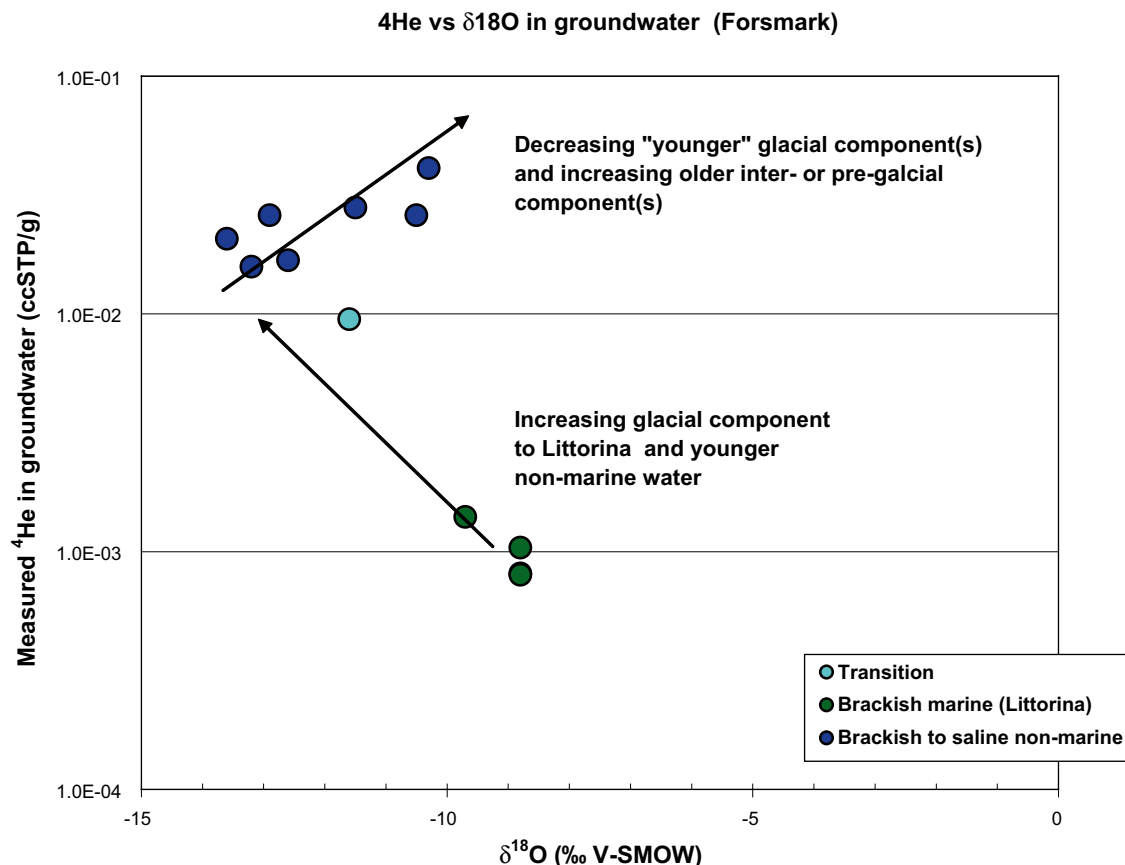

Figure 4-35. *Helium versus δ^{18}O showing the two different evolutionary trends.*

- Older groundwaters of a distinct Littorina type occur from approximately 150 m to depths of around 300–600 m (depending on the location and fracture transmissivity). The radiocarbon analyses support a postglacial origin for the brackish marine (Littorina) groundwater, and 45–53 pmC in the organic phase is in accordance with palaeohydrogeological estimations which suggest an age of approximately 5,000–6,000 years covering the period of maximum salinity during the Littorina stage (4500–3000 BC).

- Because of the relatively short residence time these fresh to brackish marine groundwaters described above have been influenced, in addition to being mixed, mostly by fast reactions such as ion exchange and calcite dissolution together with microbial modifications. Generally, aluminium silicate reactions may also be significant.

- Significantly older groundwaters, found at depths greater than around 300–600 m (depending on the location and fracture transmissivity) to around 1,000 m, are characterised initially by brackish non-marine groundwaters which become successively more mineralised with increasing depth (to saline in type) by water/rock interaction, mixing with (unknown) deep saline water, and exchange with the rock matrix porewater. Hydraulic conditions at these depths indicate low groundwater flow to stagnant conditions and suggest residence times that appear to be considerable. From chlorine-36 the residence time of the brackish to saline non-marine groundwaters can be shown to extend back to at least 1.5 Ma, which is in accordance with the helium-4 systematics.

- No highly saline groundwaters (> 20,000 mg/L Cl) have been sampled at Forsmark, but as indicated by the porewaters /Waber et al. 2008a/ there is a high probability that they exist at greater depths (e.g. KLX02 in the Laxemar subarea) and are at least as old as the shallower brackish non-marine groundwaters.

4.10 Evaluation of uncertainties

4.10.1 Measured and modelled uncertainties in field data and interpretation methods

Before constructing the site descriptive hydrogeochemical model, various uncertainties have to be taken into account. These uncertainties are quantified or discussed below.

Major sources of uncertaintes

During every phase of the hydrogeochemical investigation programme, i.e. drilling, sampling, analysis, evaluation, modelling etc, uncertainties are introduced which have to be accounted for, addressed fully and clearly documented to provide confidence in the end result, whether it will be the site descriptive model or repository safety analysis and design /Smellie et al. 2002/. Handling the uncertainties involved in constructing a site descriptive model has been documented in detail by /Andersson 2003/. The uncertainties can be conceptual uncertainties, data uncertainties, spatial variability of data, chosen scale, degree of confidence in the selected model, and error, precision, accuracy and bias in the predictions. Many of the uncertainties are difficult to judge, since they are results of expert judgement and not mathematical modelling. There is no undisturbed groundwater sampled prior to drilling and therefore much of the uncertainties associated with sampling are based on indirect (e.g. short circuiting) or direct indications (e.g. drilling water content).

The analytical uncertainties are addressed in /Nilsson 2008/ and the model uncertainties in mathematical models are also established. Some of the identified uncertainties recognised during the modelling exercise are discussed below.

The following data uncertainties have been estimated, calculated or modelled for the Forsmark data:

- Disturbances from drilling activities may be ± 10 to70%.

- The effects from earlier drilling activities on category 1–3 samples are set at ≤ 10%; these samples are used for detailed modelling. The high quality of the samples used for the site descriptive model will reduce the uncertainties of the descriptions.

- The redox effect from the drilling water on the groundwater composition is relatively small probably due to the large buffer capacity of the rock.

- Influence associated with pumping and the in-/de-gassing of water may be ± 10%.

- Sample handling and preparation may be ± 5%.

- Individual analytical uncertainty for each chemical and isotopic constituent and their concentration values are reported by the different analytical laboratories, but are not included in the Sicada database. Furthermore, these uncertainty values are difficult to handle in further interpretations due the large volumes of analytical data involved. General uncertainties as reported for the different methods and components are presented in /Nilsson 2008/. Analytical errors associated with laboratory measurements are generally ± 5–10% for major ions (Figure 4-36) but, for example, are less than ± 2% for $\delta^{18}O$ (Figure 4-37). However, for some elements the uncertainties can be larger as shown for bromide in Figure 4-38, see details in /Nilsson 2008/, These effects on interpretation and modelling have been tested and reported in /SKB 2005, Smellie et al. 2008, Gurban 2008/.

- The variability of the mean value of, for example, the measured chloride in groundwater during sampling (first/last sample) can be up to 25%, but the difference is generally much less /Smellie et al. 2008, Gascoyne and Gurban 2008/.

- M3 model uncertainty is ± 0.1 units within the 90% confidence interval; the effects on the modelling were tested in /SKB 2005/. The model uncertainties have been assessed in /Gimeno et al. 2008, Gurban 2008, Molinero et al. 2008/ and the M3 model tested in detail in /Gómez et al. 2006, 2008/. The risk of underestimating the Littorina signature in M3 is discussed in /Molinero et al. 2008/.

Porewaters

As detailed in /Waber et al. 2008a/, the calculation of the concentration of chloride (or any other chemically conservative element) in the porewater from out-diffusion concentrations is inversely proportional to water content in the rock sample in question. The uncertainty of the indirectly derived porewater concentrations thus strongly depends on the accuracy of the water content determination and the degree to which the measured values represent in situ conditions. This becomes especially important in crystalline rocks with low water contents.

Effects that could cause deviation in the measured water content from in situ conditions are related to de-saturation, stress release and the drilling disturbed zone on the rock sample. However, the effect of drilling fluid contamination induced by stress release was quantified to be less than 10% and the effect of the drilling disturbed zone on the porewater content and composition is considered to be less than 1%. It can thus be concluded that by using adequate sampling and conditioning procedures any detrimental effects to the porewater composition can be minimised to an uncertainty of less than 10%.

The uncertainty of porewater concentrations for conservative compounds is mainly related to the textural heterogeneity of the rock and how well the sample mass used for the water-content determination takes this into account. Because of such heterogeneities, the uncertainty band of a porewater concentration of a chemically conservative compound such as chloride or bromide is thus best described by the standard deviation of water contents derived from multiple samples, and/or to the analytical error of the water content determination in the case of a large kg-sized rock sample as used in the out-diffusion experiments.
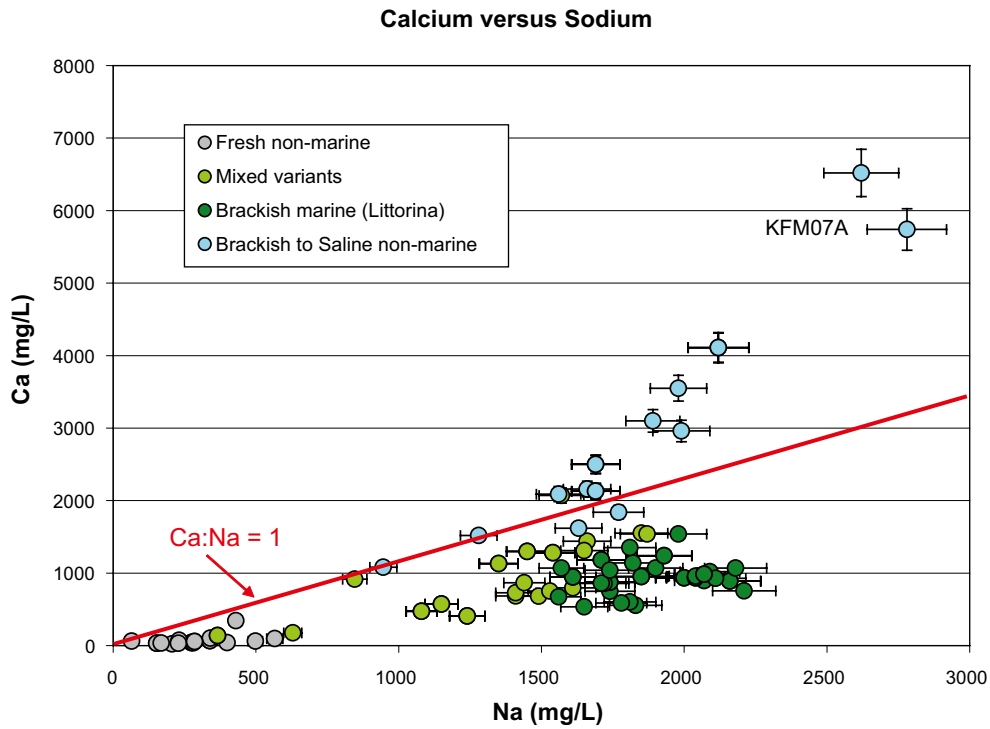
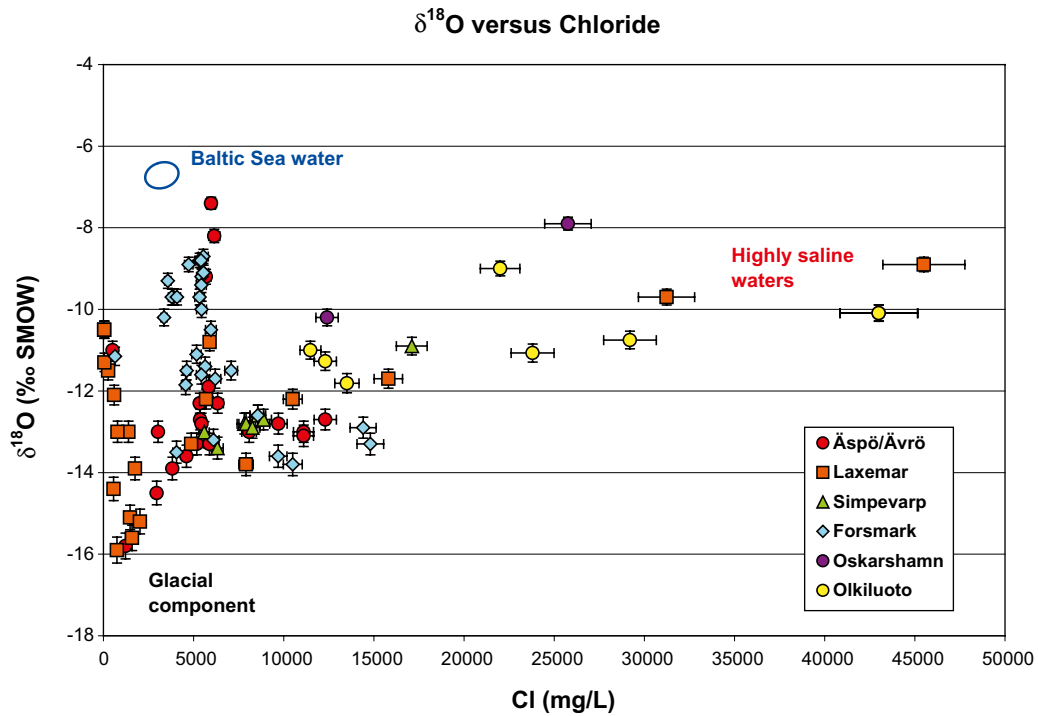**Figure 4-36.** *Calcium versus sodium with an analytical error of ± 5%.*

Figure 4-37. *δ¹⁸O plotted versus Cl with an analytical error of ± 5% for Cl and ± 2% for δ¹⁸O.*
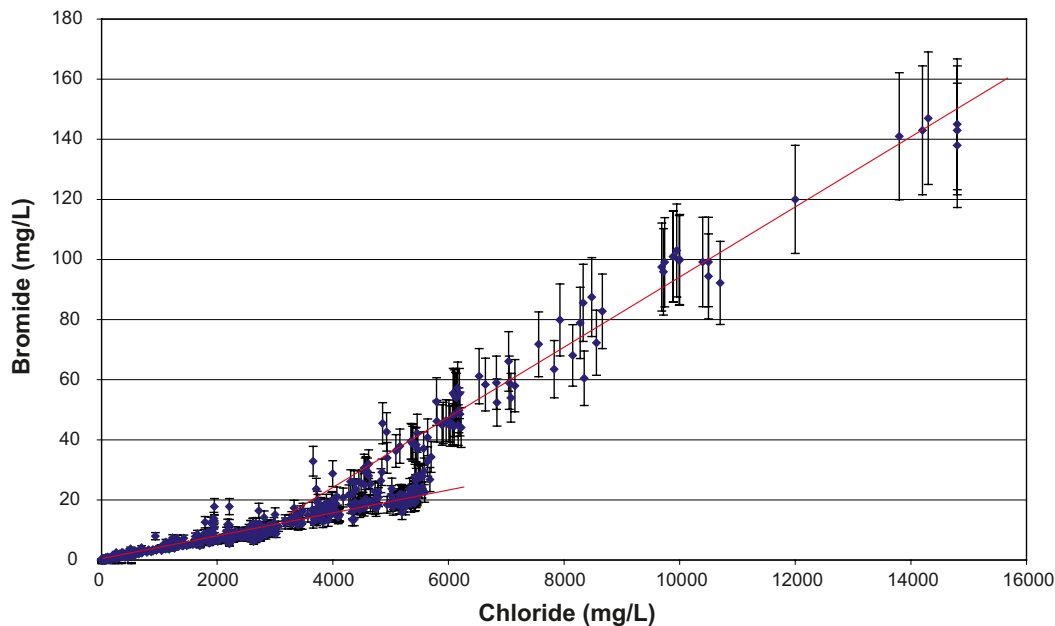
Figure 4-38. *Selected bromide/bromine values (ChemNet dataset version F.2.3) plotted versus chloride concentrations. The short red line indicates a possible marine mixing line, the longer red line a possible non-marine mixing and/or evolution line, and the error bars correspond to ± 15%. For discussion see /Nilsson 2008/.*

The concentrations obtained in the out-diffusion experimental solutions are converted to pore-water concentrations using the geochemical porosity for chemically conservative components, while those for reactive components need to be corrected for water/rock interaction during the experiment by applying geochemical modelling. Geochemical model calculations using mineral dissolution kinetics are particularly important to show that the contribution of magnesium (marine indicator) from mineral dissolution during out-diffusion to the experiment solution, contributes only a small fraction of the magnesium concentration measured in the experiment solution /Waber et al. 2008a/. Such geochemical modelling calculations show that the contribution from mineral dissolution during the experiment is limited and within 10 percent of the measured concentration in the experiment solutions.

The uncertainty of the porewater isotope composition using the isotope diffusive-exchange technique is appropriately described by the error propagated according to Gauss. Contamination by drilling fluid would affect the calculated isotope composition only in cases where such contamination would exceed about 10%. Studies have shown that such a high contamination can be excluded.

In conclusion, the water contents and water-content porosity, the chemical and isotopic composition of the porewater, and the pore diffusion coefficients derived from the out-diffusion extraction of porewater, do appear to represent in situ conditions within the given uncertainty band.

Fracture mineralogy

Uncertainties in fracture mineral frequency and fracture mineral composition are discussed in detail in /Sandstrom et al. 2008/.

Conceptual models

In the construction of conceptual models, for example, the palaeohydrogeological conceptual model, errors can occur when evaluating the influence of old water end members in the bedrock where they can only be indicated by using certain elemental or isotopic signatures. The degree of uncertainty therefore increases generally with the age of the end member. Furthermore, the effect of porewater chemistry potentially altering the groundwater is not taken into account (cf. section 4.8).

The relevance of an end member participating in groundwater formation can be tested by introducing alternative end-member compositions or by using hydrodynamic modelling to test if old water types can reside in the bedrock during prevailing hydrogeological conditions. At this model stage, a measure of validation is obtained by using statistical methods (cf. section below, and /Gimeno et al. 2008, Molinero et al. 2008/ to test the feasibility of the selected end member together with comparison with results of hydrogeological simulations. The risk of underestimating the Littorina end member influences is described in detail in /Molinero et al. 2008/.

Geochemical models

Uncertainties associated with using the PHREEQC code depend on which code version is being used. Generally, the analytical uncertainties and uncertainties concerning the thermodynamic data bases are of importance (e.g. in speciation-solubility calculations). Care is also required in order to select mineral phases which are realistic (even better if they have been positively identified) for the systems being modelled. These errors can be addressed by using sensitivity analyses, alternative models and descriptions. A sensitivity analysis was performed concerning the calculations of activity coefficients in waters with high ionic strength. This analysis and also the uncertainties of the stability diagrams and redox modelling are discussed in /SKB 2005/.

2D and 3D visualisation

The uncertainty due to 3D interpolation and 2D/3D visualisation depends on various aspects, i.e. the data quality, distribution, model uncertainties, assumptions and limitations introduced. The uncertainties are therefore often site specific and some of them can be tested by, for example, the effect of 2D/3D interpolations. The site-specific uncertainties can be tested by using quantified uncertainties, alternative models and comparison with independent models, such as hydrogeological simulations.

Modelling discrepancies

The discrepancies between different modelling approaches can be due to differences in the boundary conditions used in the models or in the assumptions made. The discrepancies between models have been used as an important opportunity to guide further modelling, including validation efforts and confidence building. In this work, the use of different modelling approaches starting from traditional geochemical approaches to advanced coupled modelling can be seen as a combined tool for confidence building. The same type of process descriptions, independent of the modelling tool or approach, increases confidence in the modelling. The use of quality assured samples and restricting the modellers to use primarily category 1–3 samples further reduces the uncertainties of the site description.

End-member tests

Extensive testing of the end members used in the M3 mixing modelling is presented in /Gimeno et al. 2008, Gurban 2008, Molinero et al.2008/. These tests are an important tool for supporting the hydrogeochemical conceptual model and for integration between hydrochemistry and hydrogeology.

A Monte Carlo method has been developed /Gimeno et al. 2008/ to obtain an independent assessment of the feasibility of the chemical composition of the end members: Deep Saline, Glacial, Littorina, and Altered Meteoric. The method computes at the same time the mixing proportions of each sample in a dataset and the composition (i.e. the concentration of several input compositional variables) of the end member waters. It is based on a Monte Carlo sampling of the end members' compositional space and the simultaneous calculation of the mixing proportions of *all samples* by a Principal Component Analysis (PCA). The aim is to try and find the right combination of mixing proportions and end-member compositions that together minimise the residuals with respect to several conservative elements.

The results of the above procedure are shown for all the elements (and end members) in the form of histograms rejecting the 100 best runs /Gimeno et al. 2008/. Each histogram has either one blue arrow pointing to a particular concentration value or two arrows spanning a range of concentrations. These are the values that characterise the composition of the proposed end members (Deep Saline, Glacial, Littorina and Altered Meteoric).

As an example of the tests applied, Figure 4-39 shows the tests on the Deep Saline end member. The blue arrow in each of the histograms point to the concentration of the given element in the end member traditionally used to compute the mixing proportions in Forsmark. These traditional end members can be actual waters, extrapolations from actual waters, or theoretical waters derived by applying several geochemical constraints and assumptions. The present approach can then be considered as an independent assessment of the feasible composition of each end member, to be compared with the composition derived from the traditional approach.

Figure 4-39 shows that magnesium and bicarbonate are not constrained by the method and any value inside the range gives similar residuals. Sodium is also poorly constrained, although it seems that values below 8,000 mg/L are less probable. As for calcium, it is only constrained in its lower end, with values below 15,000 mg/L being very improbable. Most probable values for potassium are around 40–50 mg/L, exactly matching the value used in the proposed end member.

Chlorine is around 50,000 mg/L, very close to the 47,000 mg/L selected for the Deep Saline end member; and sulphate must be above 200 mg/L and below 800 mg/L, possibly eliminating the low-sulphate end member suggested above. Finally, the isotopes are well constrained and in good agreement with the values used for the proposed end member.
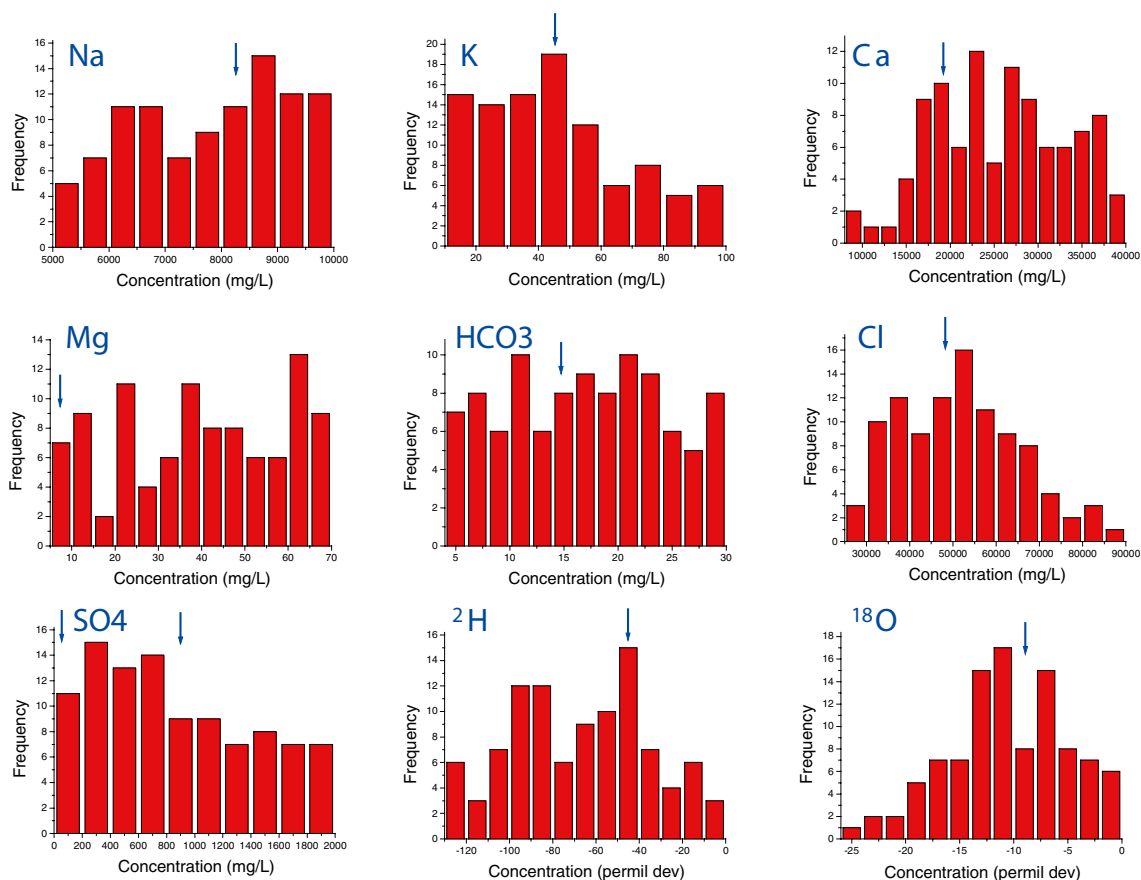
Figure 4-39. *Composition of the Deep Saline end member. The blue arrow in each histogram points to the concentration of the given element in the end member traditionally used to compute the mixing proportions in Forsmark.*

The Monte Carlo method gives an independent assessment of the chemical composition of the end members: Deep Saline, Glacial, Littorina, and Altered Meteoric. The comparison of these results with the ones obtained by more traditional approaches as summarised in sections 2.1.1 to 2.1.4 in /Gimeno et al. 2008/ serves to build confidence and reduce the uncertainty in their compositional characteristics, and at the same time place rather strict lower and upper limits for some of the elements. The value suggested by the Monte Carlo method is in most cases inside the range for the proposed end members. All the elements constrained by the method in the Deep Saline end member are within the range of the composition of the proposed end member. The same conclusion applies to the Littorina end member, although in this case more elements are not constrained by the Monte Carlo method. The only noteworthy discrepancies are thus the following:

1. For the Glacial end member, the isotopes have less negative values in the Monte Carlo method. As explained, this could mean that the 'glacial' end member is not a pure end member but a mixture of a pure glacial melt-water and old meteoric water. This is supported by the palaeohydrological history of the Forsmark site. The most probable value of –16‰ V-SMOW for $\delta^{18}O$ could then be roughly a 50–50% mixture of glacial meltwater and old meteoric water.

2. For the Altered Meteoric end member, all the elements except calcium are well constrained by the Monte Carlo method and most of them are compatible with the proposed composition of the Altered Meteoric end member. Chloride seems to be higher than the value presently used (< 181 mg/L) and the isotopes are again less negative than presently used, although the discrepancy is not large in any of the cases.

The main conclusion to be drawn from this exercise is that most elemental concentrations resulting from the Monte Carlo approach are in full agreement with most of those derived from the traditional (geochemical) approach /Smellie et al. 2008, Gimeno et al. 2008/. One potential exception is the use of the deep, highly saline Laxemar end member to evaluate the Forsmark data. Even though the most evolved Forsmark saline water component is considerably less evolved than at Laxemar, there is sufficient hydrochemical evidence to suggest that the Forsmark deep groundwaters have a different evolutionary trend to that of the Oskarshamn sites /Smellie et al. 2008/, at least enough to consider allocating a separate end member for Forsmark.

Nevertheless, most of the groundwater compositions found in the Forsmark area can be justified by the existence of simple mixing processes, the chemical reactions being of secondary importance for most major elements. This conclusion is strongly supported by the results of both independent approaches to the problem, which increases confidence on the robustness and feasibility of the general conceptual model proposed.

Effects of borehole perturbations

It is well known that site characterisation activities (mainly drilling activities) introduce perturbations in the system that can impact on the hydrochemistry of the groundwater samples collected at the site. It is of interest, therefore, to perform scoping calculations in order to evaluate how much disturbance can be allowed for a given groundwater sample at repository depth, and still meet, for example, the SKB suitability criteria /Molinero et al. 2008/. Two main approaches have been selected to deal with these scoping calculations: a) simple mixing and reaction modelling, and b) coupled reactive transport modelling. The sample (no 12354) from borehole KFM01D at 445 m depth was used to represent groundwater from repository depth. This sample was diluted with a modified meteoric water/precipitation composition.

It was concluded that suitability criteria related to TDS and pH would be fulfilled always, even for complete disturbance of the sample. The Ca+Mg criteria could be influenced with dilutions higher than 90 percent of the native groundwater sample. Furthermore, cation exchange processes have an effect by lowering the Ca+Mg concentrations in the groundwater, compared with a pure conservative mixing.

The oxygen consumption capacity of the granite bedrock has also been evaluated by using reactive transport modelling. This showed that a hypothetical pulse of oxidising water repository depth would be consumed in a relatively short period of time (about 1 year) if the maximum amounts of reported pyrite are included in the model. However, the model results have proved to be sensitive to uncertain parameters such as the exact mineralogical composition and the specific reactive surface area of such minerals. In the base case considered in the model, an interesting conclusion is that the oxygen intrusion in a borehole would only affect a very short distance into the bedrock (of about 1 cm). The modelling documented in /Molinero et al. 2008/ supports the above conclusions where the oxidising influence from drilling water on the ground-water composition was considered small, although the initially introduced drilling waters are not strongly oxidising as attempts to reduce oxidation (e.g. by flushing with nitrogen gas) are part of the routine procedure during drilling. Furthermore, the measured downhole redox potential measurements (Eh) provide evidence of the reductive capacity of the groundwater system (Figure 4-40). Despite uplifting of the equipment due to pump failure the Eh measurements show that the reducing conditions are quickly reestablished and possible oxygen contamination is quickly consumed.

4.10.2 Temporal and spatial variability

Temporal hydrochemical variability is largely dependent on the hydraulic properties of the borehole and host bedrock, and the drilling and sampling effects.

The variability of groundwater characteristics has been estimated by comparing the electrical conductivity values measured shortly after drilling with the results obtained during hydrogeo-chemical sampling (tube sampling) and by studying the time series and subsequent monitoring (see /Smellie et al. 2008, Gimeno et al. 2008, Gurban 2008/). Figure 4-41 illustrates a case in which the groundwater electrical conductivity (EC) measured in two sections sampled for complete chemical characterisation (CCC) in borehole KFM06A are compared with EC results from earlier open hole flow logging and from tube sampling. The measurements where conducted during a time period of almost three years (December 2003 to October 2006). The upper section
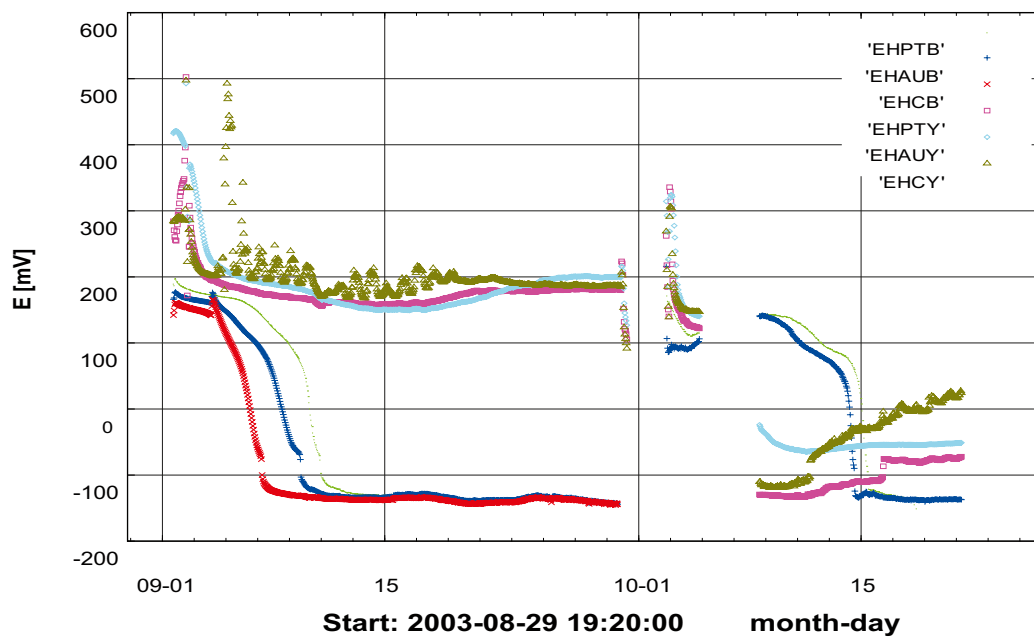
Figure 4-40. *Redox potential measurements (Eh, mV) in KFM02A, 509.0–516.1 m borehole length using platinum, gold and carbon electrodes in the borehole section (EHPTB, EHAUB and EHCB) and at the surface (EHPTY, EHAUY and EHCY).*
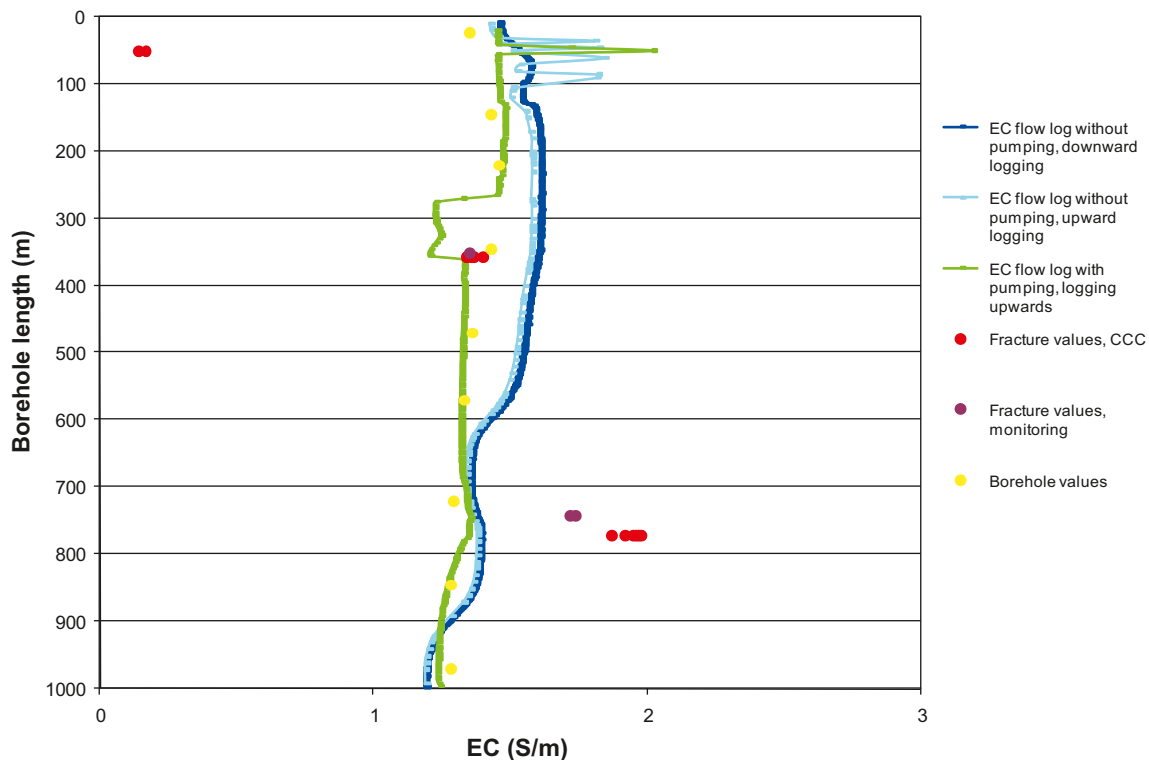
Figure 4-41. *The electrical conductivity is measured during hydraulic logging of the freshly drilled borehole KFM06A (borehole values); green line indicates pumping, blue and turquoise lines indicate no pumping. The borehole values have been inserted to compare with the conductivity of the samples taken: a) in the open borehole (borehole values as yellow infilled circles), and b) with time series (red circles) taken during hydrogeochemical sampling from fractures. The fracture groundwater samples are collected during complete chemical sampling (CCC) and during the monitoring programme.*

(around 370 m core length) showed similar water composition through all the sampling campaigns. In contrast, the deeper section (around 770 m core length) showed much higher salinity in the CCC sampling compared with the open-hole sampling and EC flow logging. During the monitoring phase, a section just above the fracture sampled for CCC was sampled and this showed slightly lower salinity and also some mixing with brackish and partly marine waters. This indicates sampling in, or close to, a transition zone between brackish and saline waters (see /Smellie et al. 2008, Gurban 2008/). The large amount of data from different measurements and time periods can be used to indicate the temporal variability of the groundwater in the bedrock and lends support to the quality of the samples used in the site description.

To address the spatial variability 3D plots can be used to show how the measured samples vary in the 3D bedrock volume. To address the possible groundwater variability between the boreholes coupled modelling shouled be used /Auqué et al. 2008/. The methodology combines results from the hydrogeological site descriptive model with a mixing and reaction-path simulation using PHREEQC. This coupling provides the theoretical but detailed compositional characters of the groundwaters in a rock volume (constituted by a grid with about one million points) that represents the whole regional area of Forsmark down to 2.3 km depth (for details see /Gimeno et al. 2008/).

4.10.3 Forsmark local scale hydrogeochemical site visualisation

The hydrogeochemical site visualisation (section 6.2) is based on a systematic, step-wise approach to determine depth trends and hydrochemical groupings of the groundwaters as detailed throughout chapter 4 and the porewaters as outlined in section 4.8. Understanding

of the system therefore reflects the interpretation of hydrochemical data which has undergone a rigorous quality check and categorisation; in other words a high degree of confidence. Coupled with the results of quality assured hydrogeological measurements and modelling, which in turn is based on geological models of high standard, the input properties to the hydrogeochemical visualisation should represent the best quality available at this moment of time. Uncertainties undoubtedly still remain, perhaps stemming from inadequacies in the geological model which may impact on the hydrogeological interpretation and possibly therefore on the integrity of the hydrogeochemical model and visualisation. However, the close agreement between all three disciplines indicates that the degree of uncertainty associated with the input data to the visualisation is low.

The upper 300–700 m of the bedrock are fairly well characterised with corresponding low uncertainties. The main uncertainties are associated with the spatial lack of hydrochemical data, both laterally (particularly in the case of the porewater), and at depths greater than 700 m (particularly in the case of the fracture groundwater), such that a large degree of expert judgement has been used to extrapolate the hydrochemistry along the extent of the cross-sections. There is, however, a greater geological and hydrogeological coverage documented to depth, in particular the latter, which has helped to extrapolate the hydrochemistry and porewater data, therefore reducing the uncertainties. Moreover, the uncertainties were further reduced with the realisation that at depths greater than 700 m, the fracture groundwater and porewater chemistries increase fairly uniformly in salinity and laterally appear to be quite homogeneous.

4.10.4 General confidence level

The following aspects of the hydrogeochemical model are associated with the highest confidence:

*   The origin of most of the end members (meteoric, marine, glacial) and major processes (qualitative control concerning Eh and pH buffer capacity, major reactions) affecting the present water composition at the sampled locations.

*   Predictability concerning expected groundwater composition.

The main reasons for this confidence are the many consistent time and spatial data to support the description concerning the origin, most of the major end members and major processes. Integration with hydrogeology supports the palaeohydrogeological description of the site. Various approaches such as modelling reactions, interpretation of different isotope ratios (Sr, S, C), buffer capacity measurements (Eh, pH) and microbe data, support the process understanding.

Reasons for the composition of matrix porewaters are fairly well established and correspond closely to the present conceptualisation of the Forsmark area.

The following aspects are associated with the lowest confidence:

*   Variations in site redox conditions (e.g. redox front propagation) with time; additional high-quality data are required.

*   Mineral phases giving rise to the elevated uranium values in the groundwater; additional mineralogical data of primary and/or secondary uranium-bearing phases in water-conducting fractures would help to support the present hypothesis.

*   The regional salinity distribution outside the target volume; important to resolve the issue of a deep saline Forsmark sample for modelling purposes.

*   The in situ concentration of sulphide; requires careful groundwater monitoring to exclude possible anthropogenic effects.

*   The sources, production rate and transport mechanisms of geogas.

The implications of these uncertainties are potentially important and need to be assessed further in the SR-Site programme.

5 Input from the hydrogeological modelling

5.1 Introduction

Close integration of hydrogeochemistry and hydrogeology is a necessary prerequisite to achieve site understanding. Hydrogeology requires hydrogeochemical information, for example, salinity distributions, groundwater residence time and end-member compositions, palaeohydrogeochemical input to help constrain model boundary conditions etc. Hydrogeology, on the other hand, can provide the groundwater flow parameters related to the geological framework so that the spatial distribution of hydrochemical signatures (laterally and vertically) can be interpreted and visualised. Within the Forsmark investigations, the following steps have helped shape the interaction between hydrogechemistry and hydrogeology.

1) **Palaeo-conceptual model** construction for the site based on available Quaternary geological information. The model was used to set the boundary conditions for the hydrogeochemical and hydrogeological modelling.

2) **Parameter values and modelling results** such as major ions and isotopes and M3 mixing proportions and porewater data were delivered to HydroNet and used for flow model calibrations and comparisons.

3) **Collaboration** in the form of regular discussions focussed on boundary conditions and their relevance to the conceptual site modelling, and to the development of the palaeohydrogeological and palaeohydrogeochemical conceptual models.

4) **Hydrogeochemical site descriptive model** is based on a common nomenclature of groundwater types and groundwater flow understanding achieved through discussion and interaction.

5.2 Model interaction

Hydrodynamic assessment of the hydrochemical evolution is based largely on conservative hydrochemical constituents such as $\delta^{18}O$ and deuterium, chloride and bromide. $\delta^{18}O$ (and deuterium) may indicate not only the distribution of one or more cold climate signatures, but also input of marine waters usually characterised by enriched $\delta^{18}O$ signatures. Chloride is used as an indicator of fresh versus saline water influences. The predicted salinity distribution provides important feedback from hydrogeology and is used to understand the flow directions and salinity distribution in 3D and, consequently, support to the site descriptive hydrogeochemical models presented in Figure 6-1, Figure 6-2 and Figure 6-3. The conservative behaviour of bromide, however, has been disputed by /e.g. Upstill-Goddard and Elderfield 1988/ who have shown that bromide can be released from organics during diagenesis, thus enhancing its concentration in groundwaters and thereby changing the original sea water Br/Cl ratios. In Forsmark this process is believed to be relatively small since there is a clear marine signature based on the Br/Cl ratios in the groundwaters with Littorina signatures.

In contrast, considerable uncertainty exists at Forsmark around the bromide and chloride issue associated with the deeper saline groundwater (i.e. highest salinity at Forsmark is 14,000 to 15,000 mg/L Cl) from depths greater than 1,000 m. In this respect it should be pointed out that the deep saline Br/Cl ratio for Laxemar has been used in the Forsmark stage 2.2 hydrogeological model simulations, thus resulting in lower than expected estimated ratios/values. This discrepancy has led to a misfit between modelled values when compared to the measured ones. However, the hydrogeological model still detects the switch from brackish marine to brackish non-marine waters with increasing depth displayed in the hydrogeochemical conceptual model /Follin et al. 2007a, 2008b/.

For the major non-conservative groundwater constituents, i.e. sodium, calcium, potassium, magnesium, sulphate and bicarbonate, these are also of interest but, primarily, from a qualitative point of view. Indeed, reactions involving ion exchange and microbiologically-mediated processes clearly affect the composition of these non-conservative constituents and may mislead interpretation of the physical system studied, if mixing alone is assumed for the flow model calibration. Nevertheless, magnesium, for instance, has been an excellent indicator in distinguishing between marine versus non-marine saline groundwater conditions in the Forsmark area /SKB 2005, 2006b/. The uncertainty associated with magnesium is discussed in /Molinero et al. 2008/.

Indications of present-day flow conditions are exemplified by the characteristic groundwater decrease in tritium at a depth of around 150 m which represents the limit of fresh, meteoric recharge waters of a young age (i.e. less than 55 years) based on the amounts of atmospheric thermonuclear tritium from the 1950's still present in the recharge precipitation and shallow groundwaters (cf. section 4.9.3 and Figure 4-29). The persistent 1–3 TU with increasing depth is due to various sources of contamination /Smellie et al. 2008/.

Generally, tritium and ^{14}C indicate that near-surface groundwaters have short residence times in the order of a few hundred years to only a few decades. This is in agreement with palaeohydrogeological evidence which indicates emergence commencing some 2,500 years ago at Forsmark with the establishment of meteoric water recharge and circulation some 900 years ago.

For much of the target volume (footwall bedrock including fracture domains FFM01 and FFM06), the sharp transition between tritiated (young) and non-tritiated (> 55 years old) groundwaters is due to the shallow bedrock aquifer comprising a lattice of sub-horizontal fractures of high transmissivity mainly at depths from 50–200 m in the uppermost part of the footwall bedrock (i.e. fracture domain FFM02). This shallow bedrock aquifer facilitates the rapid flushing of these young recharge waters towards the Baltic Sea to the north-east, and also limits active recharge into the underlying, less water-conductive bedrock represented by fracture domain FFM01 /cf. section 9.3.1, and Follin et al. 2007a/. This is a good example of interaction between hydrogeology and hydrogeochemistry, producing a consistent decription of the site observations

To evaluate the extent of mixing between glacial meltwater and the Littorina type waters a larger data set is used, including category 5 samples, many of which originate from the SFR site. Infiltration of Littorina Sea water and the resulting mixing with glacial water has been gradual, and this is especially important in interpreting the SFR samples which represent the upper approximate 200 m of the bedrock and plot along a mixing line between the glacial and marine groups. Between 200–300 m depth, some brackish waters with a significantly depleted $\delta^{18}O$ signature are present, representing samples from boreholes KFM12A and KFM11A located outside the candidate area. These waters are not typically brackish-marine, but show instead salinity compositions which indicate complex mixing between brackish marine, brackish non-marine and glacial waters, and therefore are referred to as transition zone or brackish glacial samples. These examples suggest a limited reservoir of glacial water preserved, for example, in pockets or lenses or dead-end fractures etc in the upper bedrock of the footwall closely associated with the shallow bedrock aquifer. Generally in the candidate area, at depths below 500 m and down to the maximum sampled depth at around 970 m, there is a depletion trend in $\delta^{18}O$ indicating an increasing glacial component, which does not necessarily represent the last deglaciation.

These characteristic groundwater mixing features are illustrated in Figure 5-1 which plots $\delta^{18}O$ against elevation to show the distribution of cold climate and brackish marine input to the Forsmark bedrock. The figure is based on category 1 to 5 data from percussion and cored boreholes within and close to the candidate area, and category 5 data (i.e. all available data are of uncertain quality) from the SFR site. In the figure the original range of $\delta^{18}O$ values for the Littorina Sea and for glacial meltwater are also indicated. Apparent is that all groundwaters plot in the area between these two extremes, and all show signs of mixing.
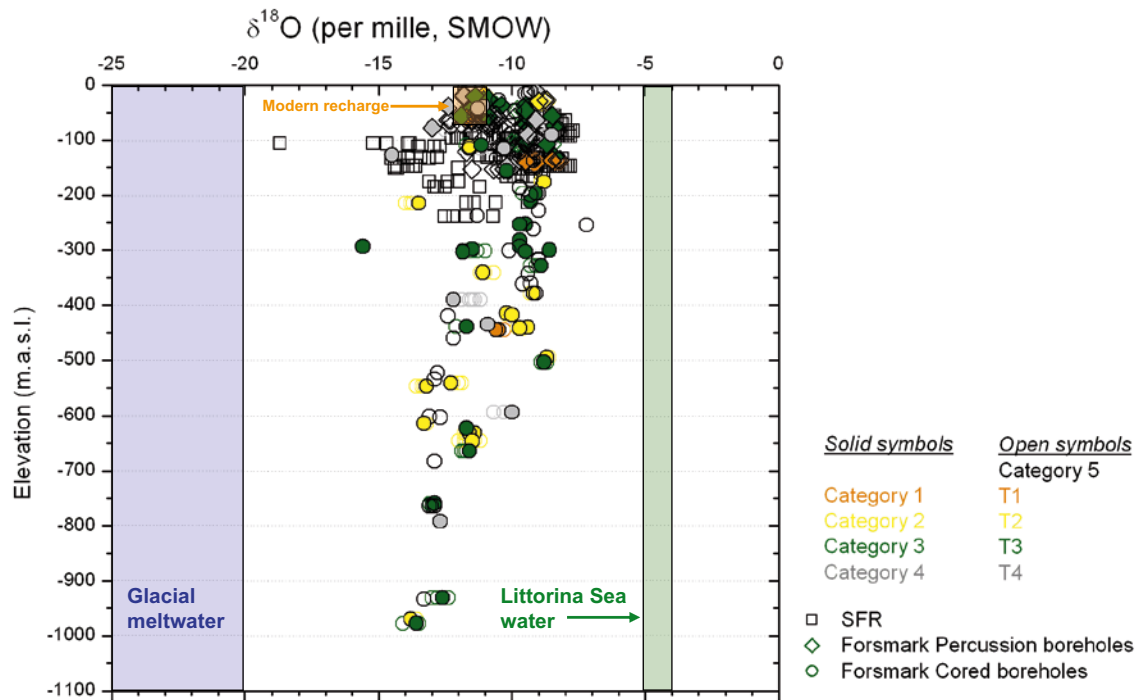
Figure 5-1. *$\delta^{18}O$ versus elevation based on category 1–5 data from all percussion and cored boreholes, and category 5 data from SFR (Final Repository for Radioactive Operational Waste). The modern recharge, glacial and marine influences are recognised; see text for discussion. The reference to T1–T4 indicates time-series data measured from some of the borehole sections; these data are shown as a horizontal series of open circles colour coded, with the actual categorised sample infilled.*

In the upper approximately 100 m, $\delta^{18}O$ values between –12 to –11‰ V-SMOW (and also corre-spondingly high tritium values) represent meteoric recharge water typical of the Forsmark area. These waters have undergone to various degrees localised mixing with waters from different sources, either naturally (especially brackish marine (Littorina) groundwaters which sometimes occur close to the surface), or due to anthropogenic influences (i.e. borehole activities). This gives rise to waters with $\delta^{18}O$ values between –11 and –7.5‰ V-SMOW.

At depths greater than about 100 m three groups can be distinguished: a) one group of values between –13 to –10‰ V-SMOW extending down to around 950 m which show possible mixing beween deep water and shallow meteoric or marine waters, b) another group showing $\delta^{18}O$ values between –13 to –16‰ V-SMOW, indicating a significant glacial component; these waters can be found at various depths from 100 m down to around 1,000 m, and c) a group of waters showing values between –10 to –7‰ V-SMOW extending down to around 600 m indicating a significant brackish marine input. The last group corresponds mainly to the brackish marine (Littorina) groundwaters.

The waters with low $\delta^{18}O$ (< –13‰ V-SMOW) in the upper 100–200 m are mainly related to mixing between brackish marine waters of Littorina type and glacial meltwater. Infiltration of Littorina Sea water and the resulting mixing with glacial water is gradual and is especially important in the samples collected from SFR which plot along a mixing line between the glacial and marine groups (Figure 5-1). Between 200–300 m some brackish groundwaters with a significantly low $\delta^{18}O$ signature are present, representing samples from boreholes KFM12A and KFM11A located outside the candidate area. These groundwaters are not typi-cally brackish-marine, but show instead salinity compositions which indicate complex mixing between brackish marine, brackish non-marine and glacial waters, and therefore are referred to as transition zone samples. These examples suggest a limited reservoir of glacial water, for example in pockets or lenses or dead-end fractures etc, in the upper bedrock. At depths below

500 m and down to the maximum sampled depth at around 970 m, there is a decreasing trend in $\delta^{18}O$ indicating an increasing glacial component, which does not necessarily represent the last deglaciation.

The $\delta^{18}O$ distinction with depth reflects the change to lower transmissivity at 500–600 m along the gently dipping zones in the hanging wall bedrock segment, i.e. the limit of the Littorina Sea incursion.

Figure 5-2a, b and c shows examples of hydrogeochemical and hydrogeological interaction, where modelled TDS and mixing proportions of meteoric and glacial waters are the output from the hydrogeological simulation model /Follin 2008, R-08-95/, The simulated proportions of these different input waters are displayed along a similar 2D cross-section to that used for the site descriptive model visualisation described in Figure 6-1, with the exception of drill site 8 which is included in Figure 6-2. The realisations show obvious differences between the footwall and the hanging wall which are due to the structural-hydraulic differences between the bedrock segments and to the differences these cause regarding the initial conditions used. As a precaution /Follin et al. 2008b/ point out that the results shown in Figure 5-2 represent the deterministic stage 2.3 base case simulation and that there is significant variability between realisations when heterogeneity is considered.

There is a general consistency when the modelled TDS is compared with the measured chloride concentrations (compare to Figure 6-1), and also the general distribution of meteoric and glacial water proportions relate to that expected when considering present observations of tritium and $\delta^{18}O$ (Figure 5-1). This is also reflected in the M3 mixing proportion calculations as discussed in section 4.2. The results of the simulation with the hydrogeological model show fair agreement with measured concentrations of Br/Cl ratio (cf. discussion above) and HCO_3 in the boreholes. These hydrogeological simulations also support the hydrochemical observations in surface water and shallow groundwater locations that indicate the probable absence of ongoing deep discharge into the freshwater surface system within the area covered by the well-connected and highly transmissive fractures/sheet joints of the shallow bedrock aquifer in the uppermost approximate 200 m of the bedrock.

Furthermore, the simulation results comply with the field observations of relict marine remnants, which also include deep saline signatures, in the groundwater at relatively shallow depths in the Quaternary deposits in restricted areas outside these structures. One such area is Lake Gällsboträsket, which coincides with the Eckarfjärden deformation zone (Figure 3-1).

5.3 Concluding remarks

Interaction between hydrogeochemistry and hydrogeology has been a common goal since the initiation of the site investigation programme at Forsmark. Important at an early stage was the use of a generalised palaeo-conceptual site model by the two disciplines which essentially was similar /Follin et al. 2008a/. As investigations progressed, hydrogeochemistry provided some insight into the present and past evolution of the different groundwater types within the approximate 0–1,000 m bedrock interval sampled at Forsmark. In turn, these observations provided important interaction with the hydrogeological modelling programme /Follin et al. 2008a/. From a hydrogeochemical perspective, the present hydrogeochemical site descriptive models discussed in section 6 are the result of close interaction with hydrogeology, where input concerning confirmation of flow directions, flow properties and possibilities to maintain different water types in the bedrock, have been of great importance in supporting the modelling results. Quantitative agreement between the models are, however, restricted to comparison between predicted and measured groundwater constituents as discussed in /Follin et al. 2008b/.
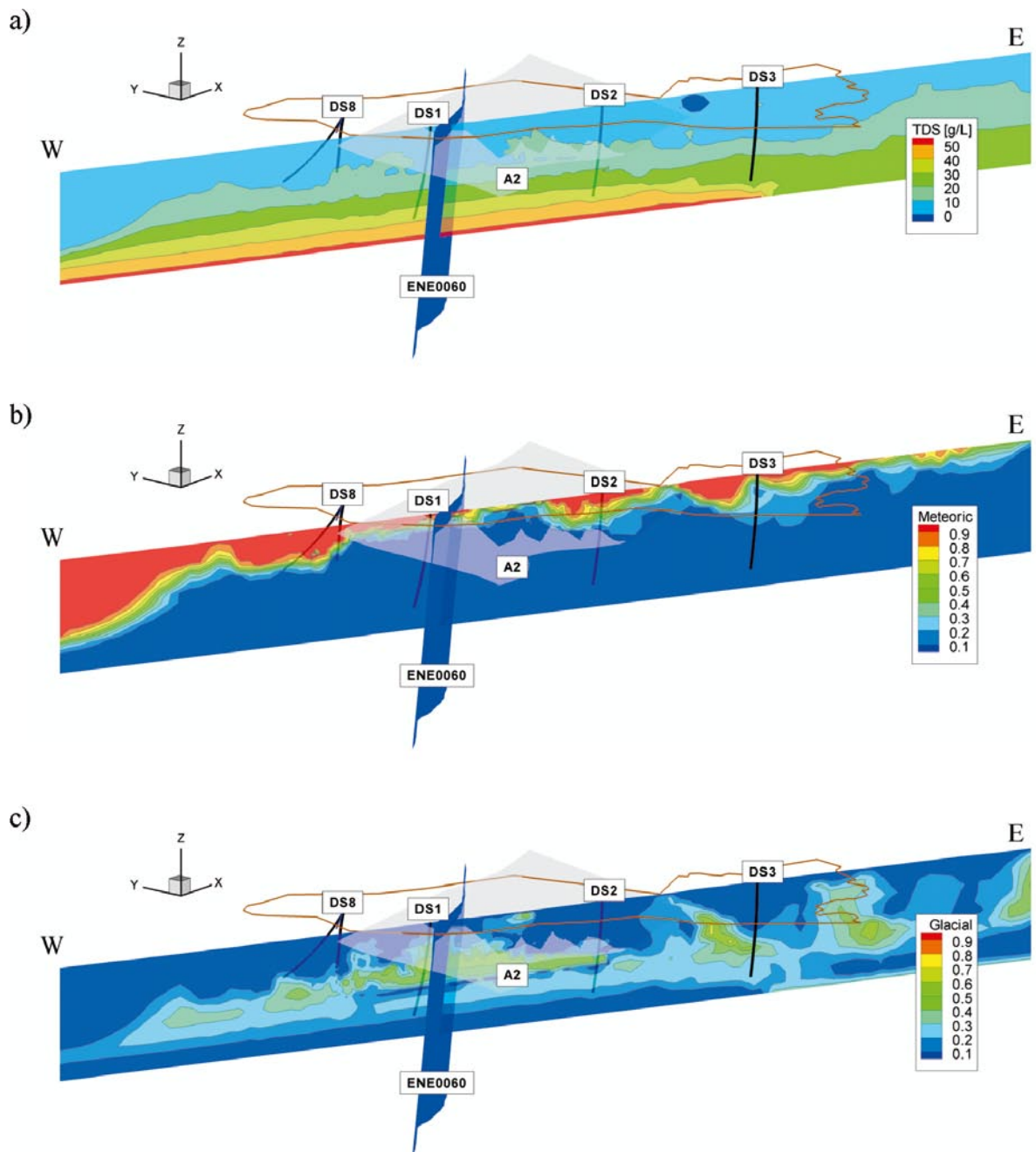
Figure 5-2. *Examples of simulations from the hydrogeological modelling studies used for calibrating the hydrogeochemical model: a) TDS (Total Dissolved Solids), b) mixing proportions of meteoric water, and c) mixing proportions of glacial water /Follin 2008, R-08-95/.*

6 Hydrogeochemical site description

6.1 Introduction

The main aim of the hydrogeochemical site descriptive model is to present an understanding of the site based on measurements and model contributions described in the previous chapters and detailed in /Smellie et al. 2008/. The site descriptive model is a combination of a quantitatively-derived hydrogeochemical model (e.g. based on site measurements) and a qualitatively-derived hydrogeochemical model (e.g. more descriptive, process-oriented conceptual model). The main objective is to describe the chemistry and distribution of the groundwater and porewater in the bedrock and the groundwater close to the interface between bedrock and the overburden, and the hydrogeochemical processes involved in its origin and evolution. This description is based primarily on measurements of the groundwater composition, but also incorporates the use of available geological and hydrogeological site descriptive models. The description also serves as the basis for possible hydrogeochemical simulations of the palaeohydrogeochemical evolution of the site and also to predict future changes. The construction of the Forsmark hydrogeochemical site descriptive model is described in detail in /Smellie et al. 2008/.

In this chapter, visualisation of the Forsmark hydrogeochemical site descriptive model is presented together with a concluding summary of the main hydrogeochemical properties of the site.

6.2 Hydrogeochemical visualisation

The Forsmark candidate area can be divided by the combination of two major gently dipping deformation zones (ZFMA2 and ZFMF1) and one steeply dipping deformation zone (ZFMNE0065) into a footwall bedrock segment (i.e. target volume; fracture domains FFM02 and FFM01) to the north-west, and a hanging wall bedrock segment (i.e. fracture domain FFM03) to the south-east (cf. Figure 2-6 and Figure 2-8, and Figure 6-1 below). Fracture domain FFM02 and the contiguous deformation zones in the uppermost part of the bedrock represent a shallow bedrock aquifer between around 50–200 m depth /Follin et al. 2007a/. This aquifer is characterised by a high frequency of sub-horizontal and gently dipping fractures with apertures, including sheet joints, as well as the near-surface extension of some deformation zones. It effectively: a) rapidly transports near-surface recharge waters laterally towards the north-east, and b) limits meteoric recharge to deeper bedrock levels. Fracture domain FFM01 (footwall underlying FFM02) differs from FFM02 in that at increasing depths below approximately 200 m and, particularly beneath 400 m, there is an overall lower intensity of open, flowing fractures and progressive lower fracture transmissivity. The hanging wall bedrock segment consists of a high frequency of transmissive, gently dipping deformation zones. The transmissivity of these zones is significantly reduced below approximately 500 m depth.

The higher fracture transmissivities especially in the upper approximately 200 m in the footwall bedrock and along the gently dipping deformation zones in the hanging wall bedrock have facilitated, during the last deglaciation and Holocene time, the incursion and mixing of waters from: a) the last deglaciation, b) the Littorina Sea transgression, and c) as yet, limited meteoric recharge. In turn, these events have subsequently changed or modified the rock matrix porewater chemistry by altering the diffusion concentration gradients between fracture groundwater and porewater.

Visualisation of the hydrogeochemical site understanding is based on the exploratory analysis part of the programme outlined in section 4, interfaced with relevant input from the geological and hydrogeological site descriptive models. To visualise the groundwater chemistry, two cross-sections were selected (cf. Figure 2-1) that best illustrate the candidate area based on stage 2.2 of the geological model /Stephens et al. 2007/. The cross-sections were subsequently simplified to meet hydrogeochemical requirements and these versions are described in /Smellie et al.

2008/. Selected examples are presented in Figure 6-1, Figure 6-2 and Figure 6-3 where specific aspects of the groundwater and porewater hydrochemistry are highlighted. The groundwater types represented, and their subdivisions with respect to elevation and chemistry, are largely based on chloride content (and magnesium) because of its direct correlation with depth and specific water types. These subdivisions are supported by other major ions. For the WNW-ESE cross-section the background porewater chemistry is visualised (Figure 6-3), subdivided on the same basis of depth and chloride contents /Smellie et al. 2008/.

To provide a more realistic visualisation of groundwaters in a fractured crystalline rock environment (i.e. to avoid giving a porous medium impression to the bedrock), the groundwater types are shown confined to the major water-conducting fractures and deformation zones. The WNW-ESE section (Figure 6-1) is particularly well suited to this type of visualisation because it cuts the major structures, in contrast to the ENE-WSW section (Figure 6-2) which cuts parallel to the major structures. In the latter case, the groundwater types and salinities are confined to the borehole sections sampled.

The cross-sections illustrate clearly the depth of disturbance following the last deglaciation caused by the intrusion of the brackish marine (Littorina) waters to around 600 m along gently dipping deformation zones in the hanging wall bedrock, compared with a maximum depth of around 150–300 m in the footwall bedrock (i.e. the target volume).

Included in the visualisations are brief summaries of the chlorinity, depth intervals, origin, the main reactions and the redox conditions for each groundwater type. Important reactions range from weathering and potential calcite dissolution in the near-surface bedrock environment, to possible calcite precipitation at intermediate levels and long-term water/rock interactions being dominant in the deep bedrock characterised by low flow to stagnant groundwater conditions with increasing depth. Microbially-mediated reactions (e.g. those due to iron-reducing and sulphate-reducing bacteria) occur, particularly in the shallow to intermediate depths where active groundwater flow takes place. Redox conditions range from oxidising/reducing near the surface to reducing with increasing depth.

The target volume at depths greater than 200–300 m, visualised in Figure 6-1 and Figure 6-2, has been largely shielded from influences occurring after the last deglaciation by the presence of the shallow bedrock aquifer. This is clearly shown by the distribution of glacial meltwater (e.g. discussion in section 5.2) and the Littorina Sea waters (cf. section 4.1), both of which are restricted to the upper 100–300 m, depending on location. However, there is evidence of cold climate signatures at different locations from 200–300 m and also to the maximum depths sampled indicating the intrusion of glacial meltwater at some time in the past along the water-conducting deformation zones. Unfortunately, it is not possible to distinguish between past and recent glacial events using $\delta^{18}O$ measurements, and ^{14}C systematics are both restricted in timescale (approximately 30,000 years) and also in interpretation which becomes inceasingly uncertain with the passing of time. For example, the influence of different carbon sources which enter and mix with the groundwater system can be extremely problematic because the bicarbonate contents are very small, are extremely sensitive to disturbances, and therefore not conducive for ^{14}C analysis or interpretation.

With respect to the rock matrix porewaters, these are visualised for the WSW-ENE cross-section in Figure 6-3 and the variation in chloride is colour coded. This visualisation provides the opportunity to directly compare the fracture groundwater chemistry with that of the porewater in the surrounding bedrock matrix. The porewater patterns in the upper approximately 700 m of bedrock are an attempt to illustrate the effects of a dynamic flow system on the rock matrix porewater compositions derived from the samples studied. For example, this includes: a) the presence of recent, out-diffusion gradients resulting in a dilution of porewaters in the rock matrix adjacent to the gently-dipping deformation zones, with an upward 'fingering' of older, higher porewater salinities still preserved between the deformation zones, and b) a more advanced situation, where only small residual concentrations or 'islands' of older more saline porewaters have been preserved in rock volumes of sufficient extent, and therefore more slowly influenced by on-going diffusion processes between the surrounding hydraulically-active fractures and the rock matrix.
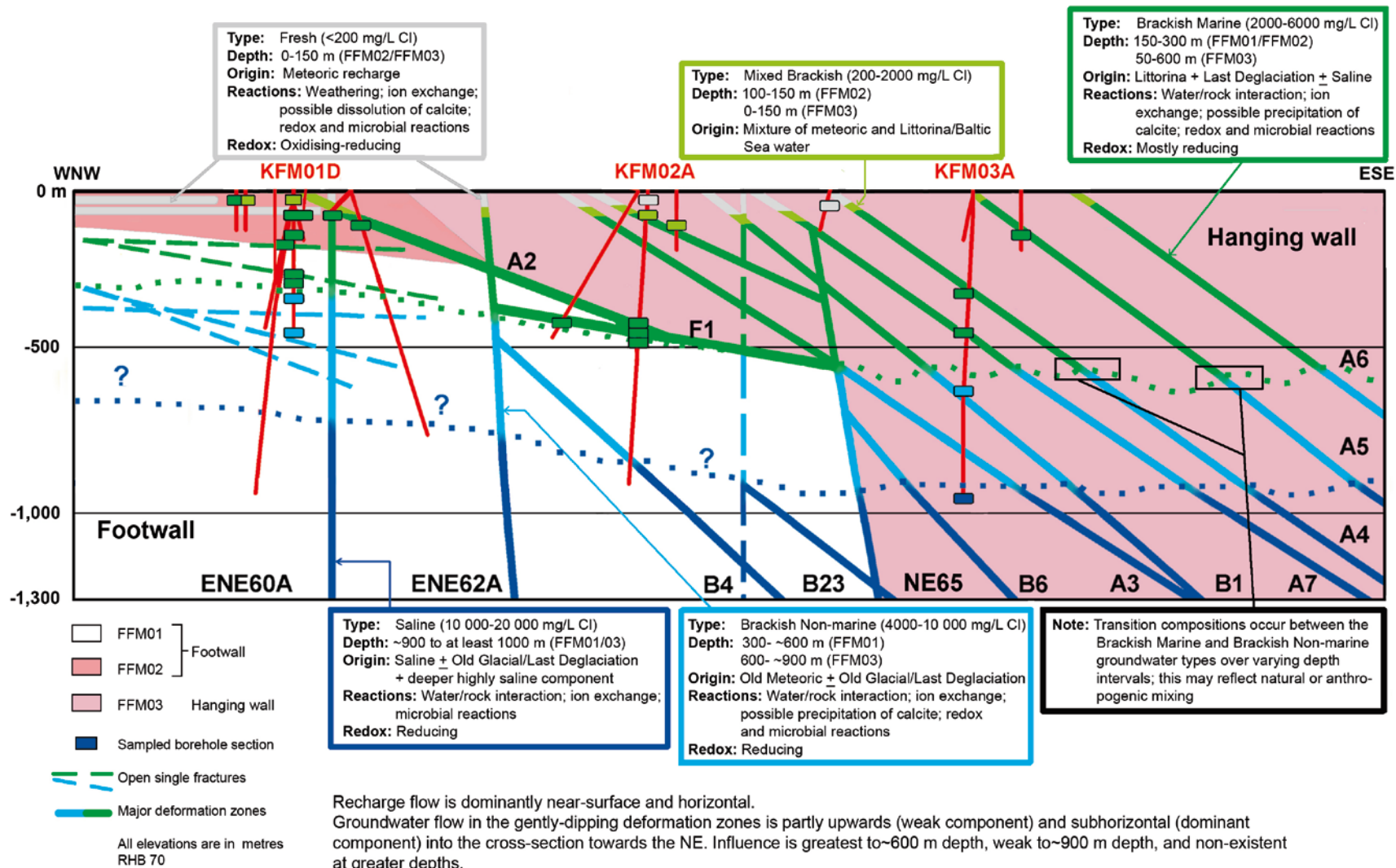
Figure 6-1. *WNW-ESE 2D cross-section through the central part of the candidate area showing the groundwater types and their properties (salinity, origin, major reactions and redox conditions). The footwall (FFM01 and FFM02) and hanging wall (FFM03) bedrock segments are indicated, separated by the gently dipping deformation zones ZFMA2 and ZFMF1 (abbreviated to A2 and F1), and the steeply dipping deformation zone ZFMNE0065. The dotted lines in different colours crossing the section represent the approximate depths of penetration of (or extrapolation of) the major groundwater types along hydraulically-active fracture zones. (Cross-section length = 6,790 metres).*
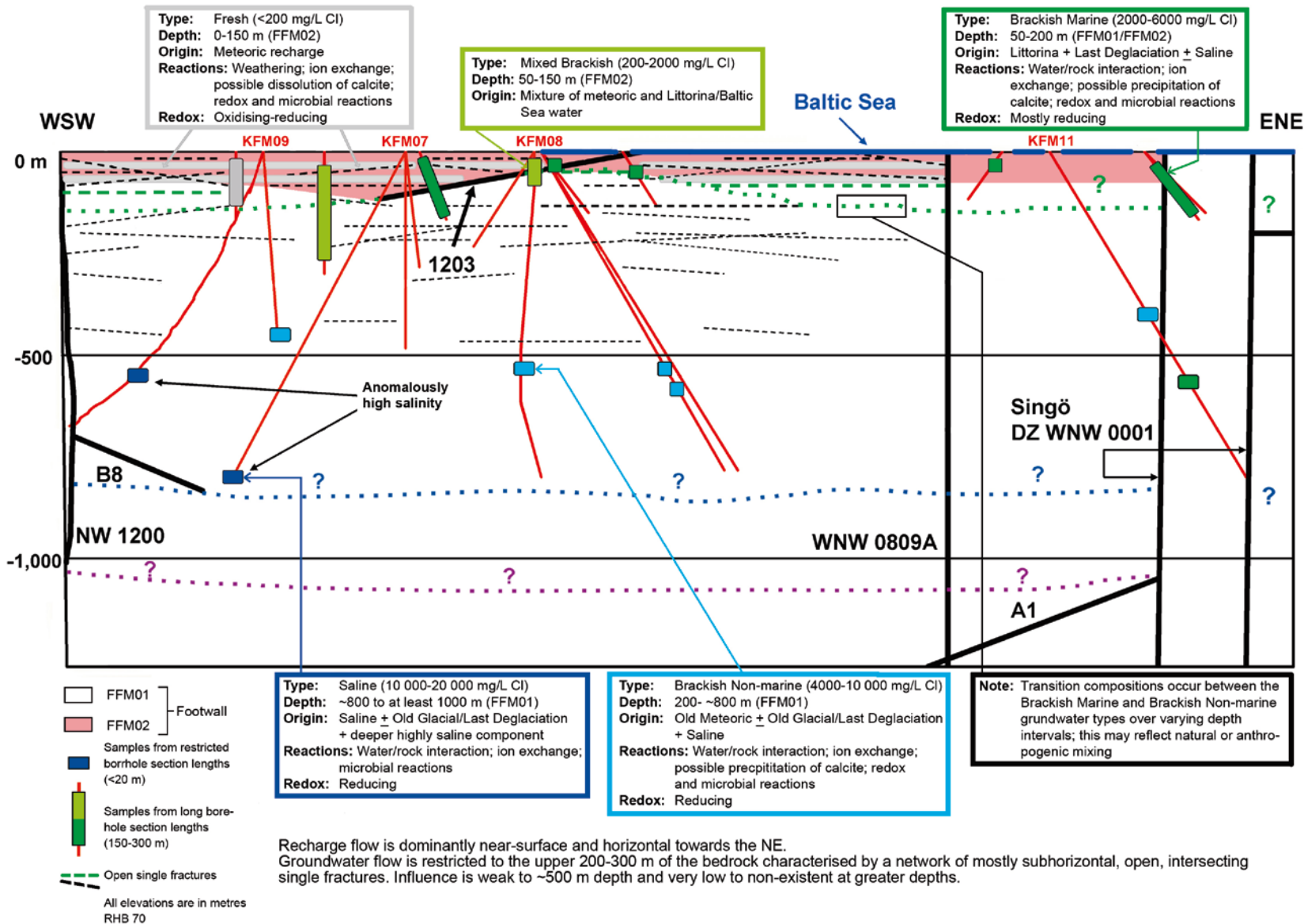
Figure 6-2. *ENE-WSW 2D cross-section through the target volume showing the groundwater types and their properties (salinity, origin, major reactions and redox conditions). Fracture domains FFM01 and FFM02, comprising the footwall, are indicated. Dashed lines in the upper bedrock are only schematic to illustrate generally the gently dipping to sub-horizontal fractures commonly present. The dotted lines in different colours crossing the section represent the approximate depths of penetration of (or extrapolation of) the major groundwater types along hydraulically-active fracture zones. (Cross-section length = 2,975 metres).*
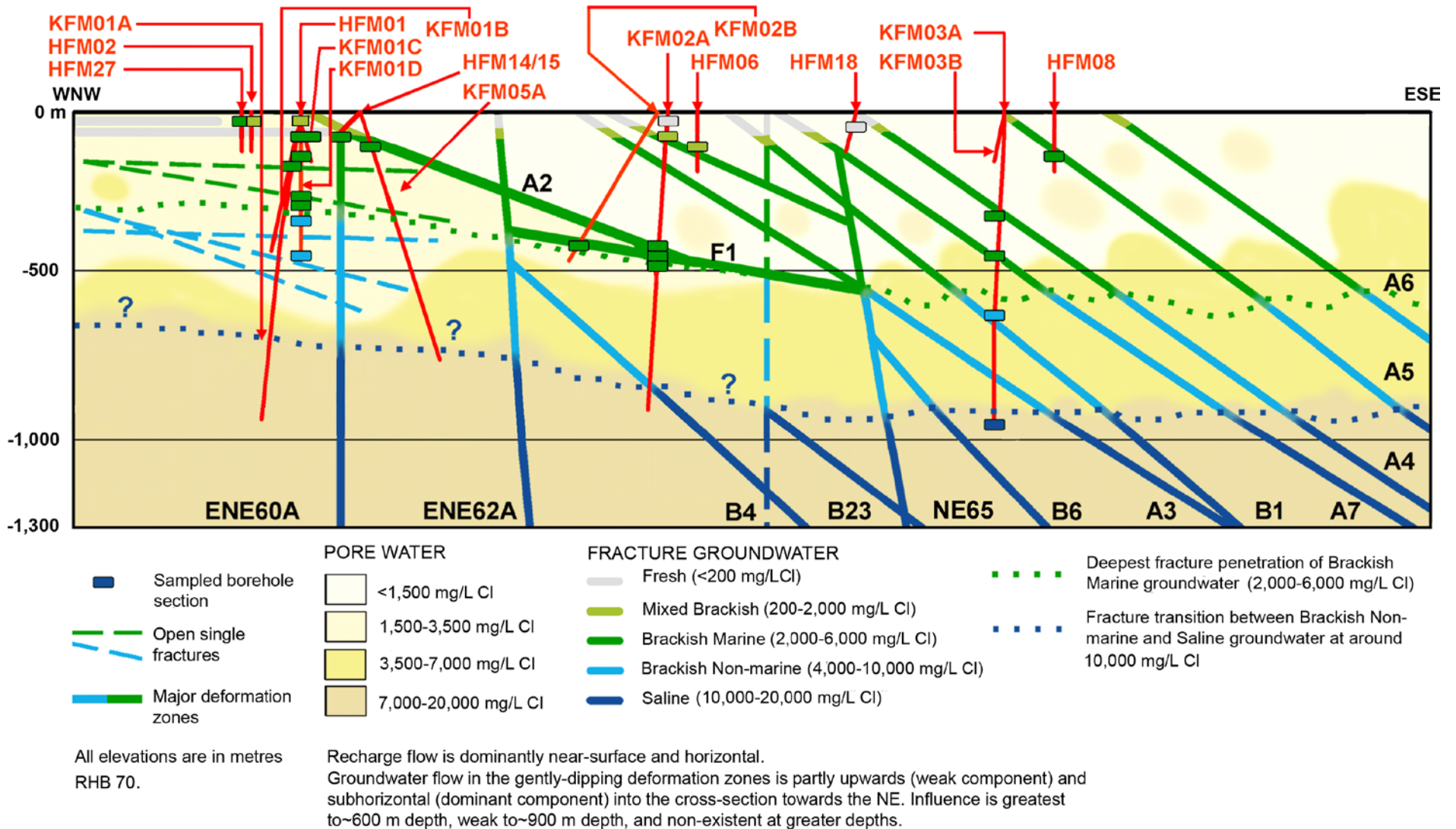
Figure 6-3. *Forsmark 2.3 visualisation of the hydrochemical data along cross-section WNW-ESE. Shown are: a) the location of the boreholes and the sections which have undergone hydrochemical sampling, b) the main fracture groundwater types which characterise the site, c) the chloride distribution with depth along the major deformation zones and minor single open fractures, and d) the chloride subdivisions of the rock matrix porewater. The groundwater flow directions are explained in the legend. The dotted lines in different colours crossing the section represent the approximate depths of penetration of (or extrapolation of) the major groundwater types along hydraulically-active deformation zones. (Cross-section length = 6,790 metres).*

The footwall bedrock down to around 700 m (dominantly fracture domain FFM01), represented by borehole KFM01D in Figure 6-3, generally the porewater has a lower chloride content (1,500–3,500 mg/L Cl) than the surrounding fracture groundwaters. Furthermore, the porewater is enriched in $\delta^{18}O$ compared with the fracture groundwaters (cf. section 4.8.5; /Waber et al. 2008a/). This indicates that a transient state is established between the porewater and groundwater down to at least 650 m below surface, although the concentration differences become smaller with increasing depth. No groundwater samples are available from greater depths. The preservation of a transient state with more dilute signatures in the porewater reflects the low conductivity of these rock portions and consequently the long time required to overprint an older signature once established in the porewaters. These dilute signatures are thought to represent old meteoric waters from temperate and cold climates which pre-date the last deglaciation (cf. section 2.5.3).

In the hanging wall bedrock, represented by borehole KFM03A and the upper part of borehole KFM02B (Figure 6-3), a close to steady-state situation between porewater and fracture groundwater is suggested down to about 200 m depth. This reflects the high frequency and close proximity of the open, water-conducting gently dipping deformation zones, and the circulation of significant volumes of water in the area. At greater depths in the bedrock, porewaters have lower chloride contents than the fracture groundwaters which are dominated by a strong brackish marine (Littorina) component; this disparity indicates a transient state between dynamic groundwater flow in the fractures and porewater within the rock matrix.

A porewater drillcore profile specifically sampled in borehole KFM02B and orientated perpendicular across the gently dipping deformation zones ZFMA2 and ZFMF1 into the surrounding rock matrix, indicated that the brackish marine (Littorina) type groundwaters in the fractures have started to overprint the older more dilute porewater compositions, but not yet having attained steady state (cf. sections 4.8 and 7.2.3) .

6.3   Summary of site hydrogeochemical properties

The major properties of the site are described below (cf. Figure 6-1, Figure 6-2 and Figure 6-3):

Near-surface waters (0–20 m): Within this 0–20 m depth interval, including the overburden, *Fresh groundwaters* (< 200 mg/L Cl) comprise the most recent recharge compositions and therefore their hydrogeochemical evolution is mainly determined by weathering reactions, in particular reactions influenced by limestone. The extensive presence of limestone blocks in the Quaternary overburden, a feature normally very uncommon in the rest of the Swedish soils, promotes an overall distinctive character to the near-surface groundwaters with respect to that observed in other areas (e.g. the Laxemar-Simpevarp area). Properties include variable but higher pH values (usually higher than 7) and variable but higher calcium concentrations (mostly between 50 and 200 mg/L) depending on the biogenic carbon dioxide input. This fact, together with the kinetically much slower weathering of the aluminosilicates (which otherwise would consume carbon dioxide) and the localised presence of especially intense biogenic input, contribute to the higher bicarbonate values observed (between 200–900 mg/L).

Groundwater redox conditions at these shallow levels are oxidising/reducing in character.

No rock matrix porewater data are available from these very shallow levels.

Shallow groundwaters (20–200 m): This depth interval in the upper part of the footwall bedrock (i.e. target volume) includes the shallow bedrock aquifer which facilitates the rapid transport of recharged meteoric groundwaters laterally towards the north-east and effectively limits further recharge to deeper levels. This shallow bedrock aquifer is not developed in the hanging wall bedrock segment.

In the footwall bedrock, these shallow groundwaters consist of a large percentage fresh groundwater which has persisted to the depths of the shallow bedrock aquifer. However, not surprisingly they do not share the same variability and high bicarbonate or calcium contents as the near-surface fresh groundwaters. Only waters with short residence time in the overburden (fast paths), and therefore more diluted, are effectively recharging these shallow hydrological systems. If the biological activity becomes more restricted in the future due to a decrease in nutrient supply or dispersion (e.g. during glaciations), the intensity of weathering will decrease and recharge waters will probably be even more dilute, but not necessarily transported rapidly to depth (or in large volumes) because of the shallow bedrock aquifer. In the hanging wall bedrock, fresh groundwaters persist to varying depths down to around 200 m depending on whether recharge or decharge conditions dominate the gently dipping deformation zones that intersect the bedrock surface.

This uppermost 20–200 m in the footwall and the hanging wall bedrock is also characterised by brackish groundwaters displaying a wide chemical variability which may be: a) due to the natural mixing of fresh recharging waters and discharging (or flushed out) groundwaters of increasing salinity (i.e. recent Baltic or old Littorina Sea relicts), and/or b) due to mixing resulting from anthropogenic effects related to drilling and sampling activities. Collectively, these two types are referred to as *Mixed Brackish groundwaters* comprising varying proportions of fresh and brackish waters with a chloride range of 200-2,000 mg/L (Figure 6-1). These shallow mixing processes occur throughout the Forsmark area but are much more prevalent in the hanging wall bedrock where no shallow bedrock aquifer exists, and variable discharge is occurring along the gently dipping deformation zones.

These hydrogeochemical and hydrogeological observations are supported by environmental isotope studies which show that recent to young fresh groundwaters, some showing signs of mixing, characterise the upper approximate100–200 m of bedrock. This is shown by tritium and carbon-14 which indicate that near-surface groundwaters have short residence times mainly in the order of a few hundred years to only a few decades. This is in agreement with palaeo-hydrogeological evidence which indicates land emergence about 2,500 years ago followed by the flushing of the relatively flat and moderately undulating topography within the Forsmark candidate area by meteoric water which became established some 900 years ago.

Few data exist for the redox characterisation of this shallow groundwater system. Nevertheless, tentative calculations from measurements in both the hanging wall and footwall bedrock suggest the existence of a generalised anoxic state with possible episodic inputs of oxidising waters. Furthermore, although drillcore material from 0–100 m depth interval is limited to only eight boreholes /Sandström et al. 2008/), there are enough data to suggest that these oxidising episodes have not been intense enough to exhaust the reducing capacity of fracture filling minerals which are still present in the shallow system (e.g. Fe(II) chlorite or pyrite). Goethite is found in some fractures mainly associated with deformation zones, and Mössbauer analyses of fracture fillings from hydraulically conductive fractures in the upper 50 metres show $Fe^{3+}/Fe(tot)$ ratios between 0.35 and 0.75. These observations support the fact that redox conditions have varied both in time and space within the uppermost part of the bedrock. At present, the dissolved ferrous iron groundwater contents are high and represent post-oxic environments in which iron-reducing bacteria (IRB) activity seems to be dominant /Hallbeck and Pedersen 2008a/. Locally, sulphidic environments with high contents of dissolved sulphide, probably active precipitation of amorphous monosulphide and, therefore, important sulphate-reducing bacteria (SRB) activity, can also be found.

Mobilisation as well as deposition of uranium in the upper 150 m of bedrock is indicated by uranium decay series analysis of fracture filling material. This is ascribed to the transition from near-surface oxidising conditions to more reducing conditions at depth within the last 1 Ma.

Only very few porewater data are available from the rock matrix within this depth interval and genrally these suggest that close to steady-state conditions have been achieved in the hanging wall but not in the footwall bedrock.

Intermediate depth groundwaters (200–600 m): During the Littorina Sea transgression, the Forsmark bedrock was under water with no active hydraulic gradient such that the sea water penetrated downwards by density intrusion flow. The bulk of the Littorina Sea waters, i.e. *Brackish Marine groundwaters* (2,000–6,000 mg/L Cl), preferentially entered the bedrock in the hanging wall bedrock along the gently dipping, highly transmissive deformation zones where a shallow bedrock aquifer is not developed. These waters mixed and eventually came to rest when older *Brackish Non-marine groundwaters* of similar to higher salinity (4,000–10,000 mg/L Cl, Figure 6-1) were increasingly encountered. The average depth of penetration at the present time along the gently dipping deformation zones is approximately 600–700 m (Figure 6-1). Penetration depth may also have been influenced by a decrease in transmissivity along these deformation zones.

In the footwall bedrock dominated by fracture domains FFM01 and FFM02, the situation was somewhat different; the shallow bedrock aquifer subsequently became saturated by Littorina Sea water which persisted until recent uplift stimulated an increase in the local hydraulic gradient. The bulk of the Littorina waters then were flushed out, a process which is still on-going. However, Littorina Sea water components are still present down to 250–300 m depth in the footwall (FFM01), as illustrated by data from borehole KFM01D, where subhorizontal to very gently dipping transmissive discrete single fractures within the upper 300 m bedrock (i.e. the defined fracture domain) have been sampled (Figure 6-1 and Figure 6-3). Here, the Littorina Sea component is weak to intermediate probably from mixing with fresh groundwaters during the on-going flushing out process. The gently dipping single fractures sampled may connect with the shallow bedrock aquifer and act as conduits bringing some brackish marine (Littorina) groundwaters down to around 300 m depth.

The major chemical composition in this intermediate depth groundwater system is mainly controlled by mixing and their values depend on the proportion of each mixed end member. The mixing proportions are different in the two main groundwater systems at Forsmark, i.e. fracture groundwaters in the hanging wall bedrock, compared to fracture groundwaters in the footwall bedrock including fracture domain FFM01. Groundwaters from the latter have a larger contribution of *Brackish Non-Marine groundwater* (or the Old meteoric ± Glacial + Saline end member) at shallower depths (around 300 m) and the same could be said for the influence of the deeper *Saline groundwater* component (10,000–20,000 mg/L Cl; Figure 6-1 and Figure 6-2). This contrasts with the groundwaters from the series of gently dipping deformation zones in the hanging wall bedrock which have a much higher proportion of the Littorina end member (almost double) existing to a greater penetration depth (around 600–700 m). It also follows that a higher Littorina component generally results in higher sulphate and magnesium contents.

Radiocarbon studies of organic/inorganic phases support a Holocene origin for the brackish marine (Littorina) groundwaters. This is in accordance with palaeohydrogeological estimations suggesting an age of approximately 5,000–6,000 years covering the period of maximum salinity during the Littorina stage (4500–3000 BC).

Even though the compositional characteristics of these intermediate groundwaters are mainly determined by mixing processes, the quickly responding pH and Eh are controlled to a large extent chemical reactions and microbial activity and for example, thereby also the sulphur and carbon species. The pH is mainly controlled by calcite dissolution-precipitation reactions and of secondary importance is the influence of other common chemical processes, such as aluminosilicate dissolution or cation exchange.

Most of the brackish groundwaters sampled at this depth interval in the hanging wall seem to be associated with the presence of lenses with an important Littorina contribution and their presence represents a discontinuity in the normal evolution of the system with depth, thus introducing a degree of uncertainty when trying to describe the redox conditions. The dissolved ferrous iron contents are generally lower than in the shallow groundwater system. The iron system seems to be disturbed, as suggested by the occurrence of amorphous iron oxyhydroxides now evolving towards more crystalline phases. The presence of this intermediate iron

oxyhydroxide with higher solubility than a truly crystalline phase, is considered possible in these brackish groundwaters if a brief oxidising disturbance has taken place and, moreover, iron debris may have been added during the drilling operation /Dideriksen et al. 2007/. Most of the Eh values determined in these brackish groundwaters (at depths between 110 and 646 m) seem to be controlled by the occurrence of these intermediate crystalline phases.

Elevated uranium contents in some groundwater samples and a few fracture coatings from depths of 200–700 m have been found related to deformation zones of different orientation.

Dissolved sulphide concentrations are systematically low and may be locally controlled by the precipitation of amorphous Fe(II)-monosulphides, linked to the activity of SRB. However, future measurements of dissolved sulphide will be an important part of the groundwater monitoring programme in order to achieve a better understanding of the sulphide production in the different groundwaters.

From approximately 300–650 m in the footwall bedrock in fracture domain FFM01, where there is a marked decrease in open fracture frequency and transmissivity, there is greater disparity between the porewater chemistry and the adjacent groundwater compositions, the former being significantly more dilute (cf. Figure 6-3). This depth interval represents transient conditions where the porewater has retained a very old, dilute and warm-climate water signature, much older than the surrounding fracture groundwaters which have been dated to at least 1.5 Ma. Oxygen-18 is enriched and therefore indicates no obvious cold climate signature, which contrasts with the adjacent groundwaters.

In the hanging wall an overall transient state also is established down to about 650 m. The lower chloride contents and an isotope signature increasingly depleted in oxygen-18 with increasing depth, indicate that the porewater in these zones stores a dilute water signature with a probable cold-climate signature. The significantly negative $\delta^{18}O$ values (–13‰ V-SMOW) preserved far from the water-conducting fractures indicates that this cold-climate signature was a glacial water circulating for a considerable time period in the fractures at these depths. Since the last deglaciation the porewater signature has become overprinted with a Littorina and/or a Baltic-type signature as indicated by chloride, magnesium and oxygen-18 in porewaters sampled closer to the conducting fracture.

Deep groundwaters (> 600 m): Under this heading are included the *Brackish Non-Marine groundwaters* and the *Saline groundwaters* previously referred to as potential mixing components with the brackish marine (Littorina) groundwater at shallower levels. In the hanging wall bedrock, the transition from brackish marine (Littorina) type fracture groundwaters to the brackish non-marine groundwaters is quite sharp and occurs at around 550–600 m depth. From 600–930 m depth, the chloride content increases steadily from 5,500–8,500 mg/L before levelling out at just under 10,000 mg/L at 1,000 m depth, i.e. the transition to the saline groundwater member (cf. Figure 6-1).

There are inadequate data at the moment to indicate the nature of the salinity increase (i.e. gradual or sharp) at depths greater than 600 m in the footwall bedrock including fracture domain FFM01.

The highest salinities are associated with boreholes KFM07A and KFM09A in groundwaters sampled from steeply dipping deformation zones outside the target volume to the north-west of the candidate area (Figure 2-2). These anomalously high salinities at intermediate depths (600–750 m) are considered to reflect natural and/or anthropogenic effects either due to glacial rebound (after the maximum glacial loading) or up-coning resulting from different borehole activities including groundwater sampling. The former possibility is supported by equivalent porewater chloride contents at similar depths to the groundwaters sampled, and the latter by heavy pumping activities prior to sampling. With the available data, however, a definitive interpretation cannot presented that supports either a natural or anthropogenic origin.

With respect to redox conditions, the dissolved sulphide concentrations increase at depths greater than 600 m. This is consistent with the occurrence of sulphate-reducing bacteria (SRB) and with the active precipitation of Fe(II)-monosulphides. The iron system seems to be limited by crystalline oxides (mainly hematite) reflecting the pristine conditions of the geochemical system. This is coherent with the reducing character and long residence time of these groundwaters, where low crystallinity phases are not expected. The sulphide values are a subject for further monitoring to assess their behaviour under different flow conditions.

Hydrochemical observations of fracture groundwaters and porewaters show that the brackish to saline non-marine groundwaters become more mineralised with increasing depth (to saline in type) by water/rock interaction and exchange with the rock matrix porewater. Coupled to hydraulic conditions at these depths (> 600 m), which indicate low fracture transmissivities, all qualitative and quantitative evidence points to groundwater residence times that are significant and may indicate that these brackish to saline non-marine groundwaters represent part of the salinity gradient that existed prior to the last deglaciation. This hypothesis is further strengthened by the transient rock matrix porewater composition present in the 300–600 m depth interval discussed above, which has around 2,000 mg/L Cl, compared to around 6,000 mg/L Cl in the fracture groundwaters (cf. Figure 6-3). This porewater falls under the general heading of 'Old Meteoric ± Old Glacial + Saline' in type, in this case with no glacial component, and is considered to represent a snap-shot of the salinity profile at this depth prior to the last deglaciation.

The most saline groundwater in Forsmark deviates from the saline groundwater at Laxemar/Simpevarp in having higher Br/Cl ratios and much lower SO_4 contents. In addition, element ratios like Sr/Cl and Li/Br are quite different and overall there is a suggestion of a different evolution trend. Unfortunately, the most saline groundwaters sampled at Forsmark only reach 15,000 mg/L Cl making comparisons with the saline water at Laxemar (45,000 mg/L Cl more uncertain).

Colloids and gases: The average colloid concentration found in the Forsmark groundwater system is 58.4 µg/L, which compares with the results of average concentrations from crystalline rock groundwaters in Switzerland (30 and 10 µg/L) and in Canada (300 µg/L), where the same sampling approach was used. The colloids are composed mostly of aluminium, silica, iron and sulphur, although caution is required for the iron and sulphur varieties which may represent artefacts, for example, from oxidation or microbial consumption related to drilling activities.

Although the gas concentrations generally increase with depth, the gases are not oversaturated at the depths at which they were sampled. The only sample that displays indications of biologically-produced methane is from borehole KFM01D at a depth of 445 m. The methane in all other samples appears to originate from abiotic sources (unless anaerobic methane oxidation (AOM) is operating). The helium, hydrogen and nitrogen gases are probably of crustal and/or mantle origin.

Uranium: Elevated uranium concentrations in some of the sampled groundwater sections (up to 148 µg/L U), corresponding to a narrow range of chlorinity and usually at intermediate depth, coincide mostly, but not always, with the brackish marine (Littorina Sea) groundwaters. In addition, uranium-rich phases are present in some of the fracture coatings (max 2310 ppm U measured in bulk filling material), although to date only one small grain of pitchblende has been identified. To describe and explain these elevated uranium concentrations have been an integral part of the hydrogeochemical studies presented in this report.

The origin of the uranium rich phases is largely unknown but it can be concluded that uranium has been circulating throughout the geological history of the site indicated by: a) some of the pegmatites show slightly enriched uranium values (a maximum value of 62 ppm is indicated by gamma spectrometric measurements, b) redistribution and deposition of uranium irregularly along permeable structures during the Proterozoic is documented in the area just outside Forsmark, and c) Palaeozoic, potentially uranium-rich alum shales that once covered the area may have contributed uranium to the system. Of special interest for understanding the present

groundwater/mineral systems is the potentially late (Quaternary) redistribution of uranium, and this has been evaluated using uranium decay series analyses of groundwater and contact fracture coatings. The main conclusions on the uranium system are given below.

- The highest uranium contents in both fracture coatings and groundwaters are found in open, water-conducting fractures. It is important to note that at the same depth interval low uranium contents are found in both fracture coatings and groundwater samples.

- The uranium present in groundwaters associated with fracture coatings is dominantly enriched in the oxidised U(VI) state. Assuming no anthropogenic effects, the uranium is believed to result from in situ dissolution of a mainly U(VI)-bearing mineral phase(s).

- Transmissive fractures in the upper 150 metres of the hanging wall and footwall bedrock show more pronounced deposition and leaching of uranium during the last 1 Ma, compatible with a dynamic and heterogeneous groundwater flow system.

- The accumulation of oxidised uranium at around 500 m depth does not necessarily mean that oxidised water has penetrated to this depth. Instead, it is shown that that mildly reducing groundwaters with sufficient HCO_3 (> 30 mg/L) are capable of keeping U(VI) mobile, and this has resulted in variable accumulations occurring within the fracture zones down to maximum depths of around 500 m.

- At some stage, dissolved uranium has become concentrated where there is a transition from high to low fracture transmissivity, corresponding to the transition from brackish marine (Littorina) to brackish non-marine groundwaters.

- The deposition of uranium is not confined to any specific periods of recent groundwater circulation, for example, since the last deglaciation, but has been shown to have occurred within the last 1 Ma as indicated by U-series data.

- Speciation-solubility calculations indicate solubility control by an amorphous uranium-phase for the groundwaters with the highest uranium contents /Gimeno et al. 2008/.

- Colloidal uptake has played only a minor role in the mobilisation and transport of uranium.

- Microbial activity (possibly enhanced by perturbation in connection with the drilling) may have increased the uranium mobility, but there is no direct evidence for this at the moment.

Uncertainties: Uncertainties in the Forsmark data have been estimated, calculated or modelled. The major perturbation is from borehole activities such as drilling and sampling events; other uncertainties (e.g. analytical, modelling etc) are generally of less importance and easier to quantify. Categorisation of water samples takes into account the different perturbations and uncertainties affecting the samples. For detailed modelling only the highest quality samples (category 1–3 samples) were generally used.

Coupled modelling approaches to quantify possible ingress of oxygen into the groundwater system during borehole activities, show that large borehole disturbances can be accommodated by the redox buffering capacity of the rock. In addition, depletion of oxidising conditions during the sampling process was supported by in situ time series analysis of O_2 in the sampled sections.

The 3D modelling of the spatial variability of TDS, alkalinity, pH, Ca, HCO_3^-, K and redox values shows that even if these are variable and heterogeneously distributed at repository depths, all of them fulfill SKB's safety criteria when extrapolated for the candidate area.

Remaining areas of uncertainty include: a) a lack of evidence to the presence or otherwise of a propagating redox front in the near-surface part of the bedrock (< 20 m depth), b) the nature of the uranium-rich fracture mineral phases potentially contributing to the elevated uranium contents in some of the groundwaters, c) the regional salinity distribution outside the target volume, and d) the reason why sampled sulphide contents are variable, and continue to be so. In contrast, the uncertainties concerning the site description are regarded to be fairly well understood and described.

7 Present status of hydrogeochemical understanding of the Forsmark site

7.1 Overall changes since previous model version

The previous model version 1.2 and model stage 2.1 /SKB 2005, 2006b/ concluded that the complex groundwater evolution and patterns at Forsmark are a result of many factors such as: a) the present-day topography and proximity to the Baltic Sea, b) past changes in hydrogeology related to glaciation/deglaciation, land uplift and repeated marine/lake water regressions/ transgressions, and c) organic or inorganic alteration of the groundwater composition caused by microbial processes or water/rock interactions. The sampled groundwaters reflect to various degrees processes relating to modern or ancient water/rock interactions and mixing and these conditions are confirmed by the results of modelling stages 2.2 and 2.3.

Integration of the Forsmark 2.2 and 2.3 data has resulted in significant modifications to the stage 2.1 site understanding. Additional hydrochemical data from strategically located boreholes, reflecting a greater temporal and spatial understanding of the groundwaters, support previous understanding of the site, for example, in relation to groundwater origin and evolution, the major hydrochemical processes that distinguish the site, the selected major end members for conceptualisation and modelling purposes and, importantly, the close agreement with hydrogeology on the palaeohydrogeological description of the site. Improved process understanding has been achieved through different isotopic approaches (e.g. Sr, S, C, O, H, B, Cl and the U-decay series), more reliable Eh and pH measurements, integration of microbial experience from Forsmark with that from other Fennnoscandian sites, and various modelling applications (e.g. geochemical reactive modelling, modelling of groundwater mixing proportions and rock buffer capacity, and modelling of helium gas compositions to derive groundwater residence times). Matrix porewater studies are now established, giving support to the palaeo-understanding of the site in addition to providing evidence that matrix diffusion in crystalline rock is active over distances of metres to tens of metres; preliminary modelling of solute diffusion rates has also been attempted. The differences between the properties of the footwall and hanging wall groundwaters are now fairly well understood and long residence times (at least 1.5 Ma) of some of these groundwaters (together with results from the porewater studies) have brought a new dimension to the interpretation and conceptualisation of the groundwater conditions in the period before the last deglaciation.

7.2 Overall understanding of the site

Explorative analyses and modelling of groundwater chemistry data measured in samples from cored boreholes, percussion boreholes, porewater from bedrock and shallow soil boreholes have been used to evaluate the hydrogeochemical conditions at the site in terms of origin of the groundwater and the processes that control the groundwater composition. Although the data set is rather limited, the results provide an overall understanding of the site. The effects from changing climate (and shoreline movement), on the measured groundwater, matrix porewater and fracture minerals have been determined with respect to origin, reactions and evolution.

7.2.1 Post glacial evolution

Several water types which are now present in the bedrock can be associated with past climatic events in the late Pleistocene, including inter-glaciations, glaciations, deglaciations, and associated changes in the shoreline in connection with marine/non-marine transgressions and

regressions. Among these, the last deglaciation and post glacialperiod is the most important for the groundwater development in the Fennoscandian shield, especially in terms of land uplift and shorelevel displacement as well as the development of the Baltic Basin.

The post glacial development reveals that when the continental ice melted and retreated from the Forsmark area around 8800 BC, glacial meltwater was hydraulically injected under considerable head pressure into the bedrock. The exact penetration depth is unknown, but, according to hydraulic simulations depths exceeding several hundred metres are possible. Although the last deglaciation of the Forsmark region coincided with the end of the Yoldia period, there are no signs of Yoldia Sea water in the bedrock. The Ancylus Lake (8800 to 7500 BC) was lacustrine and developed after the deglaciation. This period was followed by the brackish Littorina Sea (7500 BC to present). During the Littorina Sea stage, the salinity was considerably higher than at present, reaching a maximum of about 15‰ in the period 4500 to 3000 BC. Dense brackish sea water from the Littorina Sea penetrated the bedrock, resulting in a density intrusion that affected the groundwater in the more conductive parts of the bedrock and, for example, becoming slightly diluted with portions of glacial water. The initial emergence of the Forsmarkregion from the sea occurred ca. 2,500 years ago, and the recharge system of meteoric water circulation became established around 900 years ago forming a freshwater layer on top of the saline water because of its low density. As a result of the flat topography of the Forsmark area and of the short time period elapsed since the area emerged from the sea, the out-flushing of saline water has been limited, and consequently a freshwater layer remains at shallow depth.

Past Quaternary evolution has affected the groundwater chemistry at Forsmark, but this is not restricted to post glacial time since there is groundwater and porewater evidence that indicates a pre-Pleistocene warm-climate derived meteoric water component. The hydrochemistry of the Forsmark area cannot be explained without recognising this older component. The present groundwaters therefore are a result of mixing and reactions over a long period of geological time. The interfaces between different water types are not sharp but reflect the variability in the structural-hydraulic properties.

7.2.2   Groundwater composition

Groundwaters in the uppermost 20–200 m of the bedrock display a wide chemical variability with chloride concentrations in the range 200–5,000 mg/L suggesting influence of both fresh meteoric water and brackish marine water (i.e Baltic Sea water and Littorina Sea relicts). Furthermore, a sharp decrease in tritium content at about 150 m depth as well as ^{14}C data indicate that these shallow groundwaters have short residence times that are mostly in the order of a few hundred years to only a few decades.

At depths greater than around 200 m, the groundwater composition is indicative of a brackish marine water with chloride concentrations in the range 2,000–6,000 mg/L (i.e. slightly diluted with portions of glacial water) and with a clear Littorina component, as indicated by concentrations of magnesium and the bromide to chloride ratio. This water type is recognised down to 600–700 m depth in the hanging wall bedrock segment, i.e. in the transmissive gently dipping deformation fracture zones in the south-eastern part of the candidate volume. In the footwall bedrock segment (including fracture domains FFM02 and FFM01) the maximum penetration depth is to around 300 m where the frequency of water-conducting fractures is low. Below these respective depths, the groundwater composition indicates brackish to saline non-marine groundwaters (i.e. absence of Littorina influence), reflecting processes which have occurred prior to the intrusion of the Littorina Sea waters. These groundwaters show a further increase in calcium with depth (compared with sodium), which is a well recognised trend and indicative for water/rock interactions that occur under low flow to stagnant groundwater conditions with increasing depth.

7.2.3 Rock matrix porewater

Porewater in fracture domain FFM01 generally has lower chloride content and is enriched in $\delta^{18}O$ compared to the fracture groundwaters, indicating a transient state between the porewater and groundwater down to at least 600 m depth. A signature with low chloride, low magnesium and enriched in $\delta^{18}O$ and δ^2H has been preserved far away from conducting fractures at a depth of 640 m, suggesting that these porewaters have evolved from an earlier, very long established circulation of old dilute groundwaters in a few fractures. This is also consistent with the still prevailing transient state between this porewater and fracture groundwater from equivalent depths that, based on ^{36}Cl and ^4He dating, have residence times of more than 1.5 Ma. South-east of the target volume in the hanging wall bedrock, a situation close to steady-state is suggested between porewater and fracture groundwater down to about 200 m depth, reflecting the high frequency of water conducting, gently dipping deformation zones, and the rapid circulation of significant volumes of water in this area. At greater depth, the porewater has a lower chloride content than the fracture groundwater indicating a transient state down to about 650 m depth. The lower chloride content and an isotope signature increasingly depleted in $\delta^{18}O$ with increasing depth indicate that the porewater in these zones stores both a dilute water signature and a cold-climate signature. Since the last deglaciation, the porewater signature has become overprinted with a Littorina and/or a Baltic-type signature as indicated by Cl, Mg and $\delta^{18}O$ in porewaters sampled close to the major gently dipping deformation zone ZFMF1.

7.2.4 Water rock interaction

Transport of water volumes and mixing (both advection-dispersion and molecular diffusion) are major processes giving rise to present-day groundwater compositions. However, mixing also induces reactions and therefore the separation of these two processes is not only very challenging, but also important for the site understanding in order to indicate effects from past/present transport and reactions. Reactions involve interaction with the bedrock and fracture minerals, and in particular the alkalinity and redox buffering capacity of the bedrock is of key importance for groundwater composition and predicting future changes due to, for example, potential infiltration of dilute and oxidising waters.

Weathering and potential calcite dissolution under acidic conditions in the near-surface bedrock environment is promoted by the extensive presence of limestones in the overburden and controlled by biogenic input of carbon dioxide. This gives rise to pH values usually above 7, calcium concentrations mostly between 50 and 200 mg/L and bicarbonate concentrations in the range 200 to 900 mg/L in the near-surface waters (down to around 20 m depth). Concentrations then decrease to very low values at greater depths. However, bicarbonate is relatively high in most of the brackish marine groundwaters hosted in the upper 600 m of the gently dipping fracture zones south-east of the target volume, whereas brackish non-marine groundwaters below 300 m in fracture domain FFM01 have low bicarbonate contents.

The pH buffering capacity in Forsmark groundwaters at depths greater than 100 m appears to be controlled by the carbonate system, and modelling indicates that this water is in equilibrium with calcite. Investigation of fracture minerals show that calcite in fractures is abundant and that no extensive leaching has occurred in response to past glaciation/deglaciation events. These findings suggest that the buffering capacity against infiltrating dilute groundwater is sufficient, although no quantification has yet been made. However, a study aiming at quantifying fracture minerals is currently on-going and will be reported separately as a complement to the site descriptive modelling reports.

According to data analyses and modelling of the redox system, reducing conditions currently prevail at depths greater than about 20 m. Most of the Eh values determined in brackish groundwaters (at depths between 110 and 646 m) seem to be controlled by the occurrence of an amorphous iron oxyhydroxide with higher solubility than a truly crystalline phase. This indicates that the iron system is disturbed, which also is supported by mineralogical investigations

that have identified the presence of fine-grained amorphous to poorly crystalline phases now evolving towards more crystalline phases. Dissolved sulphide concentrations are systematically low, possibly due to the precipitation of amorphous Fe(II)-monosulphides, linked to the activity of sulphate-reducing bacteria (SRB).

At depths greater than 600 m, the dissolved sulphide concentrations increase, which is consistent with the occurrence SRB and with the active precipitation of Fe(II)-monosulphides. The iron system at these depths seems to be limited by crystalline oxyhydroxides, mainly hematite.

Note: However, for both iron and sulphide there is a degree of uncertainty to the reliability of the present data from suspected anthropogenic disturbances due to drilling and sampling procedures. Caution, therefore, needs to be exercised.

Elevated concentrations of uranium have been detected in groundwaters associated with a Littorina component and the highest concentrations are found in waters in the gently dipping deformation zones south-east of the target volume. There are indications that these elevated concentrations are related to easy dissolvable uranium fractions in fracture coatings in contact with these waters. Speciation-solubility calculations support this conclusion and indicate that the high uranium contents are the result of the control exerted by an amorphous (and very soluble) uranium phase present in the system, and the weakly reducing Eh values which may allow uranium complexation and re-equilibrium depending on Eh and dissolved carbonate.

The presence of goethite (FeOOH) in some hydraulically active fractures and fracture zones (mainly within the major gently dipping deformation zones ZFMA2 and ZFMF1) in the upper part of the hanging wall bedrock, indicates circulation of oxidising fluids during some period in the past (potentially Quaternary). However, the presence of pyrite in the same zones suggests that the circulation of oxidising fluids has been concentrated along channels in which different redox micro environments may have been formed. Furthermore, mobilisation as well as deposition of uranium in the upper 150 m of the bedrock is indicated by U-series decay analyses of fracture coatings.

Analyses of the current redox system at Forsmark have consistently indicated that sampling (or drilling-induced) perturbation may have altered the original redox conditions of the hydrochemical system. Examples include oxygen intrusion and precipitation of amorphous iron oxyhydroxides, as indicated by the colloidal composition (see section below) and mineralogical determinations. Additionally, there could have been modification of the original Eh and/or alkalinity by drilling waters, and the increase in dissolved uranium contents or changes in sulphide contents could have been caused partly by one or more of these disturbances. Despite these potential disturbances, the buffer capacity of the system maintains a noticeable reducing character below 100 m. Concerning the potential redox buffering capacity of the fracture system, it is concluded that previous oxidising episodes have not been intense enough to exhaust the reducing capacity of fracture filling minerals, which are still present in the shallow system (for example chlorite and pyrite).

7.2.5 Dissolved gases and colloids

Analyses of gas dissolved in groundwater at Forsmark have shown that the gas content increases with depth, but the waters are far from being oversaturated by gas. The major gas components are nitrogen and helium. Methane has also been detected, but generally in small amounts (less than 0.2 mL/L). Currently, it is not known whether the methane is of biogenic or non-biogenic origin.

Colloid amounts in Forsmark groundwater are comparable to that found in other granitic environments. The colloids are composed mostly of aluminium, silica, iron and sulphur. Uranium associated to the colloids was found in boreholes KFM02A and KFM06A, in line with the high groundwater uranium concentrations found in these boreholes. The uranium

content on the colloids is about 10% of the uranium concentration in the groundwater and colloidal transport is, therefore, the result but not the origin to the high uranium content in the groundwater.

7.2.6 Confidence

There is generally a high confidence in the description and understanding of the current spatial distribution of groundwater composition, mainly due to the consistency between different analyses and modelling of the chemical data, but also due to the agreement with the hydrogeological understanding of the area. In addition, the existence of a near-surface redox reaction zone appears to be well established based on water chemistry from the shallow groundwater, even if there is uncertainty in the data interpretation, and abundant existence of calcite suggests there is buffering capacity against dilute acid groundwaters. Furthermore, even though quantification of the bedrock buffering capacity is not yet achieved, general indications from the Forsmark area as a whole point to a bedrock which has a sufficiently large buffering capacity to maintain pH values in the range 7 to 8.5 and Eh values lower than –140 mV. One important remaining uncertainty concerns the increase in sulphide concentrations measured in the on-going monitoring programme. Initial drilling and pumping may have disturbed the system or may have facilitated sulphate reduction, but this issue remains to be resolved. The monitoring programme will also support the overall understanding of the long term behaviour of other groundwater parameters such as uranium, DOC and tritium.

7.3 Summary of important issues in site understanding

7.3.1 General

The Forsmark site investigations have produced a good hydrogeochemical understanding of the site, both of present and past conditions, and have emphasised the different groundwater behaviour of the footwall bedrock to that of the hanging wall bedrock. Focussing on the target volume (i.e. footwall), this does not represent a 'traditional' site in that there is no systematic hydrogeochemical evolution from surface recharge to the maximum depths sampled as seen, for example, in the Laxemar area. A key issue in this respect is the behaviour of the shallow bedrock aquifer in the upper approximately 100–200 m of the footwall, which serves to limit the downward percolation of recharging groundwaters to the equivalent of repository depths in the target volume, apart from that suspected to occur along some steeply dipping deformation zones that intersect the bedrock surface. This shallow bedrock aquifer demarcates a sharp hydrochemical boundary from recent, near-surface groundwaters, to deeper and much older and evolved groundwaters. Furthermore, rock matrix porewaters of a much older origin are also present below this aquifer.

Major hydrogeochemical issues of importance to site understanding are addressed below which include: a) the redox buffering capacity of the bedrock system, b) changes in groundwater composition with depth based on palaeohydrogeochemical events, c) the presence of sulphide in groundwaters, d) the presence of methanogenic bacteria and methane in groundwaters, and e) the presence of elevated uranium in groundwaters.

7.3.2 Bedrock redox buffer capacity

There is good evidence to show that the bedrock has provided a long term and efficient redox barrier to recharging oxidising meteoric groundwaters at depths down to and exceeding 100–150 m. This is supported by detailed mineralogy and geochemistry of mineral phases in fractures and host rock (e.g. uranium decay series studies). These studies show that although

redox conditions have varied, these appear to have been restricted to the upper 100–150 m of the bedrock during the last 1 Ma. Within this bedrock interval, which corresponds to the maximum extent of the shallow bedrock aquifer, the distribution of redox conditions is very heterogeneous. Under present-day conditions, active redox buffering is occurring in the upper approximately 20 m of the bedrock based on groundwater chemistry.

The rapid reducing capacity of the bedrock has been illustrated by the use of redox potential time series measurements monitored at depth in some borehole sections which have been subject to contamination with oxidising drilling water (and/or oxidising near-surface groundwaters). During monitoring over periods of days, there has been a systematic reduction in the measured redox potential due to the reducing capacity of the isolated borehole section.

7.3.3 Glacial meltwaters

There are groundwater chemical and isotope data from the footwall bedrock (i.e. target volume) indicating that significant volumes of glacial meltwaters from the last deglaciation have not penetrated to depths greater than the shallow bedrock aquifer (100–200 m). Along the steeply dipping fracture zones the glacial meltwater penetration may have reached the depth of 500 m in the hanging wall. However, there is some evidence of glacial signatures of unknown age at depths around 600 m in the footwall and 900 m in the hanging wall bedrock associated with steeply dipping fracture zones.

Given similar conditions to the last glaciation, it is unlikely that large volumes of glacial meltwaters will penetrate to repository depths in the present target volume. Moreover, accepting the possibility that meltwaters under more severe conditions may penetrate to greater depths along steeply dipping zones, the probability of the glacial meltwaters retaining their oxidising character is doubtful, especially considering the buffer capacity of the bedrock addressed above. This is supported by studies from the Äspö-Laxemar sites that indicate that even though glacial meltwater signatures are found in the bedrock, there are no signs of this water having been oxidising at depths below 100 m.

7.3.4 Calcium variability in groundwater

A groundwater calcium content of more than 1 mM/L is presently the SKB limit for repository safety analysis based on a preliminary assessment on the stability of bentonite colloids. Palaeohydrogeochemical studies show periodic changes in groundwater composition at shallow depths which, in common with the glacial meltwaters described above, indicate that these groundwaters have also been restricted in the target volume by the shallow bedrock aquifer. This is supported by tritium which shows a rapid decrease for modern recharge waters below around 200 m depth. Furthermore, present shallow groundwaters at Forsmark to 200 m depth in the target area are characterised by elevated calcium contents exceeding 1 mM/L. Calcium content in groundwater is governed by mixing and reactions, in this latter case particularly ion exchange with sodium in the bedrock. Some insight into these problems at Forsmark can be illustrated by the incursion of Littorina Sea water. This marine infiltration and mixing with glacial water took place 2500–1000 BC, followed by partial mixing with dilute meteoric recharge waters when the Forsmark site emerged following uplift. However, despite this mixing, the brackish marine (Littorina) groundwaters have gained calcium through ion exchange with the bedrock, and during silicate weathering.

For dilute groundwater incursions, there have been two critical periods for potential lowering of the calcium content; the incursion of dilute glacial meltwaters (described above) and later meteoric recharge waters following uplift. However, in essence, the target volume below the shallow bedrock aquifer has been shielded from these different incursions apart from some potential restricted influence to deeper levels via larger, steeply dipping transmissive deformation zones.

7.3.5 The presence of sulphide

Sulphate and sulphide have been measured in the groundwaters at Forsmark and the major sulphur source is marine (to the largest extent associated with Littorina type waters). The sulphur isotope ratios and the fact that sulphate-reducing bacteria are present, suggest that sulphide is and has been produced in the system. However, measurements of sulphide at different sampling occasions have yielded very different results and continued sampling in association with the monitoring programme is needed before more detailed interpretations should be attempted. Because Fe^{2+} is produced in the system, it is probable that S^{2-} will be controlled by Fe-monosulphide solubility during undisturbed conditions.

The magnitude and variability of sulphide at repository depths is still, therefore, an open question.

7.3.6 Microbes and methane

Anaerobic methanogenic bacteria were identified in trace amounts in most of the groundwaters in Forsmark, with the exception of boreholes KFM03A at depths of 340 and 640 m, where slightly higher numbers were recorded. Gas analyses show low contents of methane in all boreholes except for KFM01D at 445 m. No correlation was found between methane content and number of methanogenic bacteria.

To understand the relationship between anaerobic methanogenic bacteria and methane content is a question of general interest to establish the origin of methane in the Forsmark system. However, the studies have been inconclusive and the question remains unresolved.

7.3.7 Elevated uranium contents

Elevated concentrations of uranium have been detected in groundwaters associated mainly with the Littorina component and the highest concentrations are found in groundwaters in the gently dipping deformation zones in the hanging wall, south-east of the target volume. There are indications that these elevated concentrations are related to easy dissolvable uranium fractions in fracture coatings in contact with these. Speciation-solubility calculations support this conclusion and indicate that the high uranium contents are the result of the control exerted by an amorphous (and very soluble) uranium phase present in the system, and the weakly reducing Eh values which may allow uranium complexation and re-equilibrium depending on Eh and dissolved carbonate. This is important considering the possible modification of the natural conditions undergone by these waters. The alteration of an originally more reducing environment, and/or the increase of dissolved carbonate could have caused the increase in uranium-carbonate complexation, in turn enhancing the dissolution of uranium phases and increasing the contents of dissolved uranium with respect to that originally present in the system. Such a situation is not restricted to the Littorina type groundwaters, but may also occur if dilute recharge waters with significant bicarbonate content penetrate to greater depths.

8 Acknowledgements

9 References

Andersson J, 2003. Site descriptive modelling – strategy for integrated evaluation. SKB R-03-05, Svensk Kärnbränslehantering AB.

Appelo C A J, Postma D, 2005. Geochemistry, groundwater and pollution. Balkema, Rotterdam, The Netherlands (2nd. edition).

Auqué L F, Gimeno M J, Gómez J, Puigdoménech I, Smellie J, Tullborg E-L, 2007. Groundwater chemistry around a repository for spent nuclear fuel over a glacial cycle Evaluation for SR-Can. SKB TR-06-31, Svensk Kärnbränslehantering AB.

Auqué L, Gimeno M J, Gómez J, Nilsson A-C, 2008. Potentiometrically measured Eh in groundwaters from the Scandinavian Shield. Appl. Geochem. 27, 1820–1833.

Ball J W, Nordstrom D K, 2001. User's manual for WATEQ4F, with revised thermodynamic data base and test cases for calculating speciation of major, trace, and redox elements in natural waters. U.S. Geol. Sur., USA. Open File Report 91-183.

Banwart S A, 1999. Reduction of iron (III) minerals by natural organic matter in groundwater. Geochim. Cosmochim. Acta, 63, 2919–2928.

Berg C, Bergelin A, Wacker P, Nilsson A-C, 2006. Forsmark site investigation. Hydrochemical characterisation in borehole KFM08A. Results from the investigated section at 683.5–690.6 (690.8) m. SKB P-06-63, Svensk Kärnbränslehantering AB.

Björck S, 1995. A review of the history of the Baltic Sea 13-8 ka, Quaternary International, 27, 19–40.

Blomqvist R, Ruskeeniemi T, Kaija J, Ahonen L, Paananen M, Smellie J, Grundfelt G, Pedersen K, Bruno J, Pérez del Villar L, Cera E, Rasilainen K, Pitkänen P, Suksi J, Casanova J, Read D, Frape S, 2000. The Palmottu Natural Analogue Project. Phase II: transport of radionuclides in a natural flow system. European Commission Final Report, Phase II, EUR-19611, 171 p.

Blyth A, Frape S, Blomqvist R, Nissinen P, 2000. Assessing the past thermal and chemical history of fluids in crystalline rock by combining fluid inclusion and isotopic investigations of fracture calcite. Appl. Geochem. 15, 1417–1437.

Bosson E, Gustafsson, L-G, Sassner M, 2008. Numerical modelling of surface hydrology and near-surface hydrogeology at Forsmark. Site descriptive modelling, SDM-Site Forsmark. SKB R-08-09, Svensk Kärnbränslehantering AB.

Budai J M, Martini A M, Walter L M, Ku T C W, 2002. Fracture-fill calcite as a record of microbial methanogenesis and fluid migration; a case study from the Devonian Antrim Shale, Michigan Basin. Geofluids 2, 163–183.

Byegård J, Selnert E, Tullborg E-L, 2008. Bedrock transport properties. Data evaluation and retardation model. Site descriptive modelling. SDM-Site Forsmark. SKB R-08-98. Svensk Kärnbränslehantering AB.

Carman R, Rahm L, 1997. Early diagenesis and chemical characteristics of interstitial water and sediments in the deep deposition bottoms of the Baltic proper. J. Sea Res., 37/1-2, 25–47.

Cederbom C, Larson S Å, Tullborg E-L, Stiberg J P, 2000. Fission track thermochronology applied to Phanerozoic thermotectonic events in central and southern Sweden. Tectonophysics, 316, 1-2, 153–167.

Degueldre C, 1994. Colloid properties in groundwater from crystalline formation. Paul Scherrer Institute, Villigen, Switzerland.

Dideriksen K, Christiansen B C, Baker J A, Frandsen C, Balic-Zunic T, Tullborg E-L, Mørup S, Stipp S L S, 2007. Fe-oxide fracture-fillings as a palæo-temperature and -redox indicator: Structure, crystal form, REE content and Fe isotope composition. Chem. Geol., 244, 330–343.

Drever J I, 1997. The geochemistry of natural waters: surface and groundwater environments. Prentice Hall. Upper Saddle River, N.J. 436 pp.

Eydal H S C, Pedersen P, 2007. Use of an ATP assay to determine viable microbial biomass in Fennoscandian Shield groundwater from depths of 3–1000 m, J. Microbiol. Meth., 70 363–373.

Follin S, Johansson P-O, Hartley L, Jackson P, Roberts D, Marsic N, 2007a. Hydrogeological conceptual model development and numerical modelling using CONNECTFLOW, Forsmark modelling stage 2.2. SKB R-07-49, Svensk Kärnbränslehantering AB.

Follin S, Levén J, Hartley L, Jackson P, Joyce S, Roberts D, Swift B, 2007b. Hydrogeological characterisation and modelling of deformation zones and fracture domains, Forsmark modelling stage 2.2. SKB R-07-48, Svensk Kärnbränslehantering AB.

Follin S, 2008. Bedrock hydrogeology Forsmark Site descriptive modelling, SDM-Site Forsmark. SKB R-08-95, Svensk Kärnbränslehantering AB

Follin S, Stephens M B, Laaksoharju M, Nilsson A-C, Smellie J A T, Tullborg E-L, 2008a. Modelling the evolution of hydrochemical conditions in the Fennoscandian Shield during Holocene time using multidisciplinary information. Appl. Geochem., 23, in press.

Follin S, Hartley L, Jackson P, Roberts D, Marsic N, 2008b. Conceptual model development and numerical modelling using CONNECTFLOW, Forsmark modelling stage 2.3. SKB R-08-23, Svensk Kärnbränslehantering AB.

Frape S K, Fritz P, 1987. Geochemical trends from groundwaters from the Canadian Shield. In: P. Fritz and S.K. Frape (eds). Saline waters and gases in crystalline rocks. Geol. Assoc. Canada Spec. Paper 33, 19–38.

Fredén C, 2002. Berg och Jord, Sveriges Nationalatlas. 208 pp.

Garrels R M, Christ C J, 1965. Solutions, minerals and equilibria. New York, Harper & Row, 450 p.

Gascoyne M, 2004. Hydrogeochemistry, groundwater ages and sources of salts in a granitic batholith on the Canadian Shield, southeastern Manitoba. Appl. Geochem., 19, 519–560.

Gascoyne M, Laaksoharju (ed), 2008. High-level radioactive waste disposal in Sweden: Hydrogeochemical characterisation and modelling of two potential sites. Appl. Geochem., 23/7, ISSN 0883-2927. Elsevier.

Gascoyne M, Gurban I, 2008. Application of the Drilling Impact Study (DIS) to Forsmark groundwaters. In: B. Kalinowski (ed), 2008. SKB R-08-87, Svensk Kärnbränslehantering AB.

Gimeno M J, Auqué L F, Gómez J B, Acero P, 2008. Forsmark area version 2.2–2.3. Contribution from the University of Zaragoza. SKB R-08-86, Svensk Kärnbränslehantering AB.

Gómez J B, Laaksharju M, Skårman E, Gurban I, 2006. M3 version 3.0: Concepts, methods, and mathematical formulation. SKB TR-06-27, Svensk Kärnbränslehantering AB.

Gómez J, Laaksoharju M, Skårman E, Gurban I, 2008. M3 version 3.0: Verification and validation. SKB Report (in preparation), Svensk Kärnbränslehantering AB.

Grenthe I, Stumm W, Laaksoharju M, Nilsson A C, Wikberg P, 1992. Redox potentials and redox reactions in deep groundwater systems. Chem. Geol., 98, 131–150.

Gurban I, 2008. Forsmark Site: M3 modelling and 2D visualisation of the hydrochemical parameters in Forsmark groundwater data 2.2 and 2.3. In: B. Kalinowski (ed), 2008. SKB R-08-87, Svensk Kärnbränslehantering AB.

Hallbeck L, Pedersen K, 2008a. Explorative analyses of microbes, colloids and gases together with microbial modelling. Forsmark area version 2.3. SKB R-08-85, Svensk Kärnbränslehantering AB.

Hallbeck L, Pedersen K, 2008b. Characterization of microbial processes in deep aquifers in the Fennoscandian Shield. Appl. Geochem., 23, 1796–1819.

Kalinowski B (ed), 2008. Background complementary hydrogeochemical studies. SKB R-08-87, SKB, Svensk Kärnbränslehantering AB.

Kölling M, 2000. Comparison of different methods for redox potential determination in natural waters. In: L. Schüring, H.D. Schulz, W.R. Fischer, J. Böttcher and W.H.M. Duijnisveld (eds.), Redox. Fundamentals, processes and applications. Springer. Chapter 4, 42–54.

Laaksoharju M, Wallin B (eds), 1997. Evolution of the groundwater chemistry at the Äspö Hard Rock Laboratory. Proceedings of the second Äspö International Geochemistry Workshop, June 6–7, 1995. Äspö HRL ICR-Rep. ICR-97-04, Svensk Kärnbränslehantering AB.

Laaksoharju M, 1999. Groundwater Characterisation and Modelling: Problems, Facts and Possibilities. Dissertation TRITA-AMI-PHD 1031; ISSN 1400-1284; ISRN KTH/AMI/PHD 1031-SE; ISBN 91-7170-. Royal Institute of Technology, Stockholm, Sweden. SKB TR-99-42, Svensk Kärnbränslehantering AB.

Laaksoharju M, Tullborg E-L, Wikberg P, Wallin B, Smellie J, 1999. Hydrogeochemical conditions and evolution at the Äspö HRL, Sweden. Appl. Geochem., 14, 835–859.

Laaksoharju M, Smellie J, Tullborg E-L, Gimeno M, Molinero J, Gurban I, Hallbeck L, 2008. Hydrogeochemical evaluation and modelling performed within the site investigation programme. Appl. Geochem., 23, 1761–1795.

Molinero J, Arcos D, Duro L, 2008. Contribution to ChemNet activities. Forsmark model 2.2-2.3. In: B. Kalinowski (ed), 2008. SKB R-08-87, Svensk Kärnbränslehantering AB.

Nilsson A-C, 2008. Forsmark site investigation. Quality of hydrochemical analyses (DF version 2.2/2.3). In: B. Kalinowski (ed), 2008. SKB R-08-87, Svensk Kärnbränslehantering AB.

Nordstrom D K, Plummer L N, Langmuir D, Busenberg E, May H M, Jones B F, Parkhurst D, 1990. Revised chemical equilibrium data for major water-mineral reactions and their limitations. In: Melchior, D.C. and Basset, R.L. (eds.), Chemical Modelling of Aqueous Systems II. ACS Symp. Ser. pp. 398–413.

O'Neil J R, Clayton R N, Mayeda T K, 1969. Oxygen isotope fractionation in divalent metal carbonates. J. Chem. Phys., 51, 5547–5558.

Olofsson I, Simeonov A, Stephens M, Follin S, Nilsson A-C, Röshoff K, Linberg U, Lanaro F, Fredriksson A, Persson L, 2007. Site descriptive modelling Forsmark, stage 2.2. A fracture domain concept as a basis for the statistical modelling of fractures and minor defprmation zones, and interdisciplinary coordination. SKB R-07-15, Svensk Kärnbränslehantering AB.

Parkhurst D L, Appelo C A J, 1999. User's Guide to PHREEQC (Version 2), a computer program for speciation, batch-reaction, one-dimensional transport, and inverse geochemical calculations. Water Res. Res. Invest. Rep., 99-4259, 312 p.

Pedersen K, Hallbeck L, Arlinger J, Jahromi N, Erlandson A-C, 1997. Investigation of the potential for microbial contamination of deep granitic aquifers during drilling using molecular and culturing methods. J. Microbiol. Meth., 30:179–192.

Pedersen K, **2001.** Diversity and activity of microorganisms in deep igneous rock aquifers of the Fennoscandian Shield. In Subsurface microbiology and biogeochemistry. Fredrickson, J. K. & Fletcher, M., Eds. New York: Wiley-Liss Inc., 97–139.

Pedersen K, **2005.** Forsmark site investigation. Control of microorganism content in flushing water used for drilling of KFM06A. SKB P-Rep. (P-05-81), Svensk Kärnbränslehantering AB.

Pedersen K, Arlinger J, Eriksson S, Hallbeck A, Hallbeck L, Johansson J, 2008. Numbers, biomass and cultivable diversity of microbial populations relate to depth and borehole-specific conditions in groundwater from depths of 4–450 m in Olkiluoto, Finland. ISME-J doi: 10.1038/ismej.2008.43.

Pitkänen P, Luukkonen A, Ruotsalainen P, Leino-Forsman H, Vuorinen U, 1999. Geochemical modelling of groundwater evolution and residence time at the Olkiluoto site. Posiva Tech Rep. (98-10), Posiva, Helsinki, Finland.

Pitkänen P, Partamies S, Luukkonen A, 2004. Hydrogeochemical interpretation of baseline groundwater conditions at the Olkiluoto site. Posiva Tech. Rep. (2003-07), Posiva, Helsinki, Sweden.

Påsse T, 1997. A mathematical model of past, present and future shore level displacement in Fennoscandia. SKB TR-97-28, Svensk Kärnbränslehantering AB.

Ruskeeniemi T, Ahonen L, Paananen M, Frape S, Stotler R, Hobbs M, Kaija J, Degnan P, Blomqvist R, Jensen M, Lehto K, Moren L, Puigdomenech I, Snellman M, 2004. Permafrost at Lupin. Report of Phase II. Permafrost project GTK-SKB-POSIVA-NIREX-OPG. Report YST-119, Geol. Surv. Finland, Helsinki, Finland.

Samper J, Delgado J, Juncosa R, Montenegro L, 2000. CORE2D v 2.0: A Code for non-isothermal water flow and reactive solute transport. User's manual.ENRESA Technical Report 06/2000.

Sandström B, Tullborg E-L, 2006. Forsmark site investigation. Mineralogy, geochemistry, porosity and redox capacity of altered rock adjacent to fractures. SKB P-06-209, Svensk Kärnbränslehantering AB.

Sandström B, Page L, Tullborg E-L, 2006a. Forsmark site investigation. $^{40}Ar/^{39}Ar$ (adualaria) and Rb-Sr (adularia, prehnite, calcite) ages of fracture minerals. SKB P-06-213, Svensk Kärnbränslehantering AB.

Sandström B, Tullborg E-L, De Torres T, Ortiz J E, 2006b. The occurrence and potential origin of asphaltite in bedrock fractures, Forsmark, central Sweden. GFF 128, 233–242.

Sandström B, Tullborg E-L, Smellie J, MacKenzie A B, Suksi J, 2008. Fracture mineralogy of the Forsmark site. Final report. SKB P-08-87, Svensk Kärnbränslehantering AB.

SKB, 2004. Preliminary site description Forsmark area – version 1.1. SKB R-04-15, Svensk Kärnbränslehantering AB.

SKB, 2005. Hydrogeochemical evaluation. Preliminary site description Forsmark area – version 1.2. SKB R-05-17, Svensk Kärnbränslehantering AB.

SKB, 2006a. Groundwater chemistry around a repository for spent nuclear fuel over a glacial cycle. Evaluation for SR-Can. SKB TR-06-31, Svensk Kärnbränslehantering AB.

SKB, 2006b. Site descriptive modelling Forsmark stage 2.1. Feedback for completion of the site investigation including input from safety assessment and repository engineering. SKB R-06-38, Svensk Kärnbränslehantering AB.

SKB, 2006c. Hydrogeochemical evaluation. Preliminary site description Laxemar subarea – version 1.2. SKB R-06-12, Svensk Kärnbränslehantering AB.

SKB, 2006d. Hydrogeochemical evaluation. Preliminary site description Laxemar subarea – version 2.1. SKB R-06-70, Svensk Kärnbränslehantering AB.

SKB, 2007. Hydrogeochemical evaluation of the Forsmark site, modelling stage 2.1 – issue report. SKB R-06-69, Svensk Kärnbränslehantering AB.

SKB, 2008. Site description of Forsmark at completion of the site investigation phase, SDM-Site Forsmark. SKB TR-08-05, Svensk Kärnbränslehantering AB.

Smellie J, Laaksoharju M, Tullborg E-L, 2002. Hydrogeochemical site descriptive model – a strategy for the model development during site investigations. SKB R-02-49, Svensk Kärnbränslehantering AB.

Smellie J, Tullborg E-L, Nilsson A-C, Gimeno M, Sandström B, Waber N, Gascoyne M, 2008. Hydrogeochemical evlauation. Forsmark area (version 2.2/2.3). SKB R-08-84, Svensk Kärnbränslehantering AB.

Stephens M B, Fox A, La Poinre P, Simeonov A, Isaksson H, Hermanson J, Öhman J, 2007. Geology Forsmark. Site descriptive modelling. Forsmark stage 2.2. SKB R-07-45, Svensk Kärnbränslehantering AB.

Stumm W, Morgan J, **1996.** Aquatic chemistry, 3rd Edition. John Wiley, New York.

Svensson U, 1996. SKB Palaeohydrogeological programme. Regional groundwater flow due to advancing and retreating glacier-scoping calculations. In: SKB Project Report U 96-35, Svensk Kärnbränslehantering AB.

Söderbäck B (ed), 2008. Geological evolution, palaeoclimate and historical development of the Forsmark and Laxemar-Simpevarp areas. Site descriptive modelling, SDM-Site. SKB R-08-19, Svensk Kärnbränslehantering AB.

Söderlund P, 2008. $^{40}Ar/^{39}Ar$, AFT and (U-Th)/He thermochronologic implications for the low-temperature geological evolution in SE Sweden. Ph.D. Thesis, Department of Geology, Lund University. Litholund Theses no. 16.

Thunehed H, Pitkänen T, 2007. Transient electromagnetic soundings at Forsmark and the regional surroundings. Estimations of depth to saline groundwater. Forsmark site investigation. SKB P-07-165, Svensk Kärnbränslehantering AB.

Tröjbom M, Söderbäck B, 2006. Chemical characteristics of surface systems in the Forsmark area. Visualisation and statistical evaluation of data from shallow groundwater, precipitation, and regolith. SKB R-06-19, Svensk Kärnbränslehantering AB.

Tröjbom M, Söderbäck B, Tullborg E-L, Johansson P-O, 2007. Evaluation of the hydrochemistry in the Forsmark area with focus on the surface system. SKB R-07-55, Svensk Kärnbränslehantering AB.

Tullborg E-L, Drake H, Sandström B, 2008. Palaeohydrogeology: A methodology based on fracture mineral studies. Appl. Geochem., 23, 1881–1897.

Upstill-Goddard R C, Elderfield H, 1988. The role of diagenesis in the estuarine budgets of iodine and bromine. Continental Shelf Res., 8, 405–430.

Waber H N, Smellie J A T, 2004. Oskarshamn site investigation. Borehole KSH02: Characterisation of matrix porewater (Feasibility Study). SKB P-04-249, Svensk Kärnbränslehantering AB.

Waber H N, Smellie J A T, 2005. Forsmark site investigation. Borehole KFM06: Characterisation of porewater. Part I: Diffusion experiments. SKB P-05-196, Svensk Kärnbränslehantering AB.

Waber H N, Smellie J A T, 2007. Forsmark site investigation. Borehole KFM01D, KFM08C, KFM09B: Characterisation of porewater. Part I: Diffusion experiments and porewater data. SKB P-07-119, Svensk Kärnbränslehantering AB.

Waber H N, Smellie J A T, 2008. Characterisation of porewater in crystalline rocks. Appl. Geochem., 23, 1834–1861.

Waber H N, Gimmi T, Smellie J A T, 2008a. Porewater in the rock matrix. Site descriptive modelling, SDM-site Forsmark. SKB R-08-105, Svensk Kärnbränslehantering AB.

Waber H N, Gimmi T, Smellie J A T, deHaller A, 2008b. Porewater in the rock matrix. Site descriptive modelling. SDM-Site Laxemar. SKB R-08-112, Svensk Kärnbränslehantering AB.

Wallin B, Peterman Z E, 1999. Calcite fracture fillings as indicators of paleohydrology at Laxemar at the Äspo Hard Rock Laboratory, southern Sweden. Appl. Geochem., 14, 953–962.

Welin E, 1964. Uranium dissemination and vein fillings in iron ores of northern Uppland. Geologiska Föreningens i Stockholm Förhandlingar GFF, 51, 51–82.

Westman P, Wastegård S, Schoning K, Gustafsson B, 1999. Salinity change in the Baltic Sea during the last 8,500 years: Evidence, causes and models. SKB TR-99-38, Svensk Kärnbränslehantering AB.

Vilks P, Miller H, Doern D, 1991. Natural colloids and suspended particles in the Whiteshell Research area, Manitoba, Canada, and their potential effect on radiocolloid formation. Appl. Geochem., 565–574.